DOCTOR OF PHILOSOPHY

Regulation and role of the LKB1-AMPK pathway

Gowans, Graeme J.

Award date:
2014

DOCTOR OF PHILOSOPHY

Regulation and role of the LKB1-AMPK pathway

Graeme J. Gowans

2014

University of Dundee

Regulation and role of the LKB1-AMPK pathway

Graeme J. Gowans

A thesis presented for the degree of Doctor of Philosophy

University of Dundee

February 2014

CONTENTS

LIST OF FIGURES

LIST OF TABLES

LIST OF AMINO ACIDS

Amino acid	Three letter symbol	One letter symbol
Alanine	Ala	A
Arginine	Arg	R
Asparagine	Asn	N
Aspartic acid	Asp	D
Cysteine	Cys	C
Glutamic acid	Glu	E
Glutamine	Gln	Q
Glycine	Gly	G
Histidine	His	H
Isoleucine	Ile	I
Leucine	Leu	L
Lysine	Lys	K
Methionine	Met	M
Phenylalanine	Phe	F
Proline	Pro	P
Serine	Ser	S
Threonine	Thr	T
Tryptophan	Trp	W
Tyrosine	Tyr	Y
Valine	Val	V

ABBREVIATIONS

4E-BP	eukaryotic translation initiation factor 4E-binding protein
ACC	acetyl Co-A carboxylase
ADP	adenosine 5'-diphosphate
AICAR	5-amino-imidazole carboxamide riboside
AID	autoinhibitory domain
AMP	adenosine 5'-monophosphate
AMPK	AMP-activated protein kinase
Atg	autophagy related
ATP	adenosine 5'-triphosphate
AU	arbitrary units
Bis	bis-acrylamide
BSA	bovine serum albumin
CaMKK	Ca^{2+}/calmodulin-depedent protein kinase kinase
CBM	carbohydrate binding module
CBS	cystathionine-β-synthase
CPT1	carnitine:palmitoyl-CoA transferase 1
CRTC2	CREB-regulated transcription co-activator 2
CTD	C-terminal domain
DEPTOR	DEP domain-containing mTOR-interacting protein
dKO	double knockout
DMEM	Dulbecco's modified Eagle's medium
DMSO	dimethyl sulfoxide
DN	dominant-negative

DNA	deoxyribonucleic acid
DNP	2,4-dinitrophenol
DTT	dithiothreitol
EDTA	ethylenediaminetetraacetic acid
EGTA	ethylene glycol tetraacetic acid
eIF	eukaryotic initiation factor
ePK	eukaryotic protein kinase
FBS	foetal bovine serum
FKBP12	FK506 binding protein
FLAG	DYKDDDDK peptide
FOXO	Forkhead box O
FRT	Flp-recombinase target
GAP	GTPase activating protein
GATOR	GTPase-activating protein activity toward Rags
GBD	glycogen binding domain
GDP	guanosine-5' diphosphate
GEF	guanine nucleotide exchange factor
GFP	green fluorescent protein
GLUT	glucose transporter
GST	glutathione-S-transferase
GST	glycogen synthase
GTP	guanosine-5'-triphosphate
HDAC	histone deacetylase
HEK293	human embryonic kidney 293 cells

HEPES	N-2-hydroxyethylpiperazine-N'-2-ethane sulfonic acid
HMGR	3-hydroxy-3-methyl-glutaryl-CoA reductase
IGF	insulin-like growth factor
IPTG	isopropyl-β-D-thiogalactopyranoside
IRS	insulin receptor substrate
KD	kinase domain
kDa	kilodalton
LB	Luria-Bertrani broth
LDS	lithium dodecyl sulphate
LKB1	liver kinase B1
M	molar
MEF	mouse embryonic fibroblast
mLST8	mammalian lethal with SEC13
MO25	mouse protein 25
MOPS	3-(n-morpholino) propane sulfonic acid
mTOR	mechanistic target of rapamycin
mTORC1	mechanistic target of rapamycin complex 1
mTORC2	mechanistic target of rapamycin complex 2
OCR	oxygen consumption rate
PAGE	polyacrylamide gel electrophoresis
PARP	poly (ADP-ribose) polymerase
PCR	polymerase chain reaction
PDK	3-phosphoinositide-dependent protein kinase 1
PFKFB	6-phosphofructo-2-kinase/fructose-2,6-bisphosphatase

PGC1α	peroxisome proliferator-activated receptor gamma coactivator 1-α
PI3K	phosphatidylinositide 3-kinase
PIKfyve	FYVE domain-containing phosphatidylinositol 3-phosphate 5-kinase
PIP2	phosphatidylinositol (3,4)-bisphosphate
PIP3	phosphatidylinositol (3,4,5)-trisphosphate
PJS	Peutz-Jeghers syndrome
PKA	cyclic AMP-dependent protein kinase
PKB	protein kinase B
PKC	protein kinase C
PMSF	phenylmethylsulfonylflouride
PP	protein phosphatase
PRAS40	40 kDa Pro-rich Akt substrate
PROTOR	protein observed with rictor
PTEN	phosphatase and tensin homologue
Rab	Ras-related in brain
Raptor	regulatory associated protein of mTOR
Rheb	Ras homolog enriched in brain
Rictor	rapamycin insensitive companion of mTOR
RNA	ribonucleic acid
rpm	revolutions per minute
SBTI	soya bean trypsin inhibitor
SD	standard deviation
SDS	sodium dodecyl sulphate
SEM	standard error of the mean

SGK	serum and glucocorticoid induced protein kinase
SNF	sucrose non-fermenting
SREBP	sterol regulatory element-binding protein
STRAD	ste20-related protein
TBS	tris buffered saline
TOP	terminal oligopyrimidine tract
TOR	target of rapamycin
Tris	Tris (hydroxymethyl) methylamine
TSC	tuberous sclerosis complex
TZD	thiazolidinedione
ULK1	Unc-51-like kinase 1
WPW	Wolff-Parkinson-White
WT	wild-type
ZMP	5-aminoimidazole-4-carboxamide ribonucleoside monophosphate
α-RIM	α regulatory-subunit-interacting motif

ACKNOWLEDGEMENTS

Firstly, I would like to thank my supervisor, Professor Grahame Hardie, for all his valuable support and guidance throughout my PhD. I would also like to thank all past and present members of the Hardie lab who have helped out when things were not going so well. I would especially like to thank Dr Fiona Ross and Dr Simon Hawley for all their advice, seemingly endless patience, and for buying me many drinks.

I would also like to thank AstraZeneca for providing generous funding for my PhD research and allowing me to present the results at various scientific meetings. Thanks to the DSTT for providing reagents.

Finally, I must thank my family and friends, especially my parents, for all their support during the last four years, and for putting up with me talking about AMPK a lot.

DECLARATIONS

I hereby declare that the following thesis is based on results of investigations conducted by myself, and that this thesis is my own composition. Work other than my own is clearly indicated in the text. This dissertation has not in whole, or in part, been previously presented for a higher degree.

Graeme J. Gowans

I certify that Graeme J. Gowans has spent the equivalent of at least nine terms in research work in the Division of Cell Signalling and Immunology, University of Dundee, and that he has fulfilled the conditions of the Ordinance No 39 of the University of Dundee and is qualified to submit the accompanying thesis in application for the degree of Doctor of Philosophy.

Prof. D. Grahame Hardie

SUMMARY

The AMP-activated protein kinase (AMPK) is a sensor of cellular energy that is activated by increases in the intracellular AMP:ATP or ADP:ATP ratios. Once active, AMPK activates catabolic pathways and inhibits anabolic pathways to restore cellular energy homeostasis. AMPK activity can be increased by phosphorylation of Thr172, a conserved residue in the activation loop of the kinase domain, by either LKB1 or CaMKKβ. Increases in Thr172 phosphorylation can be mediated by either protecting this site against dephosphorylation by protein phosphatases, or by promoting its phosphorylation by upstream kinases, both of which were proposed to be mediated by binding of AMP or ADP to the γ-subunit of AMPK. AMPK is also allosterically activated by binding of AMP, but not ADP.

Recently, ADP has been proposed as the major regulator of AMPK and the role of AMP has been questioned. The reasons for this are: (i) while both AMP and ADP can increase phosphorylation of Thr172, ADP is present at higher concentrations in the cell and it was proposed that AMP would be unable to compete with ADP for binding at the γ-subunit; (ii) allosteric activation by AMP was reported to increase AMPK activity by less than 2-fold, whereas changes in the phosphorylation of Thr172 can increase AMPK activity by 100-fold.

Using cell-free systems and intact cells, the regulation of Thr172 phosphorylation and AMPK activity by AMP, ADP and ATP was re-investigated. AMP promoted Thr172 phosphorylation by LKB1 but not by CaMKKβ, while ADP had no effect on Thr172 phosphorylation by either upstream kinase. Additionally, while both AMP and ADP

could protect Thr172 against dephosphorylation, AMP was more potent. The allosteric activation of AMPK by AMP was demonstrated to be a significant component of the overall activation mechanism. Using phosphorylation of ACC (a downstream target of AMPK) as a marker, allosteric activation of AMPK was observed under conditions where there were no changes in Thr172 phosphorylation. The changes in Thr172 phosphorylation and AMPK activity observed in intact cells in response to AMPK activators were also examined, and demonstrated to be far lower than the maximal effects observed in cell-free systems. Taken together, these results demonstrate that AMP is a true physiological regulator of AMPK activity.

The regulation of LKB1 has also been the subject of much interest. Whilst it appears that LKB1 is constitutively active, several groups have reported that LKB1 activity is regulated by post-translational modifications, particularly phosphorylation. The role of phosphorylation of LKB1 on Ser31 by AMPK was investigated. While AMPK could phosphorylate LKB1 in a cell-free system, an effect lost in an LKB1 [S31A] mutant, this phosphorylation was not observed in intact cells. Additionally, mutation of Ser31 did not appear to alter LKB1 activity. These results suggest that phosphorylation of Ser31 of LKB1 by AMPK, whilst possible, may not be a physiologically relevant event.

The mTOR pathway is a key regulator of cell growth and protein synthesis in response to a number of stimuli, including growth factors, nutrients and energy status. The mTOR pathway is frequently deregulated in a number of cancers and cancer syndromes, and inhibition of mTOR is a promising therapeutic approach. The nature of the genetic lesion in tumours may determine the response of cells to mTOR inhibition. The LKB1-AMPK pathway, as well as being a negative regulator of the mTOR pathway,

is also frequently inactivated in human cancers. The role that the LKB1-AMPK pathway plays in determining the cellular response to AZ4, a dual mTORC1 and mTORC2 inhibitor, was investigated. AZ4 induced apoptosis in a number of cell lines, confirming its potential as an anti-cancer therapeutic. However, the presence of an active LKB1-AMPK pathway protected cells against AZ4-induced apoptosis, suggesting that the status of this pathway may determine how cells respond to mTOR inhibition.

PUBLICATIONS

Some of the results in this thesis have been presented in the following publications:

Gowans, G.J., Hawley, S.A., Ross, F.A., Hardie, D.G., 2013. AMP Is a True Physiological Regulator of AMP-Activated Protein Kinase by Both Allosteric Activation and Enhancing Net Phosphorylation. Cell Metab. 18, 556–566.

Hawley, S.A., Ross, F.A., **Gowans, G.J.**, Tibarewal, P., Leslie, N.R., Hardie, D.G., 2014. Phosphorylation by Akt within the ST loop of AMPK-α1 down-regulates its activation in tumour cells. Biochem J. (epub ahead of print).

CHAPTER 1: INTRODUCTION

1.1 Protein phosphorylation

Protein phosphorylation is a form of post-translational modification whereby a phosphate group is transferred from ATP to the hydroxyl group of a serine, threonine or tyrosine residue on a target protein. This is catalysed by a group of enzymes termed protein kinases. Phosphorylation is a reversible modification, with the phosphate group being removed by a protein phosphatase (Fig 1.1). Proteins can therefore cycle between phosphorylated and dephosphorylated states and this can modify their function in a variety of ways, including: (i) increased or decreased biological activity; (ii) altered interaction with other proteins; (iii) changes in subcellular location; (iv) increased stability. Protein phosphorylation is an essential component of many signal transduction pathways. Indeed, it has been estimated that 30% of proteins in the human genome are phosphorylated, and abnormally regulated phosphorylation events are present in a number of diseases (Cohen, 2002a). Indeed, the importance of protein phosphorylation events in human diseases is illustrated by the number of kinase inhibitors either approved for clinical use or undergoing clinical trials for a range of conditions (Cohen and Alessi, 2013; Cohen, 2002b).

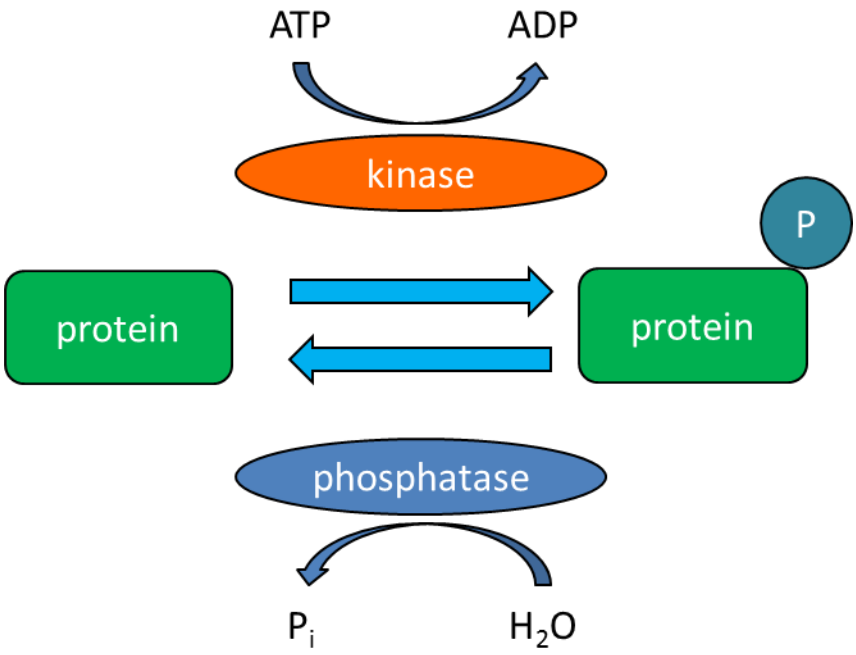

Figure 1.1: Protein phosphorylation
Schematic diagram of a protein phosphorylation/dephosphorylation cycle. Phosphorylation of the target protein is catalysed by a protein kinase and dephosphorylation by a protein phosphatase. The phosphate group is donated from ATP, producing ADP.

The first protein that was demonstrated to be reversibly regulated by phosphorylation was glycogen phosphorylase. Conversion of inactive phosphorylase *b* to active phosphorylase *a* could be achieved in the presence of Mg.ATP and an enzyme termed phosphorylase kinase (Fischer and Krebs, 1955). The conversion of active to inactive phosphorylase by protein phosphatase-1 was subsequently demonstrated (Ingebritsen and Cohen, 1983). The concept of protein kinases acting as signalling cascades was demonstrated when cyclic-AMP dependent protein kinase (PKA) was shown to phosphorylate and inactivate phosphorylase kinase (Walsh et al., 1968). Protein phosphorylation is now universally accepted as playing a major role in the regulation of almost all cellular processes.

1.2 The human kinome

The publication of the human genome sequence allowed for the identification of protein kinase genes by searching sequences for the presence of eukaryotic protein kinase (ePK) catalytic domains. A total of 518 kinases were identified, comprising 478 typical protein kinases and an additional 40 atypical protein kinases (Manning et al., 2002). The latter, while possessing kinase activity, lack sequence similarity to the ePK domain. Kinases therefore comprise nearly 2% of the total genes in the human genome. The kinases, the full complement of which is termed the kinome, were grouped into families based upon the sequence similarities of their catalytic domains, the domain structure outside the catalytic domain and known biological functions (Manning et al., 2002). A number of these identified kinases are actually considered to be catalytically inactive, lacking key conserved residues within the kinase domain. These pseudokinases are proposed to regulate the function of active kinases, and may also function as scaffolds in the formation of protein complexes (Boudeau et al., 2006; Manning et al., 2002).

1.3 AMP-activated protein kinase

1.3.1 Discovery and historical background

1.3.1.1 HMG CoA-reductase

3-Hydroxy-3-methylglutaryl coenzyme A reductase (HMGR), a key enzyme in the cholesterol biosynthesis pathway, converts HMG-CoA to mevalonic acid. Beg et al (1973) reported that HMGR activity associated with microsomes extracted from rat liver was reduced by incubation with Mg.ATP. This inactivation was dependent upon a cytosolic fraction, as the HMGR activity of washed microsomes was not reduced by

Mg.ATP unless the cytosolic fraction was included in the incubation. The authors also demonstrated that inactivated HMGR could be reactivated by incubation with a cytosolic fraction distinct from the inactivation factor (Beg et al., 1973). This was the first evidence that HMGR activity was converted from an active to inactive state and that this modulation was dependent upon a cytosolic fraction. The authors suggested that the inactivation could be due to protein phosphorylation.

Brown and colleagues (1975) reported that an HMGR inactivation factor was present in human fibroblast extracts. This factor could inactivate both fibroblast HMGR and the rat liver HMGR described by Beg et al (1973). HMGR activity was reduced by Mg.ATP, an effect prevented by EDTA. A number of observations in this study pointed to the inactivation factor in the fibroblast extract being an enzyme:

i. although ATP was required for inactivation, a derivative of ATP with a non-hydrolysable γ-phosphate group had no effect, suggesting that the cleavage or transfer of a phosphate group was necessary;

ii. an examination of the kinetics of HMGR inactivation demonstrated that a small amount of inactivation factor could inactivate the same amount of HMGR as a larger amount of inactivation factor, but over a longer period of time;

iii. the reduction in HMGR activity required a direct association between the fibroblast extract and the microsomal HMGR, as incubation of either component alone, followed by enzymatic inactivation and addition to fresh HMGR, resulted in no decrease in HMGR activity. This proved that the reduction in activity was not due to the production of an allosteric inhibitor and required the presence of an active fibroblast extract.

Interestingly, the authors also proposed that the activity of the inactivation factor was itself regulated, as the activity was present in samples isolated under conditions where HMGR activity was both high and low (Brown et al., 1975). This was early evidence for the presence of an upstream regulator of the HMGR inactivation factor.

Work by Nordstrom et al (1977) demonstrated that the inactivation of HMGR could be reversed by the addition of an activating factor, supporting the earlier work of Beg and colleagues (1973). This protein, present in the cytosol, could completely reverse the effects of HMGR inactivation by Mg.ATP. The activating factor was completely inhibited by sodium fluoride, a protein phosphatase inhibitor, suggesting that the activity of HMGR was regulated by changes in phosphorylation status. This was confirmed when it was demonstrated that incubation of HMGR with Mg^{2+} and [γ-^{32}P]ATP resulted in a reciprocal increase in ^{32}P incorporation into the enzyme and a decrease in enzyme activity (Beg et al., 1978). Incubation with partially purified phosphatase released ^{32}P and increased enzyme activity (Beg et al., 1978). This was the first conclusive evidence that HMGR activity was rapidly and reversibly regulated by a cycle of phosphorylation and dephosphorylation, being active when dephosphorylated and inactivate when phosphorylated.

Work by Ingebritsen et al (1978) demonstrated that the HMGR reactivating system could be replaced by a purified phosphatase. The authors also demonstrated that the inactivating system, the HMGR kinase, was itself regulated by phosphorylation. In this case the HMGR kinase was inactivated by the purified phosphatase and activated by an upstream kinase present in a microsomal extract, supporting the previous suggestion of Brown et al (1975).

Early work on the HMGR pathway had suggested that the inactivation of HMGR required both ATP and ADP, with the former proposed as a substrate for the HMGR kinase and the latter as an allosteric regulator (Brown et al., 1975). This theory was disproved when Ferrer et al (1985) demonstrated that AMP, and not ADP, was the activating ligand for the HMGR kinase. It is possible that the early preparations used were contaminated with adenylate kinase and it was the conversion of ADP to AMP that was necessary for activation of the HMGR kinase. HMGR activity was therefore proposed to be regulated by phosphorylation by an upstream kinase, HMGR kinase, which was itself regulated by phosphorylation. These effects were antagonized by protein phosphatases. Furthermore, HMGR kinase activity was allosterically increased by 5'-AMP.

1.3.1.2 Acetyl Co-A Carboxylase

In parallel, but unrelated, studies to the work on HMGR, Carlson and Kim (1973) discovered that acetyl Co-A carboxylase (ACC), a key enzyme in long-chain fatty acid synthesis, was inactivated by incubation with ATP. The reduction in catalytic activity mirrored the incorporation of ^{32}P into ACC. This inactivation was dependent upon time, temperature and the presence of a protein fraction, termed ACC kinase, leading to the proposal that ACC is inactivated by phosphorylation (Carlson and Kim, 1973). In addition to this, incubation of ACC with $MgCl_2$ caused an activation that was sensitive to sodium fluoride, suggesting the activity of a phosphatase (Carlson and Kim, 1973). This was confirmed by the demonstration that inactive ACC could be reactivated by incubation with partially purified phosphatase and that this correlated with ^{32}P release from ACC (Lee and Kim, 1977). That the reactivation was due to dephosphorylation was shown conclusively by purification of ACC in the presence and absence of sodium

fluoride (Hardie and Cohen, 1979). In the presence of fluoride, ACC was less active and contained more covalently bound phosphate than ACC prepared in the absence of fluoride. ACC could be converted to a more active form by incubation with highly purified protein phosphatase-1, which also reduced the amount of covalently bound phosphate (Hardie and Cohen, 1979).

Kim's group had reported that 5'-AMP stimulated the inactivation of ACC, although this was incorrectly attributed to a direct effect of AMP on ACC itself (Yeh et al., 1980). This mechanism of regulation therefore bore remarkable similarity to that seen with HMGR, and evidence was obtained to show that the same kinase inactivated both ACC and HMGR, in an AMP-stimulated manner (Carling et al., 1987). The kinase activity towards ACC and HMGR co-purified through six chromatography steps, confirming that they were functions of the same protein kinase (Carling et al., 1989). As the protein kinase now had two distinct substrates, neither of the original names, ACC kinase or HMGR kinase, were deemed suitable and AMP-activated protein kinase (AMPK) was proposed as the unifying name for the two previously distinct activities (Munday et al., 1988). This latter paper marked the first appearance of the name AMPK in the literature.

1.3.2 Identification of AMPK subunits

The first subunit to be identified was the catalytic α subunit, with an apparent molecular mass of 63 kDa (Carling et al., 1989). Using ATP-γ-Sepharose affinity chromatography, AMPK was subsequently purified to homogeneity and two additional polypeptides of 38 and 35 kDa were identified (Davies et al., 1994). Independently, AMPK purified from porcine liver was demonstrated to contain polypeptides of 63, 40

and 38 kDa (Mitchelhill et al., 1994). The three polypeptides co-migrated through gel filtration (Davies et al., 1994) and were present in a molar ration of 1:1:1 (Davies et al., 1994; Mitchelhill et al., 1994). This suggested that AMPK existed as a heterotrimeric complex. The three polypeptides identified, p63, p38 and p35, are now referred to as the α, β and γ subunits respectively (Fig. 1.2).

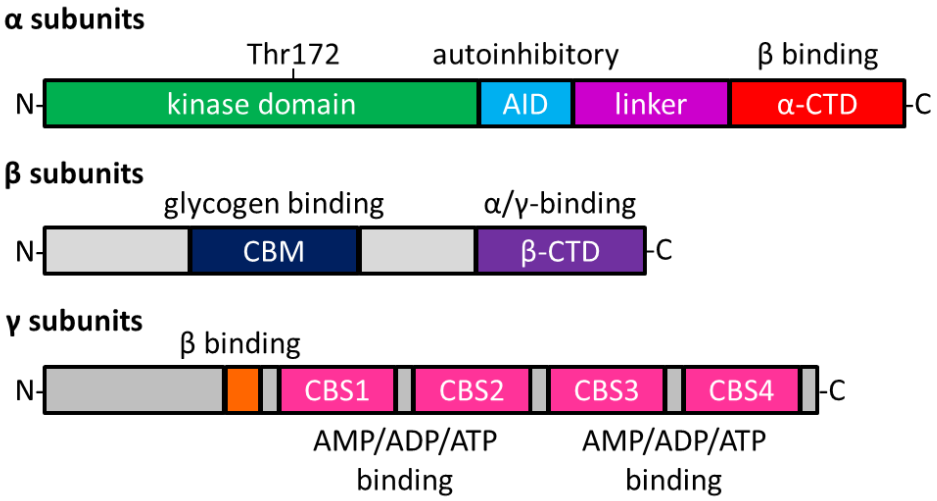

Figure 1.2: The α, β and γ subunits of AMPK
Domain maps of typical mammalian AMPK. AMPK exists as heterotrimeric complexes composed of α, β and γ subunits in a 1:1:1 ratio. AID, autoinhibitory domain; CTD, C-terminal domain; CBM, carbohydrate binding module; CBS, cystathione β synthase.

1.3.2.1 The α subunit

The mammalian AMPK-α subunit was cloned and showed a remarkable degree of sequence homology to the yeast sucrose non-fermenting (Snf1) protein (Carling et al., 1994). AMPK and Snf1 were demonstrated to be functionally homologous when their roles in the regulation of ACC function were shown to be conserved (Woods et al., 1994). In addition, Snf1 was shown to phosphorylate the SAMS peptide, a relatively specific substrate for AMPK, and, like AMPK, to be regulated by reversible phosphorylation (Woods et al., 1994). A second α subunit was later identified, named α1, with the original subunit renamed α2 (Stapleton et al., 1996). The two isoforms

also differed in their tissue distribution, assessed by probing for both mRNA and protein. Whilst α1 was evenly distributed throughout tissues, α2 was found to be more abundant in skeletal muscle, cardiac muscle and liver (Stapleton et al., 1996). The two isoforms, despite being encoded by distinct genes, share a high degree of sequence identity of 90% within the kinase domain, and 61% elsewhere (Stapleton et al., 1996).

The α subunits contain conventional kinase domains at their N-termini, with the conserved Thr172 residue in their activation loop. Phosphorylation of this residue by upstream kinases is required for AMPK activation (Hawley et al., 1996). The C-terminal domain (CTD) of the α1 subunit (residues 392-548) was reported to be required for interaction with the β and γ subunits (Crute et al., 1998). Further truncation of the α1 subunit to residue 312 resulted in a large increase in kinase activity, suggesting the presence of an autoinhibitory domain (AID) between residues 313 and 392 (Crute et al., 1998). This sequence was mapped to residues 313-335 of α1 (residues 311-333 of α2) and was predicted to be α-helical in nature (Pang et al., 2007). This helix was proposed to bind to the kinase domain, restricting its mobility and resulting in autoinhibition (Chen et al., 2009). A short linker region between the AID and the CTD appears to interact with the γ subunit and may play a key role in regulation of the kinase by nucleotides (Xiao et al., 2011; Chen et al., 2013). Regulation of AMPK is discussed further in section 1.4.

1.3.2.2 The β subunit

In mammals, there are two β isoforms, termed β1 and β2, encoded by two distinct genes and sharing 71% sequence identity (Woods et al., 1996a; Thornton et al., 1998) Expression of β1 protein is highest in the liver and the brain, whereas β2 protein is

most abundant in skeletal muscle (Thornton et al., 1998). The mammalian β subunits are closely related to the Sip1/Sip2/Gal83 proteins in budding yeast (Woods et al., 1996a). These proteins were known to interact with Snf1, the yeast homologue of AMPK-α, further supporting the conserved functions of the SNF1 and AMPK complexes (Jiang and Carlson, 1997). The C-terminal domain of the β subunit interacts with both the α and the γ subunits, functioning as a scaffold for complex assembly (Woods et al., 1996a). A conserved region in the C-terminus of the AMPK-β subunits (186-270) is homologous to the ASC domain present in the Sip1/Sip2/Gal83 proteins (Jiang and Carlson, 1997) and is required for binding to the α and γ subunits (Hudson et al., 2003; Iseli et al., 2005).

The β subunits also contain a carbohydrate-binding module (CBM), which causes the kinase to associate with glycogen particles (Hudson et al., 2003; Polekhina et al., 2003). The functional significance of this is unclear, although it may localize AMPK close to glycogen-bound substrates, such as glycogen synthase. Alternatively, AMPK activity may be regulated by glycogen itself and therefore respond to energy stores in the cell (Hardie, 2007). Indeed, AMPK activity is negatively regulated by glycogen both in purified cell-free systems (McBride et al., 2009) and in skeletal muscle (Wojtaszewski et al., 2002).

The β subunits are also subject to extensive post-translational modifications. Several phosphorylation sites have been mapped, including Ser24/25, Ser108 and Ser182 (Mitchelhill et al., 1997). Phosphorylation at Ser24/25 or Ser182 had no effect on AMPK activity. However, mutation of Ser108 reduced AMPK activity (Warden et al., 2001). In addition, the β subunits are N-terminally myristoylated at Gly2 (Mitchelhill et

al., 1997). Mutation of this residue to an alanine increased AMPK activity, as measured by immunoprecipitation and subsequent kinase assay (Warden et al., 2001).

1.3.2.3 The γ subunit

Three mammalian γ subunits are encoded by three distinct genes (Woods et al., 1996a; Cheung et al., 2000). The first isoform to be characterized, γ1, lacks a variable N-terminal extension present in the other two isoforms (Cheung et al., 2000). In contrast to the variable N-terminal regions, the C-terminal regions are highly conserved across the three isoforms, with sequence identities of 63 to 77% (Cheung et al., 2000). The tissue distribution varies amongst the isoforms, with γ1 and γ2 being ubiquitously expressed whilst γ3 expression appears to be restricted to skeletal muscle (Cheung et al., 2000). Evidence was also presented to suggest that the γ subunit was responsible for nucleotide binding, based upon its covalent labelling using the reactive AMP analogue 8-azido-[^{32}P]AMP, an effect that was abolished by adding unlabelled AMP (Cheung et al., 2000).

The γ subunits contain four tandem repeats of a 60 amino acid sequence motif termed a cystathionine β synthase (CBS) motif (Bateman, 1997). These repeats, labelled CBS1-4 in Fig. 1.2, associate in pairs to form AMP-binding domains (Scott et al., 2004). It was proposed that AMPK could bind two AMP molecules with positive co-operativity (Scott et al., 2004). A recent crystal structure of AMPK has revealed that the four CBS repeats appear to form a flattened disc, with nucleotides binding in the clefts between CBS repeats 1 and 2 and CBS repeats 3 and 4 (Xiao et al., 2011). Thus, AMPK contains four potential binding sites for nucleotides, which are numbered 1-4 according to the number of the CBS repeat carrying an aspartate residue that is positioned to bind the

ribose ring of the nucleotide (Kemp et al., 2007). Sites 1 and 3 were proposed to reversibly bind AMP or ATP, whilst site 4 was proposed to contain a permanently-bound AMP molecule. Site 2, which lacks the key aspartate residue, appeared to be empty (Xiao et al., 2011). The crystal structure also revealed that ADP could bind at site 1 or site 3 and played a role in regulation of AMPK activity (Xiao et al., 2011). The crystal structures and the regulation of AMPK are discussed in further detail in section 1.4.

Point mutations in the human γ2 CBS domains are associated with familial hypertrophic cardiomyopathy (abnormal thickening of the heart walls) and Wolff-Parkinson-White (WPW) syndrome (a condition characterized by ventricular pre-excitation, a premature electrical excitation of the ventricles, the large chambers of the heart) (Gollob et al., 2001). These mutations, when introduced in mammalian heterotrimers, reduced the sensitivity of the kinase to AMP (Daniel and Carling, 2002) and impaired AMP binding to the CBS domains (Scott et al., 2004). Interestingly, the mutations also increased the basal activity of the kinase, most likely due to the CBS domains also displaying reduced binding of the inhibitor ATP (Daniel and Carling, 2002; Hawley et al., 2010). Two of the more severe mutations, R531Q and R384T, were associated with death during infancy (Burwinkel et al., 2005; Akman et al., 2007). A common feature of the phenotype caused by the mutations is elevated cardiac glycogen content which may (when present during foetal development of the heart) prevent the normal electrical separation of the atria and ventricles, leading to ventricular pre-excitation (Arad et al., 2003; Gollob, 2003; Hardie, 2007). A similar mutation in the γ3 subunit of pigs caused elevated glycogen storage in skeletal muscle (Milan et al., 2000).

1.4 Regulation and crystal structures of AMPK

1.4.1 Regulation by phosphorylation and AMP

When AMPK was proposed as the unifying name for HMGR kinase and ACC kinase, it was already known that the kinase was allosterically activated by AMP and regulated by changes in phosphorylation. Early studies of its role as an HMGR kinase had found evidence for an upstream kinase present in the crude preparations, but it was not known how its phosphorylation was regulated *in vivo*. Moore et al (1991) reported that treatment of isolated rat hepatocytes with 20 mM fructose caused reciprocal changes in the activities of AMPK and ACC over time. Measurement of nucleotide levels in the isolated cells revealed a transient increase in the AMP:ATP ratio following addition of fructose, which returned to basal values with time. This correlated with a transient activation of AMPK and a transient inactivation of ACC. The transient inactivation of ACC in response to fructose could be explained by AMP allosterically activating AMPK and consequent ACC phosphorylation. However, the changes in AMPK activity, which were measured with saturating AMP in the assays (200 μM), could not be explained by allosteric activation and must have been due to changes in phosphorylation of AMPK itself. Moore et al (1991) also performed experiments with partially purified AMPK suggesting that, while AMP seemed to have little effect on dephosphorylation, the phosphorylation by the upstream kinase (at that time unidentified) was almost completely dependent upon AMP. This paper provided the first evidence that changes in AMPK phosphorylation might be mediated by nucleotide levels. However, the AMPK preparation used was relatively impure, containing both AMPK and the upstream kinase (AMPK kinase or AMPKK), and further investigation into this mechanism required purification of the individual components of the kinase cascade.

Further support for the idea that AMP promoted phosphorylation of AMPK by the upstream kinase came when Weekes et al (1994) succeeded in separating the AMPK and AMPKK activities. Phosphorylation of AMPK was dependent upon the addition of the upstream kinase and this was stimulated by AMP. It appeared at the time that AMP could allosterically activate the upstream kinase (Hawley et al., 1995). An important breakthrough came when Thr172, a conserved residue within the activation loop of the catalytic subunit, was identified as the target site for the upstream kinase (Hawley et al., 1996). Site-directed mutagenesis later confirmed the necessity of this residue for AMPK activation (Stein et al., 2000). The upstream kinase was also isolated at a far higher purity than that obtained previously, although its identity still remained unclear (Hawley et al., 1996).

Work in *Saccharomyces cerevisiae* identified three kinases (Elm1, Pak1/Sak1 and Tos3) that could activate Snf1 (the yeast homologue of AMPK) by phosphorylating Thr210 (equivalent to Thr172 in mammals) in a partially redundant manner (Hong et al., 2003; Sutherland et al., 2003). The catalytic domains of these kinases are closely related to that of the kinase LKB1 in mammals, and it was reported that LKB1 could phosphorylate and activate bacterially-expressed AMPK (Hong et al., 2003). Subsequently, three groups independently reported that LKB1, acting in a complex with STRAD and MO25, was the major upstream kinase acting on AMPK (Hawley et al., 2003; Woods et al., 2003; Shaw et al., 2004). In contrast with previous suggestions, however, it was demonstrated that LKB1 was not allosterically activated by AMP and that the effects of AMP on AMPK phosphorylation by the upstream kinase were substrate-mediated (Hawley et al., 2003). This view was, however, opposed by Woods et al (2003) who did not detect any effect of AMP on promotion of Thr172

phosphorylation by LKB1. The original observation that the upstream kinase was allosterically activated by AMP was made with less pure preparations and could have been due to contaminants.

Although LKB1 appeared to be the major kinase upstream of AMPK in many different cell types (Sakamoto et al., 2005; Shaw et al., 2005) it was clear that there must be an alternative upstream kinase, as LKB1-null cell lines still retained a basal Thr172 phosphorylation and AMPK activity. Earlier work had demonstrated that Ca^{2+}/calmodulin-dependent protein kinase kinase (CaMKK) purified from pig brain could phosphorylate and activate AMPK in cell-free assays (Hawley et al., 1995). However, the partially characterised upstream kinase (LKB1) being studied at that time was not activated by Ca^{2+} (Hawley et al., 1995). In 2005, it was demonstrated that CaMKKβ, one of the two isoforms of CaMKK, could also act as an upstream kinase for AMPK, with particular relevance in neuronal tissue (Hawley et al., 2005; Hurley et al., 2005; Woods et al., 2005). In contrast to LKB1, however, AMP did not promote Thr172 phosphorylation by CaMKKβ (Hawley et al., 2005). The effect of AMP, therefore, appeared to be specific for LKB1.

Remarkably, AMP was found to elicit a third effect on AMPK, when it was demonstrated that AMP protected the kinase from dephosphorylation by protein phosphatases (Davies et al., 1995). Like the effects on promoting phosphorylation, this was proposed to be substrate-mediated, for a number of reasons: (i) the IC_{50} for the effect of AMP on dephosphorylation was very similar to the EC_{50} for allosteric activation; (ii) the effect was mimicked by AMP analogues that allosterically activated the kinase; (iii) the effect was not specific for a particular phosphatase; and (iv) the

activity of the phosphatases themselves were unaffected by AMP. This was later confirmed when it was demonstrated that mutation of the nucleotide binding sites on the γ subunit abolished AMP-mediated protection against dephosphorylation (Sanders et al., 2007b). The effects of AMP on inhibition of dephosphorylation are therefore substrate-mediated.

A model for AMPK regulation was therefore proposed where AMP elicited three effects:

1. allosteric activation of AMPK;
2. inhibition of dephosphorylation of Thr172 by protein phosphatases;
3. promotion of phosphorylation of Thr172 by LKB1.

This model suggested that AMPK represented an ultrasensitive system in which small increases in the AMP:ATP ratio can produce large changes in the final output (i.e. AMPK activity) (Hardie et al., 1999). Later work, however, cast doubt on mechanism 3 above, proposing instead that the observed increase in net phosphorylation induced by AMP was due to contamination of one of the preparations used with a protein phosphatase (Sanders et al., 2007b).

1.4.2 Crystal structures of AMPK and regulation by ADP

Further insight into the regulation of AMPK came from crystal structures of the complex. In 2007, the crystal structure of a mammalian heterotrimer, consisting of the C-terminal regions of α1 and β2, and full length γ1 with bound AMP, was solved (Xiao et al., 2007). The structure revealed that the two pairs of CBS repeats (CBS1:CBS2 and CBS3:CBS4) in the γ subunit were arranged in a pseudosymmetrical, head-to-head

manner, generating 4 potential nucleotide binding sites in the centre. Sites 1 and 3 appeared to reversibly bind AMP, site 4 appeared to contain a permanently bound, “non-exchangeable”, AMP molecule, while site 2 was empty (in site 2 the key aspartate residue is replaced by an arginine, and this was proposed to prevent nucleotide binding). Thus it appeared that AMPK could bind 3 molecules of AMP in total. Earlier work investigating binding of [^{14}C]AMP to isolated CBS repeats had suggested that AMPK could bind only 2 molecules of AMP (Scott et al., 2004). However, this remains consistent with the new results (Xiao et al., 2007), which suggested that AMP bound in an exchangeable manner at two sites (1 and 3) and in a non-exchangeable manner at a third site (site 4), where [^{14}C]AMP would not be able to displace the endogenous, unlabelled AMP.

In the crystal structure (Xiao et al., 2007) AMP was bound in pockets at the interfaces between the two CBS repeats (CBS1:CBS2 and CBS3:CBS4), making interactions with a number of nearby basic residues. Interestingly, mapping of mutations present in Wolff-Parkinson-White patients onto the γ subunit structure revealed that the majority of these involve amino acids in very close proximity to the AMP binding sites (Xiao et al., 2007). ATP was shown to compete with AMP for binding at sites 1 and 3 but no major differences in conformation were observed between the AMP- and ATP- bound forms of the γ subunit (Xiao et al., 2007). A simple model was proposed whereby, under basal conditions, sites 1 and 3 contain mainly ATP. However, small rises in AMP levels were proposed to progressively replace ATP at these sites, resulting in AMPK activation.

Another important development came when ADP, despite having no effect on allosteric activation of AMPK, was reported (like AMP) to protect the kinase from

dephosphorylation in a substrate-mediated manner (Xiao et al., 2011). Investigation of the binding affinities of the two different binding sites for AMP, ADP and ATP was performed by using coumarin adducts of ADP and ATP as fluorescent reporters, and deriving the binding constants for unlabelled nucleotides by competition assays. The results suggested that the two exchangeable sites, 1 and 3, bound AMP, ADP and free ATP (ATP^{4-}) with similar affinities but that one (thought to be site 1) bound all three nucleotides with ≈30-fold higher affinity (K_D = 2.5, 1.5 and 1.7 μM respectively) than the other (K_D = 80, 50 and 65 μM respectively). Interestingly, the affinities for $Mg.ATP^{2-}$ (K_D = 18 and 230 μM at the two sites) were estimated to be 5- to 10-fold lower than those for free ATP (ATP^{4-}). Since the bulk of cellular ATP is present as the $Mg.ATP^{2-}$ complex, this provides a partial explanation as to how AMP and ADP can compete with the much higher levels of ATP normally present in the cell. Based upon the nucleotide concentrations giving half-maximal effects on allosteric activation and protection against dephosphorylation, and comparing these to the modelled binding affinities, it was proposed that binding of AMP or ADP to the lower affinity binding site, (thought to be site 3), was responsible for protection against dephosphorylation, while binding of AMP at the higher affinity binding site (thought to be site 1) was responsible for allosteric activation of the kinase.

The more complete crystal structure for AMPK that was obtained in this study, consisting of the majority of the α subunit, the C-terminus of the β subunit and the complete γ subunit, provided further clues as to how AMPK was regulated by nucleotide binding (Xiao et al., 2011). In the structure of the active complex (phosphorylated on Thr172) that was determined, the activation loop containing Thr172 could be seen to bind to the C-terminal domains of the α and β subunits, and

this was proposed to limit access of protein phosphatases to Thr172. Another region of the α subunit, called the α hook (part of the extended linker that connects the auto-inhibitory domain and the C-terminal domain) appeared to interact with the molecule of AMP that was bound in site 3. This was proposed to stabilize the association of the α and β C-terminal domains with the activation loop, thus protecting the kinase against dephosphorylation when AMP was bound in site 3. Based on previous structures (lacking the α-hook) that had ATP bound at site 3, it was thought that binding of ATP at site 3 would disrupt α-hook binding to site 3, weakening the association of the α/β C-terminal domains with the activation loop and allowing access of phosphatases to Thr172. Further modelling suggested that ADP binding at site 3 would not disrupt binding of the α-hook, explaining how ADP protects against dephosphorylation, like AMP. This model was supported by mutation of residues in the β subunit that would be predicted to weaken the interaction between the α/β C-terminal domains and the activation loop, which exhibited an increased rate of dephosphorylation. Mutation of residues within the α-hook region also removed the protective effects of AMP and ADP on dephosphorylation.

The proposed model, therefore, was that the γ subunit of mammalian AMPK contains four potential nucleotide binding sites although one (site 2) appears to be unused. Site 4 contains a permanently bound, non-exchangeable, AMP molecule, which is presumably inserted during synthesis and initial folding of the heterotrimeric complex. Sites 1 and 3 reversibly bind AMP, ADP or ATP, with one site (thought to be site 1) having a higher affinity for all three nucleotides. Binding of AMP at site 1 was proposed to cause allosteric activation, while binding of AMP or ADP at site 3 was proposed to cause protection of Thr172 from dephosphorylation. This was thought to be due to

increased association of the α-hook region with AMP or ADP bound in site 3, leading to stabilization of the interaction between the α/β C-terminal domains and the activation loop, restricting access of protein phosphatases to Thr172 (Xiao et al., 2011).

A somewhat different model has also been proposed. The ATP-bound crystal structures outlined above were determined by soaking AMP-bound crystals with ATP. Using this method, no conformational changes were apparent when comparing the AMP- and ATP-bound structures (Xiao et al., 2007). However, when the core of the heterotrimer was crystallized independently with AMP or ATP, small changes in the conformation of the γ subunits were observed (Chen et al., 2012). In contrast to the previous structure (Xiao et al., 2011), ATP was able to bind at site 4 (Chen et al., 2012), which had previously been proposed to be a "non-exchangeable" site for AMP (Xiao et al., 2007). It was also suggested (Chen et al., 2012) that binding of ATP site 4 would preclude binding of any nucleotide at site 3. Mutation of site 1, the proposed allosteric regulatory site, was also reported to have no effect on allosteric activation by AMP, while this was completely abolished by mutation of sites 3 or 4 (Chen et al., 2012). The conformational changes observed upon AMP binding to the γ subunit were most apparent around site 3, and the authors suggest that this conformational change may contribute to the allosteric activation of AMPK by AMP (Chen et al., 2012).

The role of the α-hook region in the α-subunit linker has also been questioned. The α subunit of AMPK contains an auto-inhibitory domain (AID), the removal of which increases kinase activity (Pang et al., 2007). The AID was proposed to comprise three α-helices which bind to the kinase domain, promoting an "open" conformation and reducing kinase activity (Chen et al., 2009). Mutation of key residues at this interface

prevented allosteric activation by AMP and the authors proposed that binding of AMP at the γ subunit disrupts the interaction between the AID and the kinase domain, thus activating AMPK (Chen et al., 2009). Rather than the α-hook interacting with the γ subunit, a small section of the α-subunit linker region, termed the α-RIM (regulatory-subunit-interacting motif) was proposed to be important for transmitting the signal from AMP binding at the γ subunit to the kinase domain (Chen et al., 2013). Mutation of residues at the interface between the α-RIM and the kinase domain abolished allosteric activation by AMP, whereas mutation of the proposed α-hook region had no effect (Chen et al., 2013). However, the authors did not examine the effects of α-RIM mutation on protection against dephosphorylation, an effect lost in α-hook mutants which themselves had no effect on allosteric activation (Xiao et al., 2011).

Interestingly, ADP was originally proposed to be an activating ligand for the HMGR kinase, (Brown et al., 1975) one of the activities that was later renamed as AMPK. However HMGR kinase was later shown to be much more sensitive to AMP (Ferrer et al., 1985) and the original results were attributed to contamination of the crude preparations of HMGR kinase used with adenylate kinase, which would generate AMP from ADP. Prior to the observations that ADP could protect AMPK from dephosphorylation (Xiao et al., 2011), ADP was also reported to bind to the AMPK orthologue from the fission yeast *Schizosaccharomyces pombe* (Jin et al., 2007). Binding occurred at two sites, one of which was equivalent to site 4 and was unique for ADP binding, while the other (equivalent to site 3) was also able to accept either AMP or ATP. However, the functional significance of these results remains unknown, because the regulation of the *S. pombe* enzyme by adenine nucleotides has never been studied. The SNF1 complex, the AMPK orthologue from budding yeast (*S. cerevisiae*,

which is only very distantly related to *S. pombe*) is not allosterically activated by AMP (Mitchelhill et al., 1994; Woods et al., 1994). However, activation of the complex in intact cells starved for glucose, which is due to phosphorylation at Thr210 (equivalent to Thr172 on AMPK) correlated with large decreases in cellular ATP and increases in ADP and AMP (Wilson et al., 1996). This was later demonstrated to be due to a decreased rate of dephosphorylation of Thr210 by protein phosphatases, rather than an increase in the rate of phosphorylation by upstream kinases (Rubenstein et al., 2008). The signal for this remained unclear, as AMP was shown to have no effect on dephosphorylation of the SNF1 complex (Sanders et al., 2007b). It has recently been demonstrated that dephosphorylation of the SNF1 complex was regulated by ADP, rather than AMP (Mayer et al., 2011). The mechanism for this seems to be similar to that in the mammalian enzyme, with ADP promoting association of the activation loop with the Snf1 and Gal83 subunits (equivalent to the α and β subunits in mammals) and preventing access of phosphatases. The mechanism is not identical, however, because AMP has no effect on dephosphorylation of Thr210.

1.4.3 Promotion of phosphorylation by AMP and ADP

Although a proposed aspect of the original regulatory mechanism for AMPK by AMP (Moore et al., 1991), the role of AMP to promote phosphorylation of Thr172 had been challenged, as discussed above (Sanders et al., 2007b). However, work from the Kemp laboratory suggested that Thr172 phosphorylation and activation of AMPK could indeed be promoted by AMP, although only when the β subunit was myristoylated on Gly2 (Oakhill et al., 2010). This effect was demonstrated for both LKB1 and CaMKKβ, in contrast to the previous work from Hawley et al (2005) where no effect of AMP on phosphorylation by CaMKKβ had been observed. Mutation of Gly2 had no effect on

either allosteric activation of AMPK or the ability of AMP to protect against dephosphorylation. During attempts to define which nucleotide binding site was responsible for promotion of phosphorylation, mutation of the conserved aspartate residues in sites 1, 3, and 4 all resulted in a reduction of both promotion of phosphorylation and allosteric activation by AMP. This suggests that there is a close interaction between the three nucleotide binding sites, casting doubt on the proposals that a specific effect can be attributed to a particular binding site. Positive co-operativity of binding of AMP or ATP to a construct containing all 4 CBS motifs of AMPK-γ2 had previously been observed (Scott et al., 2004), although this has not been reported in other studies.

The myristoyl group of the β subunit was known to promote AMPK association with cellular membranes (Warden et al., 2001) and a number of AMPK substrates are membrane-associated, including ACC2 and HMGR. Glucose deprivation induced Thr172 phosphorylation and membrane association of wild-type AMPK, with the effect being lost with the non-myristoylatable G2A mutant (Oakhill et al., 2010). A myristoyl-switch mechanism for AMPK regulation was proposed, similar to that of other proteins, such as recoverin (Ames et al., 1997). In the model for AMPK, high ATP levels result in the myristoyl group associating with the kinase domain and preventing access of upstream kinases to Thr172. In response to cellular stresses, AMP replaces ATP at the γ subunit and causes a release of the myristoyl group, promoting membrane association (thus targeting AMPK to its substrates) and also promoting Thr172 phosphorylation by LKB1 or CaMKKβ. The continued presence of AMP also causes allosteric activation and protects against dephosphorylation. Rising ATP levels reverses the switch and inactivates AMPK (Oakhill et al., 2010).

In addition to AMP, ADP was also reported to promote phosphorylation of AMPK by CaMKKβ (Oakhill et al., 2011). The concentrations of AMP (73 μM) and ADP (56 μM) giving half-maximal effects on the promotion of phosphorylation by CaMKKβ were similar. The promotion of phosphorylation by ADP when LKB1 was the upstream kinase was not investigated. Mutation of the aspartate residues in nucleotide binding sites 1 and 3 (but not 4) prevented ADP from promoting Thr172 phosphorylation, as did use of a truncated α subunit, rather than an αβγ heterotrimer. The effect was also lost with a non-myristoylated G2A mutant of the β subunit. This suggested that β subunit myristoylation, and nucleotide binding sites 1 and 3, were required for promotion of Thr172 phosphorylation. The current model for AMPK regulation is shown in Fig. 1.3.

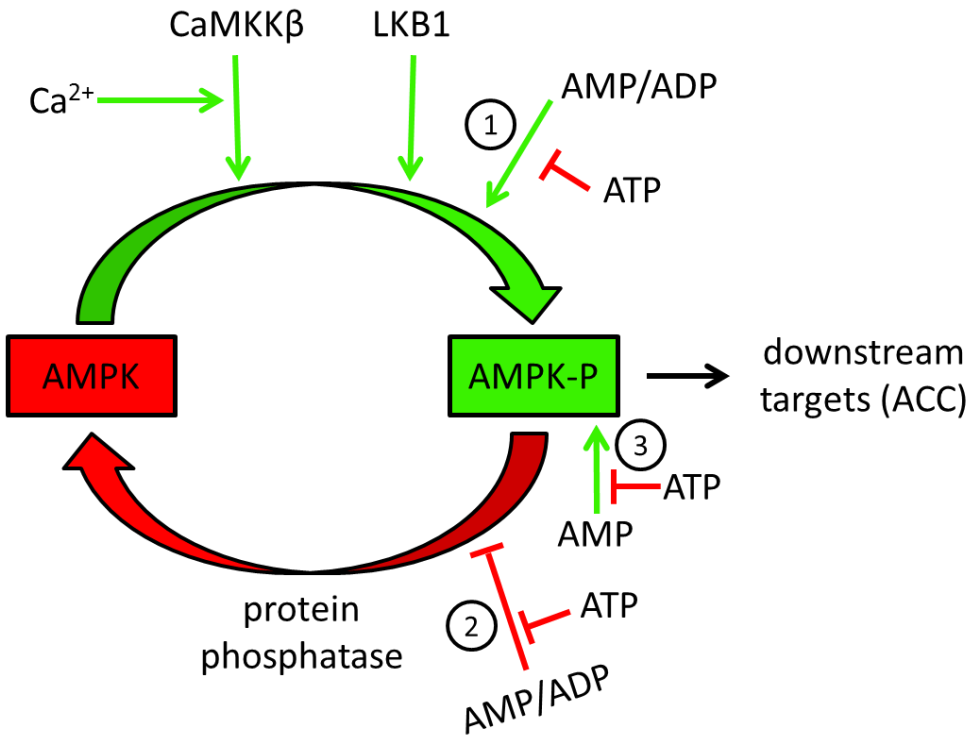

Figure 1.3: Regulation of AMPK
Proposed mechanism by which AMP and ADP regulate AMPK, based on Xiao et al (2011) and Oakhill et al (2011): (1) binding of AMP/ADP to AMPK promotes Thr172 phosphorylation; (2) binding of AMP or ADP protect Thr172 against dephosphorylation by protein phosphatases; (3) binding of AMP causes allosteric activation of AMPK. All three effects are antagonized by binding of ATP.

1.5 Activators of AMPK

AMPK is activated in mammalian cells primarily during energetic stresses that increase the AMP:ATP and ADP:ATP ratios in the cell. This can occur either by increasing ATP consumption (e.g. muscle contraction during exercise) or by decreasing ATP production (e.g. ischaemia or hypoxia). AMPK is also activated by a large number of drugs and xenobiotics (Hardie et al., 2012) and hormones (Kahn et al., 2005). The diverse mechanisms available to activate AMPK are discussed below.

1.5.1 Activation of AMPK by exercise

The classical, physiological mode of AMPK activation is via muscle contraction during exercise, observed in both rodents (Winder and Hardie, 1996) and humans (Wojtaszewski et al., 2000) in an intensity-dependent manner. Both AICAR (discussed below) and contraction caused an increase in muscle glucose uptake coupled with AMPK activation (Hayashi et al., 1998). The activation of AMPK in response to muscle contraction, and the associated glucose uptake, is dependent upon LKB1 (Sakamoto et al., 2005). The AMPK-related kinases, which are also targets of LKB1, are not activated by muscle contraction, suggesting that the LKB1-dependent effects on glucose uptake in skeletal muscle are mediated by AMPK (Sakamoto et al., 2004). AMPK may also be responsible for other beneficial effects of exercise, including increased mitochondrial biogenesis (Zong et al., 2002) and fatty acid oxidation (Aschenbach et al., 2004).

1.5.2 Activation of AMPK by other metabolic stresses

In addition to exercise, AMPK is regulated by other metabolic stresses, such as glucose deprivation (Salt et al., 1998). Although total glucose withdrawal from cells would be unlikely to happen *in vivo*, specialized glucose-sensing cells in the pancreas (Salt et al., 1998; da Silva Xavier et al., 2003; Beall et al., 2010) and the hypothalamus (Minokoshi et al., 2004; Beall et al., 2012) respond to glucose levels and regulate hormone secretion in an AMPK-dependent manner. Hypoxia, by inhibiting mitochondrial function and decreasing ATP levels, also activates AMPK (Evans et al., 2005). Once activated, AMPK phosphorylates and inhibits K^+ channels in carotid body type I cells (Ross et al., 2011; Wyatt et al., 2007), resulting in membrane depolarization, increased intracellular calcium levels and neurosecretion. The secreted neurotransmitters increase afferent discharge to the central nervous system and increase breathing.

1.5.3 Activation of AMPK by hormones

AMPK is regulated by a range of hormones secreted from adipocytes, termed adipokines (Kahn et al., 2005). Leptin, produced in proportion to the fat levels of the body and generally acting as an appetite suppressor, increases fatty acid oxidation and glucose uptake in skeletal muscle in an AMPK-dependent manner (Minokoshi et al., 2002). Leptin has a distinct role in the hypothalamus, where it decreases AMPK activity and thus acts to suppresses appetite (Minokoshi et al., 2004). AMPK, as well as dictating local responses to energy depletion, may thus also play a key role in regulating global energy intake via changes in appetite.

Adiponectin, released by adipocytes in a manner inversely proportional to body fat, also regulates AMPK in the hypothalamus, although in this case it activates the kinase

to promote feeding (Kubota et al., 2007). Similarly, the hormone ghrelin also increases AMPK activity in the hypothalamus (Andersson et al., 2004) in a CaMKKβ-dependent manner (Anderson et al., 2008). The activation of AMPK by ghrelin in response to hunger is proposed to form part of a positive feedback loop promoting Ca^{2+} release from intracellular stores, maintaining AMPK activity and release of the appetite-stimulating peptides AGRP and NYP. This imparts a form of memory to the circuit, with the circuit being reset by leptin released from adipocytes (Yang et al., 2011).

1.5.4 Activation of AMPK by drugs and xenobiotics

AMPK is activated by a diverse range of compounds (Fig 1.4), acting by a variety of mechanisms. Key to the understanding of the mode of action of these compounds was the development of HEK293 cells expressing an AMP-insensitive mutant of the AMPK-γ2 subunit, the R531G mutant (Hawley et al., 2010). This residue, which is mutated in some cases of WPW syndrome, is located in CBS repeat 4 and its mutation to glycine disrupts nucleotide binding to the γ subunit, rendering the kinase insensitive to changes in nucleotide levels. Compounds that activated complexes containing both wild-type γ2 and the R531G mutant of γ2 are clearly operating through AMP-independent mechanisms, whereas those that activated only wild-type γ2 complexes are dependent upon changes in nucleotides (Hawley et al., 2010). The compounds that activated the wild-type cells only were also demonstrated to increase the ADP:ATP ratio and to alter mitochondrial function, both hallmarks of disrupted energy status (Hawley et al., 2010).

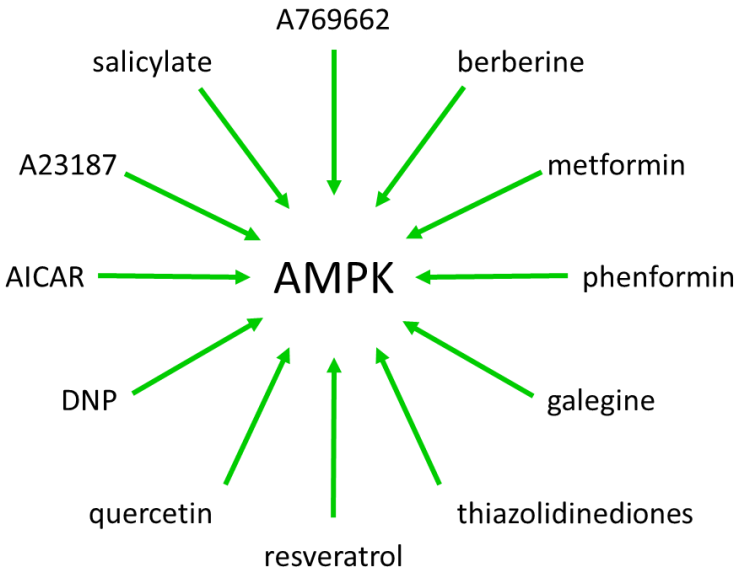

Figure 1.4: Drugs and xenobiotics acting on AMPK
A wide range of drugs and xenobiotics activate AMPK, some of which are shown here.

1.5.4.1 AICAR

The first compound identified to activate AMPK in intact cells and *in vivo* was the nucleoside 5-aminoimidazole-4-carboxamide riboside (AICAR). AICAR enters the cell where it is converted to the monophosphate form 5-aminoimidazole-4-carboxamide ribonucleoside monophosphate (ZMP) (Sabina et al., 1985), which acts as an AMP-mimetic and activates AMPK both by allosteric activation and protection against Thr172 dephosphorylation (Corton et al., 1995). As expected, AICAR had no effect on the AMP-insensitive R531G-γ2 cells (Hawley et al., 2010). AICAR has been used extensively to characterize the downstream effects of AMPK and beneficial effects related with this in a number of pathological conditions. AICAR can reverse some of the defects associated with the metabolic syndrome and diabetes, such as improved glucose tolerance and uptake, in a variety of diabetic animal models, including the *ob/ob* mouse (Song et al., 2002) and the *fa/fa* rat (Bergeron et al., 2001). In addition, AICAR treatment can also induce the expression of genes linked to oxidative

metabolism and increased the running endurance of mice independently of any training (Narkar et al., 2008). Given these benefits, AICAR has been suspected to be used as a doping agent by professional cyclists (Benkimoun, 2009) and subsequently banned by anti-doping agencies (Thomas et al., 2010). As an AMP mimetic, AICAR can also regulate other AMP-sensitive enzymes. AICAR inhibits fructose-1,6-bisphosphatase to reduce gluconeogenesis (Vincent et al., 1991) and stimulates glycogen phosphorylase to increase glycogenolysis (Longnus et al., 2003). Thus AICAR, whilst a useful research tool for investigating AMPK, may be unsuitable for clinical use given its lack of specificity and poor oral availability.

1.5.4.2 A769662 and salicylate

A769662, identified in a high throughput cell-free screen by Abbott laboratories, is a direct activator of AMPK (Cool et al., 2006). A769662 increases AMPK activity both by allosteric activation and by protecting Thr172 against dephosphorylation (Göransson et al., 2007; Sanders et al., 2007a). Unlike AMP, A769662 activation does not require the AMP-binding sites on the γ subunit, but appears to bind to a region containing the Ser108 residue of the β subunit (Sanders et al., 2007a). The identity of the β subunit isoform also appears to be important for activation by A769662, as the compound was demonstrated to primarily activate complexes containing β1, although activation of β2 complexes is possible at high concentrations of the compound (Scott et al., 2008; Hawley et al., 2012). Treatment of *ob/ob* mice with A769662 caused a reduction in plasma glucose and triglyceride levels, as well as decreased expression of gluconeogenic and lipogenic genes (Cool et al., 2006). A769662 has poor oral availability (Cool et al., 2006) and may possess AMPK-independent functions (Moreno et al., 2008), limiting its use as a therapeutic agent.

Salicylate, a compound present in willow bark but also produced by other plants as a defence mechanism in response to infection, has been used in traditional medicine for millennia. For current medicinal use, it has been replaced by aspirin or by salsalate, both of which are broken down to form salicylate following oral administration. Both aspirin and salicylate have shown promise for the treatment of type 2 diabetes (Goldfine et al., 2010; Hundal et al., 2002). Although salicylate inhibits other targets, including prostaglandin synthesis by cyclo-oxygenases (Vane, 1971) and IKKβ (Yin et al., 1998), it has recently been demonstrated to directly activate AMPK, independent of changes in cellular energy (Hawley et al., 2012). The binding site of salicylate appears to overlap with that of A769662, as they both require the Ser108 site of the β-subunit and activate β2-containing complexes poorly. Additionally, salicylate can antagonize allosteric activation by A769662, suggesting that they are competing for binding at the same site. Salicylate, like A769662, allosterically activates AMPK (albeit to a small extent) and protects Thr172 from dephosphorylation by protein phosphatases. Salicylate treatment can alter *in vivo* metabolism, causing a switch from carbohydrate to fat utilization and decreased serum levels of fatty acids, with both effects requiring the presence of the β1 isoform of AMPK (Hawley et al., 2012). However, some of the beneficial effects of salicylate, including improved glucose tolerance, occurred independently of AMPK, suggesting that other pathways are also important in dictating the response to salicylate. In addition to the changes in metabolic function, it is also possible that AMPK is mediating some of the other benefits attributed to aspirin, such as anti-inflammatory effects and protection against cancer (Rothwell et al., 2011).

1.5.4.3 Calcium

CaMKKβ, one of the Thr172 kinases, is activated in response to rising levels of calcium (Hawley et al., 2005; Hurley et al., 2005; Woods et al., 2005). Although CaMKKβ is most highly expressed in neural tissue, there is evidence that the CaMKKβ-AMPK pathway operates in other tissues, including in endothelial cells treated with thrombin (Stahmann et al., 2006) and in T cells in response to antigen (Tamás et al., 2006). Pharmacological agents that increase intracellular calcium are potent AMPK activators, acting independently of LKB1 and changes in nucleotide levels. These include the calcium ionophores A23187 (Hawley et al., 2010) and ionomycin (Hurley et al., 2005) as well as caffeine (Jensen et al., 2007).

1.5.4.4 Metformin, phenformin and galegine

Metformin is one of the most widely prescribed drugs in the world, being the first-choice treatment for type 2 diabetes (Rena et al., 2013). Metformin, along with the related compound phenformin, is derived from galegine, a natural product of *Galega officianalis* (French lilac, also known as goat's rue) (Hardie et al., 2012). Extracts of this plant have been used for centuries to treat symptoms of diabetes.

Metformin was shown to reduce hepatic glucose production in type 2 diabetics by reducing gluconeogenesis (Hundal et al., 2000) but the molecular mechanism was unclear. Metformin was demonstrated to activate AMPK in intact cells, resulting in decreased glucose production and increased glucose uptake (Zhou et al., 2001) and both phenformin and galegine are potent AMPK activators (Hawley et al., 2003; Mooney et al., 2008). Metformin had no effect on *in vitro* AMPK activity, suggesting

that the effects were indirect (Hawley et al., 2002). A candidate for this was changes in cellular nucleotide levels, as metformin had been shown to inhibit complex I of the mitochondrial chain (El-Mir et al., 2000; Owen et al., 2000) and this was confirmed using the R531G-γ2 mutant cell line (Hawley et al., 2010). A similar mechanism of action was demonstrated for both phenformin and galegine (Hawley et al., 2010). The effects of metformin appeared to be AMPK-dependent as they were reversed by the addition of compound C, an AMPK inhibitor (Zhou et al., 2001). Compound C, however, is a relatively non-specific inhibitor and may have several off-target effects (Bain et al., 2007). Further support for AMPK as the key mediator of the beneficial effects of metformin came from studies where LKB1 has been genetically deleted from the liver of adult mice (Shaw et al., 2005). These mice had hyperglycaemia and impaired glucose tolerance as well as increased expression of gluconeogenic and lipogenic genes. Metformin, whilst reducing the blood glucose of wild-type mice or *ob/ob* mice, had no effect on mice which had lost expression of LKB1 in the liver (Shaw et al., 2005).

Controversy over the role of AMPK remains, as mice with both catalytic subunits of AMPK deleted from the liver displayed normal responses to metformin (Foretz et al., 2010). In the same study, hepatocytes from mice lacking liver LKB1 also displayed normal responses to metformin (Foretz et al., 2010). A possible explanation of this is that other AMP-sensitive enzymes, such as fructose-1,6,-bisphosphatase, exist and treatment with metformin could reduce hepatic glucose production through these pathways (Hardie et al., 2012). In addition, metformin was demonstrated to inhibit TORC1 signalling (Kalender et al., 2010) and glucose uptake independently of AMPK in skeletal muscle (Kalender et al., 2010; Turban et al., 2012). One recent study has proposed that AMP produced in response to metformin inhibits adenylate cyclase,

reducing cAMP levels and PKA activity, blocking glucagon-mediated hepatic glucose output in an AMPK-independent manner (Miller et al., 2013).

However, a recent study from the Steinberg laboratory has suggested that AMPK does play a major role in the response to metformin (Fullerton et al., 2013). Mice with alanine knock-in mutations at the site phosphorylated by AMPK in both ACC1 (Ser79) and ACC2 (Ser212, equivalent to Ser79), termed double knock-in (dKI), were generated and displayed increased hepatic lipogenesis and decreased fatty oxidation compared to wild-type mice, resulting in elevated hepatic lipid content. Excess lipid storage is associated with insulin resistance and the dKI mice were found to be hyperglycaemic, hyperinsulinemic, glucose intolerant and insulin resistant, but not obese. In mice made obese by a high-fat diet (HFD), long-term treatment with metformin reduced hepatic lipid content and improved insulin-sensitivity in wild-type, but not dKI, mice. While Foretz (2010) and Miller (2013) reported AMPK-independent effects of metformin, these were short-term treatments and were performed under fasting conditions in the absence of insulin stimulation. It seems that phosphorylation and inhibition of ACC by AMPK plays a crucial role in mediating the long-term beneficial effects of metformin in type 2 diabetes, which are likely due to insulin-sensitization (Fullerton et al., 2013).

1.5.4.5 Thiazolidinediones

Another class of anti-diabetic drugs, the thiazolidinediones (TZDs), including troglitazone (LeBrasseur et al., 2006), pioglitazone (Saha et al., 2004) and rosiglitazone (Fryer et al., 2002) increase AMPK activity. TZDs are known to bind to and activate the transcription factor PPAR-γ. One effect of this is to trigger release of adiponectin, an insulin-sensitizing hormone which is itself an activator of AMPK (Yamauchi et al.,

2002). The improvements in glucose tolerance associated with adiponectin are AMPK-dependent (Yamauchi et al., 2002). Transcriptional changes and increased adiponectin release via PPAR-γ action are likely to be the main method by which the TZDs elicit their beneficial effects on diabetes, because knocking out adiponectin abolished any beneficial effects of the TZDs (Kubota et al., 2006). However, the TZDs also acutely activate AMPK by disrupting mitochondrial function (Brunmair et al., 2004; Fryer et al., 2002; Hawley et al., 2010) and caused rapid glucose uptake and fatty acid oxidation that are unlikely to be explained by changes in transcription and could be AMPK-dependent (LeBrasseur et al., 2006).

1.5.4.6 Other plant compounds

There are a large number of natural plant products that can increase AMPK activity, many of which, like salicylate, have been used in traditional medicine. These include resveratrol, present in red wine and grapes (Baur et al., 2006), berberine, from Chinese Goldthread (Turner et al., 2008), and quercetin, present in a number of fruits and vegetables (Ahn et al., 2008). How these diverse, structurally-unrelated, compounds were activating the kinase was, in many cases, unclear although some studies had suggested that it could be due to disruption of mitochondrial function (Turner et al., 2008). Use of the R531G-γ2 cell line demonstrated that most of these compounds were acting in an AMP-dependent manner, since they did not activate the AMP-insensitive R531G mutant (Hawley et al., 2010). In addition, the classical mitochondrial poisons dinitrophenol (DNP) and oligomycin operated in a similar manner.

1.6 Processes regulated by AMPK

Although first characterized as a regulator of lipid metabolism, AMPK is now thought to act as the major energy sensor of the eukaryotic cell and, once activated, regulates a wide variety of both metabolic and non-metabolic pathways (Fig. 1.5). AMPK inhibits anabolic pathways and activates catabolic pathways to protect the cell from further energy depletion and to redress the energy imbalance.

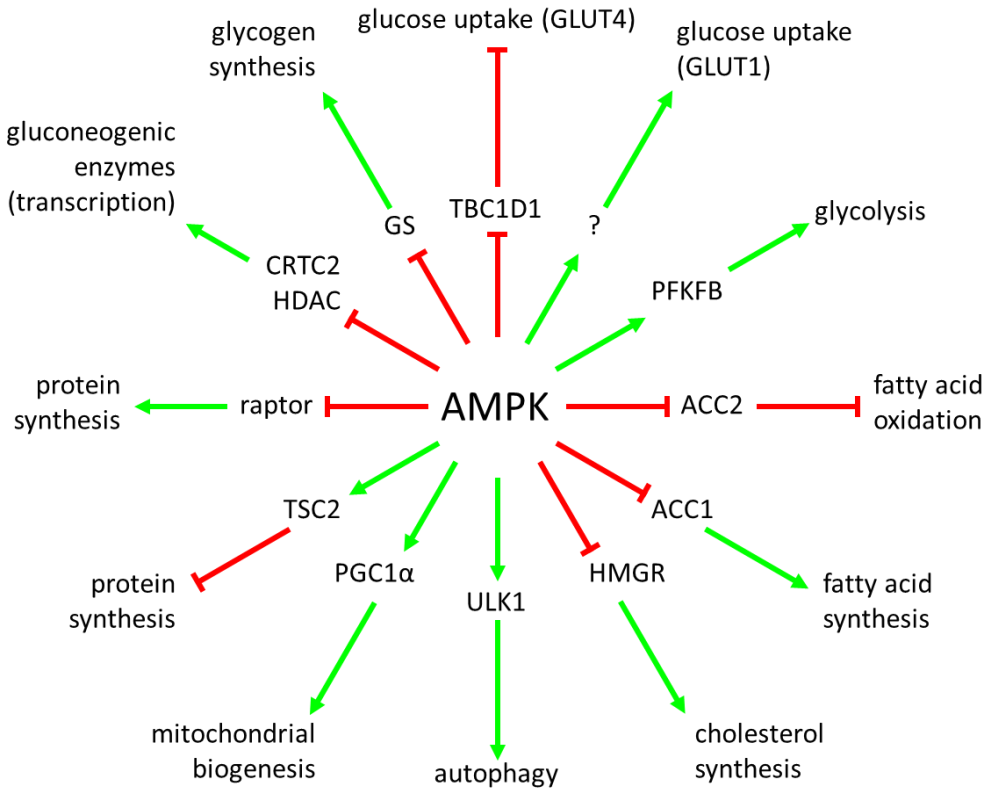

Figure 1.5: Processes regulated by AMPK
AMPK, in response to changes in energy levels, acts to redress the cellular energy balance by regulating a wide range of catabolic and anabolic pathways. Figure adapted from Hardie et al., 2012.

1.6.1 Carbohydrate and lipid metabolism

1.6.1.1 Lipid metabolism

ACC and HMGR were the first two substrates identified for AMPK (Beg et al., 1973; Carlson and Kim, 1973). ACC converts acetyl-CoA to malonyl-CoA, the first committed step in fatty acid synthesis. AMPK phosphorylates ACC1 on Ser79, reducing its catalytic activity thus inhibiting fatty acid synthesis (Davies et al., 1990, 1992). A second isoform of ACC, ACC2, is also phosphorylated and inactivated by AMPK (Winder et al., 1997). ACC2 is associated with mitochondrial membranes and is thought to increase malonyl-CoA levels at the mitochondrial surface (Abu-Elheiga et al., 2000). Malonyl-CoA is an inhibitor of carnitine:palmitoyl-CoA transferase 1 (CPT1), which mediates the entry of long-chain fatty acids into the mitochondria for fatty acid oxidation. Inhibition of ACC2 activity by AMPK phosphorylation therefore reduces the levels of malonyl-CoA and increases fatty acid oxidation (Merrill et al., 1997). It is likely, however, that there is redundancy between the two isoforms of ACC. Mice with alanine knock-in mutations at the site phosphorylated by AMPK in either ACC1 or ACC2 displayed normal hepatic lipogenesis and fatty acid oxidation compared with wild-type mice (Fullerton et al., 2013). In contrast, mice with alanine knock-in mutations at both sites (the dKI mice discussed in Section 1.5.4.4) displayed increased hepatic lipogenesis and reduced fatty acid oxidation (Fullerton et al., 2013), suggesting that the pools of malonyl-CoA generated by ACC1 and ACC2 are not separate.

AMPK also phosphorylates and inactivates HMGR, a key enzyme in the cholesterol synthesis pathway (Carling et al., 1987; Clarke and Hardie, 1990). Activation of AMPK therefore reduces fatty acid synthesis and cholesterol synthesis, whilst increasing fatty acid oxidation.

1.6.1.2 Glucose and glycogen

AMPK can increase the rate of glucose uptake via glucose transporter type 4 (GLUT4). Glucose uptake is mediated by increased translocation of GLUT4 from intracellular vesicles to the plasma membrane; this is considered a rate-limiting step (Steinberg and Kemp, 2009). Fusion of these storage vesicles with the plasma membrane requires members of the Rab family of GTPases to be in their GTP bound state. These Rabs are held in their inactive state by the action of Rab GTPase activating proteins (GAPs), including TBC1D4 (also known as Akt substrate of 160 kDa, AS160) and TBC1D1, which associate with GLUT4 vesicles. Akt (also known as PKB) phosphorylates TBC1D4 in response to insulin, and AMPK, in response to muscle contraction, phosphorylates TBC1D1, with phosphorylation at these sites inducing 14-3-3 binding (Chen et al., 2008). Phosphorylation of TBC1D4 at the PKB site is important in regulating insulin-mediated glucose uptake (Chen et al., 2011). By analogy with TBC1D4, it seems likely that AMPK phosphorylation of TBC1D1 and subsequent 14-3-3 binding would inhibit the GAP activity of TBC1D1, resulting in GTP-loaded Rabs and increased fusion of GLUT4 vesicles with the plasma membrane (O'Neill, 2013). Recent work has also proposed a role for PIKfyve (FYVE domain-containing phosphatidylinositol 3-phosphate 5-kinase) in mediating exercise-induced glucose uptake. PIKfyve catalyses the production of phosphatidylinositol 3,5-bisphosphate (PtdIns(3,5)P_2), an important regulator of vesicle trafficking. Inhibition of PIKfyve catalytic activity reduced glucose uptake and AMPK-mediated phosphorylation of PIKfyve promoted its association with endosomal vesicles (Liu et al., 2013). Interestingly, PKB phosphorylates the same site on PIKfyve as AMPK, and this is implicated in controlling insulin-mediated glucose uptake (Berwick et al., 2004).

Whether AMPK is the only regulator of contraction-mediated glucose uptake is not completely clear. The loss of AMPK-α2 in mouse muscle abolished the effects of AICAR on glucose uptake, but not the effects of contraction, while the loss of AMPK-α1 had no effect (Jørgensen et al., 2004b). In contrast, the loss of LKB1 from mouse muscle completely abolished the effects of AICAR on glucose uptake, while the effects of contraction were greatly reduced although not completely abolished (Sakamoto et al., 2005). Interestingly, muscle-specific deletion of the AMPK-β1 and -β2 subunits in mice was reported to have no effect on insulin-mediated glucose uptake, but completely prevented any contraction-mediated increases and had a severe effect on the ability of the mice to exercise (O'Neill et al., 2011). Although these latter results suggest that activation of AMPK may be entirely responsible for contraction-stimulated glucose uptake in muscle, the effects of knocking out both catalytic subunits (α1 and α2) in muscle have not yet been reported.

AMPK also increases the activity of the glucose transporter GLUT1. While the molecular mechanism for this is not currently known it appears to involve activation of GLUT1 already located at the plasma membrane, rather than its translocation to the membrane (Barnes et al., 2002).

AMPK down-regulates the expression of a number of gluconeogenic genes, including glucose-6-phosphatase, by controlling the activity of transcription factors, including CRTC2 (CREB-regulated transcription co-activator 2) (Koo et al., 2005). AMPK has also been reported to inhibit the function of class IIa histone deacetylases by promoting their nuclear exclusion (Mihaylova et al., 2011). These deacetylates act on FOXO transcription factors and promote the expression of gluconeogenic genes.

AMPK phosphorylates and inhibits glycogen synthase, causing decreased rates of glycogen synthesis (Jørgensen et al., 2004a). One function of the carbohydrate-binding module of the β subunit may be to target AMPK to glycogen synthase. AMPK can also, in certain contexts, increase the rate of glycolysis (the conversion of glucose into pyruvate), by phosphorylating and activating the PFKFB2 and PFKB3 isoforms of 6-phosphofructo-2-kinase/fructose-2,6-bisphosphatase (Marsin et al., 2000, 2002). This enzyme catalyses the generation of fructose-2,6-bisphosphate, an allosteric activator of the glycolytic enzyme phosphofructokinase.

1.6.2 Cell growth and protein synthesis

Cell growth and the production of new proteins consume large amounts of cellular energy. A key regulator of these processes, the mTOR complex 1 (mTORC1, discussed further in section 1.8), controls protein synthesis and cell growth in response to nutrients and growth factors (Zoncu et al., 2011b). In addition, the activity of mTORC1 is also sensitive to the energy status of the cell, which it senses indirectly via the LKB1-AMPK pathway. AMPK phosphorylates and activates TSC1/2, an upstream negative regulator of mTORC1, and this plays a key role in determining the cellular response to energy starvation (Inoki et al., 2003b). Interestingly, cells lacking TSC2 still respond to energy stress, although less so than wild-type cells, which suggested that additional AMPK targets may be involved in regulating mTORC1 activity (Hahn-Windgassen et al., 2005; Gwinn et al., 2008). It was subsequently demonstrated that AMPK directly influences the mTORC1 complex by phosphorylating the Raptor subunit, causing binding of 14-3-3 proteins and inhibition of mTOR catalytic activity (Gwinn et al., 2008). Mutation of the AMPK phosphorylation sites on Raptor prevents TSC2/p53 null cells from undergoing growth arrest in response to AICAR, as well as sensitizing cells to

apoptosis in response to energy stress (Gwinn et al., 2008). AMPK therefore couples cellular energy status to protein synthesis.

1.6.3 Autophagy and mitochondrial biogenesis

Autophagy is the controlled degradation of damaged or dysfunctional cellular components, such as organelles or proteins, in order to recycle valuable components such as amino acids and lipids. It is a key survival response during times of stress or starvation. Autophagy involves the formation of large vesicles that engulf cytoplasmic components, which then fuse with lysosomes to form autophagosomes. The contents of the autophagosome are digested by lysosomal hydrolases, providing a source of amino acids and nutrients when these are unavailable from elsewhere (reviewed in Mizushima et al., 2008). In yeast, autophagosomal formation is initiated by a conserved complex containing the kinase Atg1 and its subunits Atg13 and Atg17. The mammalian orthologue of Atg1, ULK1, is phosphorylated and activated by AMPK, resulting in increased autophagy and mitophagy (Egan et al., 2011). Mitophagy is a special form of autophagy by which dysfunctional mitochondria are degraded, which is important for mitochondrial turnover. In cells lacking functional ULK1 or lacking the AMPK phosphorylation site, aberrant accumulation of mitochondria was observed, along with impaired mitochondrial function (Egan et al., 2011). AMPK, by increasing autophagy, maintains the energy status of the cell under times of stress and, by increasing mitophagy, acts to maintain the health and functionality of the mitochondrial population.

Additionally, AMPK has also been proposed to increase the rate of mitochondrial biogenesis. Administration of AICAR to rats caused increased expression of

mitochondrial genes (Winder et al., 2000) and the loss of AMPK activity in muscle caused a reduction in mitochondrial content and exercise endurance (O'Neill et al., 2011). The mechanism for this may involve phosphorylation of peroxisome proliferator-activated receptor-γ co-activator 1α (PGC1α), a co-activator that enhances the activity of transcription factors acting on mitochondrial genes, including cytochrome *c*, a component of the electron transport chain (Jäger et al., 2007).

1.6.4 Membrane excitability

As discussed in section 1.5.2, AMPK responds to hypoxia and phosphorylates and inhibits membrane-bound ion channels, resulting in changes to membrane excitability in the carotid body and increases in respiration. Additionally, AMPK phosphorylates the voltage-gated K^+ channel Kv2.1, a regulator of membrane excitability and action potential firing frequency in central neurons. Phosphorylation by AMPK causes hyperpolarizing shifts in the current-voltage relationship for channel activation, causing channels to become less sensitive to membrane depolarization (Ikematsu et al., 2011). Treatment of cultured rat neurons with A769662, or the introduction of active AMPK, reduced the frequency of action potential firing (Ikematsu et al., 2011). The firing of action potentials is a major source of energy consumption in the brain and, by reducing their rate of firing, AMPK would act to conserve energy.

1.7 LKB1

1.7.1 Discovery of LKB1

Peutz-Jeghers syndrome (PJS) is an inherited, autosomal dominant, condition characterized by the formation of benign hamartomatous polyps, particularly in the gastrointestinal tract. The syndrome was first described in 1921 by Johannes Peutz and

further characterized by Harold Jeghers in the 1940s. PJS is a rare disease, with incidences estimated from 1 in 10,000 to 1 in 120,000 births (Alessi et al., 2006)

Genetic linkage analysis revealed that PJS was caused by mutation of the *LKB1* gene (Hemminki et al., 1998). Multiple mutations in LKB1 have been identified from PJS patients, the majority of which cause truncations in the kinase domain and should therefore ablate catalytic activity. A number of mutations have also been observed in the C-terminal tail of LKB1, suggesting a possible regulatory role for this region. No point mutations in the N-terminal non-catalytic region have been identified in PJS, suggesting that this region does not regulate LKB1 function (Alessi et al., 2006).

1.7.2 LKB1 as a tumour suppressor

Early work demonstrated that expression of LKB1 in HeLa and G361 cells, which were derived from human cancers (cervical and skin melanoma respectively) and lack LKB1, resulted in a cell cycle arrest. This effect was lost with catalytically-inactive LKB1 mutants and it was reasoned that the intrinsic kinase activity was necessary to halt cell division (Tiainen et al., 1999). Additionally, sufferers of PJS have a greatly increased risk of developing malignant tumours in multiple tissues (Giardiello et al., 2000). As PJS patients have mutations in the *LKB1* gene and are predisposed to cancers this, together with the effects of LKB1 on the cell cycle, suggested that LKB1 was a classical tumour suppressor and support comes from the observation that sporadic mutations in the *LKB1* gene are present in 30% of non-small cell lung cancers (Sanchez-Cespedes et al., 2002), 20% of invasive cervical cancers (Wingo et al., 2009) and 10% of melanomas (Liu et al., 2012).

1.7.3 The LKB1 complex

LKB1 exists as a heterotrimeric complex with two other proteins, STRAD (Ste-20 related adaptor) and MO25 (mouse protein 25) (Alessi et al., 2006). There are two closely related isoforms of STRAD, α and β, which possess high sequence similarity to protein kinases but lacking several crucial residues required for catalytic function. They have therefore been termed *pseudokinases*. Like STRAD, there exist two closely related isoforms of MO25, again termed α and β. LKB1, STRAD and MO25 complexes can be isolated with the three members at equal stoichiometry, suggesting they are tightly associated and form a 1:1:1 ratio in the cell (Boudeau et al., 2003a), later confirmed when the crystal structure of the complex was determined (Zeqiraj et al., 2009a)

One manner in which the complex can be regulated is through changes in subcellular localization. Cytoplasmic localization of LKB1 appears to be important for its function, as mutant forms of LKB1 found in PJS patients localize exclusively in the nucleus and are unable to suppress cell growth (Boudeau et al., 2003b). LKB1 possesses a nuclear localization sequence in the N-terminus, and overexpression of LKB1 alone resulted in the kinase localizing to the nucleus, while mutation of this sequence resulted in distribution throughout the cell (Smith et al., 1999). Co-expression of LKB1 and STRAD targeted the majority of LKB1 to the cytoplasm, although a significant amount remained nuclear, while expression of LKB1, STRAD and MO25 fully localized LKB1 to the cytoplasm.

Binding of both STRAD and MO25 is also required for the full catalytic activity of LKB1 (Hawley et al., 2003). The crystal structure of an LKB1:STRAD:MO25 complex revealed that STRAD and MO25 stabilized the active loop of LKB1 in a conformation required for

phosphorylation of substrates (Zeqiraj et al., 2009a). As a pseudokinase, STRAD does not have any catalytic activity but still binds ATP and adopts a closed conformation that is similar to that of active kinases (Zeqiraj et al., 2009b). This conformation of STRAD is critical for LKB1 activation, because mutation of residues in the ATP-binding pocket of STRAD prevent association with MO25 and activation of LKB1 (Zeqiraj et al., 2009b).

1.8 mTOR

The mTOR pathway is a key regulator of cell growth and protein synthesis. In addition to the regulation of AMPK, this thesis also examines the relationship between the LKB1-AMPK pathway and the mTOR pathway.

1.8.1 Discovery of mTOR

In 1975, a soil sample from Easter Island was discovered to contain a bacterial strain that produced an antifungal metabolite with potent growth suppressive properties against a range of organisms (Vézina et al., 1975). The metabolite was named rapamycin after Rapa Nui, the local name for Easter Island.

The target-of-rapamycin (TOR) was identified by screening the budding yeast, *Saccharomyces cerevisiae*, for mutations that caused rapamycin resistance (Heitman et al., 1991). This identified two genes, *TOR1* and *TOR2*, that were required for rapamycin sensitivity. This study also identified that rapamycin requires a cofactor, FKBP12 (FK506 binding protein), for its growth suppressive functions. FKBP12 is a cis-trans peptidyl-prolyl isomerase, and prolyl isomerization is a key step in the correct folding of proteins (Fischer and Schmid, 1990). However, inhibition of the prolyl isomerase

activity of FKBP12 was not sufficient for immunosuppression (Bierer et al., 1990), so the mechanism of action of rapamycin remains unclear. Rapamycin treatment was shown to cause a G1 cell cycle arrest in yeast (Heitman et al., 1991) and to prevent interleukin-2 induced T cell proliferation, also via a G1 arrest (Bierer et al., 1990; Dumont et al., 1990). This inhibition of proliferation by rapamycin seemed to be correlated with decreased activity of p70 S6 kinase, a known effector of the interleukin-2 response (Chung et al., 1992; Kuo et al., 1992). The deletion of *TOR1* and *TOR2* mimicked the G1 cell cycle arrest seen with rapamycin treatment, and it was subsequently demonstrated that TOR mutations prevented interactions with FKBP12-rapamycin, confirming that this was the direct target for rapamycin (Lorenz and Heitman, 1995). A mammalian homolog of the yeast TOR, mTOR (mechanistic TOR), was also shown to bind to the rapamycin-FKBP12 complex, an event necessary for rapamycin-induced cell cycle arrest (Brown et al., 1994; Sabatini et al., 1994; Sabers et al., 1995).

The product of the yeast *TOR2* gene had significant homology to PI 3-kinases (Kunz et al., 1993) and it was subsequently demonstrated that mTOR contained a kinase activity and had the ability to autophosphorylate (Brown et al., 1995; Brunn et al., 1996). mTOR was demonstrated to be the regulator of p70 S6 kinase *in vivo*, an effect that was rapamycin-FKBP12 sensitive and that required a functional mTOR kinase domain (Brown et al., 1995). mTOR was also implicated in the phosphorylation of 4E-BP1, as this was observed to be rapamycin-sensitive, with similar kinetics to that of p70 S6 kinase activation, and also required the kinase activity of mTOR (Brunn et al., 1997, 1996; Hara et al., 1997; von Manteuffel et al., 1996). Further insight came when mTOR was shown to directly phosphorylate and regulate p70 S6 kinase and 4E-BP1, two

regulators of protein synthesis, in a rapamycin-sensitive manner (Burnett et al., 1998). mTOR therefore appeared to be a central regulator of protein synthesis.

1.8.2 Identification of two mTOR complexes and their targets

1.8.2.1 mTORC1

A wide range of factors was known to regulate the *in vivo* function of mTOR, including amino acids (Hara et al., 1998), although these failed to alter the kinase activity of mTOR in cell-free assays (Hara et al., 1997). These findings, coupled with the presence of HEAT repeats and FAT domains on mTOR, both of which were suspected to mediate protein:protein interactions (Schmelzle and Hall, 2000), suggested that mTOR may exist within multiprotein complexes. Two groups independently identified Raptor (regulatory associated protein of mTOR) as a binding partner for mTOR (Hara et al., 2002; Kim et al., 2002). Raptor is a highly conserved 150 kDa protein that plays a positive role in mediating nutrient-induced mTOR signalling to p70 S6 kinase (Kim et al., 2002). In addition to Raptor, the complex contains: PRAS40 (40 kDa proline-rich Akt substrate), a negative regulator of mTOR (Sancak et al., 2007); mLST8 (mammalian lethal with SEC13), a positive regulator (Loewith et al., 2002); and the negative regulator DEPTOR (DEP domain-containing mTOR-interacting protein) (Peterson et al., 2009). In light of the discovery of a second TOR complex (see below), the complex containing Raptor is now referred to as mTORC1. The composition of mTORC1 is detailed in Fig. 1.6.

As discussed above, mTORC1 phosphorylates p70 S6 kinase on Thr389, a residue within the hydrophobic motif of the kinase domain, and this is required for the catalytic activity of p70 S6 kinase (Burnett et al., 1998). When active, p70 S6 kinase

phosphorylates a host of proteins involved in the regulation of mRNA translation, including ribosomal S6 (rS6). Although rS6 is often used as a measure of p70 S6 kinase activity, the physiological role of this remains unclear. Phosphorylation of rS6 was initially proposed to regulate the translation of 5'TOP mRNAs (an abundant subclass of mRNAs characterized by an oligopyrimidine tract at the 5' end), although this has now been disproven as p70 S6 kinase and rS6 appear to be dispensable for this process (Laplante and Sabatini, 2012). Phosphorylation of rS6 does, however, influence cell size and growth rate (Ruvinsky and Meyuhas, 2006).

Despite this, signalling through the mTORC1-p70 S6 kinase axis regulates mRNA translation through other targets. p70 S6 kinase phosphorylates eIF4B, which then enhances the activity of eIF4A, an RNA helicase. This causes an unwinding of the 5'-untranslated regions (5'-UTRs) of many mRNAs and promotes translation (Raught et al., 2004). PCDC4 (programmed cell death 4) binds to eIF4A and inhibits its helicase activity. p70 S6 kinase phosphorylates PDCD4, targeting it for degradation and preventing the inhibitory effect of PDCD4 on eIF4A (Dorrello et al., 2006).

mTORC1 also phosphorylates 4E-BP1, which plays a key role in the initiation of cap-dependent mRNA translation. The initiation factor eIF4E binds to the 5' mRNA cap and forms part of the eIF4F complex, which can then recruit ribosomes to the mRNA. 4EBP1 binds to eIF4E and prevents it from forming the eIF4F complex. When phosphorylated by mTORC1 on Thr36 and Thr45, 4E-BP1 is released, allowing formation of the eIF4F complex, ribosomal recruitment and subsequent initiation of protein translation (Pause et al., 1994).

Inhibition of TOR in yeast (Noda and Ohsumi, 1998) and in mammals (Thoreen et al., 2009) causes an increase in autophagy, a process which recycles cellular components to provide energy and nutrients during times of stress. Phosphorylation of ULK1 (the mammalian homologue of yeast Atg1) and Atg13 by mTORC1 blocks autophagosome assembly and prevents autophagy under nutrient replete conditions (Hosokawa et al., 2009; Jung et al., 2009). Other processes regulated by mTORC1 include ribosome biogenesis and the activity of transcription factors involved in mitochondrial metabolism and lipid synthesis, such as SREBP (Laplante and Sabatini, 2012).

1.8.2.2 mTORC2

Most of the work characterizing the targets of mTOR had been performed using rapamycin. In yeast, however, it was known that there were two TORs, one of which, TOR2, had unique properties and was rapamycin-insensitive (Helliwell et al., 1994; Zheng et al., 1995). Yeast TOR was shown to exist as two complexes: TORC1 and TORC2 (Loewith et al., 2002). TORC1 comprises the catalytic TOR1 or TOR2, KOG1 (the yeast homolog of raptor) and LST8. TORC2 comprises TOR2, LST8, AVO1, AVO2 and AVO3. TORC1 is rapamycin-sensitive and was proposed to regulate temporal control of cell growth, whereas TORC2 was rapamycin-insensitive and proposed to regulate the spatial control of cell growth. Similar findings were made in mammalian cells when a rapamycin-insensitive complex, mTORC2, was identified (Jacinto et al., 2004; Sarbassov et al., 2004). This complex was defined by the presence of Rictor (rapamycin-insensitive companion of mTOR), a homologue of AVO3. Like mTORC1, mTORC2 contains mLST8 and DEPTOR. In addition, TORC2 contains PROTOR (protein observed with Rictor) and mSin1, both of which are required for full activity of mTORC2 (Frias et

al., 2006; Pearce et al., 2011, 2007; Yang et al., 2006). The composition of mTORC2 is detailed in Fig 1.6.

mTORC2 was initially characterized as a kinase phosphorylating PKCα (Guertin et al., 2006; Sarbassov et al., 2004) but other targets of mTORC2 were soon identified. Full activation of PKB in response to growth factors, such as insulin, requires phosphorylation of Thr308 in the activation loop and Ser473 in the C-terminal hydrophobic motif (Alessi et al., 1996). PDK1 was determined to be the Thr308 kinase (Alessi et al., 1997) but the identity of the Ser473 kinase remained unknown. Subsequently, mTORC2 was identified as the elusive PDK2 acting on Ser473 of PKB (Sarbassov et al., 2005). mTORC2 was also demonstrated to phosphorylate and activate serum- and glucocorticoid-induced protein kinase 1 (SGK1), like PKB a member of the AGC family of protein kinases (García-Martínez and Alessi, 2008).

TOR, either in yeast or in mammals, therefore exists as two complexes. TORC1 is defined by the presence of Raptor, is rapamycin-sensitive and phosphorylates p70 S6 kinase, 4E-BP1 and ULK1. Rapamycin-insensitive TORC2 is defined by the presence of Rictor and phosphorylates PKCα, PKB and SGK.

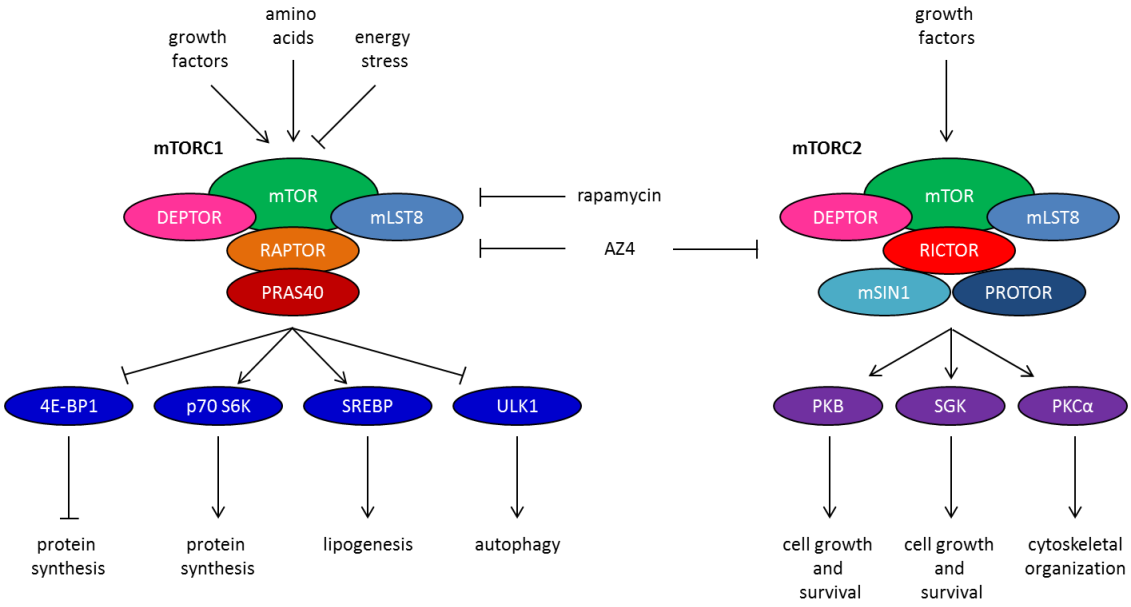

Figure 1.6: Summary of the two mTOR complexes and their targets
The components of the two TOR complexes are shown, together with some of their immediate downstream targets. Also shown are two inhibitors of the mTOR complexes, rapamycin (mTORC1 specific) and AZ4 (dual mTORC1/mTORC2 inhibitor). Discussed further in Chapter 5.

1.8.3 Regulation of mTOR

As depicted in Fig 1.7, mTOR is a nexus for signalling inputs from a large number of pathways (Zoncu et al., 2011b). The mTORC1 pathway responds to growth factors, like insulin or insulin-like growth factors (IGFs), via the PI3K (phosphatidylinositide 3-kinase) pathway. Binding of the growth factors to their membrane-bound receptors results in autophosphorylation on key tyrosine residues and subsequent recruitment and phosphorylation of the membrane-bound insulin-receptor substrate (IRS). PI3K is recruited to bind to phosphorylated IRS, where it is activated and converts phosphatidylinositol 4,5-bisphosphate (PIP_2) to phosphatidylinositol 3,4,5-trisphosphate (PIP_3). PKB is recruited to the plasma membrane by interaction of its pleckstrin homology domain with PIP_3, where it is phosphorylated by PDK1 (at Thr308 in the activation loop) and mTORC2 (at Ser473 in the hydrophobic motif). PKB then phosphorylates and inactivates the TSC1/TSC2 complex, which contains a GTPase

activator protein (GAP) acting on Rheb (Inoki et al., 2003a). GDP-bound Rheb, does not activate mTORC1, but binding of GTP converts it to an activator of mTORC1 (Long et al., 2005). Inactivation of TSC1/TSC2 therefore promotes the GTP-bound form of Rheb and activates mTORC1.

The activity of mTORC1 is also regulated by amino acids. Withdrawal of amino acids, particularly leucine, from the culture medium abolishes mTORC1 activity (Hara et al., 1998); available evidence suggests that amino acid levels are sensed intracellularly, rather than at the cell surface (Christie et al., 2002). The Rag family of GTPases, which exist as a heterodimer of either RagA or RagB with either RagC or RagD, change their GTP loading state in response to amino acids (Sancak et al., 2008). GTP-bound RagA or RagB bind to Raptor and recruit mTORC1 to the lysosome, where the mTORC1 activator Rheb resides. This recruitment is mediated by a recently discovered protein complex termed the Ragulator (Sancak et al., 2010). Amino acids enter the lysosomal lumen where, via the vascuolar-ATPase, they promote the guanine nucleotide exchange factor (GEF) activity of the Ragulator complex towards the Rag proteins (Bar-Peled et al., 2012; Zoncu et al., 2011a). This results in the exchange of GDP for GTP on RagA or RagB, followed by the dissociation of the Rag proteins from the Ragulator complex and subsequent recruitment of mTORC1 to the lysosome, where it can be activated by Rheb. In addition to the GEF activity of Ragulator, a protein complex termed GATOR (GAP activity towards Rags) has been identified that plays a negative role in mTORC1 signalling by converting GTP-bound RagA or RagB to the GDP-bound form (Bar-Peled et al., 2013). This complex appears to play an analogous role to that of TSC1/2 in the regulation of mTORC1 activity.

As discussed in Section 1.6, the activity of mTORC1 is also opposed by the LKB1-AMPK pathway in response to energy depletion. AMPK phosphorylates and activates TSC1/2, promoting its GAP activity towards the mTORC1 activator Rheb (Inoki et al., 2003b). AMPK also phosphorylates Raptor, promoting its association with 14-3-3 proteins and inhibiting mTORC1 catalytic activity (Gwinn et al., 2008).

In contrast to the regulation of mTORC1, comparatively little is known about the upstream activators of mTORC2. Insulin stimulation of cells increases Ser473 phosphorylation of PKB by mTORC2, suggesting that the complex, like mTORC1, responds to growth factors, either directly or indirectly (Sarbassov et al., 2004) and ribosomes have recently been proposed as the regulator of mTORC2 in response to growth factors (Zinzalla et al., 2011). mTORC2 is known to phosphorylate PKB, PKC and SGK, all of which respond to different growth factors, but it remains unclear how signalling inputs are processed. One proposed model is that mSin1, one of the unique components of mTORC2, exists in multiple isoforms that are differentially regulated by growth factors (Frias et al., 2006). Recently, phosphorylation of Sin1, in response to a range of stimuli including insulin and IGF-1, was reported to dissociate Sin1 from mTORC2 and reduce the catalytic activity of the complex, providing a form of negative feedback regulation (Liu et al., 2013).

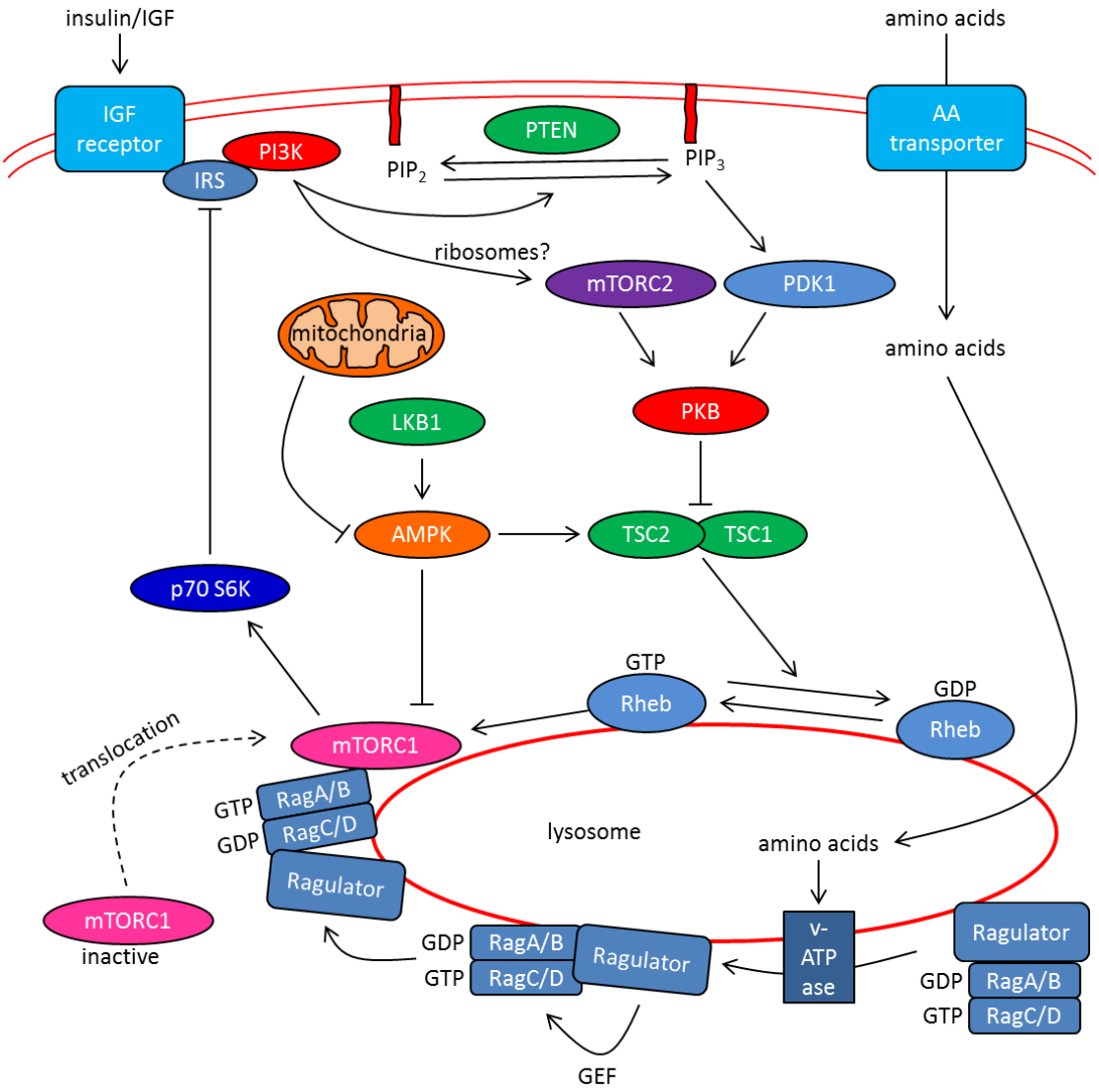

Figure 1.7: Regulation of mTORC1 and mTORC2 signalling
The mTOR complexes respond to a number of different inputs, including energy stress, amino acids and growth factors. The activity of the mTOR complexes is regulated by the activity of a number of tumour suppressors (shown in green) and oncogenes (shown in red). The downstream targets of the mTOR complexes are not shown here, with the exception of p70 S6K (dark blue), which forms part of a feedback loop to the IGF receptor. See text for more details.

1.8.4 mTOR and cancer

As mTOR plays such a central role in integrating the cellular response to growth factors and controlling cell growth, survival and proliferation, it is not surprising that it is heavily implicated in tumourigenesis. Evidence that mTOR plays a role in tumour formation comes from the study of familial cancer syndromes caused by mutations in

negative regulators of the mTOR pathway. Tuberous sclerosis (loss of TSC1/2), Peutz-Jeghers syndrome (loss of LKB1) and Cowden's syndrome (loss of PTEN) are all characterized by the formation of benign hamartomas in various tissues of the body, and in the case of Peutz-Jeghers and Cowden's syndromes there is also an increased risk of developing malignant tumours. In addition, activating mutations in PKB and PI3K, and inactivating mutations in PTEN are some of the most common mutations observed in human cancers (Yuan and Cantley, 2008). Sporadic LKB1 loss is also observed in a high proportion of lung adenocarcinomas (Sanchez-Cespedes et al., 2002). Loss of these negative regulators would result in hyperactive mTOR signalling. Additionally, activating mutations in mTOR itself have been identified in a number of human cancers (Sato et al., 2010) while overexpression of Rictor and subsequent mTORC2 activation is observed in glioma cell lines and primary tumours (Masri et al., 2007).

Over-activation of mTORC1 results in increased phosphorylation and inhibition of 4E-BP1 with subsequent activation of eIF4E. 4E-BP1 appears to play a key role in regulating cell proliferation, because MEFs lacking 4E-BP1 and 4E-BP2 displayed increased rates of proliferation (Dowling et al., 2010) and expression of 4E-BP1 is lost in a large proportion of pancreatic tumours (Martineau et al., 2013). eIF4E, which is inhibited by 4E-BP1, drives the expression of pro-tumorigenic proteins, including cyclin D3 and ornithine decarboxylase (Dowling et al., 2010) and the anti-apoptotic MCL1 (myeloid leukemia cell differentiation 1, a member of the Bcl-2 family) (Laplante and Sabatini, 2012). Additionally, the loss of 4E-BP1 and 4E-BP2 increased tumourigenesis in mice lacking p53 (Petroulakis et al., 2009). mTORC1, by phosphorylation of ULK1, inhibits autophagy, which appears to have important roles during tumourigenesis as

mice deficient in autophagic proteins are more tumour-prone than their wild-type counterparts (Yue et al., 2003). mTORC1 also drives the activation of the transcription factor SREBP which, amongst other targets, increases expression of fatty acid synthase (FAS), required to produce the high amounts of lipid required to fuel synthesis of new membranes to facilitate cellular proliferation (Menendez et al., 2009).

The activation of PKB and SGK by mTORC2 drives nutrient uptake, proliferation and cell survival. One reason is that PKB, by inhibiting TSC1/TSC2, will increase the activity of mTORC1. Additionally, both PKB (Brunet et al., 1999) and SGK1 (Brunet et al., 2001) phosphorylate members of the FOXO family of transcription factors, resulting in their exclusion from the nucleus and preventing them from regulating gene expression. The FOXO family regulate the expression of a number of genes, including those of pro-apoptotic proteins, such as Puma, and mutation of the sites phosphorylated by PKB and SGK sensitizes cells to apoptosis (Brunet et al., 1999, 2001).

PKB also has other pro-survival functions (reviewed in Manning and Cantley, 2007). The transmembrane Bcl-X_L protein prevents apoptosis by preventing cytochrome *c* release from the mitochondria, which would result in caspase cleavage and subsequent activation, followed by apoptosis. The activity of Bcl-X_L is inhibited by Bcl-2 homology domain 3 (BH3)-only family members, such as BAD (Bcl-2 associated death promoter), which sequesters Bcl-X_L and inhibits its function. In response to growth factors and mTORC2 activity, PKB directly phosphorylates BAD, resulting in 14-3-3 binding and cytoplasmic sequestration. This prevents BAD from eliciting its pro-apoptotic effects on Bcl-X_L. In addition, the expression of BH3-only proteins are controlled by FOXO transcription factors, which, as discussed above, are negatively

regulated by PKB. PKB also phosphorylates HDM2, an E3 ubiquitin ligase that triggers degradation of the pro-apoptotic tumour suppressor protein, p53. By regulating SGK and PKB, mTORC2 therefore has a key role in regulation of cell growth and survival. As mTOR regulates many pathways that impinge upon cell growth and proliferation, it is not surprising that mTOR inhibitors are considered exciting prospects for anti-cancer therapies.

1.9 Experimental aims

The role of AMP in regulating the activity of AMPK has recently been questioned. One aim of this thesis was to re-investigate the regulation of AMPK by AMP, ADP and ATP using both cell-free assays and intact cells. The crosstalk between LKB1 and AMPK was also examined by investigating whether AMPK could phosphorylate LKB1 and whether this had any functional relevance. The inhibition of mTOR is a promising avenue for anti-cancer therapies and this thesis also examines the role that the LKB1-AMPK pathway plays in determining the response of a number of cell types to mTOR inhibition.

CHAPTER 2: MATERIALS AND METHODS

2.1 Materials

2.1.1 Chemicals

Sodium fluoride, sodium pyrophosphate, Triton X-100, benzamidine, phenylmethylsulfonylfluoride (PMSF), soyabean trypsin inhibitor (SBTI), berberine chloride, A23187, sodium salicylate, phenformin, troglitazone, quercetin, 2,4-dinitrophenol (DNP), dimethyl sulfoxide (DMSO), magnesium chloride, Serva blue G, sodium pyruvate, glucose, glutathione, phenol red and Dulbecco's modified Eagle's medium (DMEM) Base were from Sigma (Poole, UK). Hepes, Tris(hydroxymethyl)methylamine (Tris), dithiothreitol (DTT) and isopropyl-α-D-thio-galactopyranoside (IPTG) were from Formedium (Hunstanton, UK). Sodium ethylenediaminetetraacetate (EDTA), sodium ethylenebis(oxyethylenenitrilo)-tetraacetate (EGTA), sodium chloride, orthophosphoric acid, Brij-35, Tween-20 ethanol, methanol and orthophosphoric acid were from VWR (UK). STO609 was from Tocris (UK). AICAR was from Calbiochem (Beeston, UK). [γ-^{32}P]ATP was from Perkin Elmer (Bucks, UK). ATP, ADP and AMP were from Melford (Chelsworth, UK). EDTA free protease cocktail inhibitor tablets were from Roche Diagnostics (Lewisham, UK). Protein G-Sepharose and 5 ml GSTrap FF columns were from GE Healthcare (Bucks, UK). Dulbecco's Modified Eagle's Medium (DMEM), McCoy's 5A medium, Opti-MEM, Foetal Bovine Serum (FBS), trypsin-EDTA, L-glutamine, penicillin-streptomycin solution (pen-strep), GlutaMax, zeocin, blasticidin, hygromycin B and Lipofectamine 2000 were from Life Technologies (UK). Effectene was from QIAGEN (Crawley, UK). FuGENE was from Promega (UK). AZ4 was supplied by Astra-Zeneca (Macclesfield, UK). A769662 was manufactured as described previously (Iyengar et al., 2005).

2.1.2 Molecular biology reagents

QIAprep Spin Miniprep kit, QIAprep Hi-Speed Plasmid Maxi kit and QIAquick PCR purification kits were from QIAGEN (Crawley, UK). Quikchange II site-directed mutagenesis kit was from Stratagene (La Jolla, CA). Molecular grade agarose and dNTPs were from Sigma (Poole, UK). Blue/orange 6X loading dye was from Promega (Southhampton, UK). XL-10 Gold, OneShot BL21 (DE3) and XL-1 competent *Escherichia coli* and the Flp-In system were from Life Technologies (UK). Liquid LB media and plates supplemented with ampicillin or kanamycin, SOC media and autoinduction media were supplied by Media Service, College of Life Sciences, University of Dundee.

2.1.3 Plasmids

Plasmids used in this thesis are outlined in table 2.1. The GST-LKB1 plasmid was provided by the DSTT (University of Dundee). Other plasmids were kindly provided by Dr. Fiona Ross, University of Dundee.

Plasmid	Vector	Expression	Tag
GST-LKB1	pGEX6P2	Bacterial	GST
GFP-LKB1	pEGFP-C2	Mammalian	GFP
AMPK-α1	pCMV	Mammalian	Myc
AMPK-α1 KD	pGEX6P2	Bacterial	GST
AMPK-α2 KD	pGEX6P2	Bacterial	GST

Table 2.1: Plasmids used in this thesis.

2.1.4 Primers

Primers were from Sigma (Poole, UK) and are outlined in table 2.2.

Mutation	Forward primer	Reverse primer
LKB1[S31A]	CACGTTCATCCACCGCATCGACGCCA CCGAGGTCATCTACCAG	CTGGTAGATGACCTCGGTGGCGTCG ATGCGGTGGATGAACGTG
LKB1[S31D]	CACGTTCATCCACCGCATCGACGACA CCGAGGTCATCTACCAG	CTGGTAGATGACCTCGGTGTCGTCG ATGCGGTGGATGAACGTG
AMPK-α[T172D]	GTCAGATGGTGAATTTTTAAGAGAT AGTTGTGGCTCACCCAACTATGC	GCATAGTTGGGTGAGCCACAACTAT CTCTTAAAAATTCACCATCTGAC
LKB1-FRT	CCCAAGCTTGGGTTACCATGGAGGT GGTGGACCCGCAG	CCGCTCGAGCGGTCACTTATCATCAT CATCCTTATAATCCTGCTGCTTGCAG GCCGACAG

Table 2.2: Primers used in this thesis.

Mutants created by site-directed mutagenesis are outlined in table 2.3.

Mutant	Plasmid DNA	Primers
LKB1 [S31A]	GST-LKB1	LKB1 [S31A]
LKB1 [S31A]	GFP-LKB1	LKB1 [S31A]
LKB1 [S31D]	GFP-LKB1	LKB1 [S31D]
AMPK-α1 [T172D]	AMPK-α1	AMPK-α [T172D]

Table 2.3: Mutants created as part of this thesis

2.1.5 Protein biochemistry reagents

XCell Surelock™ Mini-Cell, XCell Blot Module™, iBlot transfer module, NuPAGE® LDS Sample Buffer (4x), pre-cast NuPAGE® Novex 4-12% Bis-Tris gels and 3-8% Tris-acetate gels, NuPAGE® MOPS SDS running buffer (20x), NuPAGE® Tris-acetate SDS running buffer (20x), NuPAGE® Transfer Buffer (20x), SeeBlue® Plus2 Pre-Stained Standard and IRDye 680 secondary antibodies were from Life Technologies (UK). IRDye800 secondary antibodies were from Rockland (Gilbertsville, PA). BSA was from Sigma (Poole, UK). Vivaspin protein concentrators were from Sartorius (UK).

2.1.6 Peptides

The AMARA and SAMS peptides were synthesised by GL Biochem (Shanghai, China) and are detailed in table 2.4.

Peptide	Sequence	Reference
AMARA	AMARAASAAALARRR	Dale et al. 1995
SAMS	HMRSAMSGLHLVKRR	Davies et al. 1989

Table 2.4: Peptides used in this thesis

2.1.7 Proteins

CD73 5'-ectonucleotidase was from R&D systems (Abingdon, UK). Rat liver purified AMPK was prepared as described previously (Hawley et al., 1996) except that the final size-exclusion chromatography was on a Superdex 200 (Hi load 16/60) column, not a Sephacryl S-200. Human [His]LKB1-STRAD-MO25 complex was prepared using an insect cell baculovirus system (Jaleel et al., 2006) by the Division of Signal Transduction Therapy (DSTT), University of Dundee. The GST fusion of human LKB1, also prepared by the DSTT, was expressed and purified from *E. coli*. A GST-fusion of human CaMKKβ and a His-fusion of human AMPK α1[D157A]β2γ1, both kind gifts from Dr Fiona Ross, University of Dundee, were expressed and purified from *E. coli*. $PP2A_C$ was purified from bovine heart (Cohen et al., 1988) and PP2Cα from *E. coli* (Davies et al., 1995) and were kind gifts from Dr Simon Hawley, University of Dundee.

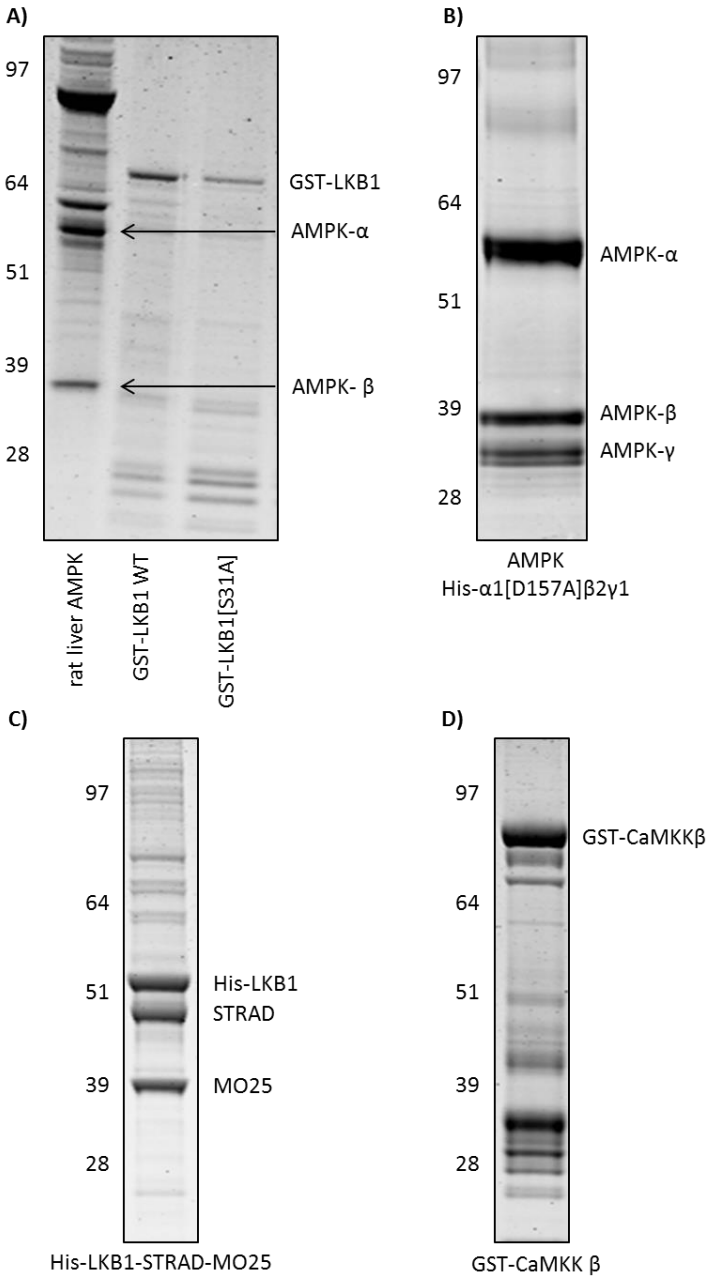

Figure 2.1: Protein preparations used in this thesis.
Proteins were resolved by SDS-PAGE and visualized using Coomassie staining. **(A)** AMPK purified from rat liver, GST-LKB1 and GST-LKB1[S31A]. **(B)** His fusion of AMPK α1[D157A]β2γ1. **(C)** His fusion of LKB1-STRAD-MO25 complex. **(D)** GST fusion of CaMKKβ.

2.1.8 Antibodies

Antibody	Species	Recognises	Company	Catalogue. No.
Phospho AMPK-α (Thr172)	rabbit	AMPK-α1 and -α2 phosphorylated at Thr172	Cell Signalling	2531
Actin	mouse	β-actin	Sigma	A5441
Phospho-PKB (Ser473)	rabbit	PKB phosphorylated at Ser473	Cell Signalling	4060
PKB	rabbit	PKB	Cell Signalling	9272
Phospho p70 S6K (Thr389)	mouse	p70 S6K and p85 S6K phosphorylated at Thr389 or Thr412 respectively	Cell Signalling	9206
p70 S6K	rabbit	p70 and p85 S6K	Cell Signalling	2708
PARP	rabbit	PARP (total and cleaved)	Cell Signalling	9542
Caspase-3	rabbit	Caspase-3 (total and cleaved)	Cell Signalling	9665
FLAG	mouse	FLAG peptide (DYKDDDDK)	Sigma	F1804
Phospho-GSK3 α/β (Ser 21/9)	rabbit	GSK3α and GSK3β phosphorylated at Ser21 or Ser9 respectively	Cell Signalling	9331
GSK3	mouse	GSK3α and GSK3β	Santa Cruz Biotechnology	sc-7291
GFP	mouse	GFP	Roche	11814460001

Table 2.5: Commercial antibodies used in this thesis.

Antibody	Species	Immunogen	Recognizes	Reference
AMPK-α1	sheep	CTSPPDSFLDDHHLTR (344-358 of rat AMPK-α1)	AMPK-α1	Woods et al. 1996
AMPK-α2	sheep	CMDDSAMHIPPGLKPH (352-366 of rat AMPK-α2)	AMPK-α2	Woods et al. 1996
Phospho-ACC	sheep	TMRPSMSGLHLVK (217-226 of human ACC2)	ACC1/ACC2 phosphorylated at Ser79/ Ser221 respectively	Hawley et al. 2003
pSer31 LKB1	sheep	TFIHRIDSTEVIYQPR (24 to 39 of LKB1)	LKB1 phosphorylated on Ser 31	N/A
Total LKB1	sheep	MDVADPQPLGLFPEGELMSVGM DTFIHRIDS (1-31 of rat LKB1)	LKB1	N/A

Table 2.6: Non-commercial antibodies used in this thesis.

2.1.9 Buffers

IP buffer (low salt):	50 mM Tris-HCl, pH 7.25, 150 mM NaCl, 50 mM NaF, 5 mM NaPPi, 1 mM EDTA, 1 mM EGTA, 1 mM DTT, 0.1 mM benzamidine, 0.1 mM PMSF, 5 μg/ml SBTI, 1% (v/v) Triton-X100
IP buffer (high salt):	as above, but containing 500 mM NaCl
Hepes assay buffer:	50 mM Hepes, pH 7.4, 50 mM NaCl, 1 mM DTT, 0.02% (v/v) Brij-35
Lysis buffer (mammalian):	50 mM Tris-HCl, pH 7.2, 50 mM NaF, 1 mM NaPPi, 1 mM EDTA, 1 mM EGTA, 1 mM DTT, 0.1 mM benzamidine, 0.1 mM PMSF, 5 μg/ml soyabean trypsin inhibitor, 1% (v/v) Triton-X100
Lysis buffer (bacterial):	50 mM Tris-HCl pH 8.2, 500 mM NaCl, 1 mM dithiothreitol, 1 mM EGTA, 1 mM EDTA with Complete Protease Inhibitor mix
Elution buffer:	50 mM Hepes, pH 8, 200 mM NaCl, 20 mM glutathione
TBS:	20 mM Tris-HCl, pH 7.4, 137 mM NaCl
TBS-T:	20 mM Tris-HCl, pH 7.4, 137 mM NaCl, 0.1% Tween-20
Coomassie stain:	50% (v/v) methanol, 10% (v/v) acetic acid and 0.1% (w/v) Coomassie blue
Coomassie destain:	10% (v/v) methanol, 10 % (v/v) acetic acid

2.2 Methods

2.2.1 Site-directed mutagenesis

Site-directed mutagenesis of DNA constructs was performed using Stratagene QuikChange® II site-directed mutagenesis kit according to manufacturer's instructions. Briefly, the mutagenesis reactions were set up in sterile 0.2 ml PCR tubes and each reaction contained: 1X reaction buffer, template plasmid dsDNA (50 ng), forward and reverse mutagenic oligonucleotide primers (0.3 µM each), 1 mM dNTPs, 2.5 U *Pfu turbo* DNA polymerase made up to a final volume of 50 µl with sterile de-ionised water. The reactions were performed in a Hybrid PCR express thermal cycler using the following conditions: [95°C (1 min)] x 1, [95°C (1 min), 55°C (1 min), 68°C (1 min/kb plasmid length)] x 18, [68°C (10 min)] x 1. After cycling, 10 U of *DpnI* restriction endonuclease was added and the reaction incubated at 37°C for 1 hour. *DpnI* digests methylated DNA (template plasmid DNA) but not non-methylated DNA (mutant plasmid). This reaction (10 µl) was used to transform competent XL-10 Gold *E. coli* cells as described in section 2.2.2. DNA constructs were verified by DNA sequencing.

Template DNA and primers used in this thesis are outlined in tables 2.1 and 2.2 respectively. Mutants created as part of this thesis are outlined in table 2.3.

2.2.2 Transformation of *E. coli*

E. coli cells were thawed on ice. DNA was added to cells and incubated on ice for 30 minutes. The cells were subjected to a heat shock at 42°C for 1 minute, before being incubated on ice for a further 5 minutes. SOC media (250 µl) was added to the cells. Cells were then incubated in a shaking incubator at 37°C for 1 hr before being streaked

onto an LB plate containing the appropriate selective antibody. Plates were incubated at 37°C overnight to allow appearance of colonies.

2.2.3 Purification of plasmid DNA from *E. coli*

2.2.3.1 Small scale purification:

Transformed *E. coli* cells were grown overnight at 37°C in 5 ml of LB broth plus the appropriate selective antibiotic. Cells were pelleted by centrifugation at 13000 rpm for 2 minutes. Plasmid DNA was then purified using the QIAGEN QIAprep® Spin Miniprep kit according to the manufacturer's instructions. Briefly, the cells were resuspended and lysed in buffers P1 and P2. These buffers contain SDS, sodium hydroxide and RNase. The SDS solubilizes the protein and phospholipid components, leading to lysis of the cells and the alkaline conditions ensure denaturation of chromosomal/plasmid DNAs and proteins. The lysates are then neutralized and adjusted to high salt conditions in buffer N3, where the chromosomal DNA, proteins and SDS precipitate. Plasmid DNA remains in solution and is separated from the precipitate by centrifugation before being applied to a column containing a silica membrane. This membrane binds the plasmid DNA under high salt conditions. Salts are then removed by washing with an ethanol-based buffer and plasmid DNA eluted using sterile de-ionized water. DNA was then sequenced (see section 2.2.5).

2.3.2.2 Large scale purification:

Transformed *E. coli* cells were grown overnight at 37°C in 200 ml of LB broth plus the appropriate selective antibody. Cells were pelleted by centrifugation (7000 rpm, 15 minutes, 4°C). Plasmid DNA was purified using the QIAGEN Hi-Speed Plasmid Maxi kit according to manufacturer's instructions. The principal behind this kit is similar to that

outlined for the small-scale purification but briefly, cells were resuspended in buffer P1 and lysed in buffer P2. The lysates were then neutralized in buffer P3 and the lysate cleared by filtration and applied to a column containing a silica membrane. DNA binds to the membrane and washed with buffer QC and eluted with buffer QF. DNA was precipitated by the addition of isopropanol and was collected using the QIAPrecipitator, before elution in sterile de-ionized water. DNA was then sequenced (see section 2.2.5).

2.2.4 DNA quantification

Plasmid DNA was diluted in deionized water to a final volume of 500 µl in a quartz cuvette. Absorbance was measured at 260 nm, against a water blank, to give an estimation of the DNA present in the sample. A DNA solution of 50 µg/ml has an absorbance at 260 nm of 1. The purity of the DNA was assessed by measuring the absorbance at 280 nm. Proteins and RNA absorb light at 280 nm. A 260 nm/280 nm ratio of 1.6 or greater was indicative of highly purified DNA.

2.2.5 DNA sequencing

DNA sequencing was performed by The Sequencing Service, College of Life Sciences, University of Dundee, using Applied Biosystems Big-Dye Ver 3.1 chemistry on an Applied Biosystems model 3730 automated capillary DNA sequencer.

2.2.6 Expression of GST-fusion proteins in *E. coli*

GST-LKB1 [Ser31A], GST-AMPK-α1 kinase domain (KD) and GST-AMPK-α2 kinase domain (KD) plasmids were used to transform BL21 (DE3) *E. coli* as outlined in section 2.2.2 and plated on LB-ampicillin plates overnight. A single colony was selected and

used to inoculate 50 ml of LB-ampicillin liquid media and grown overnight at 37°C in a shaking incubator. 10 ml of this culture was used to inoculate 1 L of LB-ampicillin liquid media. Cultures were placed at 37°C in a shaking incubator and left until the OD_{600} reached 0.4 absorbance units. The flask was placed at 2-8°C for 15 minutes. IPTG (1 mM) was added and the culture incubated at 20°C in a shaker incubator overnight. Cells were pelleted by centrifugation (7000 rpm, 15 minutes, 4°C), frozen in liquid nitrogen and stored at -20°C prior to purification (see section 2.2.7).

2.2.7 Purification of GST-fusion proteins from *E. coli*

Cell pellets prepared in section 2.2.6 were ground to a fine powder using a mortar and pestle in the presence of liquid nitrogen. The powder was resuspended in lysis buffer and clarified by centrifugation (30000 rpm, 30 minutes, 4°C). Supernatant was applied to a GST-FF column (equilibrated with lysis buffer) at 4°C and the column washed with 10 volumes of lysis buffer. Elution buffer was added and the protein collected. Proteins were concentrated using an Amicon Ultra centrifugal concentrator and stored at -80°C.

2.2.8 General mammalian tissue culture

All media and buffers used for tissue culture were warmed to 37°C prior to use. Cells were cultured and maintained in 75 cm^3 or 175 cm^3 flasks at 37°C in an atmosphere containing 5% CO_2. The cells were grown until 80-90% confluency before splitting for routine maintenance. For passaging of cells, the culture medium was aspirated, 5-10 ml of trypsin-EDTA was added and the cells were returned to the 37°C incubator for 3-5 minutes. After the cells detached from the surface of the flask, 1 ml of the cell suspension was used to seed a fresh 75 cm^3 or 175 cm^3 flask containing 15 ml or 25 ml of complete culture medium.

2.2.9 Freezing and thawing cell lines

Cells were grown to confluency in 175 cm^3 flasks and trypsinised as described in section 2.2.8. Cells were pelleted by centrifugation at 1000 rpm for 5 minutes, the trypsin aspirated and cells resuspended in growth media containing 10% (v/v) DMSO. Cells were transferred to cryo-protective tubes and placed in a cell freezer. Cells were frozen in a -80°C freezer before being transferred to liquid nitrogen for long-term storage. Frozen cell stocks were thawed in a 37°C water bath and transferred to 10 ml of pre-warmed media. Cells were pelleted and the supernatant was aspirated to remove DMSO. The cells were resuspended in fresh growth media and seeded into 75 cm^3 flasks.

2.2.10 G361 cell line

G361 cells were cultured in McCoys 5A media supplemented with 10 % (v/v) foetal bovine serum (FBS), 2 mM glutamine, 100 IU/ml penicillin and 100 µg/ml streptomycin. The G361 FRT parental cells (see section 2.2.15) were cultured as above except that the media was supplemented with zeocin (100 µg/ml). The G361 cells stably expressing AMPK-α2 [D157A] (see section 2.2.15) were cultured as above except that the media was supplemented with hygromycin B (100 µg/ml).

2.2.11 Mouse embryonic fibroblasts (MEF)

Wild-type and AMPK-$\alpha1^{-/-}$ -$\alpha2^{-/-}$ double knockout MEFs (kind gifts from Dr Benoit Viollet, Institut Cochin, Paris) were cultured in DMEM supplemented with 10 % (v/v) foetal bovine serum (FBS), 100 IU/ml penicillin and 100 µg/ml streptomycin.

2.2.12 HEK293 cell line

HEK293 cells were cultured in DMEM supplemented with 10 % (v/v) foetal bovine serum (FBS), 100 IU/ml penicillin and 100 μg/ml streptomycin. HEK293 cells stably expressing AMPK-β-FLAG, both β1 and β2 and G2A mutants, were kind gifts from Dr Fiona Ross, University of Dundee and cultured as above except that the media was supplemented with hygromycin B (200 μg/ml) and blasticidin (15 μg/ml). These HEK293 cells were generated using the Flp-In system to stably express AMPK-β under the control of a tetracycline repressor. In the absence of tetracycline, the tet repressor (constitutively expressed from a gene stably inserted into the host genome) forms a homodimer that binds to a tet operator sequence in the promoter of the gene of interest (in this case, AMPK-β-FLAG) which has also been stably inserted to the genome. This represses transcription of the gene of interest. Upon addition, tetracycline binds to the tet repressor, rendering it unable to bind to the tet operator and allowing transcription of the gene of interest. Tetracycline (1 μg/ml) was added to the cells for 48 hr prior to treatment and lysis.

2.2.13 HeLa cell line

HeLa cells were cultured in DMEM supplemented with 10 % (v/v) foetal bovine serum (FBS), 100 IU/ml penicillin and 100 μg/ml streptomycin.

2.2.14 Generation of HeLa cells expressing wild-type and kinase-dead LKB1

These cell lines were generated using Flp-In technology according to the manufacturer's instructions. HeLa cells were transfected with pFRT/lacZeo plasmid using Lipofectamine 2000 and after 48 hr washed into medium containing zeocin (100 μg/ml). The medium was replaced every 3-4 days until single clones could be

identified and expanded. The incorporation of an FRT site was measured by β-galactosidase activity.

Wild-type and kinase-dead (D194A) LKB1 plasmids, provided by the DSTT, were used as DNA templates and LKB1 was amplified by PCR using the LKB1-FRT primers (designed to incorporate a C-terminal FLAG tag and HindIII/XhoI restriction sites). The PCR reaction contained primers (0.3 µM), 100 ng dsDNA template, 0.5 mM dNTPs, 4 mM MgCl2, 5% DMSO (v/v) and 2.5 U Pfu DNA polymerase, made up to 50 µl with sterile de-ionized water. The reactions were incubated in a Hybrid PCR Express thermal cycler using the following conditions: [95°C (7 min)] x 1, [95°C (1 min), 50°C (1 min), 72°C (2 min)] x 38, [72°C (10 min)] x 1. The PCR reactions were analysed on a 1% agarose gel and the appropriate bands were excised using a sterile scalpel. The PCR products were purified using a QIAquick PCR purification kit according to the manufacturer's instructions. Purified PCR product and pFRT/FRT vector were digested with HindIII/XhoI at 37°C for 2 hours. The restriction digest reactions were analysed on 1% agarose gel and linearised plasmids were purified as above. The purified digest products were incubated overnight at 4°C with T4 DNA ligase at a vector: insert ratio of 1:7. XL-1 *E. coli* were transformed with these ligation reactions (as described in section 2.2.2) and plasmid DNA extracted from positive clones. DNA constructs were verified by DNA sequencing.

The FRT site-containing HeLa cells were transfected with the LKB1 plasmids and a plasmid (pOG44) encoding a Flp recombinase. Transfection was performed, in the absence of zeocin, using Lipofectamine, according to manufacturer's instructions. After

48 hr, hygromycin B (150 μg/ml) was added and the medium changed every 3-4 days until single clones could be identified and expanded.

2.2.15 Transient transfection of G361 cells

G361 cells were transfected with DNAs encoding GFP-LKB1 (wild-type, S31A mutant or S31D mutant), FLAG-STRADα and myc-MO25 (all human). G361 cells were grown to 60% confluency in 6 cm diameter dishes then transfected using Effectene according to manufacturer's instructions. After 36 hr, cells were treated as indicated in the figure legends for 1 hr prior to lysis.

2.2.16 Generation of G361 cells stably expressing dominant negative AMPK-α2

These cell lines were generated using Flp-In technology according to the manufacturer's instructions. G361 cells were transfected with pFRT/lacZeo plasmid using FuGENE and after 48 hr washed into medium containing zeocin (100 μg/ml). The medium was replaced every 3-4 days until single clones could be identified and expanded. The incorporation of an FRT site was measured by β-galactosidase activity. A construct encoding kinase-dead human AMPK-α2[D157A] fused to a C-terminal FLAG tag was inserted into pcDNA5/FRT plasmid. The FRT site-containing G361 cells were transfected with the AMPK-α2 plasmid and a plasmid (pOG44) encoding a Flp recombinase. Transfection was performed, in the absence of zeocin, using Effectene, according to manufacturer's instructions. After 48 hr, hygromycin B (100 μg/ml) was added and the medium changed every 3-4 days until single clones could be identified and expanded. The transfection of the G361 parental FRT cells with the AMPK-α2 construct was performed by Dr Fiona Ross, University of Dundee.

2.2.17 Transfection of AMPK $\alpha1^{-/-}$-$\alpha2^{-/-}$ double knockout MEFs

MEF cells lacking the catalytic AMPK-α subunits were transfected with DNAs encoding myc-α1, β2 and FLAG-γ1 (all human). The myc-α1 construct had either the wild-type sequence or a T172D mutation (see table 2.2). MEFs were grown to 90% confluency in 6 cm diameter dishes then transfected using Lipofectamine 2000 according to manufacturer's instructions. Cells were washed into Opti-MEM reduced serum media (in the absence of antibiotics) prior to transfection then back into growth media after 5 hr. After 48 hr cells were treated as indicated in the figure legend for 1 hr prior to lysis.

2.2.18 Lysis of mammalian cells

Cells were harvested using a rapid lysis method, a technique which minimizes activation of AMPK. Dishes were placed on ice and the media aspirated. Cells were washed twice with ice-cold PBS, lysed in 200 µl of ice-cold lysis buffer and scraped into pre-chilled 1.5 ml eppendorf tubes. Lysates were clarified by centrifugation for 10 minutes at 13000 rpm, 4°C. The supernatant was collected and the protein concentration determined. Lysates were flash frozen on liquid nitrogen and stored at -80°C. Prior to use, lysates were thawed on ice.

2.2.19 Estimation of protein concentrations

Protein concentrations were estimated using Bradford reagent. Bradford reagent was prepared by dissolving 30 mg of Serva blue in 50 ml of 100% ethanol and 55 ml of 85% (v/v) orthophosphoric acid. The solution was made up to 1 L using deionised water and filtered to 0.2 µm. The solution was stored at room temperature and protected from light. A standard curve was generated using a range of BSA concentrations. Protein concentrations of samples were determined by adding 1 ml of Bradford reagent to

protein samples in 100 µl of water and measuring the absorbance at 595 nm. The A_{595} was then read off the BSA standard curve to give an estimate of the protein concentration in the sample.

2.2.20 SDS-PAGE

SDS-PAGE resolves proteins based upon their molecular weight. The anionic detergents sodium or lithium dodecyl sulphate (SDS or LDS) are used to denature proteins and confer a negative charge proportional to their size resulting in a constant mass/charge ratio. When placed under an electric field, these proteins migrate towards the anode at a rate proportional to their molecular weight.

Samples to be resolved were denatured by the addition of Invitrogen NuPAGE 4X LDS (lithium dodecyl sulphate) sample buffer and heated to 70°C for 10 minutes. Samples, along with pre-stained molecular weight standards (Invitrogen SeeBlue Plus 2), were loaded onto pre-cast NuPAGE 4-12% bis-tris gels and resolved at 200 V for 1 hour in NuPAGE 1X MOPS running buffer. For analysis of acetyl Co-A carboxylase (ACC), pre-cast 3-8% tris-acetate polyacrylamide gels were used and proteins were resolved at 150 V for 80 minutes in NuPAGE 1X tris-acectate running buffer after which proteins were transferred to nitrocellulose membranes for immunoblotting or stained with Coomassie blue for visualization of protein bands.

2.2.21 Coomassie staining of gels

To visualize proteins after SDS-PAGE separation, gels were soaked for 30 minutes in Coomassie staining buffer. Gels were then washed in Coomassie destain buffer

overnight. All incubations were performed at room temperature on a rocker platform. Imaging was performed using the LiCor Odyssey detection system (700 nm channel).

2.2.22 Immunoblotting (Western blotting)

Proteins were resolved by SDS-PAGE and transferred to nitrocellulose membrane for immunoblotting. For gels consisting of up to 15 wells, transfers were performed using an Invitrogen XCell II Blot Module according to the manufacturer's instructions. The gel-membrane sandwich was assembled as: 2x blotting pad, 3 MM filter paper, gel, nitrocellulose membrane, 3 MM filter paper, blotting pads. The sandwich was orientated to place the gel closest to the cathode and the membrane closest to the anode. Transfers were performed at 35 V for 90 minutes using 1X NuPAGE transfer buffer containing 20% (v/v) methanol.

For gels containing more than 15 wells, transfers were performed using the Invitrogen iBlot dry blotting system according to manufacturer's instructions. The gels were soaked for 5 minutes in 2X NuPAGE transfer buffer containing 20% (v/v) methanol. The gel-membrane sandwich was prepared as: anode stack (containing nitrocellulose membrane), gel, 3 MM filter paper, cathode stack, sponge. Transfers were performed for 7 minutes at 20V.

Membranes were blocked in LiCor Odyssey blocking buffer for one hour then probed with primary antibody overnight. Membranes were washed as:

5 x 5 minutes in TBST buffer

1 x 5 minutes in TBS buffer

Membranes were then incubated with appropriate IRDye 680 or IRDye 800 secondary antibodies diluted 5000X in LiCor Odyssey blocking buffer for 1 hour. Streptavidin coupled IRDye 800 secondary antibodies, used to detect biotinylated ACC, were diluted 2000X in LiCor Odyssey blocking buffer. Membranes were washed as above and the signal detected and quantified (as required) using the LiCor Odyssey IR detection system. Where required, densitometry was performed using LiCor Odyssey software. Membrane blocking, antibody incubations and washing steps were all carried out on a rocker platform at room temperature.

2.2.23 Non-covalent coupling of antibodies to protein G-sepharose beads

Protein G-sepharose beads (stored in 20% ethanol) were washed four times with low-salt IP buffer to remove alcohol. Beads were then incubated with the required antibody (1 µg of antibody/µl of beads) on a roller mixer at 2-8°C overnight to allow coupling of antibody to beads. Beads were then washed three times in IP buffer (high salt) to remove unbound antibody. Beads were then washed twice with IP buffer (low salt) and stored as a 30% slurry in IP buffer (low salt) at 2-8°C until required.

2.2.24 Immunoprecipitation and assay of AMPK from cell lysates

Anti-AMPK-α1 and -α2 antibodies were non-covalently coupled to protein G-sepharose beads as described in section 2.2.23. Beads were then incubated with cell lysates on a roller mixer for 2 hours at 2-8°C to immunoprecipitate AMPK and washed as:

2 x IP buffer (high salt)

2 x IP buffer (low salt)

2 x Hepes assay buffer

Beads were resuspended in Hepes assay buffer and aliquoted into 1.5 ml eppendorf tubes in a final volume of 20 µl before subsequent kinase assay.

The activity of AMPK was measured by its ability to phosphorylate the synthetic AMARA peptide (AMARAASAAALARRR), which was derived from the sequence of rat acetyl-coenzyme A carboxylase (ACC), a substrate of AMPK (Dale et al., 1995). Assays were started by the addition of 30 µl of assay buffer, containing 200 µM AMP, 200 µM [γ^{32}P]-ATP, 5 mM $MgCl_2$ and 200 µM AMARA (final volume of 50 µl). Assays were incubated at 30°C in an orbital shaker for 15 minutes. Reactions were terminated by pipetting 30 µl of the assay mixture onto squares of P81 filter paper and placing these into a solution of 1% (v/v) orthophosphoric acid. Filter papers were washed with water to remove any unincorporated ATP and allowed to dry at room temperature. The radioactivity incorporated in each sample was measured using an LKB-Wallace 1214-Rackbeta scintillation counter. One unit of activity was determined as that which catalysed the incorporation of one nanomole of ^{32}P into synthetic peptide.

2.2.25 Allosteric activation of AMPK immunoprecipitated from G361 lysates

Immunoprecipitations and assays were carried out as detailed in section 2.2.24 with the following exceptions: the SAMS peptide (Davies et al 1989) was used (200 µM) in place of AMARA and the kinase reactions were performed ± AMP (200 µM).

2.2.26 AMPK assays using rat liver purified AMPK and isolated kinase domains

AMPK assays in-solution were performed using either the SAMS or AMARA peptide (200 µM) and a reaction mixture containing AMP (200 µM, except where indicated in figure legends), ATP (200 µM, except where indicated in figure legends) and $MgCl_2$

(a constant 4.8 mM molar excess over ATP was maintained). Assays (25 µl) were incubated at 30°C in a water bath for 15 minutes. Reactions were terminated by pipetting 15 µl of the assay mixture onto squares of P81 filter paper then processed as section 2.2.24.

2.2.27 Protection against dephosphorylation assays

Rat liver purified AMPK was incubated with enough PP2Cα to give approximately 70% Thr172 dephosphorylation. AMP, ADP and ATP were added at the concentrations given in the figures. Aliquots were removed for kinase assays (performed as section 2.2.24) and Western blotting (performed as section 2.2.22). When included, 5'-nucleotidase was at 3.9 µg/ml and was preincubated with nucleotides for 5 minutes prior to starting dephosphorylation reactions. All incubations were at 30°C and performed in Hepes assay buffer.

2.2.28 Promotion of phosphorylation assays

Rat liver AMPK was incubated with $PP2A_c$ to give approximately 95% Thr172 dephosphorylation. Okadaic acid (5 µM) was added to stop this reaction. Dephosphorylated kinase was then incubated with LKB1 or CaMKKβ (as indicated) plus $MgCl_2$ (5 mM) and ATP (200 µM) for 10 minutes (unless indicated otherwise), with AMP, ADP or A769662 at concentrations given in figures. Aliquots were removed for kinase assays (performed as section 2.2.24) and Western blotting (performed as section 2.2.22). When included, 5'nucleotidase was at 1.8 µg/ml. All incubations were at 30°C and performed in Hepes assay buffer. When A769662 was present in the LKB1/CaMKKβ incubations, it was also included at 1 µM in the final kinase assay. This

concentration of A769662 is sufficient to give maximal activation of AMPK in a cell-free assay.

2.2.29 Estimation of degree of Thr172 phosphorylation in intact cells

2.2.29.1 CaMKKβ phosphorylation of immunoprecipitated AMPK-α

Immunoprecipitations were carried out as detailed in section 2.2.24. Beads were then incubated ± CaMKKβ for 30 minutes at 30°C in the presence of $MgCl_2$ (5 mM) and ATP (200 μM) before being washed in Hepes buffer to remove CaMKKβ. AMPK activity was then determined using the AMARA peptide as outlined in section 2.2.23.

2.2.29.2 Comparison to bacterial protein

Bacterially-expressed kinase-dead AMPK (α1[D157A]β2γ1 complex, a kind gift from Dr Fiona Ross, University of Dundee) was incubated with LKB1-STRAD-MO25 complex or CaMKKβ (as indicated in figure legends) in the presence of $MgCl_2$ (5 mM) and ATP (200 μM) for 15 minutes. Reactions were stopped by the addition of SDS with further incubation at 70°C for 10 minutes. Bacterial protein and cell lysates (giving equivalent amounts of AMPK-α) were analysed by Western blotting (as detailed in section 2.2.22) and the membranes probed with anti-phospho Thr172 and anti-AMPK-α antibodies. The signals were quantified and the ratio of phosphorylated to total AMPK calculated.

2.2.30 LKB1 assays

LKB1 activity was measured by its ability to activate dephosphorylated AMPK. Anti-LKB1 antibodies were non-covalently coupled to protein-G-sepharose beads as described in section 2.2.23. These beads were then incubated with cell lysates on a roller mixer for 2 hours at 2-8°C to immunoprecipitate LKB1.

Beads were washed as:

2 x IP buffer (high salt)

2 x IP buffer (low salt)

2 x Hepes assay buffer

Beads were resuspended in Hepes assay buffer and aliquoted into 1.5 ml eppendorf tubes in a final volume of 20 µl. The immunoprecipitated LKB1 was incubated with bacterially-expressed AMPK αβγ heterotrimer with Mg.ATP for 20 minutes at 30°C. AMPK activity was then measured using the AMARA peptide as described in section 2.2.24.

2.2.31 Nucleotide measurements

Culture medium was aspirated from cells, followed by washing in ice-cold PBS and lysis in ice-cold 5% perchloric acid. Samples were vortexed and lysates clarified by centrifugation. The supernatant was collected and an equal volume of 1:1 mixture of tri-n-octylamine and 1,1,2-trichlorotrifluoroethane added. Samples were vortexed, centrifuged and the top (aqueous) phase collected. This procedure was repeated twice more and nucleotides stored at -20°C before analysis. All centrifugation steps were performed at 13000 rpm, 4°C for 3 minutes.

Sample analysis was performed using a Beckman Coulter P/ACE 5500 capillary electrophoresis instrument using 50 mM Na phosphate and 50 mM NaCl (pH 5.2, leading buffer) and 100 mM MES/Tris (pH 5.2, tailing buffer). Each buffer contained 0.2% hydroxyethylcellulose. Nucleotide peaks were detected by UV absorbance at 254 nm and nucleotide ratios were calculated using peak heights. Retention times for each

nucleotide were determined prior to sample analysis by running a mixture of pure nucleotides through the capillary.

2.2.32 Measurement of cellular oxygen consumption rate (OCR) of intact cells

OCR measurements were performed using a Seahorse Biosciences XF24 analyser. This instrument isolates a small volume of medium above a monolayer of cells to create a transient microchamber. Fluorescent probes then measure changes in the concentration of dissolved oxygen over time and the instrument calculates an OCR value. The microchamber is then abolished and the medium mixed to allow cellular respiration to return to baseline and prevent cells from becoming hypoxic. The instrument also has the ability, via four ports, to inject drugs directly onto the cells and measure the effect of these on OCR.

Assays were performed according to the guidelines provided by the manufacturer but briefly, cells were seeded into the wells of a microplate in a small volume (100 µl) to prevent adhesion to the side of the wells, and placed at 37°C for 3-4 hours. Extra medium was then added to the cells (150 µl) and cells left at 37°C overnight. The morning of the assay, growth media was changed for unbuffered media (pH 7.4) and cells placed in a CO_2-free incubator at 37°C for 1 hour. During this time, any required drugs were prepared in unbuffered media and the pH adjusted back to 7.4. Drugs were then loaded into the injection ports and the probes calibrated. Cells were loaded onto the instrument and the assay initiated.

2.2.33 Measurement of ^{32}P incorporation into proteins

Proteins, as indicated in the figure legends, were incubated at 30°C with $MgCl_2$ (5 mM) and 200 µM [$\gamma^{32}P$]-ATP. Reactions were stopped by the addition of 4X LDS buffer followed by further incubation at 70°C for 10 minutes. Samples were resolved by SDS-PAGE, alongside known amounts of BSA, and the gels stained with Coomassie buffer. Gels were destained overnight, imaged using the LiCor Odyssey detection system and the BSA standards used to quantify the amount of protein present. Gels were dried at 80°C, under a vacuum, for 90 minutes. Dried gels were subjected to autoradiography. Bands were excised from the dried gel and the amount of ^{32}P incorporated determined as per section 2.2.24. Stoichiometry of substrate phosphorylation was estimated as nmol of ^{32}P incorporated per nmol of protein.

2.2.34 Data analysis

Data, unless indicated otherwise, is mean ± SEM. Unless stated otherwise, statistical analysis was by ANOVA, using Bonferroni's multiple comparison test of selected data sets (*$p < 0.05$, **$p < 0.01$, ***$p < 0.001$).

CHAPTER 3: REGULATION OF AMPK BY AMP AND ADP

3.1 Introduction

Despite AMP being the historical regulator of AMPK that led to its name, the role of AMP in regulating AMPK has recently been questioned. This was in part because ADP was reported to inhibit dephosphorylation of Thr172 in a similar manner to AMP (Xiao et al., 2011). As ADP is present at about 10-fold higher concentrations than AMP in the cell, the similar binding affinities of AMP and ADP at both the high affinity site (site 1?) and the low affinity site (site 3?) of the mammalian kinase suggest that it would be ADP, not AMP, that would be the primary signal that prevented dephosphorylation (Xiao et al., 2011). Both ADP and AMP were also reported to promote Thr172 phosphorylation over a similar concentration range, which again would imply that, given the differences in cellular concentrations, ADP rather than AMP would be the stress signal that promotes Thr172 phosphorylation (Oakhill et al., 2010, 2011). Coupled with the frequent reports that allosteric activation by AMP only increases AMPK activity by 2-fold or less, compared to the >100-fold increase in activity in response to Thr172 phosphorylation (Sanders et al., 2007b; Suter et al., 2006), the physiological role of AMP as a regulator of AMPK has been questioned (Carling et al., 2012; Oakhill et al., 2012). The current model for AMPK regulation is outlined in Fig. 1.3 of Chapter 1.

3.2 Aims

Recent work has proposed a role for ADP in the regulation of AMPK, as well as casting doubt upon the role that AMP plays in the physiological regulation of the kinase. The aim of this chapter was to re-investigate the regulation of AMPK by AMP, ADP and ATP. Using cell-free systems, the ability of AMP and ADP to promote Thr172 phosphorylation by either LKB1 or CaMKKβ, and to protect against Thr172 dephosphorylation by protein phosphatases, were examined. The allosteric activation of AMPK by AMP was also investigated both in a cell-free system and in intact LKB1-null cells. The absolute changes in Thr172 phosphorylation produced in an intact cell were also investigated in response to AMPK activators, using two cultured cell models. The change in cellular nucleotides in response to various AMPK activators was also determined and this data was used to estimate the contributions of AMP and ADP to the overall activation mechanism.

3.3 Results

3.3.1 AMP, but not ADP, promotes phosphorylation by LKB1, but not CaMKKβ

To investigate the regulation of AMPK by adenine nucleotides, native AMPK purified from rat liver was used. It has been reported that rat liver AMPK exhibits greater allosteric activation by AMP than bacterially expressed human or rat AMPK (Carling et al., 1987; Sanders et al., 2007b; Suter et al., 2006). It is possible that this discrepancy stems from the fact that bacterially expressed AMPK lacks the post-translational modifications possessed by rat liver AMPK. It is also possible that bacteria do not express the necessary chaperones required for correct folding of the enzyme into its optimal 3D structure. Regardless of the explanation, AMPK purified from rat liver is more sensitive to regulation by adenine nucleotides than that purified from bacteria, and was used throughout this chapter.

It has recently been reported that AMP can promote Thr172 phosphorylation by LKB1 and by CaMKKβ, while ADP also promoted phosphorylation by CaMKKβ (LKB1 was not tested) (Oakhill et al., 2011, 2010). These effects were reported to be dependent on myristoylation of the β subunit, with experiments being performed using recombinant AMPK purified from, and expressed in, bacterial or mammalian cells. For this study, the promotion of phosphorylation was reinvestigated using AMPK purified from rat liver, which is an approximately equal mixture of α1β1γ1 and α2β1γ1 complexes (Woods et al., 1996b). AMPK was dephosphorylated by incubation with $PP2A_C$ to give approximately 95% inactivation and the dephosphorylated kinase was then incubated with LKB1 or CaMKKβ. Aliquots from this incubation were removed for kinase assays or for Western blots. Fig. 3.1 shows that AMP promoted phosphorylation by LKB1, but

not CaMKKβ. No effect of ADP was observed with LKB1, despite several attempts over a wide range of ADP concentrations (Fig. 3.2).

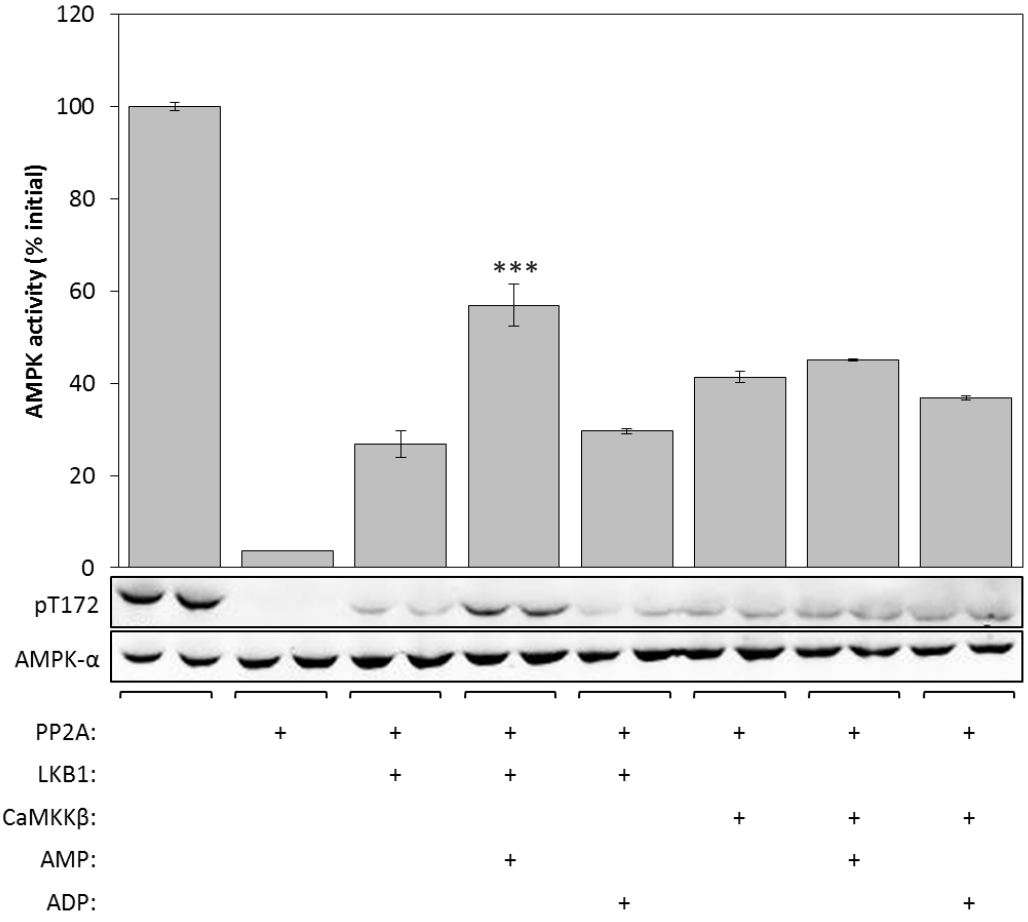

Figure 3.1: AMP, not ADP, enhances Thr172 phosphorylation by LKB1, not CaMKKβ
Purified rat liver AMPK was incubated with bacterial $PP2A_c$ to give approximately 95% inactivation and the reaction stopped by the addition of okadaic acid. The kinase was then incubated with LKB1 or CaMKKβ, with or without AMP or ADP (300 µM). Aliquots were taken for kinase assays using the AMARA peptide substrate (top) or Western blotting using the indicated antibodies (bottom). Kinase activities are expressed as % of the activity without $PP2A_C$ treatment and are mean ± SEM (n = 3). Significantly different from control without AMP by one-way ANOVA with Dunnett's multiple comparison test: ***$p < 0.001$.

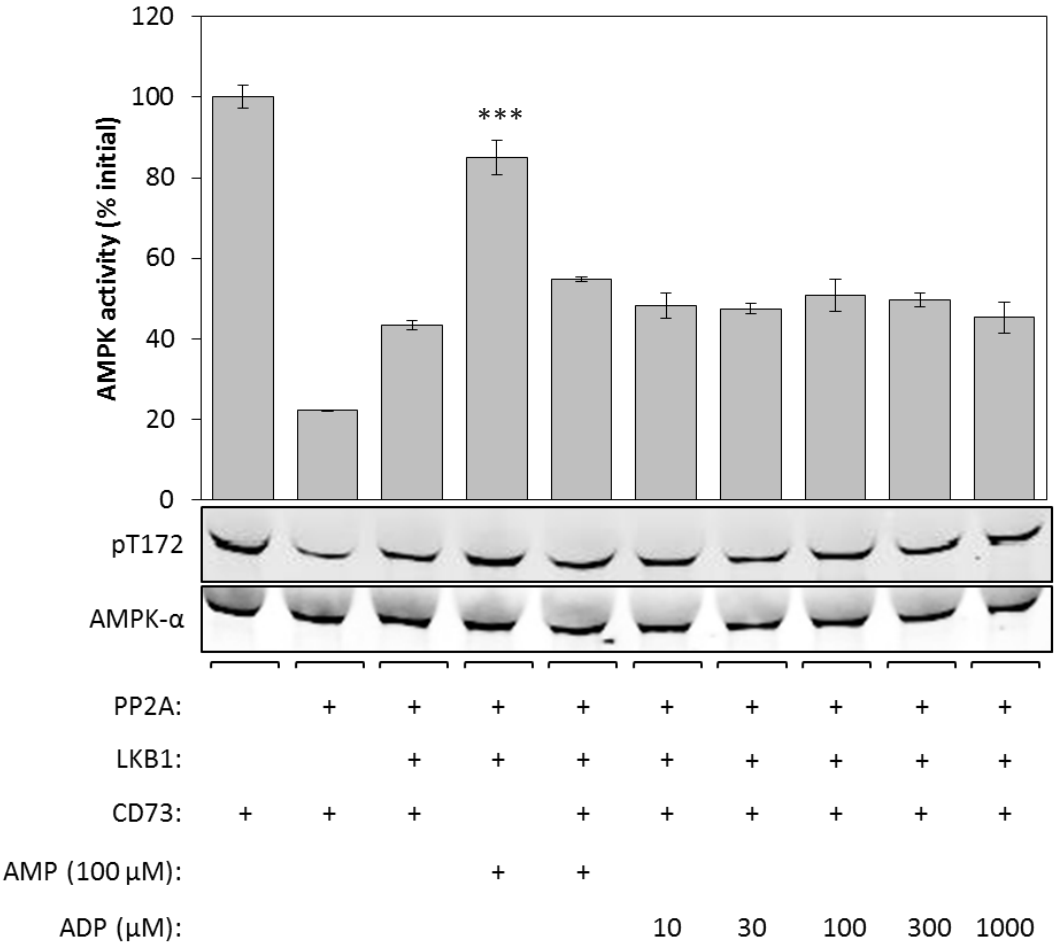

Figure 3.2: ADP does not promote phosphorylation of Thr172 by LKB1
Purified rat liver AMPK was incubated with bacterial $PP2A_c$ to give approximately 95% inactivation and the reaction stopped by the addition of okadaic acid. The kinase was then incubated with LKB1, with or without AMP or ADP. CD73 nucleotidase was included in all phosphorylation reactions to minimize the effects of contaminating AMP, with the exception of the AMP control reaction. Aliquots were taken for kinase assays using the AMARA peptide substrate (top) or Western blotting using the indicated antibodies (bottom). Kinase activities are expressed as % of the activity without $PP2A_C$ treatment and are mean ± SEM (n = 3). Significantly different from control without AMP by one-way ANOVA with Dunnett's multiple comparison test: ***$p < 0.001$.

Next, the concentration dependence of the AMP effect on LKB1-mediated Thr172 phosphorylation was determined (Fig. 3.3). AMP gave a maximum of 2.8 ± 0.2 fold stimulation of the activation rate, with a half-maximal effect (EC_{50}) of 160 ± 60 µM.

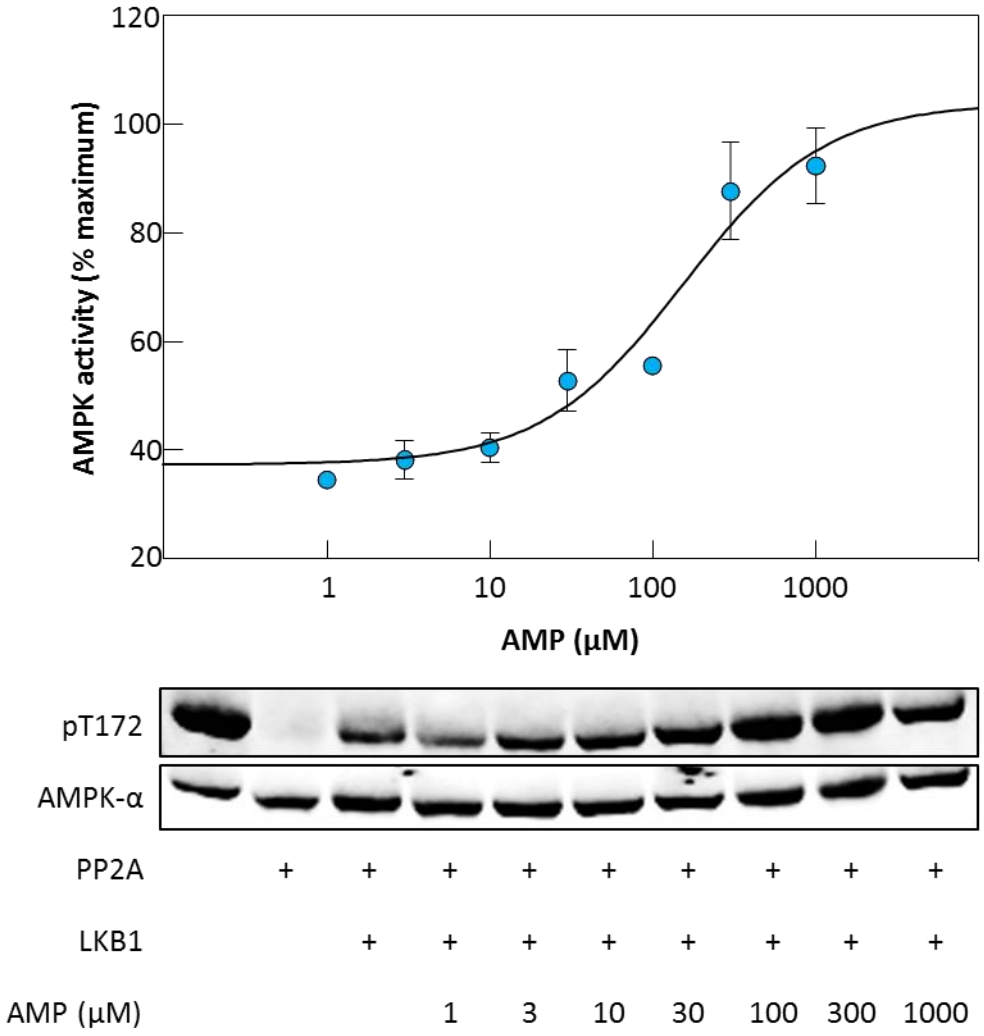

Figure 3.3: Titration of effect of AMP on LKB1-mediated Thr172 phosphorylation
Purified rat liver AMPK was incubated with bacterial $PP2A_c$ to give approximately 95% inactivation and the reaction stopped by the addition of okadaic acid. The kinase was then incubated with LKB1 and the indicated concentration of AMP. Aliquots were taken for kinase assays using the AMARA peptide substrate (top) or Western blotting using the indicated antibodies (bottom). Kinase activities are expressed as % of the activity without $PP2A_C$ treatment and are mean ± SEM (n = 3). Data were fitted to the equation: Y=basal + (((activation × basal-basal) × X)/(EC_{50}+X)), where Y is kinase activity and X is AMP concentration. The curve was generated using the following best-fit parameters: basal, 37 ± 3%; activation, 2.8 ± 0.2-fold; EC_{50}, 160 ± 60 μM.

The time courses of the effect of AMP and ADP on LKB1-mediated activation of AMPK were also investigated (Fig. 3.4). These data shows that AMP exerts its effects very rapidly: at the 2 minute time point the AMPK activity of the incubation with AMP was already twice that of the control incubation without AMP. ADP has no effect on the rate of activation up to the 10 minute time point that was used for the previous

experiments. At later time points, a small stimulatory effect of ADP was observed. However, it is likely that this effect is due to generation of AMP from ADP during the assay, as it was abolished by the addition of 5'-nucleotidase. This enzyme degrades AMP to adenosine, but has no effect on ADP or ATP (Fig. 3.5).

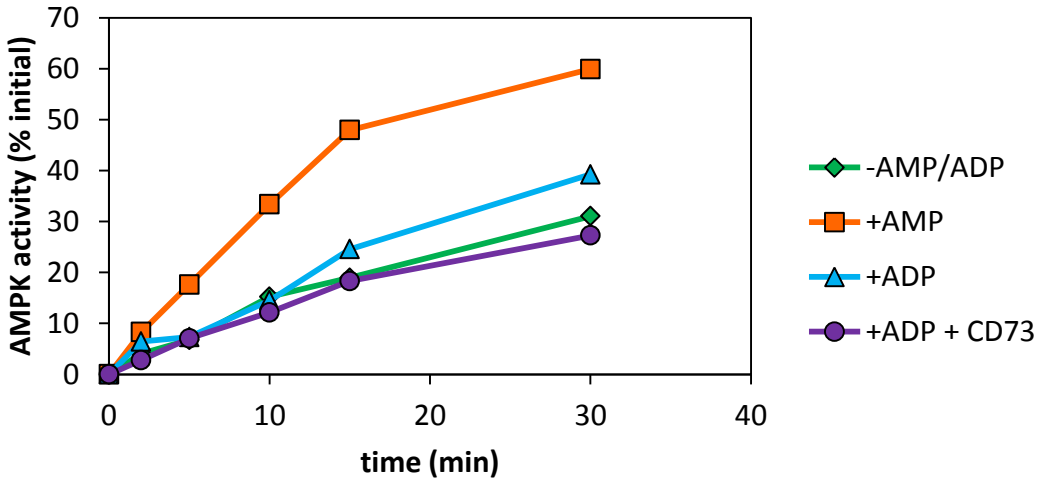

Figure 3.4: Timecourse of AMPK activation by LKB1
Purified rat liver AMPK was dephosphorylated with PP2Ac and the reaction stopped with okadaic acid. Kinase was then incubated with LKB1 either alone or with AMP (300 µM), ADP (300 µM) or ADP + CD73 nucleotidase. At each timepoint an aliquot was removed and the kinase activity determined using the AMARA peptide substrate. Kinase activities are expressed as % of the activity without $PP2A_C$ treatment.

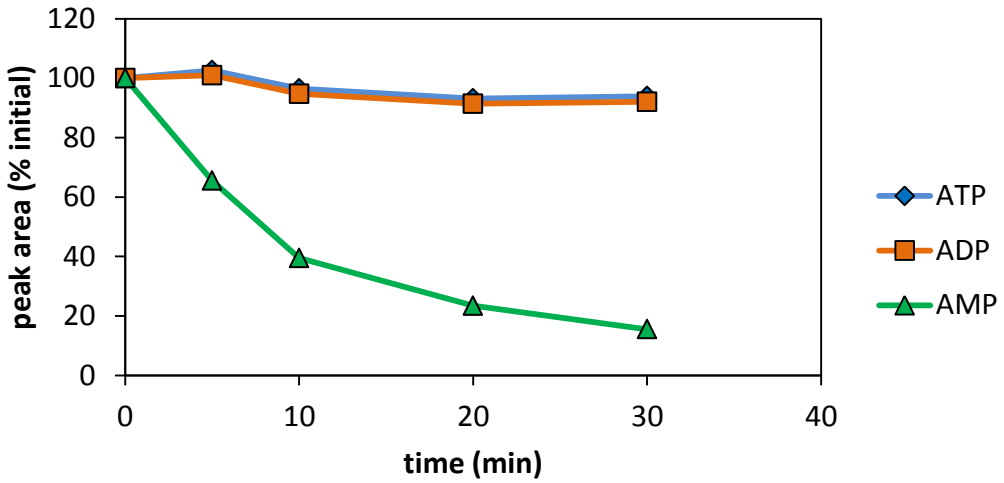

Figure 3.5: Effect of 5'-nucleotidase on AMP, ADP and ATP
AMP, ADP and ATP were incubated with 5'-nucleotidase at 30°C. Aliquots were removed and stored on ice prior to analysis by capillary electrophoresis. Results are expressed as % of initial peak area.

A769662, a direct allosteric activator of AMPK, can also protect the kinase against dephosphorylation (Göransson et al., 2007; Sanders et al., 2007a). The ability of A769662 to promote phosphorylation of Thr172 was investigated. Results in Fig. 3.6 show that, unlike AMP, A769662 has no effect on the rate of AMPK activation by LKB1. No effect of either AMP or A769662 was observed on the rate of AMPK activation by CaMKKβ. These results show that only AMP can promote Thr172 phosphorylation by LKB1.

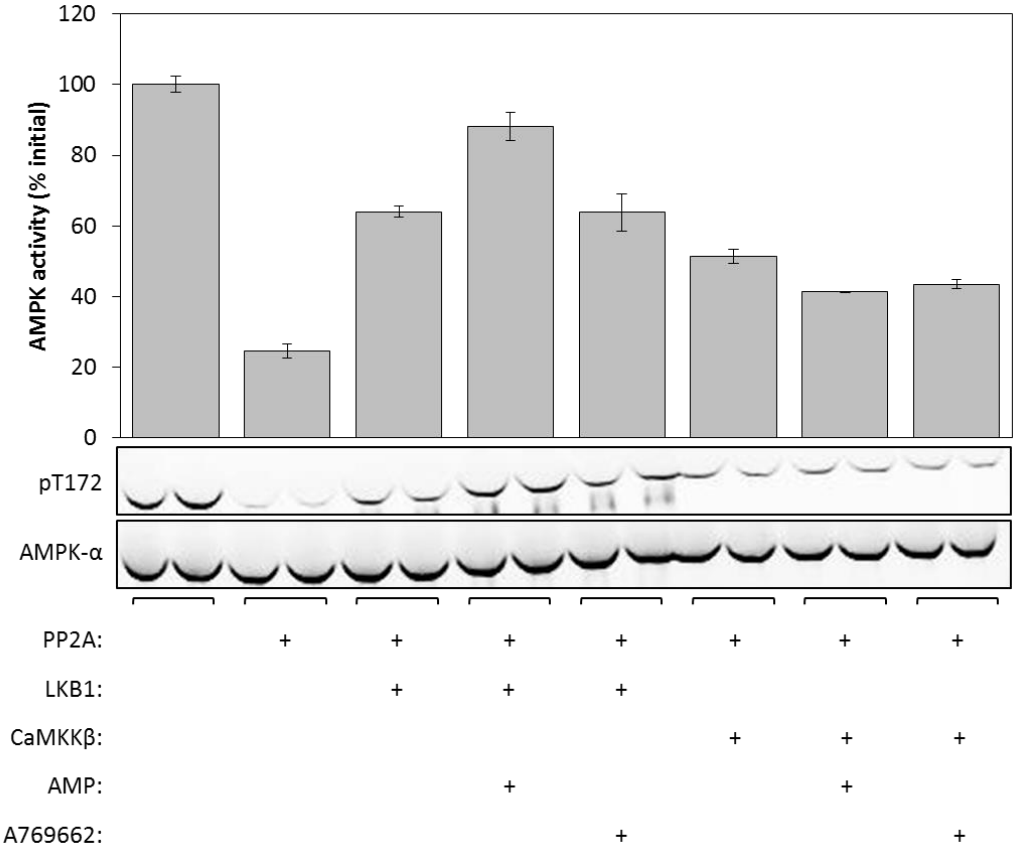

Figure 3.6: A769662 does not promote phosphorylation of Thr172
Purified rat liver AMPK was incubated with bacterial $PP2A_c$ to give approximately 95% inactivation and the reaction stopped by the addition of okadaic acid. The kinase was then incubated with LKB1 or CaMKKβ, with or without AMP (100 µM) or A769662 (1 µM). Aliquots were taken for kinase assays using the AMARA peptide substrate (top) or Western blotting using the indicated antibodies (bottom). Kinase assays were performed with either AMP (200 µM) or A769662 (1 µM) present, depending on which compound was present in the prior phosphorylation reaction. Kinase activities are expressed as % of the activity without $PP2A_C$ treatment and are mean ± range (n = 2). Results are representative of two independent experiments.

The effects of AMP on promotion of phosphorylation had previously been disputed on the basis that the effects could be explained by the contamination of one of the preparations with a Mg^{2+}-dependent protein phosphatase. If such a phosphatase was present, inhibition of dephosphorylation of Thr172 by AMP would lead to a net increase in phosphorylation. To rule this out, AMPK and LKB1 preparations were incubated with and without Mg^{2+} and the effect on Thr172 phosphorylation measured. Fig. 3.7 shows that Mg^{2+} had no effect on Thr172 phosphorylation, unless exogenous PP2C was also added to the incubation. This confirms that the effect of AMP on promotion of phosphorylation cannot be ascribed to phosphatase contamination.

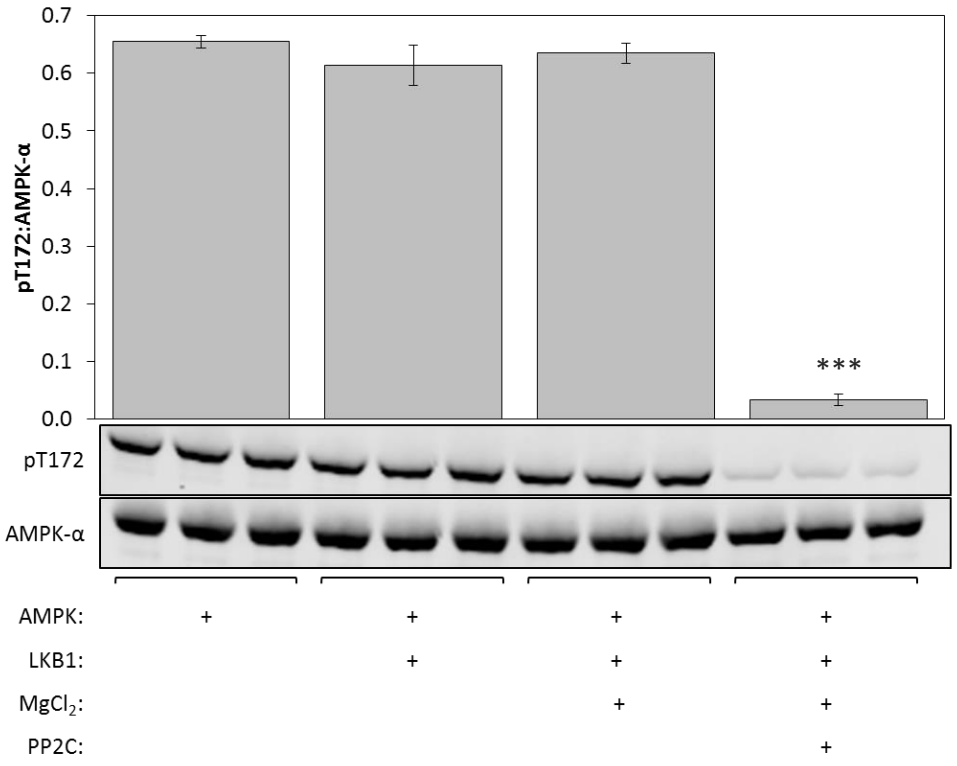

Figure 3.7: AMPK and LKB1 preparations are not contaminated with phosphatase
Purified rat liver AMPK was incubated ± LKB1, ± $MgCl_2$, ± PP2Cα for 15 minutes and samples analysed by Western blotting with the indicated antibodies. The bar chart shows the ratio of the signals obtained with anti-pThr172 and anti-AMPK-α antibodies (mean ± SEM, n = 3). Significantly different from control without AMP by one-way ANOVA with Dunnett's multiple comparison test: ***$p < 0.001$.

Recent work (Oakhill et al., 2010) had shown that the promotion of Thr172 phosphorylation was dependent on the β subunit of AMPK being myristoylated. A glycine residue at position 2 was identified as the target for this myristoylation (Mitchelhill et al., 1997; Oakhill et al., 2010). To investigate this, HEK293 cells stably expressing either wild-type (WT) or G2A mutant β1 or β2 subunits, all containing a C-terminal FLAG tag, were generated by Dr Fiona Ross. The expression of the recombinant protein was under the control of the tetracycline repressor. Expression of the recombinant protein, after 48 hr tetracycline treatment, was confirmed by anti-FLAG immunoblot (Fig. 3.8). As in Oakhill et al (2010), a small band shift was observed when comparing the WT and G2A mutant β-subunits.

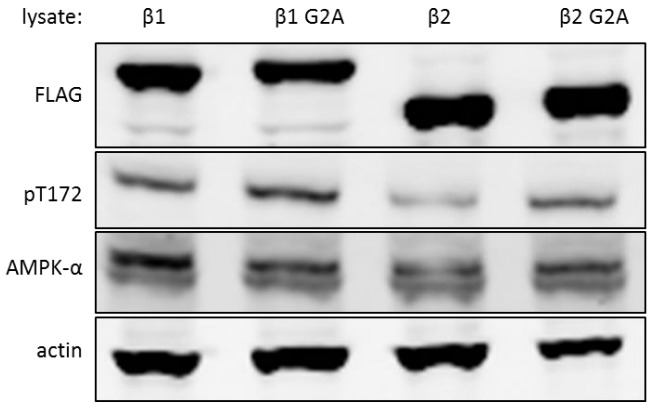

Figure 3.8: Generation of HEK293 cells expressing AMPK-β1 and AMPK-β2 mutants
DNAs encoding FLAG-tagged AMPK-β1 and AMPK-β2 (and G2A mutants) were inserted into HEK293 cells using Flp-In technology. The expression of the recombinant protein was under the control of a tetracycline repressor. To induce expression, tetracycline was added to the cells for 48 hr. Cells were harvested and subject to Western blotting using the indicated antibodies.

Treatment with the Ca^{2+} ionophore A23187, which activates CaMKKβ, caused an increase in pThr172 and pS79 ACC signals by measured by immunoblot (Fig 3.9A.), however, no AMPK activity was associated with the recombinant β subunit when anti-FLAG immunoprecipitates were assayed for AMPK activity (Fig. 3.9B).

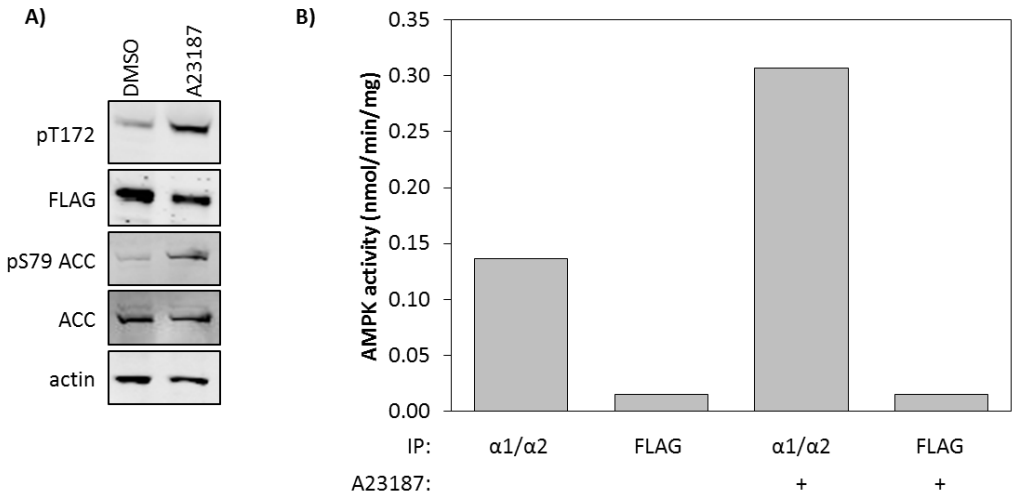

Figure 3.9: Characterisation of the HEK293 AMPK-β1 cell line
HEK293 cells were treated ± A23187 (10 µM) for 1 hr. **(A)** Cell lysates were subject to Western blotting using the indicated antibodies. **(B)** AMPK was immunoprecipitated from cell lysates using anti-AMPK-α1/α2 antibodies or anti-FLAG beads and AMPK activity determined using the AMARA substrate peptide. Results were similar for β1 [G2A], β2 and β2 [G2A] cell lines.

AMPK activity could, however, be detected when immunoprecipitation was performed using anti-AMPK-α1/-α2 antibodies. This suggested either that the recombinant-β subunit could not form a complex with the α and γ subunits, or that the complex was not catalytically active. To investigate this, cell lysates were incubated with either anti-FLAG or anti-AMPK-α1/-α2 antibodies. The supernatant from this incubation was then incubated with anti-AMPK-α1/-α2 antibodies. The immunoprecipitates were washed and kinase activity measured (Fig. 3.10). The results show that incubation with the anti-FLAG antibodies did not deplete any AMPK activity from the lysates, since the AMPK activities obtained before and after the anti-FLAG immunoprecipitation were very similar. This suggests that the recombinant β subunit is not able to form a complex with the other subunits – if it could, the AMPK activity measured after anti-FLAG immunoprecipitation should be much lower. Without the ability to selectively immunoprecipitate the mutant β complexes, attempts to investigate the requirement of β-myristoylation for promotion of phosphorylation were abandoned.

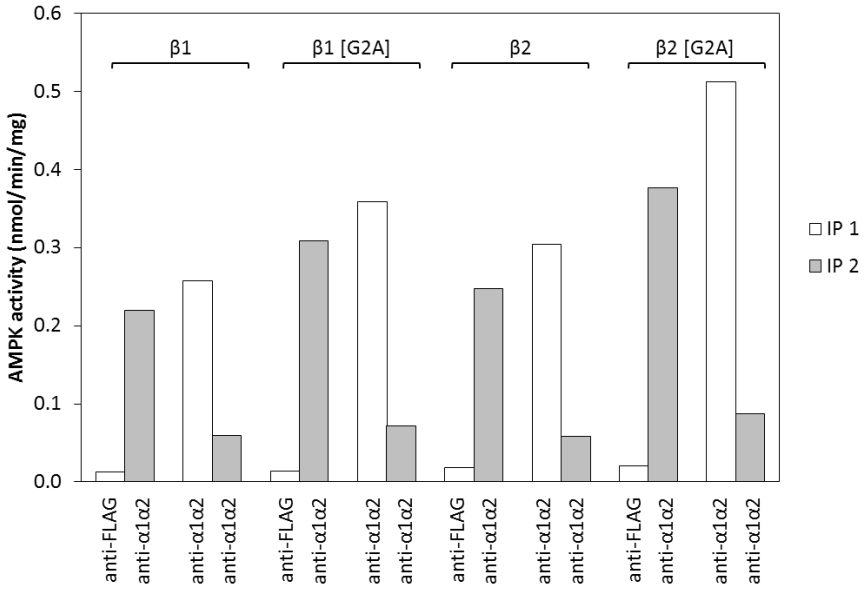

Figure 3.10: Recombinant AMPK-β cannot form a complex *in vitro*
AMPK activity was immunoprecipitated from HEK293 cell lysates (as indicated in figure) using either anti-AMPK-α1/-α2 antibodies or anti-FLAG beads. The supernatant from this IP was then subjected to a second IP using anti-AMPK-α1/-α2 antibodies. AMPK activity was determined for both sets of immunoprecipitates using the AMARA substrate peptide.

3.3.2 AMP is better than ADP at protecting AMPK against dephosphorylation

ADP has recently been reported to protect AMPK against dephosphorylation (Xiao et al., 2011). Using the preparation of rat liver AMPK, it was observed that both AMP and ADP could protect AMPK against PP2Cα-mediated Thr172 dephosphorylation and inactivation (Fig. 3.11, data courtesy of Dr Simon Hawley and Dr Fiona Ross). This confirmed the previous results of Xiao et al (Xiao et al., 2011). However, the results also show that AMP is more potent than ADP at protecting the kinase against inactivation. In experiments performed in the absence of ATP, the half-maximal effect of AMP on inactivation (EC_{50}) was 2.6 ± 0.3 μM. The EC_{50} for ADP was nearly 10-fold higher at 23 ± 3 μM. Assays were also performed at 5 mM ATP, a concentration that is within the level expected in mammalian cells (Imamura et al., 2009). ATP would be expected to compete with both AMP and ADP for binding at the γ subunit, and should

therefore increase the EC_{50} for both nucleotides. Consistent with this, the EC_{50} of AMP was increased to 196 ± 15 µM and that of ADP increased to 1.4 ± 0.1 mM. The almost 10-fold higher potency of AMP was thus retained under these conditions, again demonstrating that AMP is more potent than ADP at protecting the kinase against dephosphorylation of Thr172.

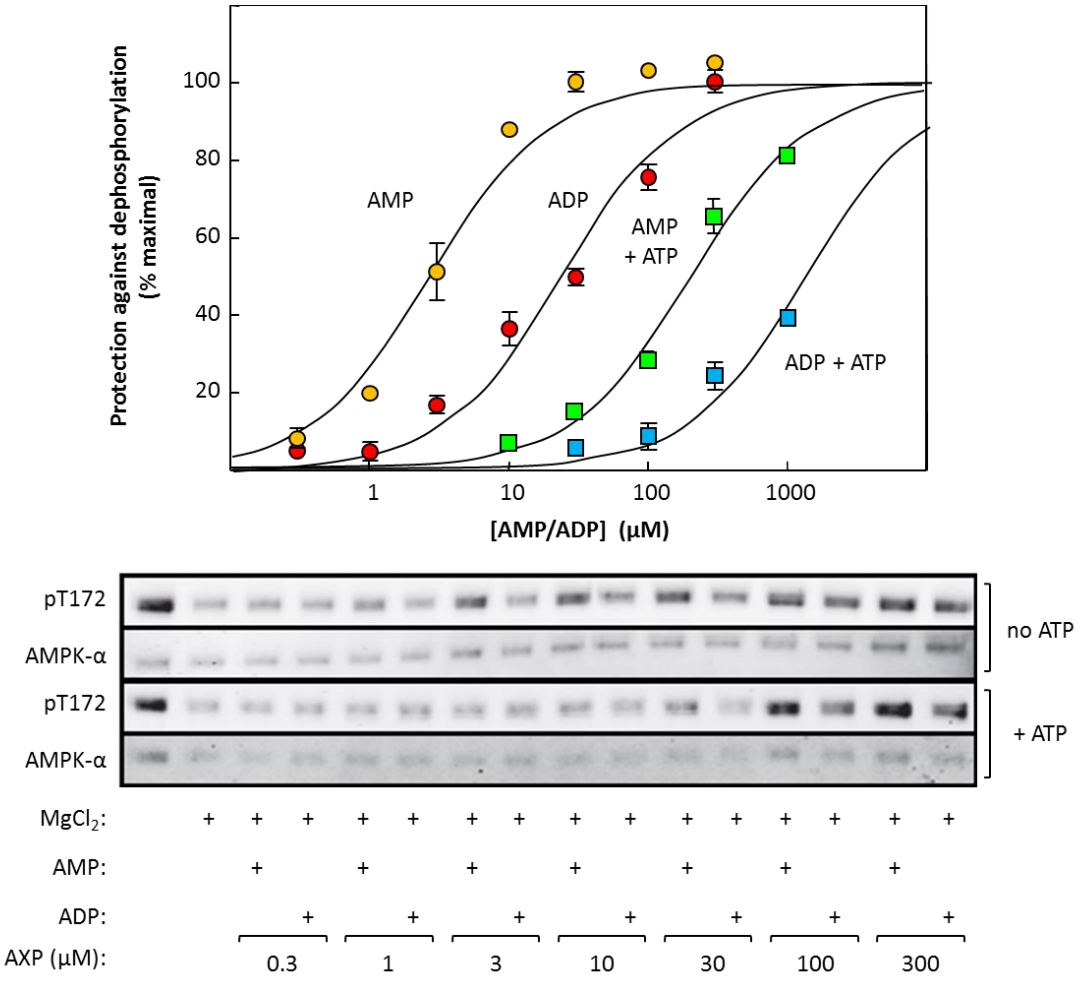

Figure 3.11: Effect of AMP and ADP on protecting AMPK from dephosphorylation
Purified rat liver AMPK was incubated with PP2Cα ± $MgCl_2$ ± ATP (5 mM) with or without AMP or ADP at the indicated concentrations. Aliquots were removed for kinase assays (top) and Western blotting (bottom). Kinase activities were determined using the AMARA substrate peptide. Protection against inactivation is defined as the activity differences in assays ± nucleotide, expressed as a percentage of the difference obtained ± optimal nucleotide (30 µM for AMP and 300 µM ADP, in the absence of ATP). Results are fitted to the equation $Y = 100 \times X/(EC_{50} + X)$ where Y = % protection and X = concentration of AMP or ADP. Curves were generated with this equation, using best-fit values for EC_{50} quoted in the text. Results are mean ± range (n = 2).

Commercial preparations of ADP, as used in these assays, are often contaminated with AMP. Analysis of the preparation used showed that this was at a level of ≈1% (Dr. Fiona Ross, personal communication). It is also likely that AMP is generated from ADP during incubations (Suter et al. 2006 and Fig. 3.4). As the difference in potencies between the nucleotides was approximately 10 fold, but the AMP contamination of the ADP preparations was only 1%, it did not seem likely that the effects of ADP on protection against dephosphorylation were caused by the small amounts of AMP present. However, to completely rule this out, the experiments were repeated using saturating amounts of the two nucleotides (100 µM AMP or 300 µM ADP) with and without the addition of 5'-nucleotidase. This enzyme, as discussed previously, hydrolyses AMP, but not ADP, to adenosine. The 5'-nucleotidase completely abolished the effects of AMP, but the effects of ADP were decreased only by a small amount (Fig. 3.12). This small reduction is likely to be due to the hydrolysis of the small amount of contaminating AMP, which, in 300 µM ADP, would be 3 µM. The remaining protection must have been caused by ADP, confirming that this is a bona fide regulator of Thr172 dephosphorylation.

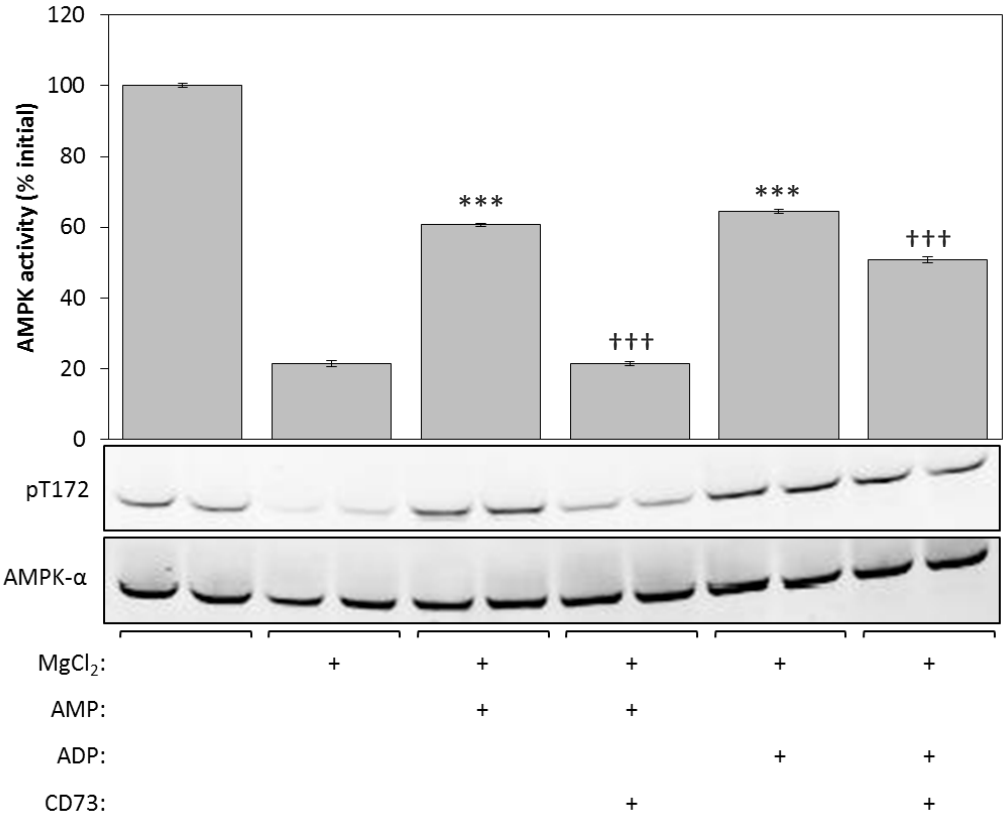

Figure 3.12: 5'-nucleotidase treatment abolishes the AMP-mediated, but not ADP-mediated, effects on protection against Thr172 dephosphorylation
Purified rat liver AMPK was incubated with PP2Cα ± $MgCl_2$ with or without AMP (100 µM), ADP (300 µM) or CD73 5'-nucleotidase as indicated. The nucleotides were pre-incubated with CD73 for 5 min at 30˚C before starting the reaction by the addition of AMPK. After 10 minutes, aliquots were removed for kinase assays (top) and Western blotting (bottom). Kinase activities were determined using the AMARA substrate peptide and are expressed as % of activity without $MgCl_2$ (mean ± SEM, n = 3). Significantly different from controls without AMP/ADP: ***p < 0.001; significantly different from control without CD73: †††p < 0.001.

3.3.3 Allosteric activation by AMP

As well as regulation of Thr172 phosphorylation, AMPK can also be regulated by allosteric activation. This allosteric activation is caused by AMP, but not ADP, binding to the γ subunit. The increase in AMPK activity in response to allosteric activation by AMP ranges has been reported as <2 fold with bacterially expressed heterotrimer (Sanders et al., 2007b; Suter et al., 2006) but seems to be consistently higher, ≈3-4 fold, when native AMPK purified from rat liver is used (Carling et al., 1987).

To determine if AMP is able to compete with ATP for binding at the site on the γ subunit responsible for allosteric activation, assays were performed not only at the standard ATP concentration (200 µM), but also at 1 mM and 5 mM ATP. These latter conditions mimic the higher concentrations of ATP that would be found in intact cells. The results in Fig. 3.13 (data courtesy of Dr Simon Hawley and Dr Fiona Ross) show that, at all three ATP concentrations tested, AMP activated AMPK at low concentrations and then inhibited at higher concentrations.

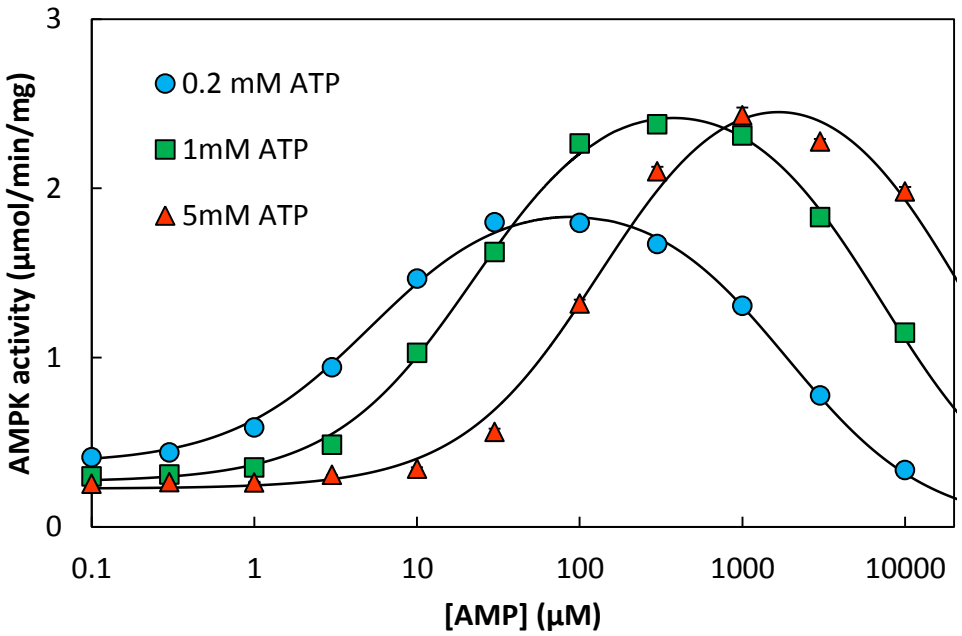

Figure 3.13: Allosteric activation of rat liver AMPK by AMP
Purified rat liver AMPK was incubated with increasing concentrations of AMP at three concentrations of ATP. Data were fitted to the equation: Y=basal + (((activation × basal-basal) × X)/(EC_{50} + X))-((activation × basal) × X/(IC_{50} + X)) where Y is activity and X is the AMP concentration. The curves were generated using this equation and the best-fit parameters quoted in the text. Results are mean ± range (n = 2).

To investigate the inhibitory effects observed at high concentrations of AMP, the AMPK-α1 and -α2 kinase domains were expressed as GST-fusions and purified from bacteria (Fig. 3.14). The kinase domains were incubated with LKB1 (as they are inactive when dephosphorylated) and then assayed in the presence of 0.2, 1 or 5 mM ATP and

a range of AMP concentrations. The results in Fig. 3.15 show that stimulation by AMP was no longer observed, but AMP did inhibit the kinase at high concentrations. Increasing the ATP concentration shifted the curve to the right, meaning that a higher concentration of AMP was required to inhibit the kinase domain. Taken together, these results show that the inhibitory effects of AMP are due to competition with ATP at the catalytic site.

The curves obtained in Fig. 3.13 also shifted to the right as ATP increased, supporting the idea that ATP competes at the activating site on the γ subunit and the catalytic site on the α subunit. The data was fitted to a simple model and the parameters obtained are outlined in Table 3.1. Thus, even when ATP is present at physiological concentrations, AMP caused a large allosteric activation of AMPK (13-fold).

	0.2 mM ATP	1 mM ATP	5 mM ATP
Fold activation	5.4 ± 0.2	10 ± 0.5	13 ± 1.3
EC_{50} for AMP activation	5.3 ± 0.4 µM	22 ± 1.1 µM	137 ± 14 µM
IC_{50} for AMP inhibition	1.9 ± 0.1 mM	7.1 ± 0.33 mM	22 ± 3 mM

Table 3.1: Parameters obtained from full length AMPK and kinase domains

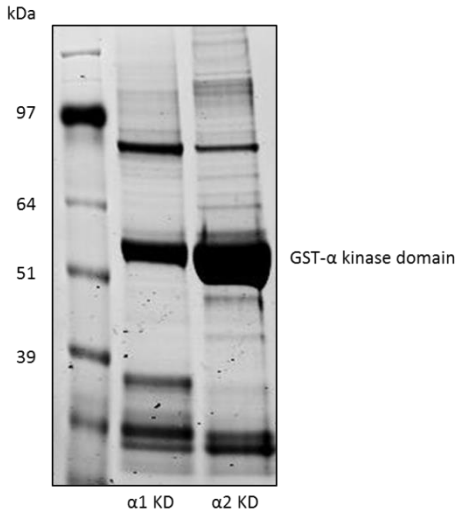

Figure 3.14: Purification of AMPK α1 and α2 kinase domains
GST-tagged AMPK-α1 and -α2 kinase domains were expressed in BL21 DE3 cells and purified using glutathione Sepharose columns. Purified protein was resolved by SDS-PAGE and stained using Coomassie Blue dye.

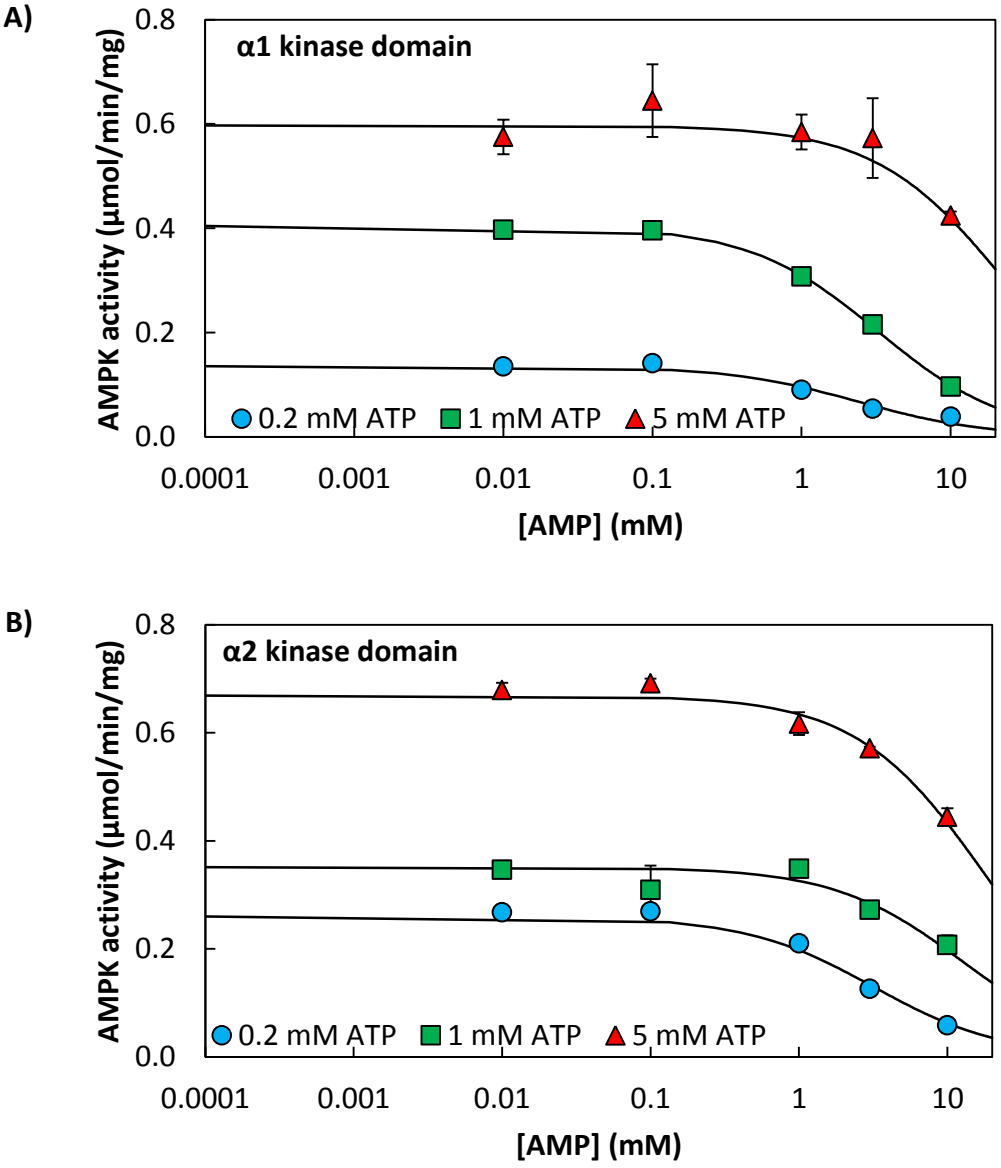

Figure 3.15: Effect of AMP on AMPK catalytic domains

GST fusions of AMPK-α1 **(A)** and -α2 **(B)** kinase domains were incubated with increasing concentrations of AMP at three concentrations of ATP. Kinase activities were determined using the AMARA peptide substrate. Results were fitted to the equation: Y = basal – (basal × X/IC_{50} + X), where Y = kinase activity and X is AMP concentration. The curves were generated using this equation and the following best-fit parameters (± SEM at 0.2, 1 and 5 mM ATP): α1 basal activity: 136 ± 5, 404 ± 6 and 598 ± 22 nmol/min/mg; IC_{50} for α1: 2.4 ± 0.4, 3.3 ± 0.3 and 23 ± 68 mM; α2 basal activity: 260 ± 6, 351 ± 7 and 669 ± 8 nmol/min/mg; IC_{50} for α2: 3.2 ± 0.4, 13 ± 1.4 and 18 ± 1.4 mM. Results are mean ± SEM (n = 3).

3.3.4 Allosteric activation of AMPK in intact cells

To determine the relative contribution of allosteric activation versus changes in Thr172 phosphorylation in the overall activation mechanism of AMPK, G361 cells were initially used. These cells, derived from a human melanoma, do not express LKB1 (Fig. 3.16).

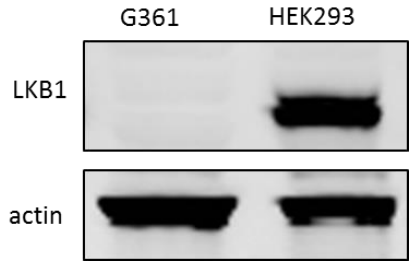

Figure 3.16: G361 cells do not express LKB1
Lysate from G361 cells and HEK293 cells were probed with the indicated antibodies.

These cells were a useful tool for these studies, because agents that increase cellular AMP do not increase Thr172 phosphorylation in LKB1-null cells (Hawley et al., 2003) so any effects observed should be entirely due to allosteric activation of the kinase. On the other hand, treatments that increase Ca^{2+}, and thus activate the CaMKKβ pathway, would activate AMPK entirely through increasing Thr172 phosphorylation. Since AMP would not be expected to increase Thr172 phosphorylation and therefore AMPK activity measured by kinase assay in an immunoprecipitate, it was necessary to use a downstream target of AMPK as a measurement of kinase activity in the intact cells. As discussed previously, AMPK phosphorylates ACC1 at S79, and phosphorylation of this site was used to monitor AMPK activity in response to a variety of treatments.

G361 cells were treated with the natural product berberine, an inhibitor of mitochondrial complex I (Hawley et al., 2010; Turner et al., 2008). As predicted, berberine did not increase Thr172 phosphorylation in these cells (Fig. 3.17) and no effect of berberine on AMPK activity was observed in well-washed

immunoprecipitates, where any bound AMP would have been removed from the kinase during the washing steps. In addition, the assays were carried out at 200 μM AMP, which, as seen in Fig. 3.13, is sufficient to give maximum allosteric activation of the kinase. These steps would therefore remove any effects of allosteric activation caused by endogenous AMP derived from the intact cells. As expected, the Ca^{2+} ionophore A23187 increased both Thr172 phosphorylation and kinase activity when measured in an immunoprecipitate. Although berberine had no effect on Thr172 phosphorylation, a large increase in phosphorylation of the downstream target ACC was nevertheless observed. An interesting observation was that the ACC phosphorylation in response to berberine was actually higher than that obtained with A23187, despite the finding that there was no increase in Thr172 phosphorylation.

The CaMKK inhibitor STO609 blocked the effects of A23187 on phosphorylation of Thr172 and AMPK activation. It also reduced the basal AMPK activity, suggesting that the low basal CaMKKβ activity was sufficient to generate some phosphorylation of Thr172. Interestingly, although the effects of berberine were reduced by STO609, they were not abolished.

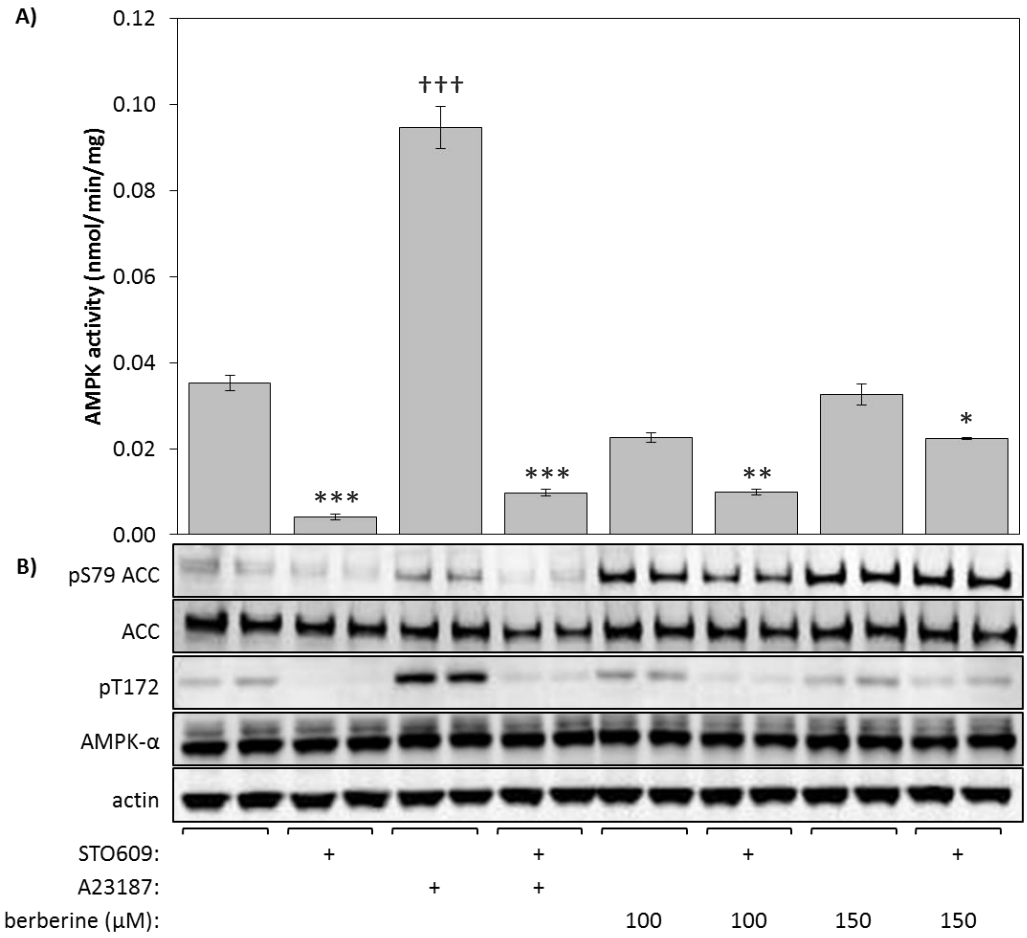

Figure 3.17: Effect of berberine on AMPK phosphorylation/activation in G361 cells
G361 cells were treated with A23187 (10 μM) or berberine (100/150 μM), in the presence or absence of STO609 (2.5 μM), for 1 hr. **(A)** AMPK was immunoprecipitated from the cell lysate using anti-AMPK-α1/-α2 antibodies and kinase activity measured using the AMARA peptide substrate. Results are mean ± SEM (n = 3). **(B)** Cell lysates were subject to Western blotting with the indicated antibodies. Significantly different from control without STO609: *p < 0.05, **p < 0.01, ***p < 0.001; significantly different from control without AMPK activator: †††p < 0.001.

Similar experiments were carried out using A769662, a direct AMPK activator. This compound does not alter cellular nucleotide ratios (Hawley et al., 2010), instead binding directly to AMPK at sites distinct from those on the γ subunit used by nucleotides (Göransson et al., 2007; Sanders et al., 2007a; Scott et al., 2008). The A769662 compound can allosterically activate the kinase as well as protect against Thr172 dephosphorylation. Like berberine, A769662 caused no increase in Thr172 phosphorylation or AMPK activity but did cause a large increase in ACC

phosphorylation (Fig. 3.18). The change in ACC phosphorylation in response to A769662 was similar to that of A23187, which did increase Thr172 phosphorylation.

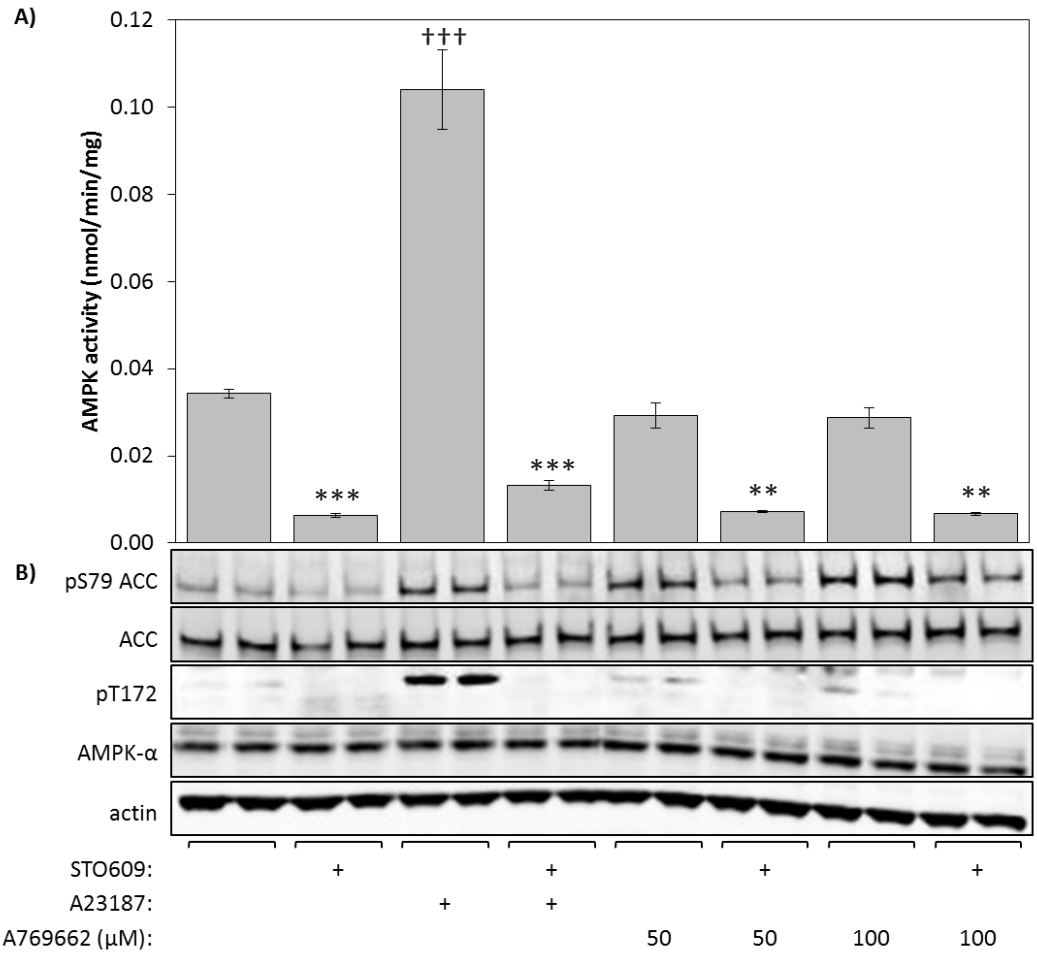

Figure 3.18: Effect of A769662 on AMPK phosphorylation/activation in G361 cells
G361 cells were treated with A23187 (10 μM) or A769662 (50/100 μM), in the presence or absence of STO609 (2.5 μM), for 1 hr. **(A)** AMPK was immunoprecipitated from the cell lysate using anti-AMPK-α1/-α2 antibodies and kinase activity measured using the AMARA peptide substrate. Results are mean ± SEM (n = 3). **(B)** Cell lysates were subject to Western blotting with the indicated antibodies. Significantly different from control without STO609: **p < 0.01, ***p < 0.001; significantly different from control without AMPK activator: ††† p < 0.001.

To further investigate the degree of ACC phosphorylation obtained with berberine and A23187, G361 cells were treated with each compound separately and together. The results (Fig. 3.19) show that the phosphorylation of ACC obtained with berberine alone is greater than that of A23187 alone and comparable to that obtained with dual treatment of berberine/A23187. This suggests that the ACC phosphorylation in

response to berberine is close to saturation as it cannot be increased further by changes in Thr172 phosphorylation. This data also suggests that AMPK phosphorylated on Thr172 can be further activated by allosteric activation – the ACC phosphorylation in response to A23187 alone is increased when berberine is included in the incubation.

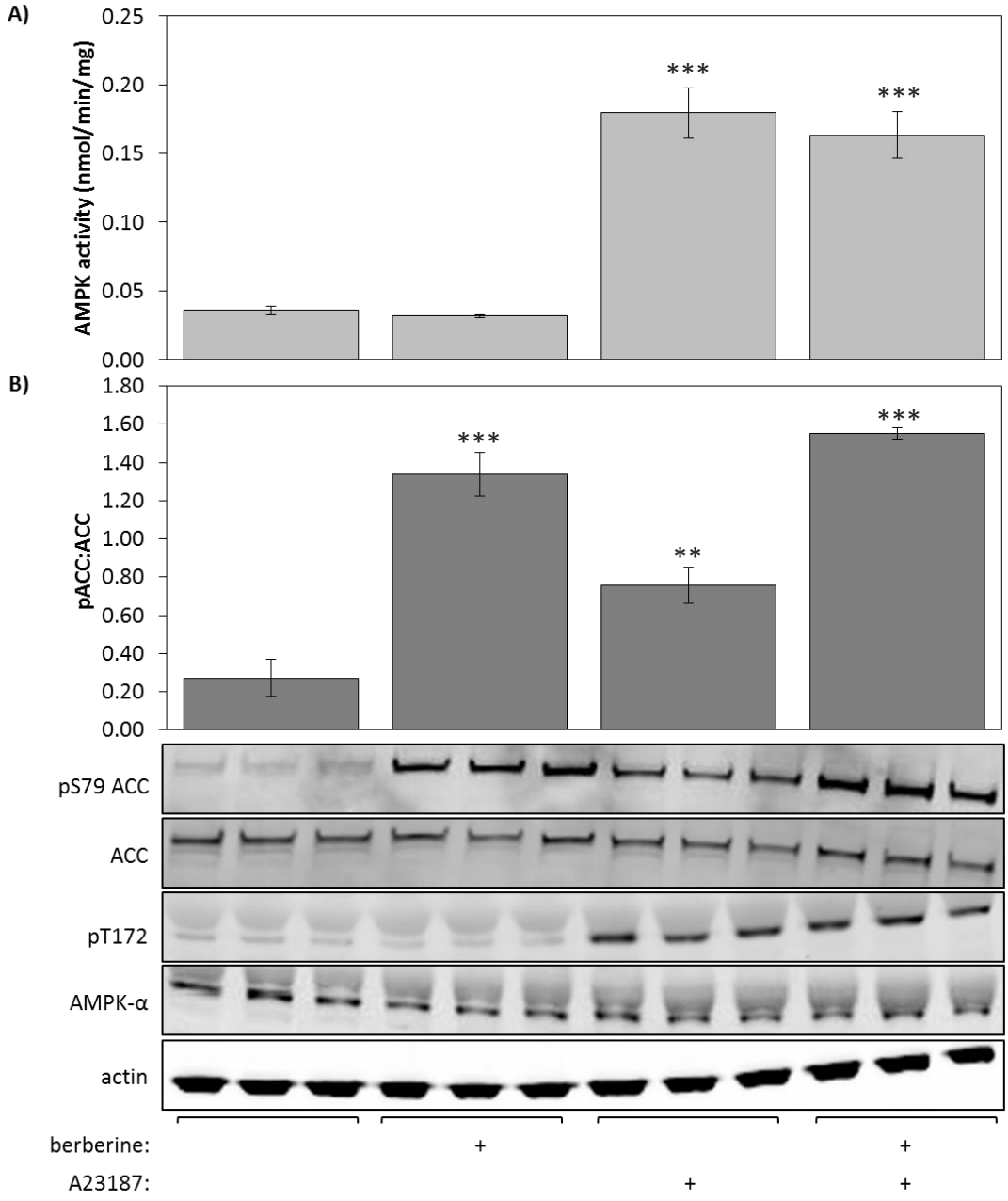

Figure 3.19: Effect of berberine and A23187 on activation of AMPK in G361 cells
G361 cells were treated with berberine (100 µM), A23187 (10 µM) or berberine and A23187 together for 1 hr. **(A)** AMPK was immunoprecipitated from cell lysates using anti-AMPK-α1/-α2 antibodies and kinase activity measured using the AMARA peptide substrate. Results are mean ± SEM (n = 3). **(B)** Cell lysates were subject to Western blotting with the indicated antibodies. The bar chart represents the pACC/total ACC ratio obtained from the blots (mean ± SEM, n = 3). Significantly different from control: **p < 0.01, ***p < 0.001.

The ability of mammalian AMPK to be allosterically activated was further examined. AMPK was immunoprecipitated from G361 cell lysates (± A23187 treatment) and assayed ± AMP (200 µM). Fig. 3.20 shows that the AMPK activity isolated from G361 cell lysates can be increased approximately two-fold in response to AMP. This is smaller than that obtained in Fig. 3.13 (using AMPK purified from rat liver) but this could be due to the kinase being bound to antibodies rather than free in solution. The restricted conformation of the antibody bound kinase may prevent the necessary structural changes required to give maximal allosteric activation in response to AMP. A recent report of the crystal structure of the AMPK heterotrimer suggested that the kinase does undergo conformational changes upon binding of AMP (Chen et al., 2012). The antibody bound conformation may therefore mimic this, giving a higher basal, or prevent this, giving decreased maximum activity, both of which could result in a lower fold activation than that observed with the kinase in solution.

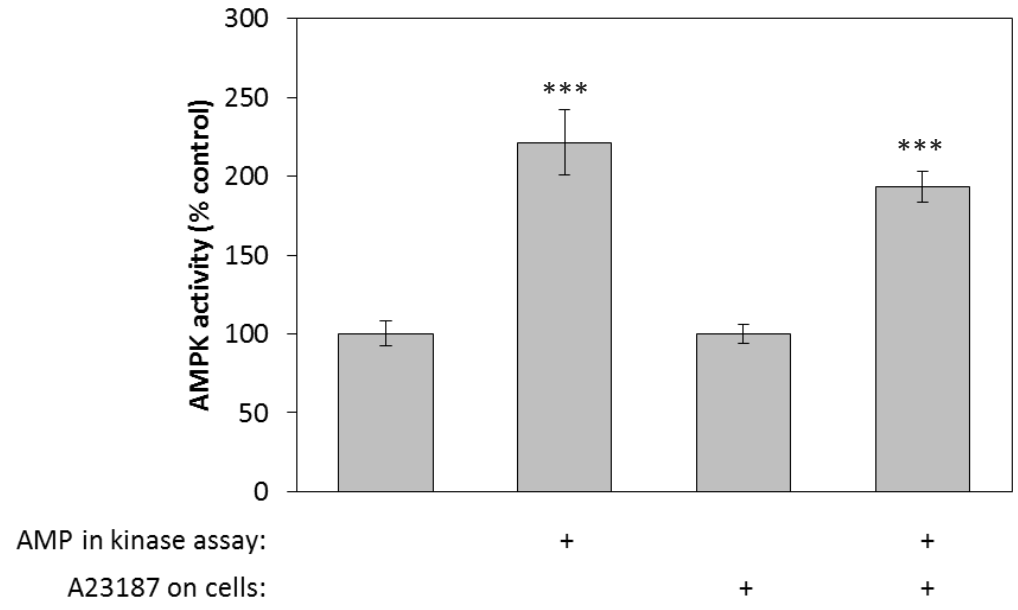

Figure 3.20: Allosteric activation of AMPK immunoprecipitated from G361 cells
AMPK was immunoprecipitated from G361 cell lysates (treated ± A23187 (10 µM) for 1 hr) using anti-AMPK-α1/-α2 antibodies. AMPK activities were then determined using the SAMS substrate peptide. Assays were performed ± AMP (200 µM). Results are mean ± SEM (n = 6) and are expressed as percentage of no AMP control. Significantly different from control without AMP: ***$p < 0.001$.

The effects of A23187, berberine and A769662 on AMPK activity, ACC phosphorylation and cellular nucleotides in G361 cells were investigated (Fig. 3.21). Like the previous experiments, all three compounds increased phosphorylation of ACC, with only A23187 having any effect on Thr172 phosphorylation or AMPK activity measured in washed immunoprecipitates. Berberine, a mitochondrial poison, caused an increase in the cellular ADP:ATP ratio. The other two compounds had no effect on this.

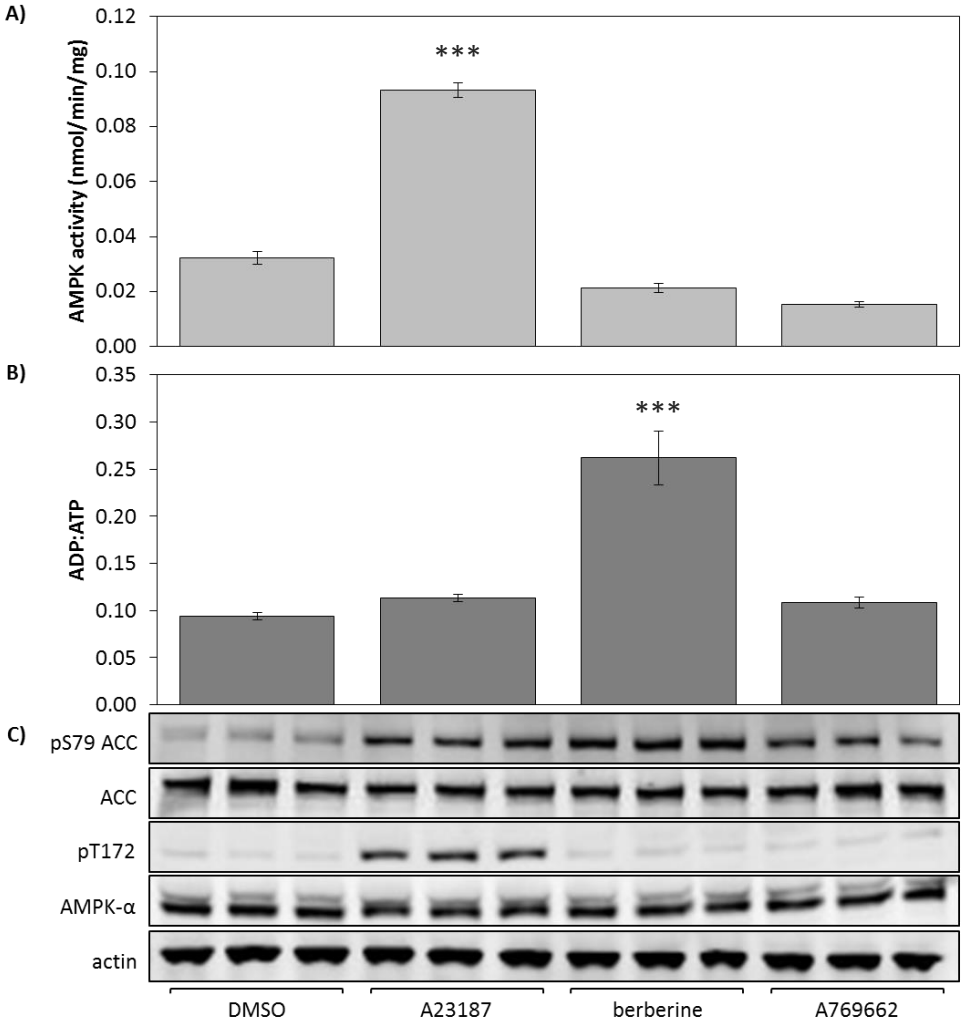

Figure 3.21: Effect of AMPK activators on G361 cellular nucleotides ratios
G361 cells were incubated for 1 hr with A23187 (10 µM), berberine (100 µM) or A769662 (100 µM) and lysed in parallel for analysis of AMPK activities or for analysis of ADP:ATP ratios. **(A)** AMPK was immunoprecipitated from cell lysates using anti-AMPK-α1/-α2 antibodies and kinase activity measured using the AMARA peptide substrate. Results are mean ± SEM (n = 3). **(B)** Samples lysed for nucleotide analysis were analysed by capillary electrophoresis and the ADP:ATP ratios estimated. Results are mean ± SEM (n = 3). **(C)** Cell lysates were subject to Western blotting with the indicated antibodies. Significantly different from DMSO control: ***$p < 0.001$.

Cellular AMP was too low to directly measure, so this was estimated from the ADP:ATP ratios. The derivation of this estimation is outlined below.

Adenylate kinase catalyses the reaction:

$$2ADP \leftrightarrow AMP + ATP$$

The equation for calculating the equilibrium constant is:

$$K(eq) = \frac{products}{reactants}$$

So for adenylate kinase:

$$K(eq) = \frac{AMP \times ATP}{ADP^2}$$

Rearranged to:

$$ATP \times AMP = K(eq) \times ADP^2$$

Divide each side by ATP^2 and simplify:

$$\frac{ATP \times AMP}{ATP^2} = \frac{K(eq) \times ADP^2}{ATP^2}$$

$$\frac{AMP}{ATP} = K(eq) \times \left(\frac{ADP}{ATP}\right)^2$$

This illustrates that the AMP:ATP ratio will increase as the square of the ADP:ATP ratio. The measurements from the cells allowed calculation of the ADP:ATP ratio. Using the equation above, and assuming that the equilibrium constant for adenylate kinase is 1.05 (Lawson and Veech, 1979), the AMP:ATP ratios could be estimated. From this information, it was possible to estimate the ATP, ADP and AMP concentrations in the cell extracts. The derivation of this is outlined below.

Assuming a total available intracellular pool of adenosine nucleotides of 5 mM gives:

$$[ATP] + [ADP] + [AMP] = 5\ mM$$

Divide each side by ATP:

$$\frac{[ATP]}{[ATP]} + \frac{[ADP]}{[ATP]} + \frac{[AMP]}{[ATP]} = \frac{5}{[ATP]}$$

Simplify:

$$1 + \frac{[ADP]}{[ATP]} + \frac{[AMP]}{[ATP]} = \frac{5}{[ATP]}$$

Multiply both sides of the equation by [ATP]:

$$\left(1 + \frac{[ADP]}{[ATP]} + \frac{[AMP]}{[ATP]}\right) \times [ATP] = 5$$

Solve for [ATP]:

$$[ATP] = \frac{5}{\left(1 + \frac{[ADP]}{[ATP]} + \frac{[AMP]}{[ATP]}\right)}$$

From this equation, and the AMP:ATP and ADP:ATP ratios previously calculated, the total [ATP] in the cell can be estimated. Using the AMP:ATP and ADP:ATP ratios, along with the [ATP], the [AMP] and [ADP] in the cell can then be estimated. This was performed for all of the samples and is outlined in Table 3.2. Fig. 3.22 shows the [AMP] and [AMP]:[ATP] ratio estimates for all samples.

	control	A23187	berberine	A769662
ADP:ATP	0.094	0.113	0.262	0.109
AMP:ATP	0.0093	0.0135	0.0737	0.0125
ATP (mM)	4.54	4.44	3.75	4.46
ADP (µM)	426	502	975	484
AMP (µM)	42.2	59.8	272.6	55.6

Table 3.2: Estimation of nucleotide concentrations and ratios in G361 cell extracts
The ADP:ATP ratio was measured by capillary electrophoresis and all other values were estimated from this information using the equations outlined above

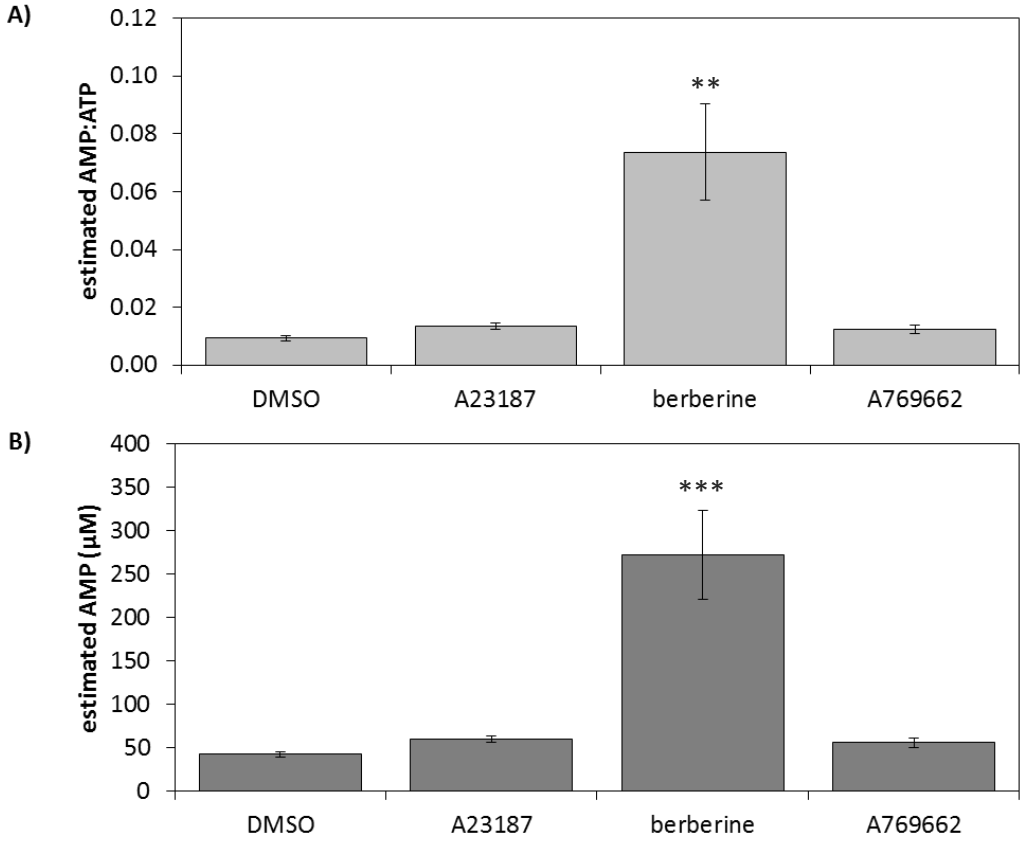

Figure 3.22: Estimate of cellular AMP:ATP ratios in G361 cells
Using the data from Fig. 3.21 and the assumptions outlined in section 3.3.4, the AMP concentrations **(A)** and AMP:ATP **(B)** ratios were estimated (mean ± SEM, n = 3). Significantly different from DMSO control: **p < 0.01, ***p < 0.001.

The estimated AMP concentrations do not increase significantly in response to A23187 or A769662 but rise dramatically in response to berberine, exhibiting a 6- to 7-fold increase from (42 ± 3 µM to 270 ± 50 µM).

3.3.5 Effect of salicylate, AICAR and other AMPK activators on G361 cells

Salicylate, the natural breakdown product of aspirin, is a direct activator of AMPK operating in a similar manner to the A769662 compound (Hawley et al., 2012). Salicylate binds to the β subunit and allosterically activates AMPK as well as protecting Thr172 from dephosphorylation. The effect of salicylate on G361 cells was examined. Treatment with salicylate increased the phosphorylation of ACC at S79 in a dose-

dependent manner while having no effect on either Thr172 phosphorylation or AMPK activity measured in well-washed immunoprecipitates (Fig. 3.23). The effects of 10 mM salicylate were comparable to those of berberine and A769662.

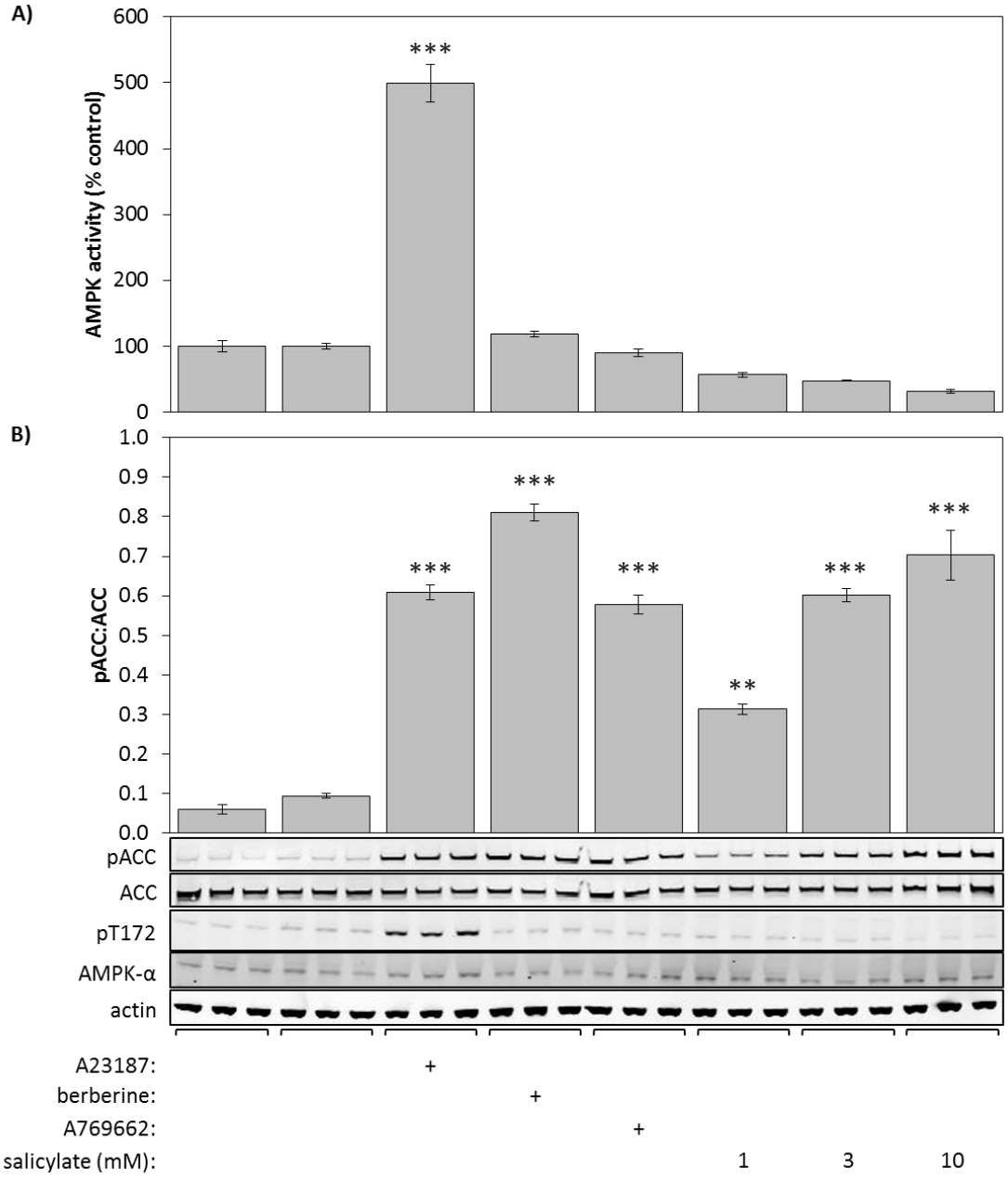

Figure 3.23: Effect of treatment of G361 cells with salicylate on AMPK activity
G361 cells were treated with A23187 (10 µM), berberine (100 µM) or salicylate (1, 3 or 10 mM) for 1 hr and lysed in parallel for analysis of AMPK activity (this figure) or for analysis of ADP:ATP ratios (Fig. 3.24). **(A)** AMPK was immunoprecipitated from cell lysates using anti-AMPK-α1/-α2 antibodies and kinase activity measured using the AMARA peptide substrate. Results are mean ± SEM (n = 3). **(B)** Cell lysates were subject to Western blotting with the indicated antibodies. The bar chart represents the pACC:total ACC ratio obtained from the Western blots. Results are mean ± SEM (n = 3). Significantly different from control: **p < 0.01, ***p < 0.001.

In HEK293 cells, it was demonstrated that at high concentrations (>10 mM) salicylate was acting as a relatively weak mitochondrial uncoupler and caused an increase in the ADP:ATP ratio (Hawley et al., 2012). To investigate if this was also the case in G361 cells, nucleotide ratios were also examined, from parallel dishes of cells to those in Fig. 3.23 (Fig. 3.24). The data shows that at concentrations of 3 mM and 10 mM, salicylate was causing a small but significant increase in the ADP:ATP ratio. The AMP:ATP and AMP, ADP, and ATP concentrations were estimated using the equations outlined in section 3.3.4. The estimates (Table 3.3 and Fig. 3.24) indicate that the concentration of AMP rose from 30 ± 5 μM to 48 ± 4 μM or 64 ± 1.2 μM (3 mM and 10 mM salicylate respectively).

These data is supported by that shown in Fig. 3.25, where the effect of salicylate on the oxygen consumption rate (OCR) of G361 cells was measured. This, like the ADP:ATP ratio, can be used to determine the effect of a compound on mitochondrial function. For example, DNP, a potent mitochondrial uncoupler, induces a large and rapid increase in OCR. This parameter has been used in the past to characterize the mechanism of action of a panel of AMPK activators (Hawley et al., 2010). Salicylate at 1 mM had no significant effect on OCR. However, as seen with the ADP:ATP ratios, salicylate at 3 and 10 mM caused a significant increase in OCR, confirming that it was disrupting mitochondrial function at these concentrations.

This data also confirms the effects of A23187, berberine and A769662. As expected, only berberine causes a change in OCR, the other two compounds have no effect. This is consistent with data obtained in HEK293 cells (Hawley et al., 2010).

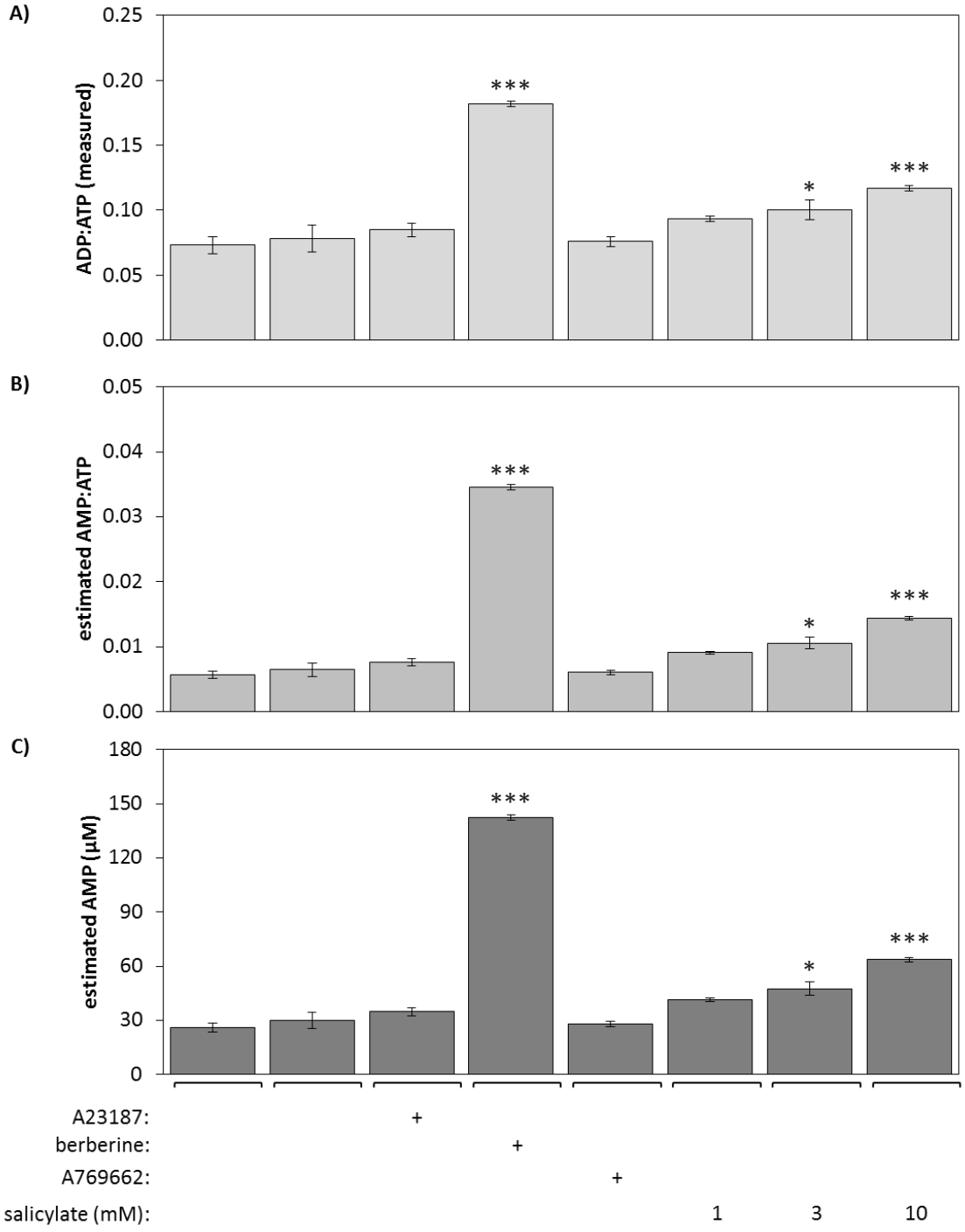

Figure 3.24: Effect of treatment of G361 cells with salicylate on nucleotide ratios
G361 cells were treated with A23187 (10 µM), berberine (100 µM) or salicylate (1, 3 or 10 mM) for 1 hr and lysed in parallel for analysis of AMPK activity (Fig. 3.23) or for analysis of ADP:ATP ratios (this figure). **(A)** Samples lysed for nucleotide analysis were analysed by capillary electrophoresis and the ADP:ATP ratios calculated. Results are mean ± SEM (n = 3). **(B)** and **(C)** using the data from (A) and the assumptions outlined in section 3.3.4, the AMP concentrations and AMP:ATP ratios were estimated. Significantly different from control: *$p < 0.05$, ***$p < 0.001$.

	DMSO	H2O	A23187	berb	A76	Sal 1 mM	Sal 3 mM	Sal 10 mM
ADP:ATP	0.073	0.078	0.085	0.182	0.076	0.093	0.100	0.117
AMP:ATP	0.0056	0.0065	0.0076	0.0346	0.0060	0.0091	0.0106	0.0144
ATP (mM)	4.64	4.61	4.11	4.54	4.50	4.42	4.62	4.58
ADP (µM)	338	360	746	422	451	517	350	389
AMP (µM)	26	30	35	142	28	41	48	64

Table 3.3: Estimation of nucleotide concentrations and ratios in G361 cell extracts
The ADP:ATP ratio was measured by capillary electrophoresis and all other values were estimated from this information using the equations outlined in section 3.3.4.

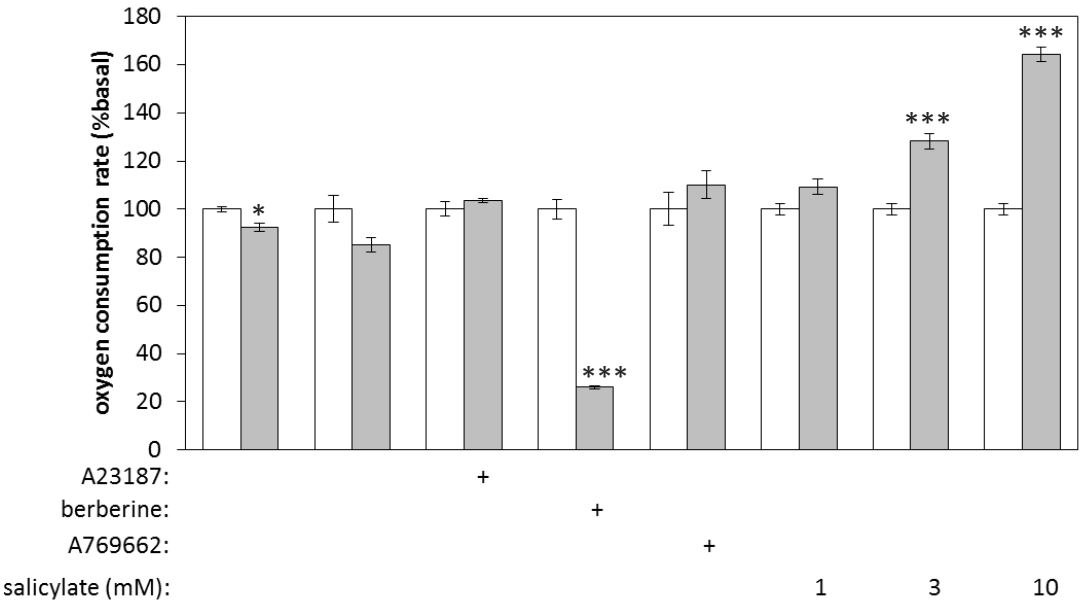

Figure 3.25: Effect of AMPK activators on the oxygen consumption rate of G361 cells
Oxygen consumption rate (OCR) analysis was performed using a Seahorse Biosciences extracellular flux analyser. G361 cells were seeded into plates and the basal OCR calculated for every well. A23187 (10 µM), berberine (100 µM), A769662 (100 µM) or salicylate (1, 3 or 10 mM) were then injected onto the cells and the OCR calculated over a 30 min period. Results are expressed as % of basal OCR before (clear bars) and after (grey bars) compound injection (mean ± SEM, n = 3). Significantly different from control before compound injection: *$p < 0.05$, ***$p < 0.001$.

5-Aminoimidazole-4-carboxamide ribonucleoside (AICAR) is a widely used activator of AMP. AICAR enters cells where it is converted to the monophosphate form 5-aminoimidazole-4-carboxamide ribonucleoside monophosphate (ZMP) (Sabina et al., 1985), an AMP mimetic, and causes allosteric activation of AMPK and protection against dephosphorylation (Corton et al., 1995). The measured fold allosteric activation of AMPK in response to ZMP is similar to that obtained with AMP, around 3-6 fold, although the latter has a much lower half-maximal effect (4.4 μM for AMP vs 164 μM for ZMP).

G361 cells were treated with increasing concentrations of AICAR for 1 hr and lysed in parallel for analysis of AMPK activity and cellular nucleotides. Similar to berberine, AICAR induced phosphorylation of ACC with no increase in AMPK activity or Thr172 phosphorylation (Fig. 3.26A and B). Analysis of the nucleotides samples obtained showed that, compared to untreated samples, a novel peak appeared in the AICAR-treated samples and increased with AICAR dose (Fig. 3.27A). The identity of this peak was confirmed as ZMP by spiking samples with an internal standard of purified ZMP (data not shown) and Fig. 3.27B shows the ZMP:ATP ratios from G361 cell extracts.

There was also no detectable increase in cellular ADP:ATP or AMP:ATP ratios (Fig. 3.26C, D and E), the latter calculated as outlined in section 3.2.4. This suggested that the effects of AICAR were due to conversion into ZMP. This data again illustrates that allosteric activation of the AMPK, regardless of the molecule causing it, can make a significant contribution to the overall activation mechanism.

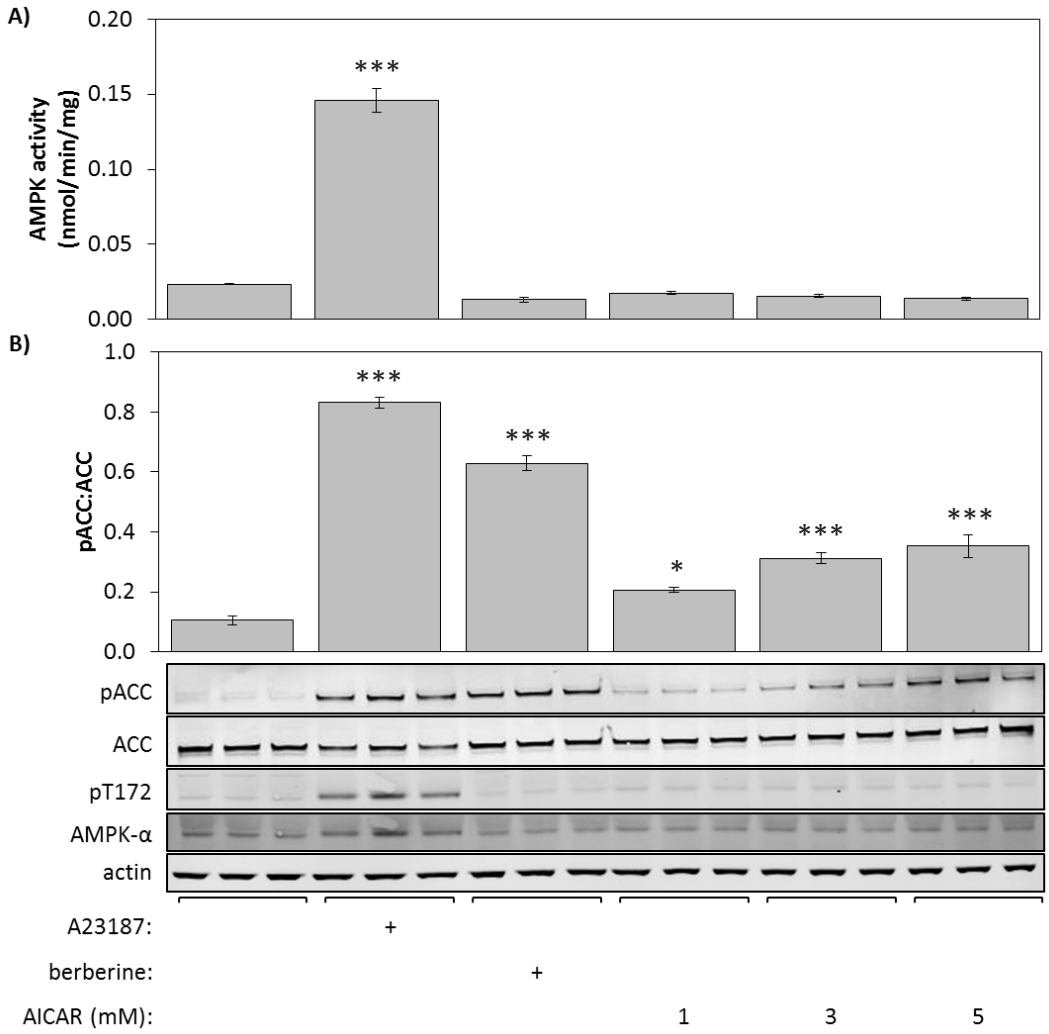

Figure 3.26: Effect of treatment of G361 cells with AICAR

G361 cells were treated with A23187 (10 µM), berberine (100 µM) or AICAR (1, 3 or 5 mM) for 1 hr and lysed in parallel for analysis of AMPK activity or for analysis of nucleotide ratios. **(A)** AMPK was immunoprecipitated from cell lysates using anti-AMPK-α1/-α2 antibodies and kinase activity measured using the AMARA peptide substrate. **(B)** Cell lysates were subject to Western blotting with the indicated antibodies. The bar chart represents the pACC:total ACC ratio obtained from the Western blots. **(C)** Samples lysed for nucleotide analysis were analysed by capillary electrophoresis and the ADP:ATP ratios calculated. **(D)** and **(E)**: using the data from (C) and the assumptions outlined in section 3.2.4, the AMP concentrations and AMP:ATP ratios were estimated. Results are mean ± SEM (n = 3). Significantly different from control: *$p < 0.05$, ***$p < 0.001$.

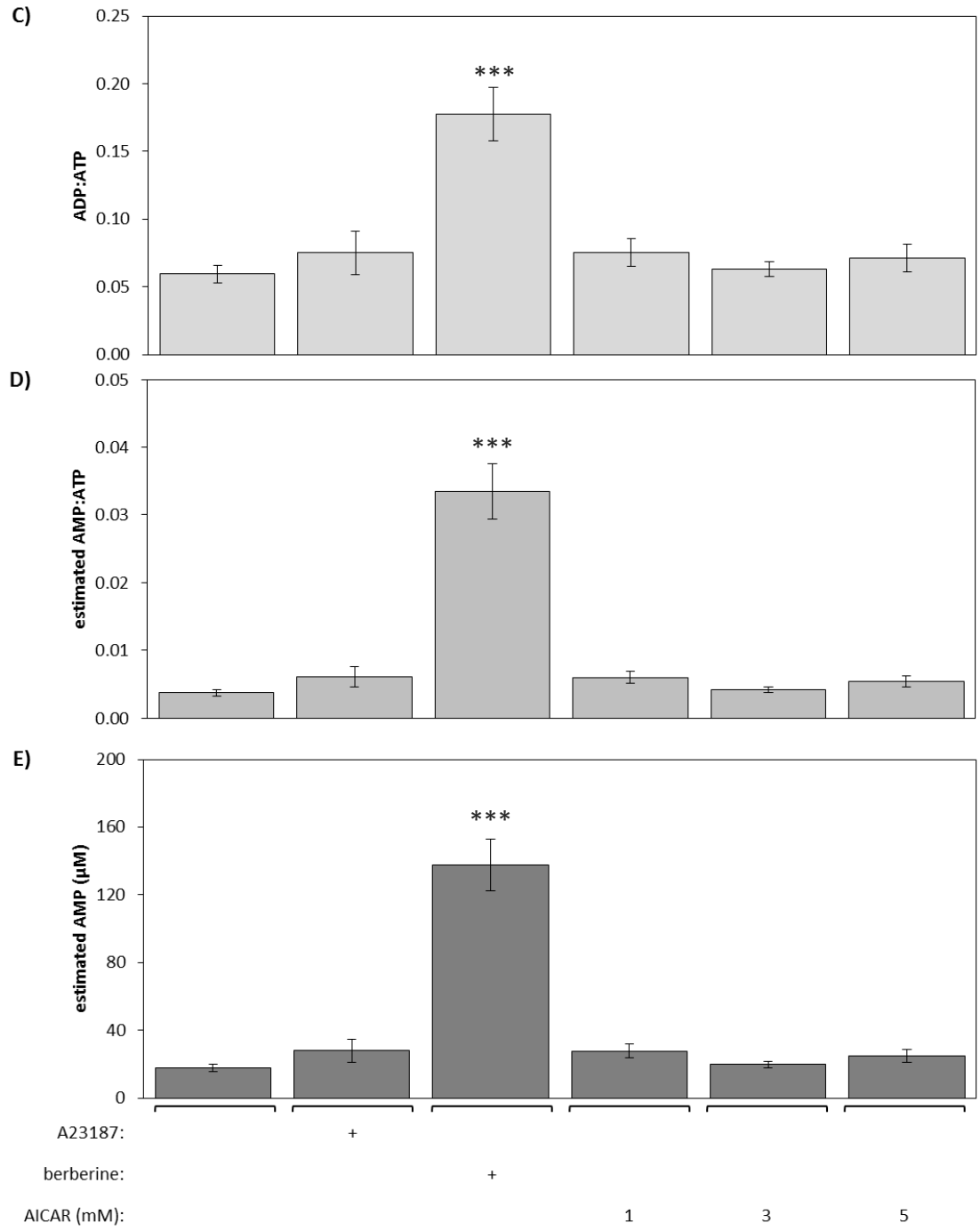

Figure 3.26: Effect of treatment of G361 cells with AICAR (continued)

G361 cells were treated with A23187 (10 µM), berberine (100 µM) or AICAR (1, 3 or 5 mM) for 1 hr and lysed in parallel for analysis of AMPK activity or for analysis of nucleotide ratios. **(A)** AMPK was immunoprecipitated from cell lysates using anti-AMPK-α1/-α2 antibodies and kinase activity measured using the AMARA peptide substrate. **(B)** Cell lysates were subject to Western blotting with the indicated antibodies. The bar chart represents the pACC:total ACC ratio obtained from the Western blots. **(C)** Samples lysed for nucleotide analysis were analysed by capillary electrophoresis and the ADP:ATP ratios calculated. **(D)** and **(E)**: using the data from (C) and the assumptions outlined in section 3.2.4, the AMP concentrations and AMP:ATP ratios were estimated. Results are mean ± SEM (n = 3). Significantly different from control: *p < 0.05, ***p < 0.001.

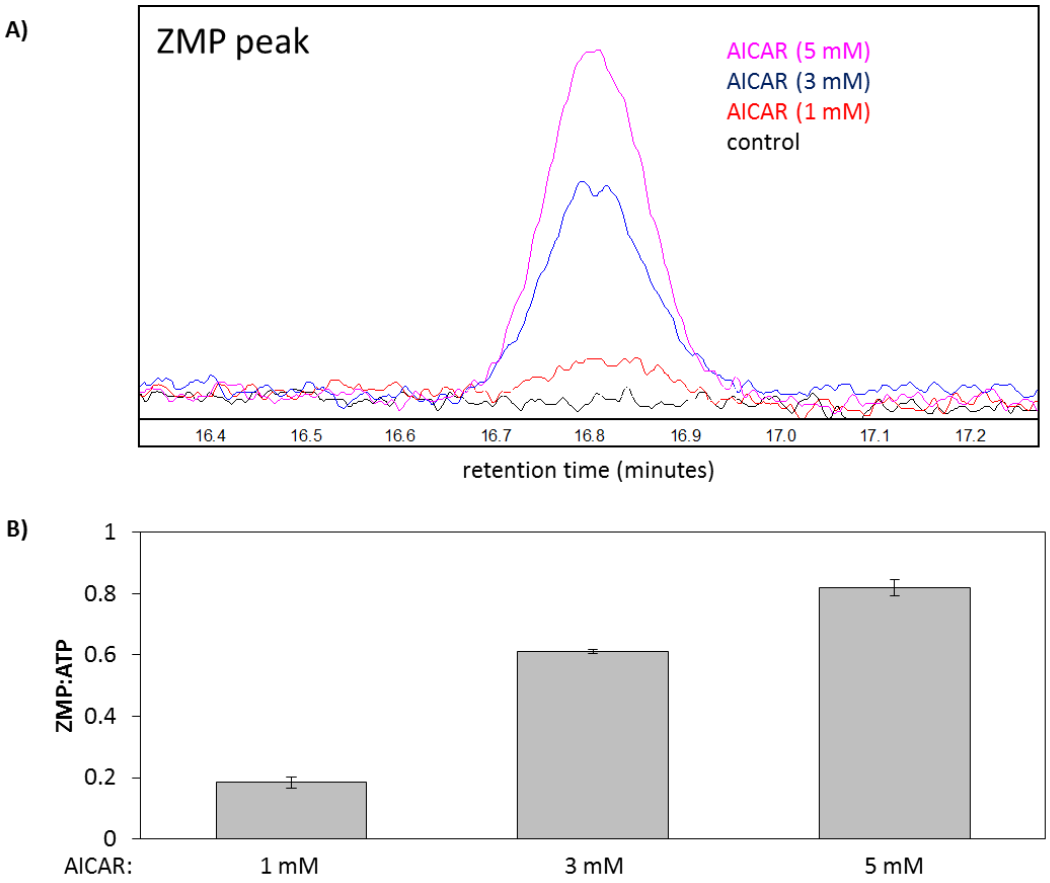

Figure 3.27: AICAR increases intracellular ZMP levels
G361 cells were treated with AICAR (1, 3 or 5 mM) for 1 hr and lysed in parallel for analysis of AMPK activity or for analysis of nucleotide ratios (same samples as Fig. 3.25). **(A)** ZMP peaks obtained from control and AICAR treated samples. Peak identity was confirmed by spiking samples with purified ZMP (data not shown). **(B)** ZMP:ATP ratio from AICAR treated samples (mean ± SEM, n = 3).

In addition to berberine, there exist a large variety of compounds that activate AMPK in an AMP-dependent manner. Many of these compounds are natural plant products used in traditional medicine. These compounds have been shown previously to disrupt mitochondrial function and increase the ADP:ATP ratio (Hawley et al., 2010). G361 cells were treated with: phenformin, a biguanide closely related to the anti-diabetic drug metformin; 2,4-dintrophenol (DNP), a proton ionophore that collapses the mitochondrial H^+ gradient; troglitazone, a member of the thiazolidinedione family of anti-diabetics and quercetin, a plant flavonoid (Fig. 3.28). All of the compounds tested

displayed similar effect to berberine in that they increased ACC phosphorylation with no detectable increase of Thr172 phosphorylation.

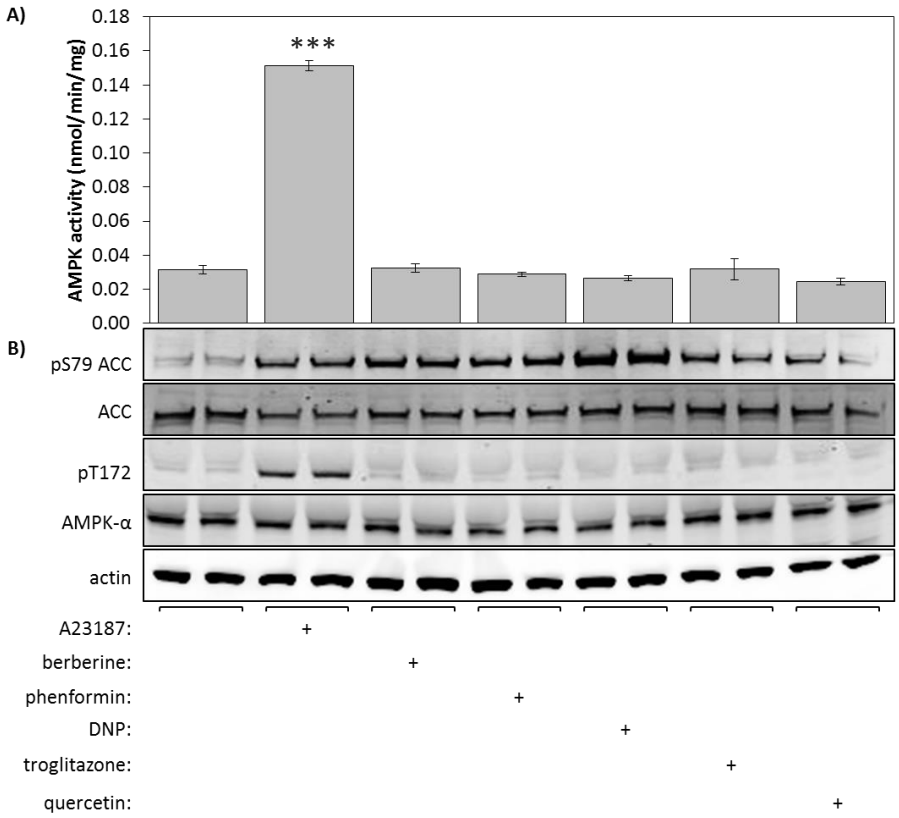

Figure 3.28: Effect of treatment of G361 cells with a range of AMPK activators
G361 cells were treated with A23187 (10 µM), berberine (100 µM), phenformin (3 mM), DNP (300 µM), troglitazone (40 µM), or quercetin (150 µM) for 1 hr. **(A)** AMPK was immunoprecipitated from the cell lysate using anti-AMPK-α1/-α2 antibodies and kinase activity measured using the AMARA peptide substrate. Results are mean ± SEM (n = 3). **(B)** Cell lysates were subject to Western blotting with the indicated antibodies. Significantly different from DMSO control: ***$p < 0.001$.

3.3.6 ACC phosphorylation is mediated by AMPK

To confirm that ACC phosphorylation is mediated by AMPK, wild-type (WT) and AMPK-$\alpha1^{-/-}$-$\alpha2^{-/-}$ double knockout (dKO) mouse embryonic fibroblasts (MEFs) were treated with a number of AMPK activators, and the effects on AMPK and ACC phosphorylation determined (Fig. 3.29). Results show that, while ACC phosphorylation is increased in the WT MEFs in response to these compounds, no effect is seen in the dKO MEFs, confirming the necessity of AMPK for ACC phosphorylation.

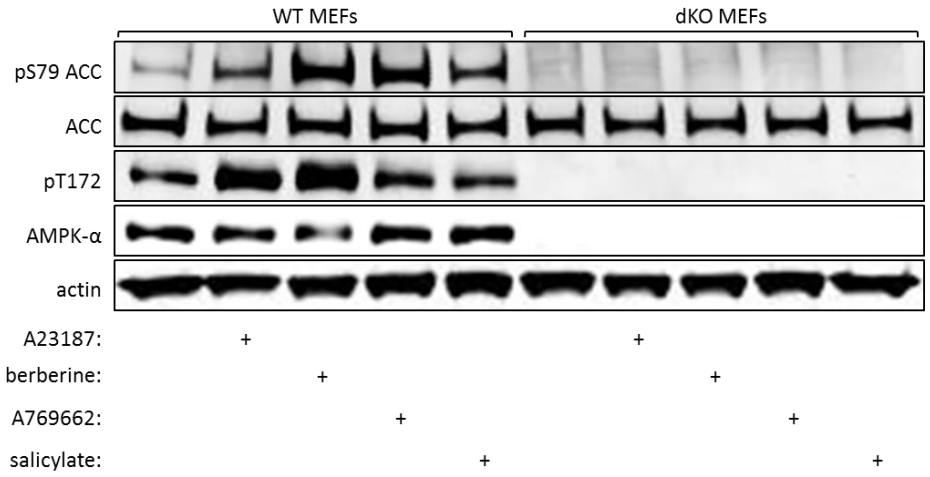

Figure 3.29: Evidence that ACC phosphorylation in MEFs is mediated by AMPK
Wild-type (WT) and AMPK-$\alpha1^{-/-}$-$\alpha2^{-/-}$ double knockout (dKO) mouse embryo fibroblasts were treated with A23187 (10 µM), berberine (300 µM), A769662 (300 µM) or salicylate (10 m M) for 1 hr. Cell lysates were subjected to Western blotting with the indicated antibodies.

G361 cells stably expressing a dominant negative AMPK-α2 mutant (D157A) were also generated. G361 cells predominantly express AMPK-α1 and by expressing the AMPK-α2 mutant it was hoped that this would compete with the endogenous α1 subunit for binding to the β and γ subunits. As AMPK is stable in a cell only as a heterotrimer, this would act as a dominant negative mutant cell line with the kinase dead α2 replacing the wild-type α1 in the heterotrimer, with the latter being degraded. This approach has been successfully used in a previous study from our laboratory (Hawley et al., 2010) where HEK293 cells overexpressing an AMP-insensitive γ subunit no longer responded to any treatment that activated AMPK through changes in AMP levels. Fig. 3.30 (data courtesy of Dr Fiona Ross) shows that treatment of the dominant-negative G361 cells with A23187 gave an AMPK activity ≈30% that of wild-type cells. This is similar to the reduction in basal activity observed and indicates that, in contrast to the results obtained with HEK293 cells, the expression of the kinase-dead α2 subunit is not sufficient to completely replace the active, endogenous α1, and a small amount of

active kinase remains. Despite this, the increase in ACC phosphorylation was reduced by a similar degree to the measured AMPK activity in the dominant negative cells. ACC phosphorylation induced by A769662 was also reduced by a similar amount (Fig. 3.30).

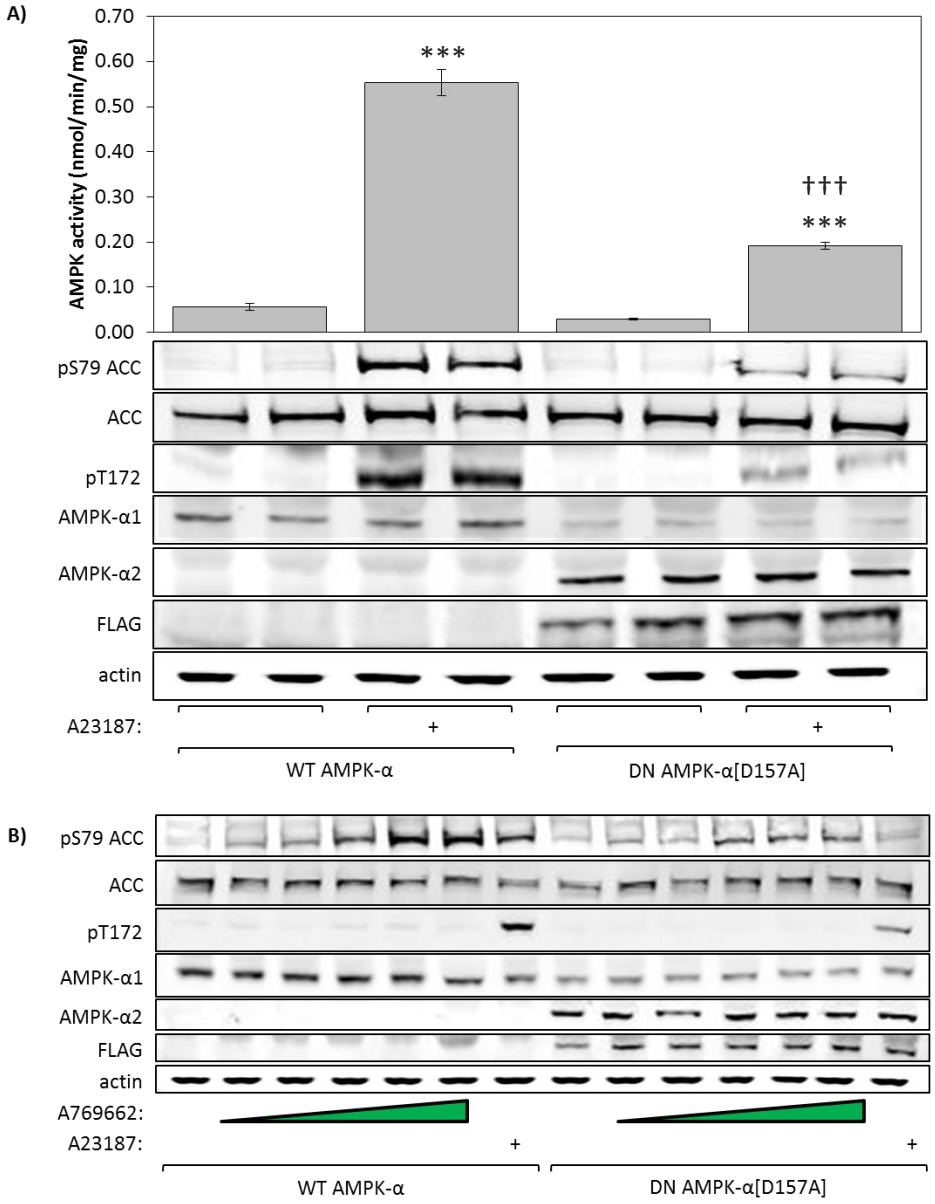

Figure 3.30: Evidence that ACC phosphorylation in G361 cells is mediated by AMPK
A FLAG-tagged inactive mutant (D157A) of AMPK-α2 was stably expressed in G361 cells to create dominant-negative (DN) cells. **(A)** Wild-type (WT) and DN G361 cells were treated with A23187 (10 µM) for 1 hr. AMPK was immunoprecipitated from cell lysates using anti-AMPK-α1/-α2 antibodies and kinase activity measured using the AMARA peptide substrate (top). Results are mean ± SEM (n = 4). Cell lysates were also subject to Western blotting with the indicated antibodies (bottom). **(B)** WT and DN G361 cells were treated with A23187 (10 µM) or A769662 (30, 100, 300, 500 and 1000 µM) for 1 hr. Cell lysates were subject to Western blotting using the indicated antibodies. Significantly different from control without A23187: ***$p < 0.001$; significantly different from wild-type AMPK plus A23187: †††$p < 0.001$.

3.3.7 Berberine increases pACC in cells expressing an α1[T172D] mutant

In this chapter, results have been presented to show that treatment of G361 cells with an AMPK activator can increase ACC phosphorylation with no measureable change in Thr172 phosphorylation or AMPK activity. The proposed mechanism for this effect is allosteric activation of the kinase. To conclusively prove that allosteric activation of AMPK is possible with no changes in Thr172 phosphorylation status, AMPK-$\alpha1^{-/-}$-$\alpha2^{-/-}$ dKO mouse embryo fibroblasts were transfected with an AMPK-α1 [T172D] mutant construct. Dephosphorylated AMPK-α is essentially inactive, as is a T172A mutant. However, the T172D mutant does retain a basal activity and can be allosterically activated by AMP, although it cannot be phosphorylated and activated by upstream kinases (Stein et al., 2000). Thus, any changes in kinase activity in this mutant must be due to allosteric activation. MEFs were transfected with plasmids encoding AMPK-β2, AMPK-γ1 and AMPK-α1 wild-type (WT) or AMPK-α1[T172D] mutant (Fig. 3.31). The recombinant proteins could not be detected by Western blotting (data not shown), probably due to the low transfection efficiency. Despite this, a significant basal activity could be detected in the cells expressing either of the α1 constructs, although the activity was lower in the T172D cells, confirming the results of others (Stein et al., 2000). The activity of WT AMPK was increased by both A23187 and berberine, with a concomitant increase in ACC phosphorylation. Interestingly, the effect of berberine on ACC phosphorylation was greater than that of A23187 although the effect of Thr172 phosphorylation and AMPK activation was smaller.

The AMPK activity, as measured by Thr172 phosphorylation or immunoprecipitation followed by kinase assay, was not increased in the T172D mutant in response to either A23187 or berberine, as expected. However, phosphorylation of ACC did significantly

increase in the T172D cells in response to berberine, which must be due to allosteric activation of AMPK.

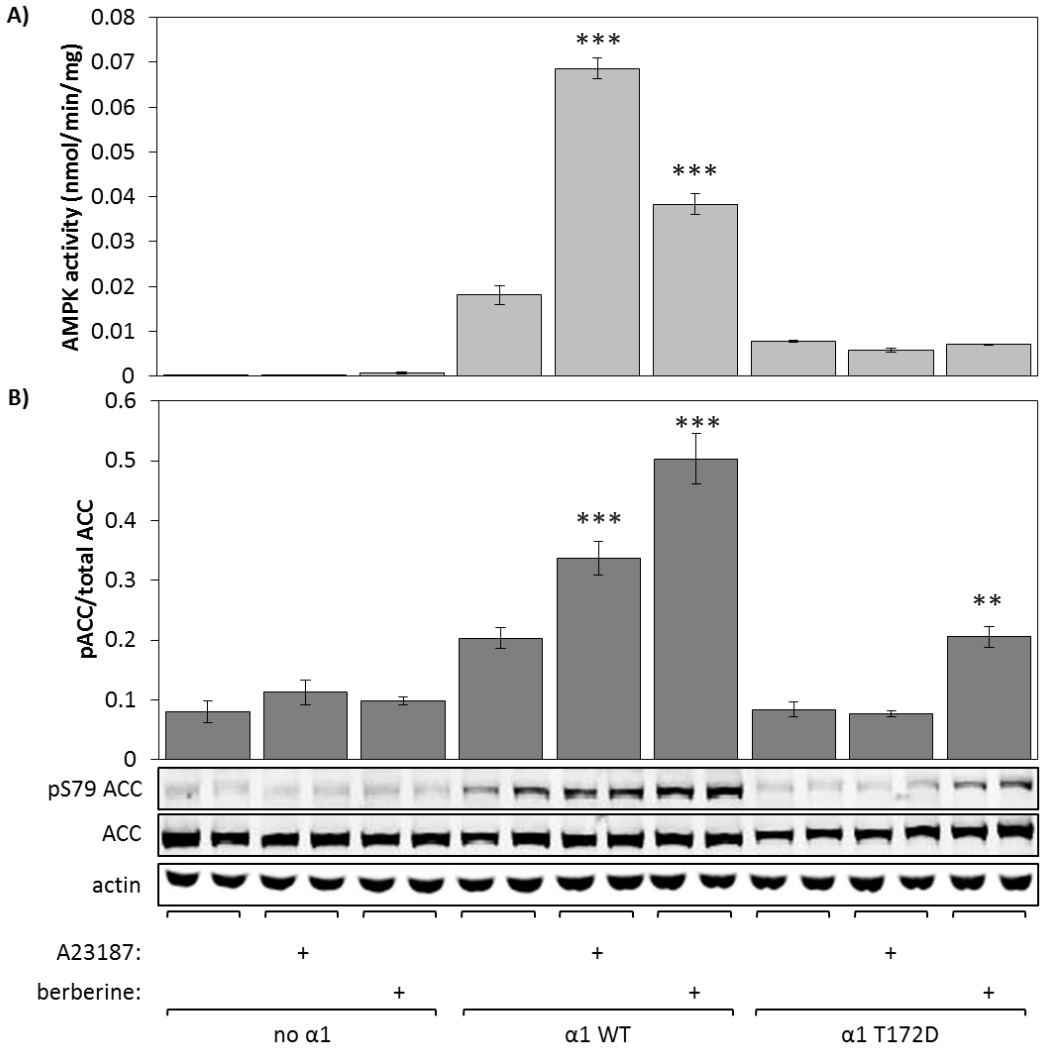

Figure 3.31: Effects of A23187 and berberine in AMPK-knockout mouse embryo fibroblasts expressing α1 [T172D] mutant

AMPK-$\alpha1^{-/-}$-$\alpha2^{-/-}$ mouse embryo fibroblasts were transiently transfected with DNAs encoding AMPK-α1 (WT or T172D mutant) together with AMPK-β2 and AMPK-γ1 for 48 hr. Cells were then treated with A23187 (10 μM) or berberine (300 μM) for 1 hr. **(A)** AMPK was immunoprecipitated from cell lysates using anti-AMPK-α1/-α2 antibodies and kinase activity measured using the AMARA peptide substrate. Results are mean ± SEM (n = 3) **(B)** Cell lysates were subject to Western blot using the indicated antibodies. The bar chart represents the ratio of pACC to total ACC quantified from these blots and results are mean ± SEM (n = 3). Significantly different from control without A23187: **p < 0.01, ***p < 0.001.

3.3.8 The changes in Thr172 phosphorylation in intact cells are modest:

Bacterially expressed AMPK complexes can be activated >100-fold in cell free assays by phosphorylation of Thr172 by either LKB1 or CaMKKβ (Suter et al., 2006). However, it remained unclear if changes in Thr172 phosphorylation in the intact cells would ever approach this maximal extent. Two methods were used to address this question. In the first, bacterially expressed kinase-dead AMPK heterotrimer (α1[D157A]β2γ1) was phosphorylated with either LKB1 or CaMKKβ until the phosphorylation, as measured by Western blotting using a phospho-Thr172 antibody, reached a maximum. The pThr172 signal obtained from equivalent amounts of AMPK-α from cell lysates was then measured. Assuming that the phosphorylation of the bacterially expressed α subunit was stoichiometric, the degree of Thr172 phosphorylation in cell lysates could be calculated. In a second approach, AMPK was immunoprecipitated from cell lysates and incubated with and without recombinant CaMKKβ. After removal of CaMKKβ by extensive washing of the beads, the kinase activity of the immunoprecipitates was determined.

Using these methods, the degree of phosphorylation of Thr172 in G361 (Fig. 3.32) and HEK293 (Fig. 3.33) cells (which are LKB1-null and LKB1-expressing respectively, see Fig. 3.15) in response to AMPK activators was determined. In G361 cells, using the bacterial complex to calibrate the signal, basal Thr172 phosphorylation was estimated at 4%, rising ≈3.5 fold to 13% of maximum after treatment with A23187. Using CaMKKβ to phosphorylate the immunoprecipitates, the basal Thr172 phosphorylation was estimated at 3.5%, rising ≈5-fold after A23187 treatment to 18% of maximum.

In HEK293 cells, the changes in Thr172 phosphorylation in response to both A23187 and berberine were determined. Using the bacterial complex, the degree of phosphorylation was estimated at 27% of maximum, rising to 36% or 50% of maximum in response to A23187 or berberine respectively. Similar results were obtained when CaMKKβ was used to phosphorylate the immunoprecipitates. A basal AMPK activity of 23% of maximum rose to 37% or 60% of maximum after treatment with A23187 or berberine respectively.

The two methods therefore gave broad agreement with each other. In LKB1-null G361 cells, Thr172 phosphorylation is initially very low. This can be increased by activation of CaMKKβ by A23187, but the Thr172 phosphorylation never approaches the maximum. As expected, HEK293 cells, which express LKB1 (thought to be constitutively active), possess a relatively higher basal level of Thr172 phosphorylation and AMPK activity compared to G361 cells. Treatment with A23187 or berberine increased the phosphorylation of Thr172, but only by <2-fold to ≈60% of maximum. Thus, even after treatment with a potent mitochondrial poison, the change in phosphorylation of AMPK-α remains quite small. It seems that in both cell lines the actual changes in Thr172 phosphorylation are quite modest and operate over a fairly narrow range. Of course, these changes would be supplemented by allosteric activation in the intact cell.

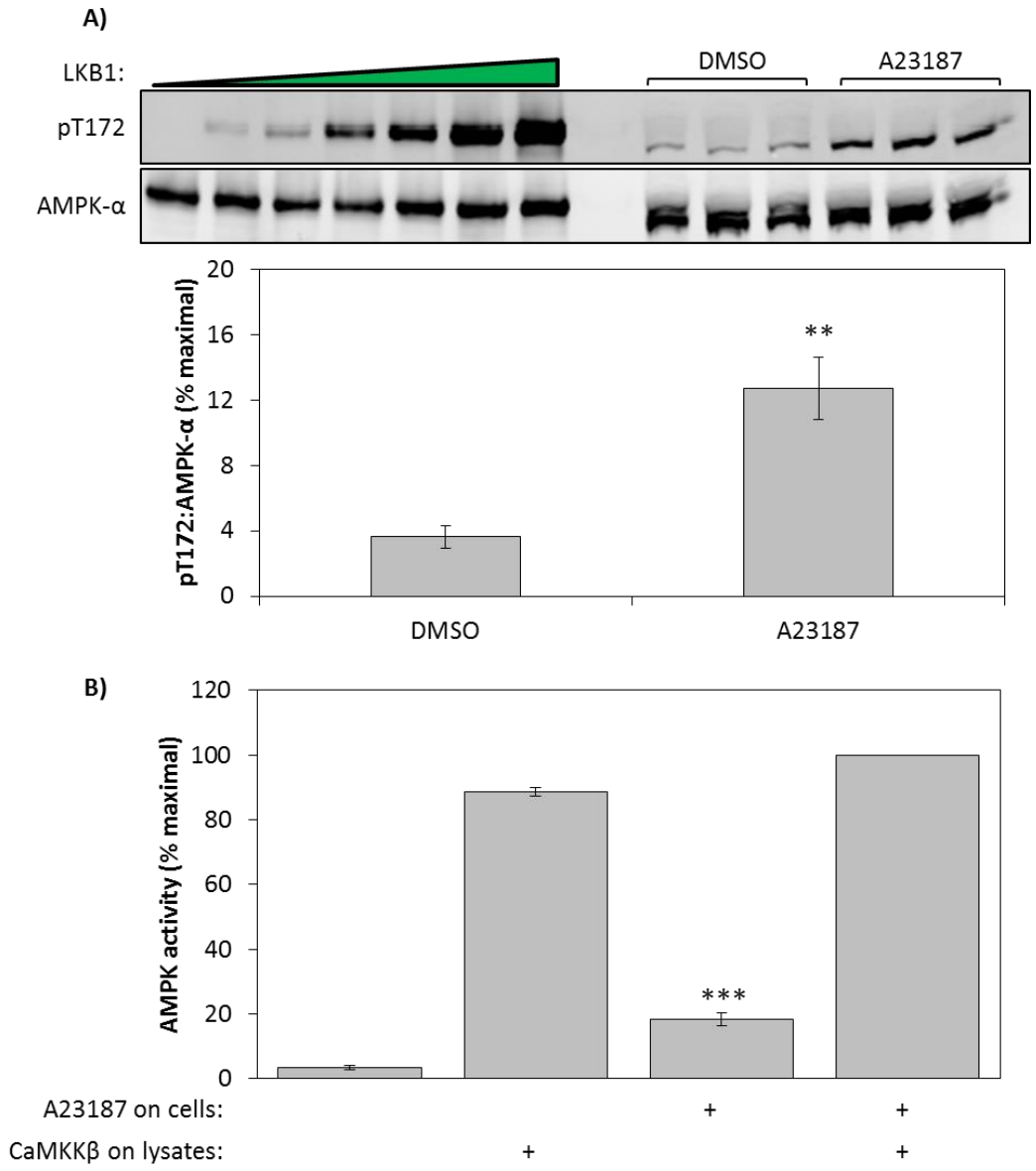

Figure 3.32: Estimation of Thr172 phosphorylation in intact G361 cells

G361 cells were treated ± A23187 (10 µM) for 1 hr. **(A)** Bacterially expressed AMPK (α1[D157A]β2γ1 complex) was incubated with increasing amounts of LKB1. Equivalent amounts of AMPK-α from G361 cell lysates and the bacterially expressed complex were analysed by Western blotting using anti-pThr172 and anti-AMPK-α antibodies. Assuming the bacterial complex is stoichiometrically phosphorylated, the degree of pThr172 in G361 cell lysates was calculated. The graph shows mean ± SEM from 5 independent experiments. **(B)** AMPK was immunoprecipitated from G361 cell lysates with anti-AMPK-α1/-α2 antibodies. AMPK activity was then measured before and after phosphorylation by purified CaMKKβ. AMPK activity was determined using the AMARA peptide substrate. Results are mean ± SEM from 3 independent experiments. Each experiment was performed using multiple samples. Significantly different from control (before CaMKKβ treatment) by one-way ANOVA with Dunnett's multiple comparison test: $^{**}p < 0.01$, $^{***}p < 0.001$.

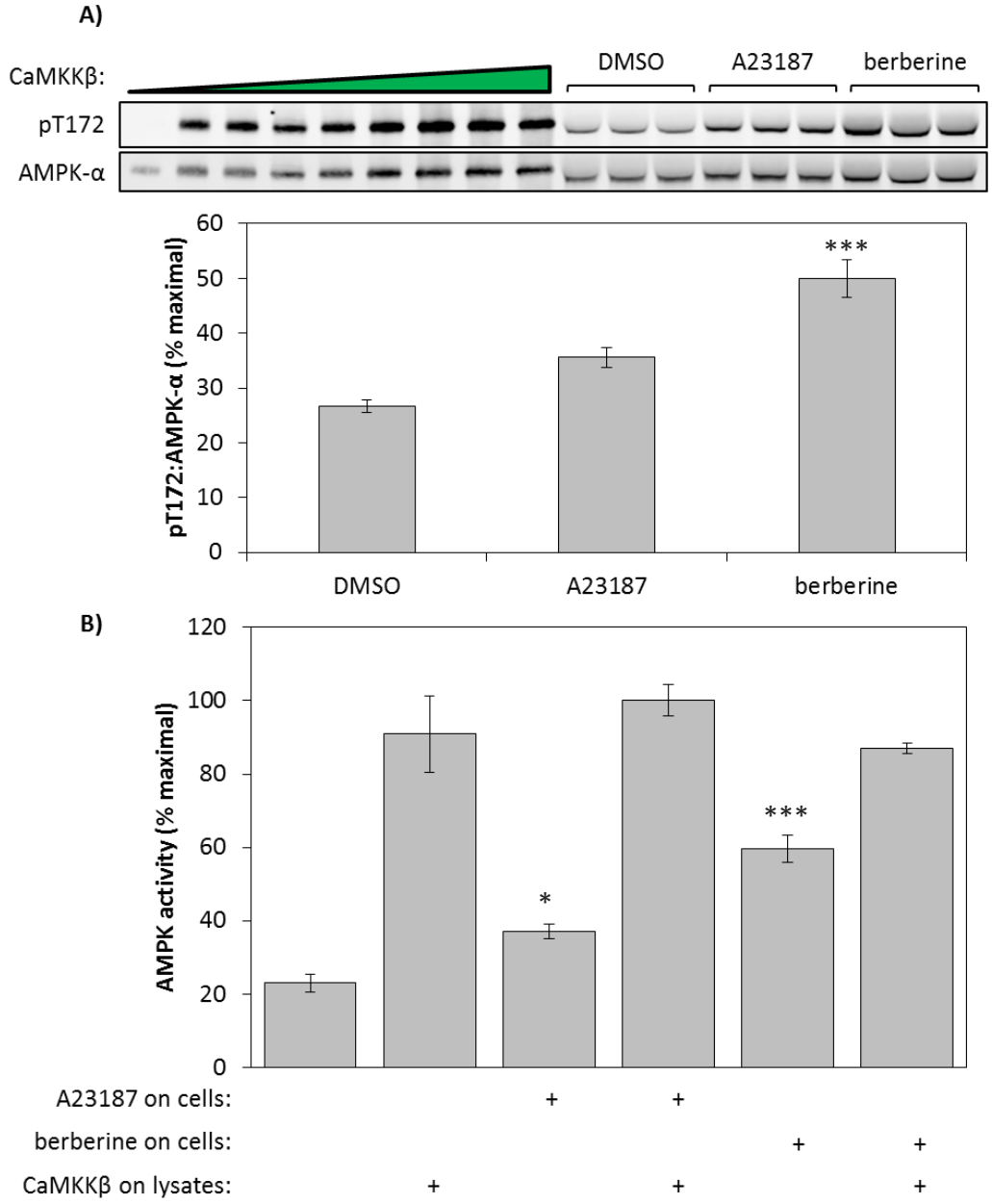

Figure 3.33: Estimation of Thr172 phosphorylation in intact HEK293 cells
HEK293 cells were treated with DMSO, A23187 (10 µM) or berberine (100 µM) for 1 hr. **(A)** Bacterially expressed AMPK (α1[D157A]β2γ1 complex) was incubated with increasing amounts of CaMKKβ. Equivalent amounts of AMPK-α from HEK293 cell lysates and the bacterially expressed complex were analysed by Western blotting using anti-pThr172 and anti-AMPK-α antibodies. Assuming the bacterial complex is stoichiometrically phosphorylated, the degree of pThr172 in HEK293 cell lysates was calculated. The graph shows mean ± SEM (n = 3) **(B)** AMPK was immunoprecipitated from HEK293 cell lysates (treated as above) with anti-AMPK-α1/-α2 antibodies. AMPK activity was then measured before and after phosphorylation by purified CaMKKβ. AMPK activity was measured using the AMARA peptide substrate. Results are mean ± SEM (n = 3). Significantly different from control (before CaMKKβ treatment) by one-way ANOVA with Dunnett's multiple comparison test: *$p < 0.05$, ***$p < 0.001$.

3.4 Discussion

3.4.1 Promotion of phosphorylation by AMP

The results presented in this chapter highlight the key role that AMP plays as a physiological regulator of AMPK.

Evidence is presented to show that AMP can promote phosphorylation of Thr172 of AMPK by the major upstream kinase LKB1, but not by the alternate upstream kinase CaMKKβ. No effect of ADP was observed with either upstream kinase. Recent papers from the Kemp laboratory (Oakhill et al., 2011, 2010) had reported that both AMP and ADP could promote Thr172 phosphorylation by CaMKKβ, results that have not been reproduced, either in this thesis or in other published work (Hawley et al., 2005). The reasons for these discrepancies are unclear, but a simple explanation could be that the experiments of Oakhill et al were contaminated with trace amounts of protein phosphatase.

The original experiments showing that AMP promoted Thr172 phosphorylation by the as-then unidentified upstream kinase were disputed by other groups as it was suggested that one of the preparations used might have been contaminated with a magnesium dependent protein phosphatase of the PPM family, and that any effects of the nucleotide on Thr172 phosphorylation were due to protecting this site against dephosphorylation by phosphatases. This protection would lead to an increase in net phosphorylation, similar to that which would be observed if AMP was promoting the phosphorylation reaction.

Indeed, a preparation of AMPK purified from rat liver used in other studies was contaminated with a PPM phosphatase (Sanders et al., 2007b). However, it seemed unlikely that this was true for the preparations used in this chapter, for two reasons:

i. The preparation used by Sanders et al was purified through two steps, whereas the preparation used in this study (see Hawley et al., 1996) was purified through a further four steps. Based on a previous analysis of this method (Carling et al., 1989), this would result in the relative purifications factors being 45-fold vs 708-fold. In fact, the method of Hawley et al (1996) has since been revised and the current method utilizes a Superdex200 column rather than a Sephacryl S-200, which is likely to further increase the purity of the preparation.

ii. If the observed effects were due to protection against dephosphorylation, then they should be observed with both LKB1 and CaMKKβ, rather than just with LKB1. The upstream kinase used should be irrelevant: it would only be there to provide the phosphate for the phosphatase to remove. This would assume that the contamination is in the AMPK preparation, not one of the upstream kinase preparations. However, based on the results in section 3.3.1, if the contamination was in the LKB1 preparation then ADP should have similar effects to AMP, which is not the case.

Taken together, these arguments seem to rule out the contamination of any of the preparations with a protein phosphatase. This was further confirmed by the mock incubations in Fig. 3.7, where no decrease in phosphorylated Thr172 was observed unless exogenous PP2C was added. This confirms that the preparations are not contaminated with a PPM family phosphatase, and that the observed effects of AMP are due to promotion of phosphorylation.

Although Oakhill et al (2010) performed an experiment similar to our Fig. 3.7 to show that the AMPK preparation used was not contaminated with phosphatase, this was not treated in the same manner as the AMPK used for the phosphorylation experiments. Prior to the phosphorylation reactions, AMPK (expressed in COS7 cells as a GST fusion) bound to glutathione-Sepharose beads was dephosphorylated using PP2C. This PP2C was also expressed as a GST fusion, although the protein had been treated with thrombin to cleave and remove the GST tag. The beads were then washed to remove PP2C. AMPK was eluted from the beads and incubated with upstream kinase and nucleotide to measure the promotion of phosphorylation. If the washing of the beads had not removed all of the PP2C (for example, if the GST cleavage had been incomplete) then trace amounts could be present in the phosphorylation reactions. The AMPK used in the contamination experiments is phosphorylated AMPK expressed in COS7 cells and has not been exposed to PP2C. This would explain why Oakhill et al observed effects of both AMP and ADP: the effects were not on the phosphorylation reaction but were rather on inhibition of the phosphatase reaction. Although this explains the results of the COS7 expressed AMPK, Oakhill et al (2010) also examined the effect on AMPK co-expressed with NMT (N-myristoyl transferase) in bacteria. Again, AMP promoted phosphorylation of Thr172 by CaMKKβ, although examination of the Thr172 immunoblots suggested that the effect was modest. It is difficult to reconcile these results with those of this chapter and other studies (Hawley et al., 2005) where no effect of AMP on CaMKKβ mediated phosphorylation was detected. Interestingly, Oakhill et al did not repeat the experiments with bacterially expressed AMPK using LKB1 as the upstream kinase. In their follow-up study reporting that ADP also promoted Thr172 phosphorylation (Oakhill et al., 2011), CaMKKβ was used for all

experiments and the effects of using LKB1 were not examined. It would have been interesting to examine if similar effects were observed using ADP and LKB1.

Instead of PP2C, the experiments performed in this chapter used PP2A to dephosphorylate purified AMPK. PP2A has the advantage that it can be completely inhibited by okadaic acid (Cohen, 1989) and therefore does not need to be removed from the incubations prior to the phosphorylation reaction. As the AMPK and LKB1 preparations were not contaminated with protein phosphatase, the effects of AMP on LKB1-mediated Thr172 phosphorylation must be via promoting phosphorylation and not by inhibiting the dephosphorylation.

The dependence of the effect on β subunit myristoylation was also investigated, but, due to technical difficulties, the attempts were not successful. The stable cell lines generated contained β1 and β2 with a C-terminal FLAG tag. The goals were to immunoprecipitate the recombinant β complexes and determine if AMP could promote phosphorylation by LKB1. However, no kinase activity was obtained after FLAG immunoprecipitation. It seems that the recombinant β subunit cannot form a complex with the α and γ subunits as an anti-FLAG immunoprecipitate, whilst having no kinase activity itself, did not deplete the kinase activity of a subsequent immunoprecipitation using anti-AMPK-α1/-α2 antibodies, suggesting that no catalytic subunits were associated with the FLAG-tagged β subunit. The complex appeared to be active in the intact cell, although without the ability to measure kinase activities of recombinant and wild-type complexes it is difficult to estimate how successfully the wild-type β has been replaced with the recombinant β. It may be that the position of the FLAG tag at the C-terminus of the β subunit interferes with complex assembly, as

examination of most complete crystal structures suggests that the activation loop of the kinase is closely associated with the C-terminus of the β subunit (Xiao et al., 2011). Placing the tag at the N-terminus would interfere with the myristoylation of Gly2. The β construct used by Oakhill et al (2010) contained no tag, suggesting that they had encountered similar problems. However, using an untagged β and performing immunoprecipitations with anti-α1/-α2 antibodies means that the contents of the immunoprecipitated heterotrimer are not well defined and may contain endogenous, rather than recombinant, β subunit.

3.4.2 Protection against dephosphorylation by AMP and ADP

The results presented in this chapter also show that dephosphorylation of Thr172 by protein phosphatases is inhibited by both AMP and ADP, with the effects of both nucleotides being antagonized by ATP. While broadly confirming those of Xiao et al (2011) these results disagree in one important respect. Xiao et al state that ADP provided protection against Thr172 dephosphorylation across a range of concentrations similar to that of AMP, however the results in this chapter clearly show that AMP is around 10-fold more potent than ADP, regardless of the ATP concentration used in the assays (Fig. 3.11). This increased potency of AMP was observed, although not commented on, in the study of Xiao et al (2011). Reanalysis of their Fig. 1B shows that AMP is at least 3 times more potent than ADP in protecting the kinase against dephosphorylation, with 30 μM AMP offering greater protection than 100 μM ADP. This is smaller than the 10-fold difference observed in this chapter, but this could be due to differences in systems being studied: Xiao et al used bacterially expressed AMPK, not rat liver purified AMPK as in this chapter. Mammalian AMPK exhibits a greater allosteric activation in response to AMP compared with the bacterially

expressed complex. It is possible that this increased degree of activation would also be observed when measuring protection against dephosphorylation. Xiao et al (2011) did examine the effects of AMP and ADP on rat liver purified AMPK, however they did so by Western blotting, which is not as quantitative as kinase assays. The rat liver preparation used was also less well defined than our preparation and they used endogenous, contaminating, phosphatases to dephosphorylate AMPK. Perhaps if these experiments were repeated under similar conditions used in this chapter a 10-fold difference between the nucleotides would be observed.

3.4.3 Allosteric activation of AMPK

Examining the allosteric activation of the rat liver purified AMPK by AMP showed that the activity of AMPK could be increased by as much as 13-fold by AMP when this was measured at 5 mM ATP, a concentration typical of that found in an intact cell (Imamura et al., 2009). These results convincingly demonstrate that AMPK can be allosterically activated by low concentrations of AMP, even when ATP is present at physiological concentrations.

The data generated from the G361 cell line also supports the role of AMP as a physiological regulator of AMPK. Treating these LKB1-null cells with berberine, a mitochondrial inhibitor, resulted in a large increase in phosphorylation of ACC with no measureable increase in phosphorylation of Thr172 by either kinase assay or Western blot. In fact, the increase in ACC phosphorylation was larger with berberine than that with the calcium ionophore A23187, which did increase Thr172 phosphorylation. This suggests that, in an intact cell, allosteric activation can be quantitatively as important as changes in Thr172 phosphorylation. This was further supported by treatment of

G361 cells with berberine alone, or berberine plus A23187 (Fig. 3.19). The data shows that the allosteric activation in response to berberine could not be increased further by the simultaneous addition of A23187, which increased Thr172 phosphorylation. The phosphorylation of ACC in response to berberine alone must already be close to maximal. These data also illustrates that, in agreement with the cell-free assays, AMP can compete with ATP for binding to the nucleotide-binding sites on the γ subunit, despite the latter nucleotide being present at far higher levels.

G361 cells were also treated with A769662, a synthetic activator of AMPK. A769662, like berberine, increased ACC phosphorylation with no change in Thr172 phosphorylation. A769662 can also protect the kinase against dephosphorylation but it appears that under these conditions in these cells it is eliciting all of its effects via allosteric activation.

The experiments performed with other AMPK activators also highlight the contribution that allosteric activation makes to the overall regulation of the kinase. Salicylate, a recently identified direct activator of AMPK (Hawley et al., 2012) was shown to activate AMPK in G361 cells independent of changes in AMP levels and Thr172 phosphorylation. Salicylate is a relatively poor allosteric activator, which explains the small change in ACC phosphorylation at 1 mM salicylate, a concentration that has no effect on the ADP:ATP ratio. At higher concentrations (3 and 10 mM) salicylate will still allosterically activate AMPK but it also increases the ADP:ATP ratio by partially uncoupling the mitochondrial respiratory chain from ATP synthesis, resulting in a rise in intracellular AMP. It seems probable that, as the more potent allosteric activator, a large proportion of the observed effects in G361 cells at 3 and 10 mM salicylate are

actually being caused by AMP, not salicylate. It was estimated that AMP rose from 30 µM to 64 µM in response to 10 mM salicylate. Plotting these data on the allosteric activation curve at 5 mM ATP suggests that this could increase the AMPK activity around 2-fold, which would presumably be high enough to contribute to ACC phosphorylation. In HEK293 cells, where LKB1 is present, salicylate is able to elicit effects on Thr172 phosphorylation as well as allosteric activation, which explains its larger effects on AMPK activity and ACC phosphorylation in these cells (Hawley et al., 2012).

Treatment of G361 cells with AICAR also resulted in a large increase in phosphorylation of ACC with no increase in Thr172 phosphorylation, and no change in cellular ADP:ATP ratios. A concentration-dependent rise in ZMP was detected in these samples and it is likely that the effects on AMPK are due to allosteric activation by ZMP, not AMP.

A range of AMP-dependent AMPK activators applied to G361 cells elicited a similar response to that of berberine. These compounds are structurally unrelated and the property they have in common is disrupting mitochondrial function and hence cellular nucleotide ratios. It therefore seems unlikely that the effects of berberine on ACC phosphorylation could be due to off-target effects and the simplest explanation is allosteric activation of AMPK by AMP.

Whilst it could be argued that the effects of berberine and the other AMP-dependent activators could be due to AMP inhibiting dephosphorylation of ACC, rather than allosterically activating AMPK, this also seems unlikely. The effect of AMP on protecting AMPK from dephosphorylation is substrate-mediated, as first demonstrated

in the original study characterizing this effect (Davies et al., 1995). The authors proposed that the protective effect of AMP was independent of the phosphatase used as the effects were present with both PP2A and PP2C. Using alternate substrates the authors also demonstrated that the phosphatases themselves were not affected by AMP (Davies et al., 1995). The authors also proposed that protection against dephosphorylation was due to AMP binding to AMPK, as the half-maximal effect of AMP was identical to that of AMP on allosteric activation of the kinase and both were increased by a similar degree when measured in the presence of 4 mM ATP. While Davies et al were unaware at that time of the location of the nucleotide binding sites on the γ subunit of AMPK, Sanders et al (2007b) demonstrated that mutation of key residues in these sites abolished the protective effects of AMP, again suggesting that the effect was substrate-mediated. This was also demonstrated for ADP (Xiao et al., 2011). In addition to this, an AMPK-α1 fragment (residues 1-312), which lacks the nucleotide binding sites on the γ subunit, was not protected against PP2Cα mediated Thr172 dephosphorylation by AMP, unlike the full-length heterotrimer (Suter et al., 2006). Thus the effects of AMP on ACC phosphorylation cannot be attributed to effects on the protein phosphatase and must be caused by increased allosteric activation of AMPK. This is also likely to be true for the effects of A769662. Serine-108 of the β1 subunit of AMPK is essential for activation by A769662. Mutation of this residue to an alanine almost completely abolished the allosteric activation and protection against Thr172 dephosphorylation by A769662, whilst the AMP-mediated effect was unchanged (Sanders et al., 2007a). These results confirm that A769662, like AMP, exerts its effects on dephosphorylation via binding to AMPK, not the phosphatase.

The data presented here also reinforces the requirement of AMPK for phosphorylation of ACC. As well as an effect on the ACC phosphatase, one other way in which the data could be explained is that the compounds tested are not increasing AMPK activity, but a distinct ACC kinase, which might explain why no change in Thr172 phosphorylation was detected. However, there is a large body of evidence to indicate that AMPK is the only kinase phosphorylating Ser79 on ACC. Using AMPK catalytic subunit knockouts, it has been demonstrated that ACC phosphorylation is abolished in a number of different cell types including mouse embryonic fibroblasts (Foretz et al., 2010), hepatocytes (Laderoute et al., 2006) and T cells (Rolf et al., 2013). It has also been shown in β1 knockout mouse hepatocytes that A769662, which only activates AMPK complexes containing β1 and not those containing β2, has no effect on ACC phosphorylation (Scott et al., 2008). This was also demonstrated following activation using salicylate, which, like A769662, only activates complexes containing β1 (Hawley et al., 2012). In addition, phosphorylation of *Drosophila* ACC was abolished in response to oligomycin when the α, β and γ subunits were knocked down by dsRNAi interference (Pan and Hardie, 2002).

Results in this chapter from mouse embryo fibroblasts (Fig. 3.29) and G361 cells (Fig. 3.30) show that AMPK is the kinase phosphorylating Ser79 on ACC and that the effects of the compounds tested are not due to off-target effects on a different kinase. This suggests that ACC phosphorylation in G361 cells, like other cell types examined, is mediated through AMPK. It is not possible to completely rule out the possibility that the low ACC phosphorylation observed in the dominant negative cells was due to a kinase other than AMPK, although this kinase would have to be activated by both A23187 and A769662, which seems unlikely. This kinase would also have to be absent

from mouse embryo fibroblasts as no effect of A23187 or A769662 on phosphorylation of ACC was observed in these cells (Fig. 3.29). Taken together, the simplest explanation is that rising AMP levels in the intact cell are allosterically activating AMPK and causing phosphorylation of ACC.

3.4.4 AMP as the key physiological regulator of AMPK

Some recent reviews have proposed that ADP, and not AMP, is the critical physiological regulator of AMPK (Carling et al., 2012; Oakhill et al., 2012). There seem to be two main reasons for these doubts. The first is that allosteric activation is reported to be quite modest, usually <2-fold, whereas stoichiometric phosphorylation of Thr172 can produce ≈100-fold AMPK activation (Sanders et al., 2007b; Suter et al., 2006). If changes in phosphorylation status can increase activity 100-fold then the relatively small 2-fold activation reported with the bacterially expressed heterotrimer would appear to be negligible. However, these estimates for the extent of allosteric activation came from studies performed using bacterially expressed heterotrimers. Using native rat liver AMPK, an allosteric activation of up to 13-fold was obtained in response to AMP, significantly higher than that of the bacterial complex.

The reasons for this discrepancy are not completely clear, but could relate in part to the bacterial complex lacking some post-translational modifications that occur with the mammalian complex. It should also be pointed out that, to obtain a 13-fold increase in AMPK activity, it was necessary to take some precautions to reduce the basal activity. As discussed previously, commercial preparations of ADP are often contaminated with AMP. This can also be true for ATP, which, by necessity, is present in the kinase assay as a source of gamma phosphate for transfer to the synthetic

peptide substrate. AMP may also be generated during the assay, most likely from non-enzymic breakdown of ADP generated during the assay. As AMPK is sensitive to low concentrations of AMP, it has already been suggested that the levels of AMP present may be high enough to increase the basal activity, thus reducing the apparent extent of stimulation (Suter et al., 2006). To alleviate this problem, freshly prepared ATP solutions that had been screened for AMP contamination were utilized. The duration of the kinase assays was also reduced to 5 minutes to help minimize the amount of AMP generated during the incubation. Another way in which the apparent sensitivity of AMPK to AMP could have been increased would have been to include 5'-nucleotidase in the control incubations lacking additional AMP. The 5'-nucleotidase would hydrolyse any contaminating AMP in the ATP preparation and may reduce the basal activity of the kinase even further.

While it is true that Thr172 phosphorylation can increase AMPK activity ≈100-fold in a cell free system, this extent of activation is observed when comparing completely dephosphorylated enzyme (which has an almost undetectable activity) to that of stoichiometrically phosphorylated enzyme. It seemed unlikely that the changes in phosphorylation of Thr172 in an intact cell would operate over such a wide range. Indeed, the results in Fig. 3.32 and Fig. 3.33 show that the changes in phosphorylation are actually much more modest. In G361 cells, which lack LKB1 and therefore exhibit a low basal AMPK activity, A23187 treatment increased AMPK activity by 4-fold, but this represented a change from only 4% to around 16% of stoichiometric Thr172 phosphorylation. In HEK293 cells, which express LKB1, the basal phosphorylation was higher, around 25%, and the increases in response to A23187 (1.5 fold) and berberine (2 fold) were even more modest. Thus, it seems that, although 100-fold changes in

AMPK activity due to Thr172 phosphorylation can be achieved in cell-free assays, the changes that occur in intact cells are generally much more modest.

The intact cell experiments also support the idea of allosteric activation being an important component of the overall regulatory mechanism. The data presented here show that the phosphorylation of ACC in G361 cells was higher with berberine than with A23187, suggesting that allosteric activation can increase AMPK activity to a greater extent than that induced by changes in Thr172 phosphorylation. Further evidence of this comes from the AMPK-α double knockout mouse embryo fibroblasts transfected with wild-type α1. The increase in ACC phosphorylation was higher in response to berberine than with A23187, despite the smaller increases in Thr172 phosphorylation. This can be explained by the effect of berberine on ACC phosphorylation being caused by both allosteric activation as well as increased Thr172 phosphorylation. That the α1[T172D] mutant AMPK could be allosterically activated in these double knockout mouse embryo fibroblasts further supports this idea. These data conclusively demonstrate that significant allosteric activation can occur in intact cells without any changes in Thr172 phosphorylation.

Another argument against AMP being the physiological regulator of AMPK came from estimates of the affinities of the nucleotide binding sites on the γ subunit for AMP, ADP and ATP (Xiao et al., 2011). The binding affinities were measured indirectly using displacement of fluorescent derivatives of ATP from the bacterially expressed heterotrimer. The estimated K_D at the higher affinity exchangeable site was around 2 μM for all three nucleotides, while the estimated K_D for the lower affinity site was around 50-80 μM for all three nucleotides. Site 1 was proposed to be the high affinity

site and it was proposed that binding at this site was responsible for allosteric activation. This was based on three observations: (i) a crystal structure of the complex obtained after co-crystallization with ADP revealed only a single molecule of the nucleotide bound at site 1, suggesting that site 1 is the high affinity site; (ii) NADH, which was proposed to bind to the high affinity site, was found to competitively inhibit allosteric activation by AMP; (iii) AMP competitively inhibited NADH binding with an estimated K_D of 1.6 μM, similar to the affinity at the high affinity site determined by competition with coumarin-ATP. Since AMP is present at much lower cellular concentrations that ADP or ATP, it was further suggested that AMP would be unable to effectively compete with ADP or ATP for binding at the high affinity site. However, the 13-fold increase in activity observed at physiological concentrations of ATP (Fig. 3.13 shows that AMP can compete with other nucleotides. This is also true in intact G361 cells, where AMP (Fig. 3.17), and ZMP (Fig. 3.26), could compete with ADP and ATP for binding at these sites.

The affinities of the nucleotide binding sites discussed above (Xiao et al., 2011) were estimated using the assumption that there were only two available sites for binding, and that these did not interact. However, given that the crystal structures show that certain basic side chains are involved in binding more than one molecule of bound AMP (Xiao et al., 2007), it seems unlikely that there would be no interaction between the three binding sites. Indeed, mutation of any of the three aspartate residues that bind the ribose ring of the bound nucleotide in sites 1, 3 or 4 was found to affect the effects of AMP both to cause allosteric activation and to enhance phosphorylation by CaMKKβ (Oakhill et al., 2010). Interaction between sites is also suggested by earlier work where the binding of AMP and ATP to the CBS domains displayed strong positive

cooperativity (Scott et al., 2004). The assumptions that there was no interaction between the binding sites therefore may not have been entirely valid. Furthermore, in another study (Chen et al., 2012), when the core of the heterotrimer was co-crystallized with AMP or ATP independently, ATP was found to bind at site 4, the proposed "non-exchangeable" site for AMP and this would preclude binding of any nucleotide at site 3. Additionally, mutation of site 1 had no effect on allosteric activation by AMP, whereas mutation of site 3 or 4 completely abolished this (Chen et al., 2012).

The half-maximal concentrations calculated in this chapter for allosteric activation, protection against dephosphorylation and promotion of phosphorylation also do not fully support the suggestion that allosteric activation is caused by binding at the high affinity site (thought to be site 1) and protection against dephosphorylation by binding at the lower affinity site (thought to be site 3) (Xiao et al., 2011). The EC_{50} for AMP on allosteric activation and protection against dephosphorylation were very similar (5 μM and 2.6 μM respectively, although the former was measured in the presence of 200 μM ATP), which suggests but does not prove that they are due to binding at the same site. These values correlate with the proposed affinity of site 1 (≈2 μM). In addition, the half-maximal effect of AMP on inhibition of dephosphorylation was approximately 10 times lower than that of ADP, suggesting that the binding affinities of the two nucleotides at the site affecting dephosphorylation are not equal. The calculated EC_{50} for promotion of phosphorylation by AMP (160 μM) is closer to the proposed affinity of site 3 (≈80 μM), although the former was measured in the presence of 200 μM ATP.

The data discussed above shows that more work is required before a specific function can be allocated to a particular nucleotide binding site. Ideally, this may require the use of novel activators of AMPK that elicit only one of the regulatory effects on the kinase (allosteric activation, inhibition of dephosphorylation or promotion of phosphorylation), as well as solving the crystal structure of the kinase in the presence of these activators. However, the most widely used activator of AMPK, A769662, does not bind to the nucleotide binding sites on the γ subunit, but rather to a site that appears to be located on the β subunit. A current goal of the AMPK field is therefore to develop and characterize novel activators or inhibitors that uniquely bind at only one of the nucleotide binding sites. However, it is entirely possible that multiple nucleotide binding sites contribute to any one regulatory mechanism and it would not be possible to assign a role to an individual site.

Nucleotide measurements from intact G361 cells also support a role for AMP in regulating AMPK. Previous estimates for AMP levels in the intact cells, based on previous estimates in the literature, were quoted to be 1-5 μM, with ADP being present at 50-200 μM (Xiao et al., 2011). However, examining these papers suggest that the levels of AMP in the cell are, in fact, higher than this. Measuring the ADP:ATP ratio and estimating the absolute changes in nucleotide levels in G361 cells gave different results. AMP was estimated to rise from 40 μM to 270 μM after berberine treatment, with ADP rising from 426 μM to 975 μM. The change in AMP concentration is therefore around-6.5 fold, compared with 2-fold for ADP. After berberine treatment the ADP concentration is predicted to be only 3-4 times the concentration of AMP.

The nucleotide estimates were plotted on the allosteric activation, protection against dephosphorylation and promotion of phosphorylation curves obtained (Fig. 3.34). The change in AMP corresponds well with the range of concentrations that were shown to induce both allosteric activation and protection against dephosphorylation (both measured at 5 mM ATP). The predicted increase in AMP also corresponds with the estimated EC_{50} for promotion of Thr172 phosphorylation of 160 µM AMP. However, the EC_{50} was measured at 0.2 mM ATP, so it is unclear how significant the promotion of phosphorylation would be at the higher ATP concentrations prevalent *in vivo*. Plotting the ADP concentrations on the dephosphorylation curve, it is also clear that the increase in ADP would only be sufficient to produce a very small effect on Thr172 phosphorylation compared with the larger effect of AMP.

One caveat is that these G361 cells are a transformed cell line from a human melanoma and may therefore have altered metabolic function compared with non-transformed cell lines. As they lack LKB1 and therefore have a low basal AMPK activity, it could also be argued that these cells would be more sensitive to any disruption to mitochondrial function, resulting in a larger fluctuation in nucleotide levels than in cells expressing LKB1. However, examining data from HEK293 cells (isolated from the embryonic kidney of a human foetus) suggests that the changes in nucleotide levels may actually be greater than those in G361 cells. An increase in ADP:ATP ratio from 0.1 to 0.6 after berberine treatment was observed (Hawley et al., 2010). Using these figures, a rise in AMP from 50 µM to 950 µM would be predicted. This difference might be explained by the operation of the Warburg effect in the G361 cells. This phenomenon, first described by Otto Warburg in 1924, is the observation that cancer cells produce their energy predominantly through high rates of glycolysis, rather than

mitochondrial oxidative phosphorylation (Warburg, 1956). Non-transformed cells, by contrast, generate the bulk of their energy through oxidative phosphorylation. HEK293 cells may therefore be more sensitive than tumour cells, such as G361 cells, to inhibitors of mitochondrial function like berberine.

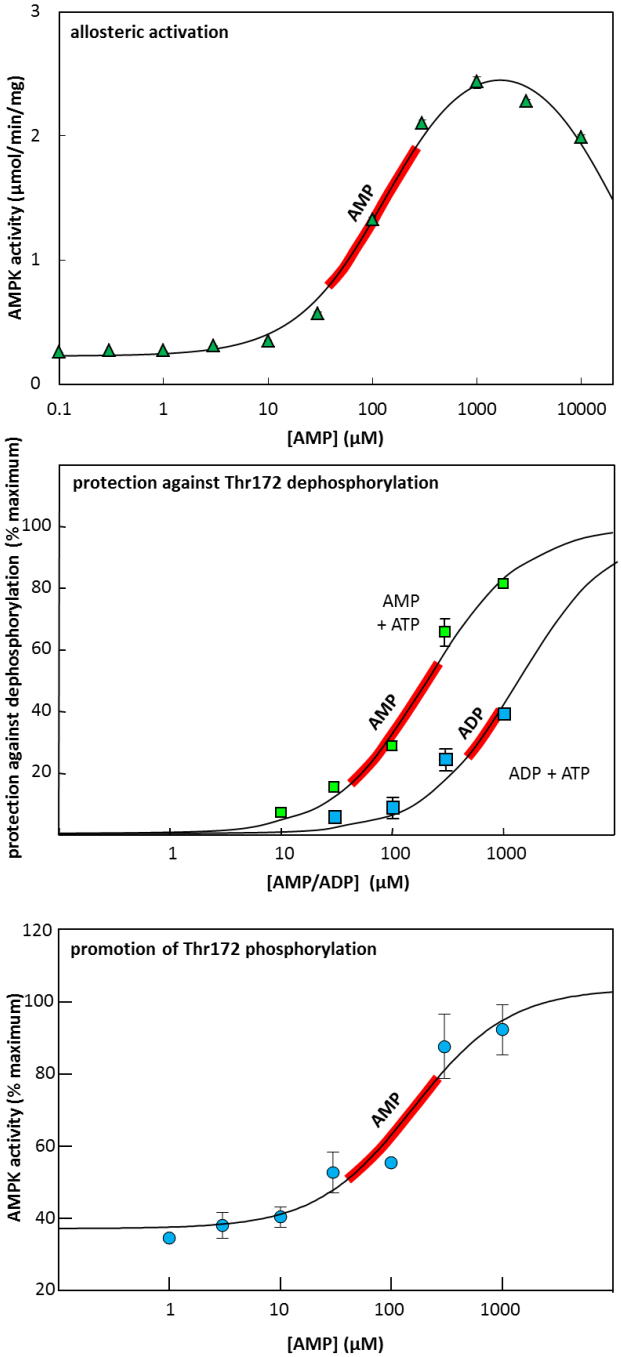

Figure 3.34: Changes in AMP and ADP levels vs. AMPK dose-response curves
Estimates of the changes in AMP and ADP levels in G361 cells in response to berberine were calculated in section 3.3.4 and plotted on the dose response curves for allosteric activation (top), protection against dephosphorylation (middle) and promotion of phosphorylation (bottom).

3.4.5 AMPK may have evolved sensitivity to AMP

Thus, allosteric activation by AMP, as discussed above, appears to be a quantitatively important part of the overall activation mechanism. An interesting proposal is that the ability to respond to AMP has arisen during evolution of the kinase. Allosteric activation by AMP has been observed with orthologues from insects (Pan and Hardie, 2002), nematodes (Apfeld et al., 2004) and mammals but not those from fungi (Mitchelhill et al., 1994; Wilson et al., 1996; Woods et al., 1994) or plants (Mackintosh et al., 1992), which seem to be regulated exclusively by phosphorylation. In *S. cerevisiae*, SNF1 activity is not regulated by AMP, either allosterically or by changes in phosphorylation (Sanders et al., 2007b). Instead, SNF1 is protected from Thr210 (equivalent to Thr172 in mammal) dephosphorylation by ADP (Mayer et al., 2011). As the effects of Thr172 phosphorylation and allosteric activation multiply together to give the overall activity of the kinase, AMPK orthologues that can respond to AMP would exhibit greater sensitivity to changes in cellular energy levels. This is further enhanced by the fact that the AMP:ATP ratio rises as the square of the ADP:ATP ratio (Hardie and Hawley, 2001). A system that is designed to respond to the former, in addition to the latter, will provide larger responses to any disruption in energy. The responsiveness of AMPK from higher organisms to AMP may represent an additional and more sensitive form of regulation than that in more primitive organisms.

3.4.6 A revised model for regulation of AMPK

Based upon the results presented in this chapter, a new model for AMPK regulation by nucleotides is proposed (Fig. 3.35). While both AMP and ADP can protect Thr172 against dephosphorylation, AMP is around 10-fold more potent. Promotion of Thr172 phosphorylation appears to be a genuine regulatory mechanism, but is only observed

with AMP and only when LKB1 is the upstream kinase. Allosteric activation by AMP appears to be much more significant, both in a cell free system and the intact cell, than previously suggested.

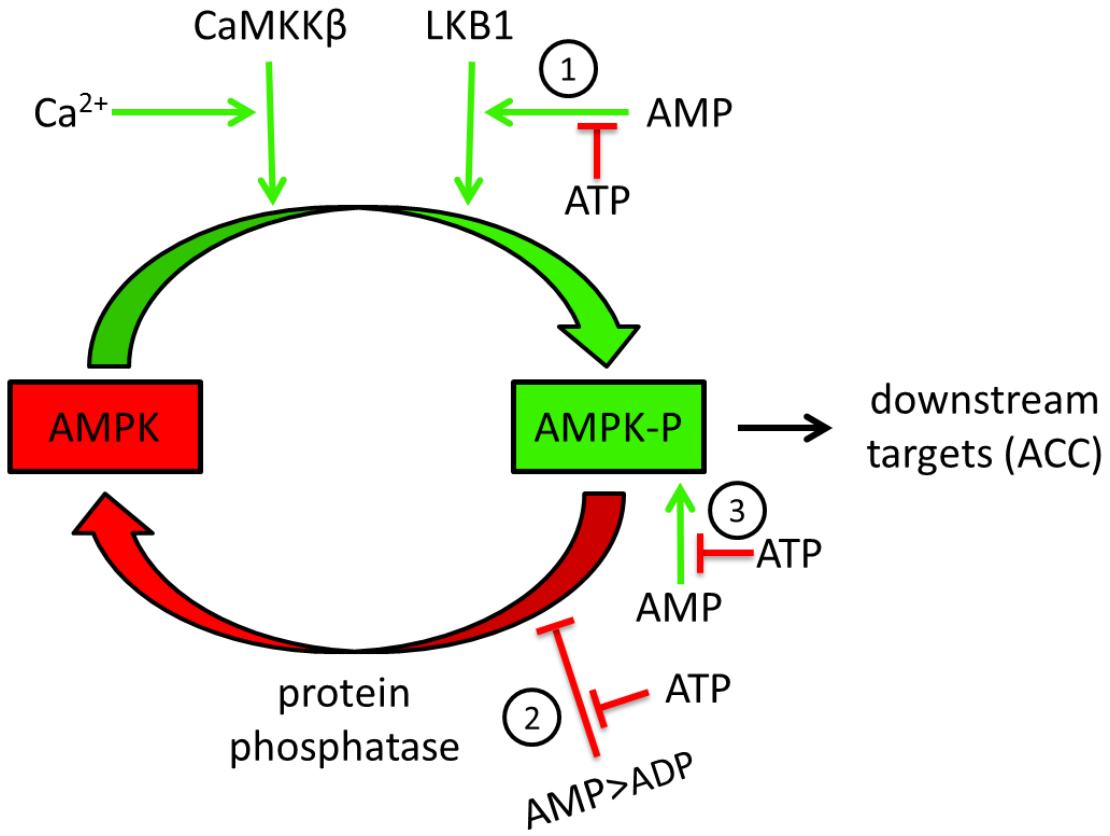

Figure 3.35: A revised model for regulation of AMPK
Mechanism by which AMP and ADP regulate AMPK: (1) binding of AMP to AMPK promotes Thr172 phosphorylation by LKB1; (2) binding of AMP or ADP protect Thr172 against dephosphorylation by protein phosphatases, although AMP is more potent; (3) binding of AMP causes allosteric activation of AMPK. All three effects are antagonized by binding of ATP.

CHAPTER 4: INVESTIGATING PHOSPHORYLATION OF LKB1 BY AMPK

4.1 Introduction

4.1.1 Regulation of LKB1 activity by post-translational modification

The LKB1 complex, as discussed in Chapter 1, is the major upstream kinase for AMPK and the AMPK-related kinases. For full activity, LKB1 is required to be present in the cytoplasm, and binding of STRAD and MO25 to LKB1 results in cytoplasmic localization of the complex. Several lines of evidence suggest that LKB1, when bound to STRAD and MO25, is constitutively active. Treatment of intact cells with phenformin or AICAR, which potently activate AMPK, has no effect on the catalytic activity of either LKB1 or the ARKs, despite increased phosphorylation and activation of AMPK (Lizcano et al., 2004). Furthermore, the activity of LKB1 or of the AMPK-related kinases was not increased in response to contraction in muscle, despite increased Thr172 phosphorylation and activation of AMPK (Sakamoto et al., 2004). The lack of effect of energy stress on the activity of the AMPK-related kinases can be explained by the observation that the AMPK-related kinases, unlike AMPK-α, do not associate with the AMPK-β or AMPK-γ subunits and cannot respond to AMP in the same manner (Al-Hakim et al., 2005). Despite this, many groups have reported that LKB1 activity is modulated by post-translational modifications, particularly phosphorylation. LKB1 is phosphorylated on multiple residues. Phosphorylation of Ser31, Ser325, Thr366 and Ser431 appear to be mediated by upstream kinases, whereas LKB1 autophosphorylates on Thr185, Thr189, Thr336 and Ser404 (Alessi et al., 2006). The figure below (4.1) illustrates the domain structure of LKB1 and the sites proposed to be modified by phosphorylation and farnesylation.

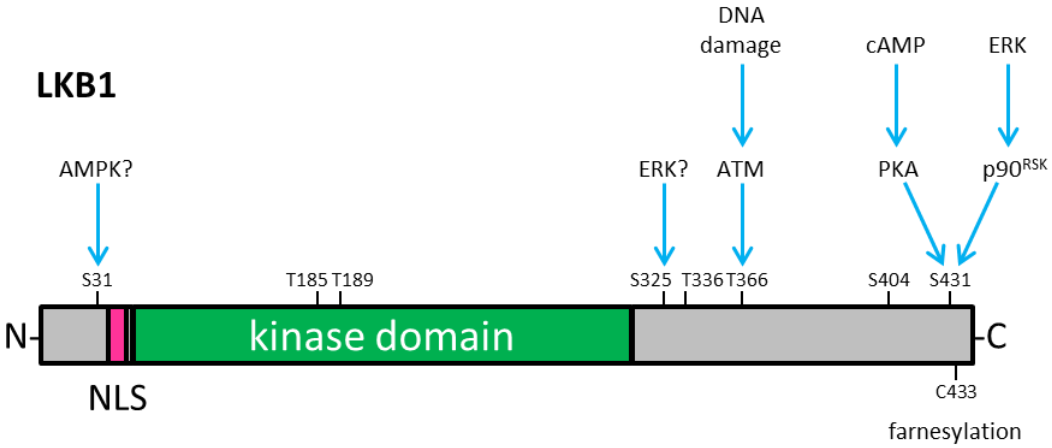

Figure 4.1: Domain structure of LKB1 and location of post-translational modifications
LKB1 has an N-terminal domain (containing an NLS), a kinase domain, and a C-terminal domain proposed to be a regulatory region. The location of phosphorylation and farnesylation sites are shown, together with the proposed upstream kinases. Sites Thr185, Thr189, Thr336 and Ser404 are autophosphorylation sites.

Phosphorylation of Ser325 has been reported to have no regulatory effect on LKB1 function, as mutation of this site to either alanine or the phosphomimetic aspartate did not alter the ability of LKB1 to reduce cell growth (Sapkota et al., 2002a). The upstream kinase(s) acting on this site are unknown, although it was suggested that, as the region around Ser325 is proline-rich, this site may be the target of a proline-directed kinase (Sapkota et al., 2002a). Recently, ERK was proposed as the upstream kinase for Ser325 (Zheng et al., 2009). Mutation of this site to alanine appeared to increase the activity of LKB1 towards AMPK in intact cells, suggesting that phosphorylation of this site inhibited LKB1 function. This result has been disputed in unpublished work from our laboratory where ERK did not phosphorylate LKB1 to any significant degree and where mutation of Ser325 to alanine had no effect on the ability of LKB1 to activate AMPK in a cell-free system (Dandapani, PhD thesis, 2013).

Mutation of Thr366 partially reduced the ability of LKB1 to suppress growth of G361 cells, although not to the same extent as a kinase-dead mutant, and seemed to have

no effect on its ability to phosphorylate either itself or p53 (Sapkota et al., 2002a). Phosphorylation of Thr366 was increased in response to ionizing radiation, and the upstream kinase was identified as ATM (Sapkota et al., 2002b). The functional consequence of phosphorylation at this site remains unclear.

The C-terminus of LKB1 was shown to be phosphorylated at Ser431 by cAMP-dependent protein kinase (PKA) in cell-free systems and in response to forskolin, a compound that raises intracellular cAMP levels and activates PKA, in intact cells (Collins et al., 2000). The authors also identified Cys433 as a prenylation site. Work from the Alessi laboratory then demonstrated that full-length LKB1 was phosphorylated at Ser431 and that this was mediated by either PKA or $p90^{RSK}$ (Sapkota et al., 2001). Mutation of Ser431 to an alanine had no effect on the ability of LKB1 to autophosphorylate or to phosphorylate p53 (AMPK had not been identified as an LKB1 substrate at the time) but did reduce the ability of LKB1 to inhibit cell growth, having a similar effect as kinase-dead LKB1. *In vivo* prenylation at Cys433 was confirmed, although this did not influence the ability of LKB1 to inhibit growth (Sapkota et al., 2001). It has recently been reported that mutation of Ser431 had no effect on the ability of LKB1 to phosphorylate and activate AMPK in either cell-free or intact cell systems (Fogarty and Hardie, 2009). Expression of an S431A mutant of LKB1 was able to halt progression of LKB1-null G361 cells through the cell cycle just as well as wild-type LKB1, suggesting that phosphorylation of Ser431 is not required for LKB1 function (Fogarty and Hardie, 2009). Further support comes from the discovery that $LKB1_S$, a splice variant of LKB1 in which the last 63 residues are replaced with a 39 residue sequence lacking the Ser431 and Cys433 sites, could activate AMPK and the AMPK-related kinases to a similar extent as the wild-type protein (Towler et al., 2008). This

short form of LKB1 appears to play a role in spermiogenesis, because male mice lacking $LKB1_S$ were sterile (Towler et al., 2008).

The function of the autophosphorylation sites is unclear. Mutation of Thr336 to glutamic acid, a phosphomimetic, had no effect on LKB1 catalytic activity but did reduce the ability of LKB1 to suppress cell growth (Sapkota et al., 2002a). More recently, phosphorylated Thr336 was proposed to bind to 14-3-3 proteins, resulting in decreased association of LKB1 with its substrates, such as AMPK (Bai et al., 2012). Overexpression of 14-3-3 proteins attenuated LKB1-induced cell cycle arrest (Bai et al., 2012).

4.1.2 Phosphorylation of Ser31 of LKB1

The original AMPK consensus sequence was defined as ϕ(β/x)xxSxxxϕ, where ϕ is a hydrophobic residue, present at the -5 and +4 positions (relative to the phosphoacceptor) and β is a basic residue at either position -3 or -4 (Dale et al., 1995). Using the sequence surrounding Ser79 of ACC1 (fused to GST) as a substrate for AMPK, an extended consensus motif was examined and revealed that AMPK interacted with its substrates over a wider area than previously thought (Scott et al., 2002). The interaction was reported as occurring over a region of 21 residues, from -16 to +4, compared with the 10 residues outlined above. In particular, a region extending from -5 to -16 was proposed to form an amphipathic helix that interacted across a hydrophobic groove in the kinase domain of AMPK, and mutation of this region increased the K_m of AMPK for ACC by around 6-fold (Scott et al., 2002). Additionally, a basic residue at -6 was identified as important in determining the activity of AMPK towards ACC (Scott et al., 2002).

This work was expanded by the use of a peptide scanning library, where each peptide contained one fixed amino acid at a given position relative to a phosphoacceptor. Each peptide was used as a substrate for AMPK and the incorporation of phosphate determined, giving a measure of the selectivity of the kinase for each amino acid at each position (Gwinn et al., 2008). In agreement with the earlier study, a basic residue was strongly selected for in the -3 and -4 positions and a hydrophobic residue in the -5 and +4 positions. Furthermore, a polar residue was selected for in the +3 position. An optimal AMPK motif was determined, with additional secondary and tertiary selections also detailed (Fig. 4.2). Serine 31 of LKB1 lies within a region that bears similarity to this AMPK consensus motif. The sequence contains a hydrophobic residue at positions -5 and +4 as well as a basic residue at -3 and -4 (Fig 4.2). The sequence, although not conforming to the consensus as closely as other well-known substrates in that there is a hydrophobic rather than a polar residue at +3, appears to be a reasonable match for phosphorylation by AMPK. Additionally, the sequence around Ser31 is highly conserved amongst higher eukaryotes, suggesting it may have some functional role.

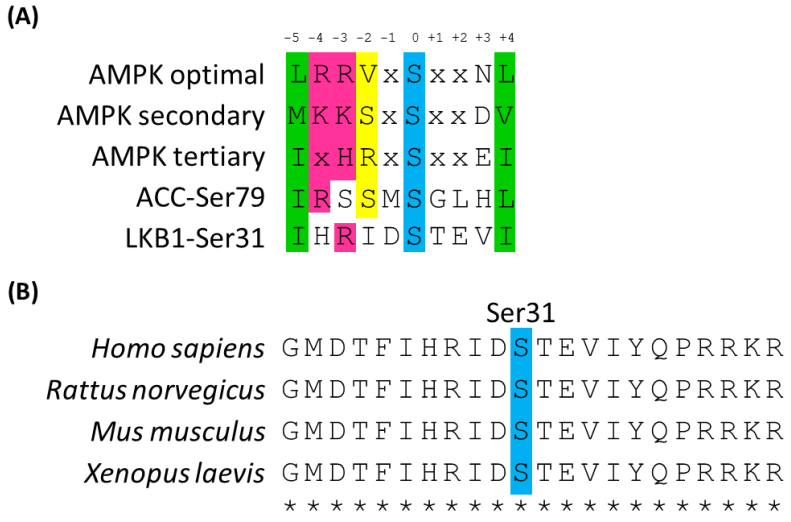

Figure 4.2: Protein sequence surrounding Ser31 of LKB1
(A) Comparison of the AMPK consensus motifs and the sequences around Ser79 of ACC1 and Ser31 of LKB1 (adapted from Gwinn et al., 2008). **(B)** The sequence surrounding Ser31 of LKB1 is conserved amongst higher eukaryotes.

4.2 Aim

The main aim of this chapter was to determine whether AMPK could phosphorylate Ser31 of LKB1 and to estimate the stoichiometry of this phosphorylation. This was investigated in a cell-free system using bacterially expressed wild-type LKB1 and a non-phosphorylatable serine to alanine mutant. Phosphorylation at this site was measured by ^{32}P incorporation and by the use of a phospho-specific antibody. The effect of Ser31 mutation on LKB1 function was investigated in intact G361 cells by measuring Thr172 phosphorylation and AMPK activity.

4.3 Results

4.3.1 AMPK can phosphorylate LKB1 in cell-free assays

The ability of AMPK to phosphorylate LKB1 was tested in a cell-free system. Bacterially expressed GST-LKB1 was incubated with increasing concentrations of native AMPK purified from rat liver with $MgCl_2$ and [γ-^{32}P]-ATP, with or without AMP. LKB1 is inactive in the absence of its binding partners STRAD and MO25, excluding the possibility of autophosphorylation or phosphorylation of Thr172 on AMPK-α.

Fig 4.3 shows that incubation with AMPK results in incorporation of ^{32}P into LKB1. This incorporation reached a maximum stoichiometry of approximately 0.14 nmol phosphate per nmol protein and was stimulated three-fold by AMP. The increase in phosphorylation in response to AMP suggests that it was mediated by AMPK and not a contaminating kinase in the rat liver preparation. AMPK alone gave significant autophosphorylation (data not shown) on the α and β subunits. This supports work performed in our laboratory where AMPK-α2 was demonstrated to autophosphorylate on Ser491 (Dr Simon Hawley, personal communication) and work in the literature where AMPK-β autophosphorylates on Ser108 (Mitchelhill et al., 1997). No autophosphorylation on the γ subunit has been reported, consistent with these results.

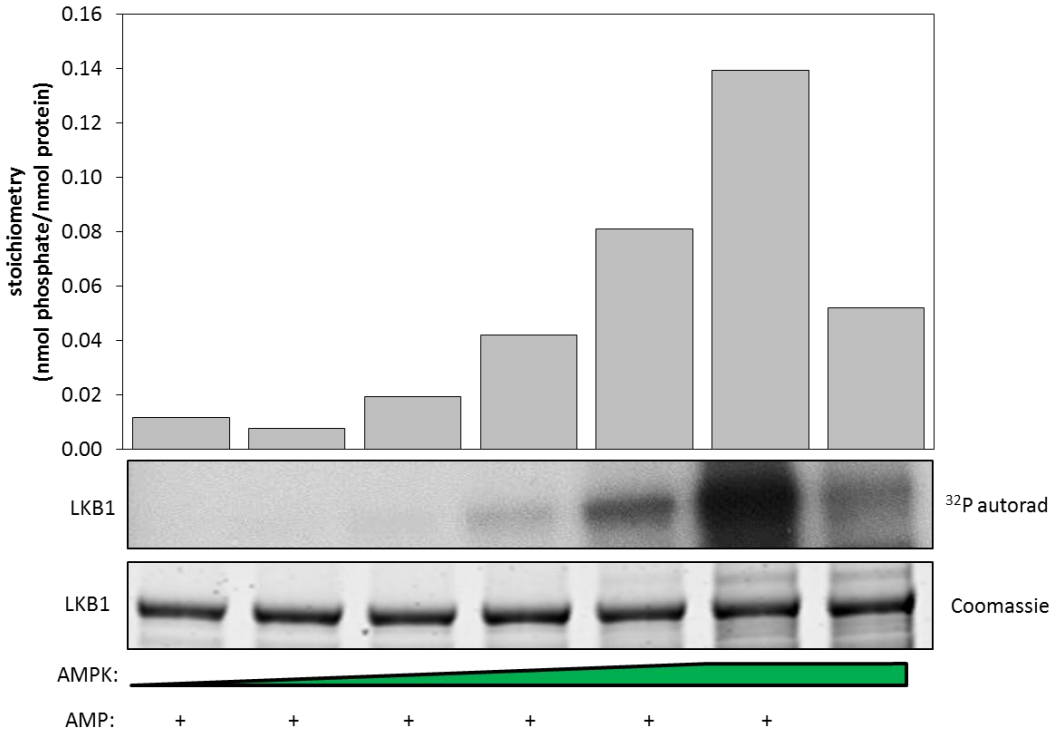

Figure 4.3: Phosphorylation of LKB1 by AMPK
Bacterially-expressed LKB1 and rat liver purified AMPK were incubated with Mg-[γ-^{32}P]-ATP for 15 minutes at 30°C. Reactions were stopped by the addition of SDS and analysed by PAGE. The gel was stained with Coomassie Blue (bottom) before autoradiography (top). The bar chart displays the incorporation of ^{32}P into LKB1.

4.3.2 Phosphorylation of LKB1 by AMPK occurs at Ser31

To investigate if the observed ^{32}P incorporation into LKB1 was at Ser31, a non-phosphorylatable alanine was introduced by site-directed mutagenesis of the wild-type construct. This generated a GST-fusion of LKB1 [S31A]. This construct was expressed and purified in *E. coli* (Fig. 4.4).

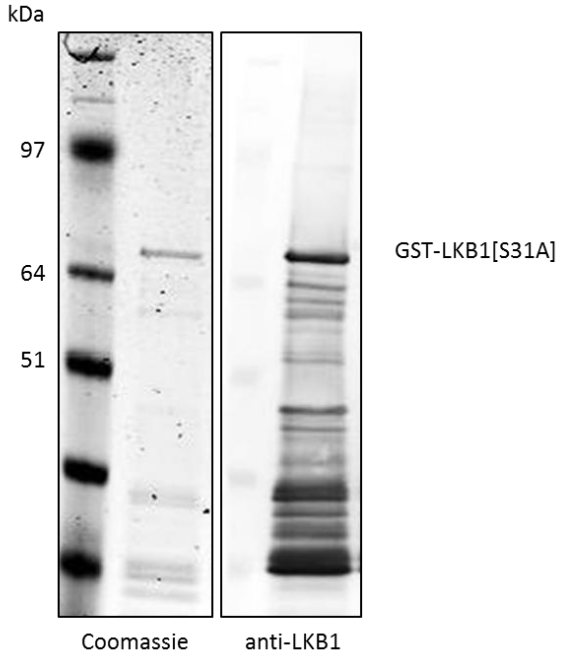

Figure 4.4: Purification of GST-LKB1 [S31A]
LKB1 containing a S31A mutation was expressed as a GST-fusion protein in bacteria and purified using a glutathione-Sepharose column. Purified protein was resolved by SDS-PAGE and visualized using Coomassie staining (left) or probed with an anti-LKB1 antibody (right).

Wild-type and S31A LKB1 were incubated with rat liver AMPK in the presence of $MgCl_2$, [γ-^{32}P]-ATP and AMP. Reactions were terminated by addition of SDS and analysed by SDS-PAGE and autoradiography (Fig. 4.5). As before, incorporation of ^{32}P was observed with wild-type LKB1 but this was lost with the S31A mutant protein, suggesting that the majority of the ^{32}P was being incorporated at Ser31 and that this site can be phosphorylated by AMPK in a cell-free assay. The stoichiometry of this phosphorylation, 0.5 mol phosphate/mol protein, was higher than that obtained in Fig. 4.3. The incubations in Fig. 4.5 were performed with a fresh preparation of rat liver AMPK which may explain the higher stoichiometry. To investigate if the ^{32}P incorporation had reached a maximum, the incubation times were increased to 30 minutes (Fig. 4.6). These results support those in Fig. 4.5, with only wild-type LKB1 displaying any significant ^{32}P incorporation. The stoichiometry of phosphorylation was

increased to 1.0 mol phosphate/mol protein for wild-type LKB1 after 30 minutes incubation with AMPK, although the stoichiometry of phosphorylation of the S31A mutant also increased to 0.3 mol phosphate/mol protein. This shows that close to stoichiometric amounts of phosphate can be incorporated at Ser31 on LKB1 by AMPK.

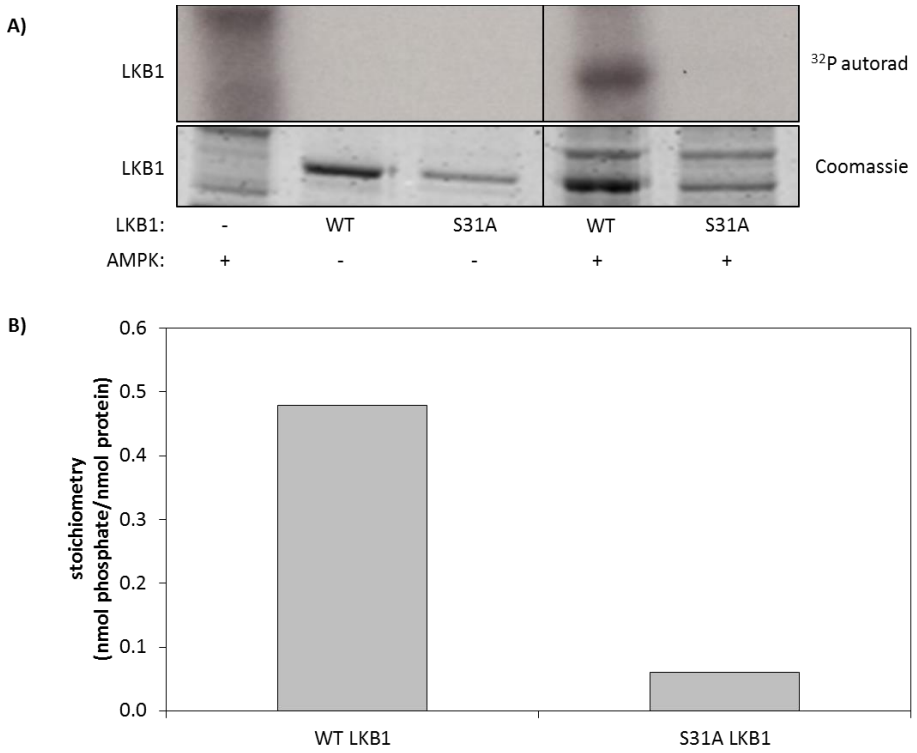

Figure 4.5: Phosphorylation of wild-type LKB1 and LKB1 [S31A] by AMPK after 15 min
Bacterially-expressed LKB1 and rat liver purified AMPK (100 U/ml) were incubated with Mg-[γ-^{32}P]-ATP for 15 minutes at 30°C. Reactions were stopped by the addition of SDS and analysed by PAGE. **(A)** The gel was stained with Coomassie Blue (bottom) before autoradiography (top). **(B)** Bar chart displays the incorporation of ^{32}P into the wild-type and S31A mutant of LKB1.

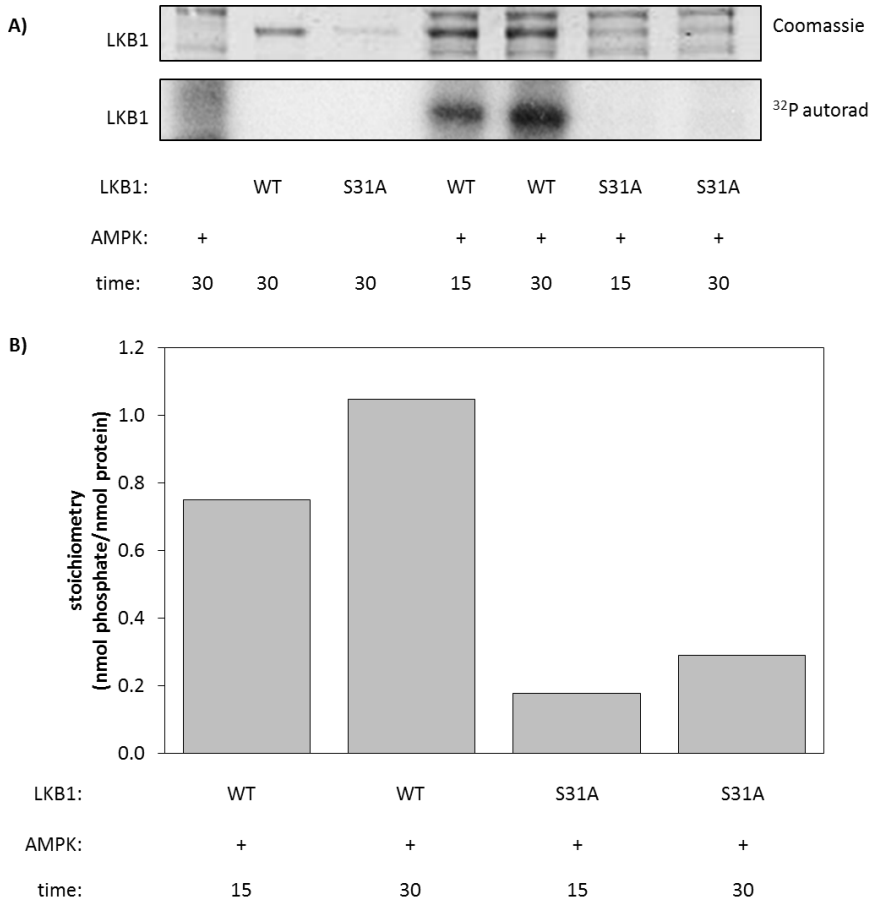

Figure 4.6: Phosphorylation of wild-type LKB1 and LKB1 [S31A] by AMPK after 30 min
Bacterially-expressed LKB1 and rat liver purified AMPK (100 U/ml) were incubated with Mg-[γ-^{32}P]-ATP for 15 or 30 minutes at 30°C. Reactions were stopped by the addition of SDS and analysed by PAGE. **(A)** The gel was stained with Coomassie Blue (bottom) before autoradiography (top). **(B)** The bar chart displays the incorporation of ^{32}P into the wild-type and S31A mutant of LKB1.

To further confirm that Ser31 was being phosphorylated, an antibody against phospho-Ser31 LKB1 was tested. Incubations of rat liver AMPK and wild-type or S31A LKB1 were carried out as above, using unlabelled ATP. Samples were analysed by Western blotting. Three different titrations of the phospho-Ser31 LKB1 antibody are shown in Fig. 4.7. The antibody shows increased reactivity with WT LKB1 that has been incubated with AMPK compared with LKB1 alone, most apparent in the 1000× antibody dilution.

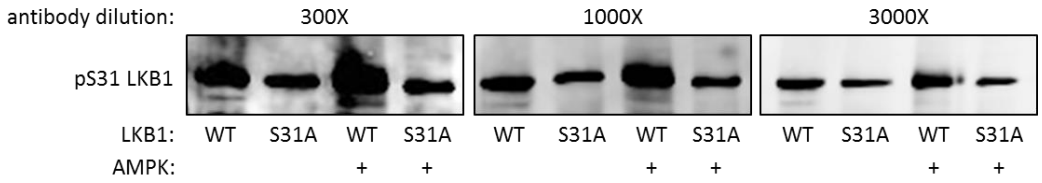

Figure 4.7: Titration of a phospho-Ser31 LKB1 antibody
Bacterially-expressed LKB1 and rat liver purified AMPK were incubated with Mg-ATP for 15 minutes at 30°C. Reactions were stopped by the addition of SDS and analysed by Western blotting using the phospho-Ser31 antibody at the indicated dilutions (stock antibody concentration was 0.7 mg/ml).

The antibody was not, however, particularly phosphospecific because a significant signal was obtained with the S31A mutant protein, although this signal did not increase in response to AMPK. The antibody had originally been purified by applying the collected sheep serum to a column bearing the phosphorylated form of the peptide originally injected, resulting in the purification of antibodies that cross-react with the phosphopeptide. This mixture may contain antibodies that also recognize the dephosphorylated form of the peptide, resulting in an antibody with poor phosphospecificity. To combat this, a dephosphorylated form of the peptide was included in antibody incubations. This dephosphorylated peptide was expected to compete with dephosphorylated LKB1 for binding to the non-phosphospecific antibody and thus reduce background for both wild-type and S31A LKB1 samples. Results from these incubations are shown in Fig. 4.8 and show that phosphospecificity has improved compared with Fig. 4.7. Quantification of the signals (at 50-fold excess of peptide) show that the signal obtained with the phosphospecific antibody increased approximately two-fold when wild-type LKB1 was incubated with Mg.ATP and AMPK, with no change observed with the S31A mutant of LKB1. These results suggest that AMPK can phosphorylate LKB1 at Ser31 and support those obtained in Fig. 4.5.

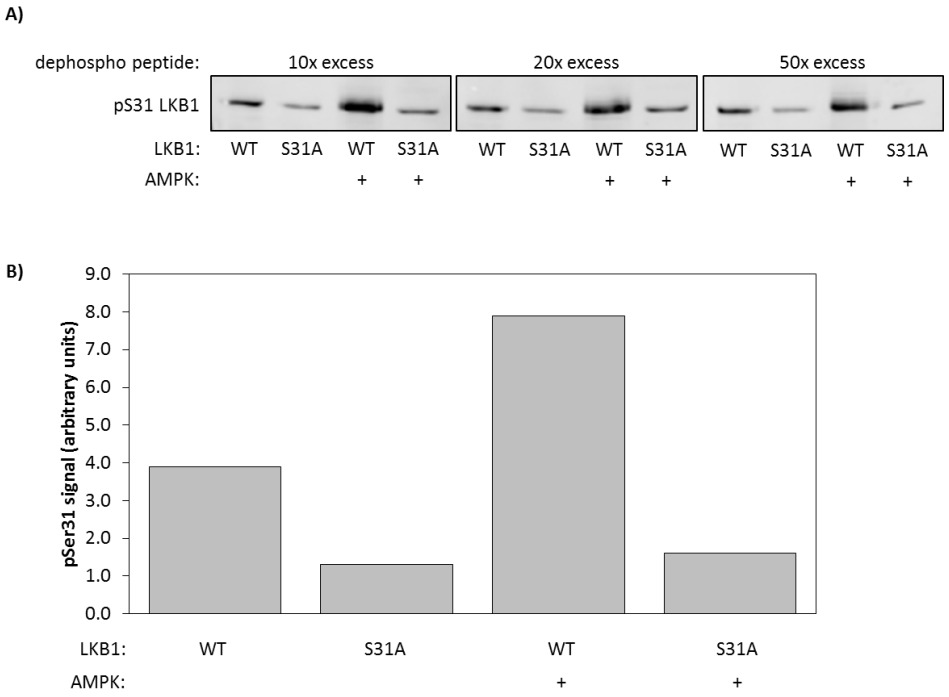

Figure 4.8: Effect of dephospho-peptide on the signal obtained using the phospho-Ser31 LKB1 antibody
Bacterially-expressed LKB1 and rat liver purified AMPK were incubated with Mg.ATP for 15 minutes at 30°C. Reactions were stopped by the addition of SDS and analysed by Western blotting using the phospho-Ser31 antibody (1000-fold dilution) and the indicated excess of dephospho-peptide. **(B)** The bar chart displays quantification of the pSer31 signal from the incubation containing 50-fold excess of dephospho-peptide.

To investigate if Ser31 of LKB1 is phosphorylated by AMPK in intact cells, HEK293 cells were treated with a range of AMPK activators and the lysates subjected to Western blotting using the phospho-Ser31 LKB1 antibody. Incubations were performed in the presence of an excess of the dephosphorylated Ser31 peptide. All treatments increased phosphorylation of ACC at S79, used as a marker for AMPK activity, but no change in Ser31 phosphorylation was detected (Fig. 4.9).

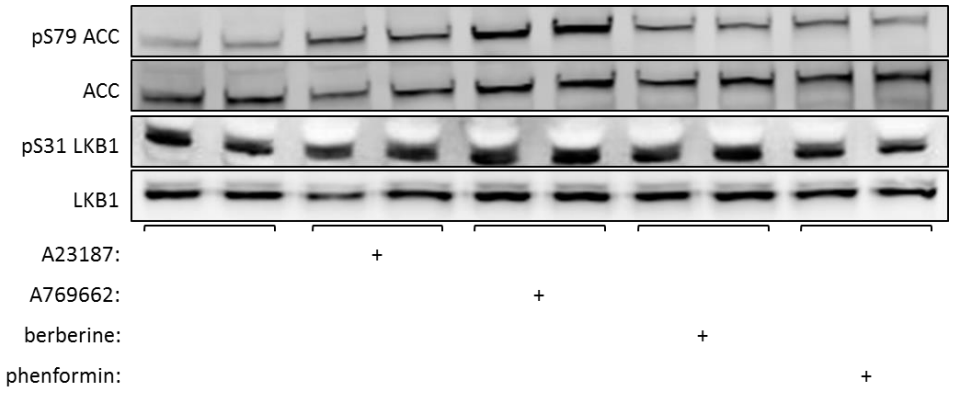

Figure 4.9: Effect of AMPK activators on phosphorylation of LKB1 at Ser31
HEK293 cells were treated with the indicated compounds for 60 min prior to lysis and cell lysates probed with the indicated antibodies. The Ser31 dephospho-peptide was included in the pSer31 LKB1 blot at a 50-fold excess.

4.3.3 Effect of Ser31 mutation in intact cells

Site-directed mutagenesis of human LKB1 fused to GFP (WT LKB1) was performed to generate alanine (S31A LKB1) and aspartic acid (S31D LKB1) mutants. G361 cells, which lack LKB1, were transfected with WT and mutant LKB1 along with its accessory proteins, FLAG-tagged STRAD-α and myc-tagged MO25-α, and cells were then treated with berberine or A23187 to activate AMPK. Berberine, via changes in AMP and ADP levels, activates AMPK via the LKB1 pathway and allosteric activation, while A23187, by increasing intracellular Ca^{2+}, activates AMPK through the CaMKKβ pathway. Fig. 4.10 shows the result of AMPK assays and Western blotting of the G361 cell lysates. Mutation of S31 to either alanine (non-phosphorylatable mutant) or aspartic acid (phospho-mimetic mutant) had no effect on the function of LKB1. In response to berberine, the S31A and S31D mutant LKB1 activated AMPK, as measured by AMPK kinase assay, Thr172 phosphorylation and ACC phosphorylation, to a similar extent as the wild-type LKB1.

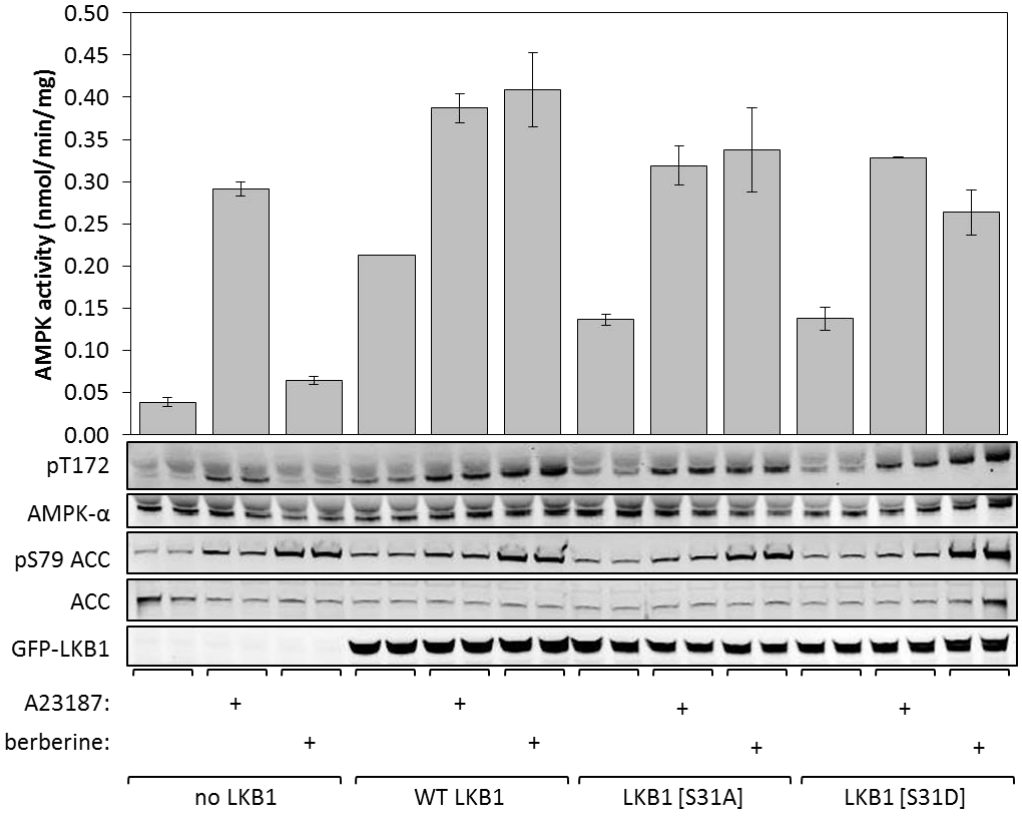

Figure 4.10: Transfection of G361 cells with LKB1

G361 cells were transfected with STRAD-α, MO25 and wild-type or mutant LKB1 (as indicated). After 36 hr, cells were treated with A23187 (10 µM) or berberine (300 µM) for a further 60 min before lysis. AMPK was immunoprecipitated from cell lysates using anti-AMPK-α1/-α2 antibodies and kinase activity measured using the AMARA peptide substrate (top). Results are mean ± range (n = 2). Cell lysates were subject to Western blotting with the indicated antibodies.

4.4 Discussion

These results demonstrate that, as predicted by others (Sapkota et al., 2002a), AMPK can phosphorylate LKB1 on Ser31. The stoichiometry of phosphorylation approaches 0.8 mol phosphate/mol protein, although the amount of AMPK required to achieve this is somewhat higher than that required to phosphorylate a *bona fide* AMPK substrate such as ACC or HMGR. Stoichiometric phosphorylation of LKB1 at Ser31 required incubation with 100 units of AMPK for 30 minutes, whereas phosphorylation of other substrates require up to 10-fold less AMPK. Ser31 appears to be the only site on LKB1 being significantly phosphorylated by AMPK, as mutation of this residue greatly reduced phosphorylation.

Although AMPK can phosphorylate LKB1 in a cell free system, it is unclear whether this occurs in intact cells. Using a phospho-specific antibody, no change in Ser31 phosphorylation was observed in response to a number of AMPK activators (Fig. 4.9). Equally, no difference in phosphorylation of Ser31 was observed when LKB1 from wild type and AMPK-$\alpha1^{-/-}$ -$\alpha2^{-/-}$ double knockout mouse embryo fibroblasts was probed with the phospho antibody (data not shown). These results, however, do not completely rule out the possibility that this site is phosphorylated by AMPK in intact cells. The antibody used displays reasonable phosphospecificity using purified LKB1 treated with and without AMPK but this may not be the case with cell lysates. Although the sequence around Ser31 is well conserved across higher eukaryotes (Fig. 4.2), the antibody was raised against the human LKB1 sequence, not mouse LKB1, and this could explain the fact that no difference was observed between the wild type and knockout mouse embryo fibroblasts. Future investigations require the generation of a more phosphospecific antibody.

Although Ser31 of LKB1 is phosphorylated in intact cells and can be phosphorylated to a reasonable stoichiometry by AMPK, it seems unlikely that the phosphorylation of Ser31 plays a major role in regulating the kinase. Mutation of Ser31 to either an alanine or aspartic acid had no effect on the ability of LKB1 to activate AMPK in G361 cells (Fig. 4.11). The basal AMPK activities in cells transfected with the Ser31 mutants were increased to the same level as that from cells transfected with wild type LKB1. Berberine, as discussed previously, increases cellular AMP levels and this increases Thr172 phosphorylation and AMPK activity in an LKB1-dependent manner. The AMPK activities measured in response to berberine treatment were similar in the cells transfected with wild type and S31A or S31D mutant LKB1. Thus, this site does not appear to be crucial for LKB1 function under the conditions examined. It is possible that the phosphorylation of Ser31 is mediated by a distinct kinase that is inactive under these conditions, explaining why no effect was observed. The data with the phosphomimetic mutant does not support this theory, but it could be that any effects on LKB1 function require the presence of a phosphate group and are not particularly well mimicked by an aspartate side chain. These results match those of Sapkota et al (2002a) where they observed no effect of S31 mutation on the ability of LKB1 to suppress growth of G361 cells. At the time, AMPK was not known to be a downstream target of LKB1 and phosphorylation of p53 or autophosphorylation was used as a measurement of LKB1 catalytic activity. However, mutation of Ser31 had no effect on LKB1 activity, agreeing with the data obtained in this chapter.

Although the phosphorylation of Ser31 on LKB1 by AMPK can be achieved in cell-free assays, it seems unlikely that this is a physiological event. The activity of LKB1 is not increased by treatment with phenformin or AICAR, two treatments that increase AMPK

activity (Hawley et al., 2003) or by muscle contraction (Sakamoto et al., 2004). Thus the physiological kinase for this site, and any functional relevance, remains to be identified.

CHAPTER 5: AMPK AND THE RESPONSE TO mTOR INHIBITION

5.1 Introduction

mTOR, in response to growth factors and nutrients, transmits pro-growth and pro-survival signals through a number of downstream targets (Laplante and Sabatini, 2012). As mTOR activity is increased in a number of different cancers and cancer syndromes, inhibition of mTOR is an attractive therapeutic option for these conditions. Rapamycin, a naturally occurring inhibitor, would appear to be an ideal candidate for this. However, there are a number of limitations to the use of rapamycin. Rapamycin is, except under certain circumstances (Sarbassov et al., 2006), a specific inhibitor of mTORC1. As seen in Fig. 1.8 of chapter 1, p70 S6 kinase forms a negative feedback loop to the insulin receptor substrate (IRS) proteins, reducing the stimulatory effect of growth factors on PI 3-kinase (PI3K). As mTORC1 is the upstream activating kinase for p70 S6 kinase, treatment with rapamycin removes this negative feedback loop and increases PI3K activity, providing pro-survival signals through PKB (Sun et al., 2005; O'Reilly et al., 2006). In addition, p70 S6 kinase inhibition activates the MAPK (Carracedo et al., 2008) and platelet-derived growth factor (Zhang et al., 2007) pathways, which act positively to mediate growth factor signalling. Treatment with rapamycin therefore increases pro-survival and proliferative signals and has not been as successful in tumour suppression as predicted, having only a cytostatic, rather than cytotoxic, effect (Efeyan and Sabatini, 2010). Additionally, rapamycin only partially inhibits phosphorylation of 4E-BP1 by mTORC1 (Chresta et al., 2010; García-Martínez et al., 2009), which, as discussed in Chapter 1, plays a key role in regulating cell proliferation downstream of mTORC1.

Recently, potent and highly-specific inhibitors that target both mTORC1 and mTORC2 have been identified, such as Torin1 (Thoreen et al., 2009), PP242 (Feldman et al., 2009) and Ku-0063794 (García-Martínez et al., 2009). Unlike rapamycin, which appears to work by weakening the interaction between raptor and mTOR and thus preventing the recruitment of certain substrates (Yip et al., 2010), these compounds function as ATP-competitive inhibitors of the mTOR catalytic subunit. By targeting both complexes, they remove the feedback inhibition problems associated with rapamycin. Thus, while inhibition of mTORC1 would still relieve the feedback inhibition loop from p70 S6 kinase to the IRS proteins, the inhibition of mTORC2 prevents the increase in phosphorylation of Ser473 on PKB (Chresta et al., 2010). Phosphorylation of Ser473 is required for subsequent phosphorylation of Thr308 and full activation of PKB. These compounds therefore dampen the increased signalling through the PI3K pathway induced by mTORC1 inhibition. In addition, and unlike rapamycin, the mTOR kinase inhibitors block phosphorylation of all mTOR targets, including 4E-BP1 (Chresta et al., 2010; García-Martínez et al., 2009). Indeed these compounds appear to be more potent than rapamycin in reducing cell proliferation (García-Martínez et al., 2009; Feldman et al., 2009).

Dual target mTOR inhibitors have been tested for anti-cancer properties in a range of *in vitro* and *in vivo* situations. AZD8055, a dual-target mTOR inhibitor, was reported to decrease tumour volume in a mouse model that spontaneously develops B-cell follicular lymphomas (García-Martínez et al., 2011). These mice are heterozygous for expression of PTEN and have depleted LKB1, resulting in elevated PKB activity and reduced AMPK activation (Huang et al., 2008). AZD8055 also induced a dose-dependent inhibition of tumour growth in mice bearing xenografts derived from cell

lines isolated from gliomas or lung adenocarcinoma (Chresta et al., 2010). Treatment of an acute myeloid leukemia cell line with AZD8055 reduced cell proliferation and cell cycle progression and increased the activity of caspase-3, part of the apoptotic cascade (Willems et al., 2011). Additionally, AZD8055 reduced the tumour volume, possibly by induction of caspase-dependent apoptosis, and increased survival of mice bearing a xenograft derived from this cell line (Willems et al., 2011). AZD8055 also decreased the proliferation and survival of primary cells isolated from acute myeloid leukemia patients, whilst having little effect on normal, immature cells (Willems et al., 2011). AZD8055 was also demonstrated to increase apoptosis, in combination with an HDAC inhibitor, in hepatocellular carcinoma cell lines and to reduce the size of tumours of mice bearing a patient-derived primary hepatocellular carcinoma xenograft (Shao et al., 2011). Finally, AZD8055 was reported to decrease tumour volume and increase survival of mice bearing a xenograft derived from a cultured head and neck squamous cell carcinoma cell line, and these effects were more potent than those observed with rapamycin (Li et al., 2013).

mTOR inhibitors are clearly promising as anti-cancer therapeutics. However, the status of other signalling pathways may determine the response to mTOR inhibitors. For example, treatment of $TSC1^{-/-}/TSC2^{-/-}$ cells with rapamycin increases their survival via removal of the p70 S6 kinase negative feedback loop and increased PKB signalling (see Fig. 1.8) (Shah et al., 2004). Given that the LKB1-AMPK pathway, like TSC1/TSC2, is a negative regulator of mTOR signalling, it is possible that this would also be the case when LKB1-null cells are treated with rapamycin. However, in the $TSC1^{-/-}/TSC2^{-/-}$ cells, the AMPK pathway would be intact whereas in the LKB1-null cells it would, under most

conditions, have a very low activity. The LKB1-AMPK pathway may therefore play a key role in determining the cellular response to mTOR inhibition.

The importance of understanding the link between LKB1-AMPK status and the response of cells to mTOR inhibition is accentuated when the extent to which the LKB1-AMPK pathway is implicated in the development and maintenance of tumours is considered. LKB1 is mutated in Peutz-Jeghers syndrome, a hereditary condition that pre-disposes suffers to cancer. Additionally, LKB1 is frequently lost in both lung (Sanchez-Cespedes et al., 2002) and cervical (Wingo et al., 2009) cancers. There is a growing body of evidence to suggest that AMPK itself can act as a tumour suppressor. In mice heterozygous for PTEN, inhibition of AMPK led to accelerated tumour development, while treatment with metformin, phenformin or A769662 delayed tumour onset (Huang et al., 2008). Further genetic evidence for the role of AMPK as a tumour suppressor *in vivo* comes from the observation that the loss of AMPK signalling in mice acts, via HIF-1α, to drive development of myc-induced B cell lymphomas (Faubert et al., 2013). These results support the idea that AMPK, rather than one or more of the AMPK-related kinases, is the key downstream mediator of the tumour suppressor effects of LKB1. Additionally, AMPK signalling appears to be down-regulated in many tumours, potentially providing them with a competitive growth advantage by removing any constraints on cell proliferation and protein synthesis (Hadad et al., 2009; Zheng et al., 2009). As the LKB1-AMPK pathway is disrupted in a large number of tumours, and mTOR inhibition is a promising therapeutic option, determining whether the LKB1-AMPK pathway influences the response to mTOR inhibition could give valuable insights into appropriate treatments for cancer.

5.2 Aims

To aim of this chapter was to characterize the response of mammalian cells to AZ4, a dual mTORC1 and mTORC2 inhibitor, and to determine if the status of the LKB1-AMPK pathway influenced this response. Using a variety of cell lines, the concentration of AZ4 required to inhibit the two TOR complexes was determined. The effect of AZ4 on AMPK activity was also investigated. The effect of mTOR inhibition on apoptosis was investigated in the presence and absence of serum, and under conditions where the AMPK pathway was either active or inactive.

5.3 Results

5.3.1 Generation of HeLa cells expressing wild-type or kinase-dead LKB1

HeLa cells, isolated from a human cervical cancer, do not express LKB1 due to a large deletion within the gene encoding it (Wingo et al., 2009). Using Flp-In technology (see Chapter 2 for details), HeLa cells expressing either wild-type LKB1 or a kinase-dead mutant were generated. The kinase-dead LKB1 contains a mutation in the DFG motif (D194A) that prevents it from binding Mg^{2+} ions and correctly positioning ATP for phosphotransfer, and is therefore catalytically inactive (Pearce et al., 2010). LKB1 function was assessed by treating cells with A23187, which increases AMPK activity via CaMKKβ, or phenformin, which activates AMPK in an LKB1-dependent manner. As expected, AMPK activity, as measured by kinase assay and phosphorylation of Thr172 and ACC, was increased in both cell lines in response to A23187, whereas only the cells expressing wild-type LKB1 responded to phenformin (Fig. 5.1). LKB1 activity was also assessed by measuring its ability to activate recombinant AMPK. LKB1 was immunoprecipitated from cell lysates, incubated with bacterially-expressed AMPK and the activity of AMPK measured. Only immunoprecipitates from wild-type LKB1 cells phosphorylated and activated AMPK (Fig. 5.2).

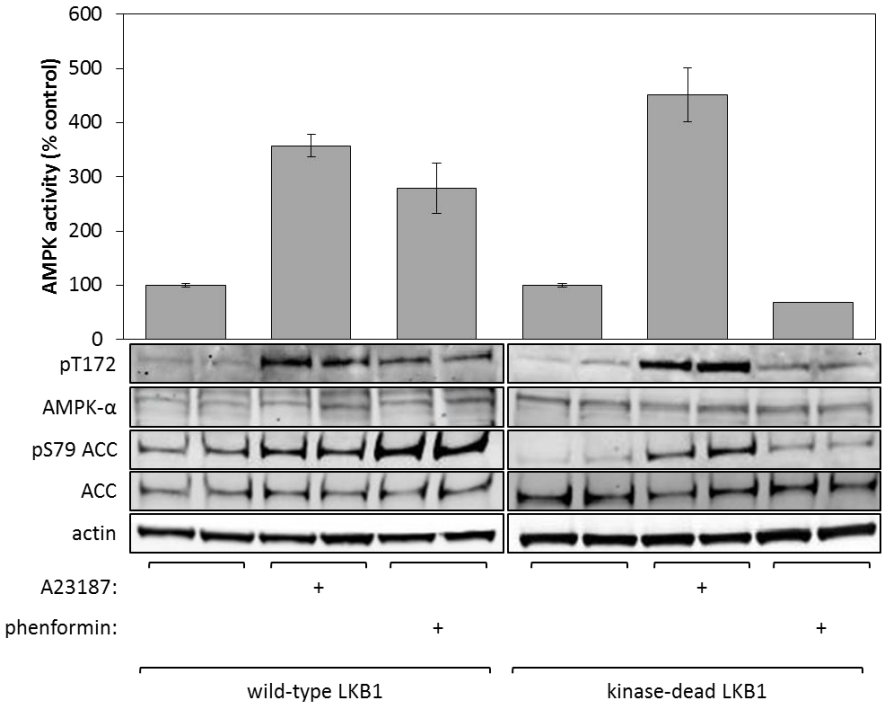

Figure 5.1: Characterization of HeLa cells expressing wild-type or kinase-dead LKB1
HeLa cells expressing wild-type or kinase-dead LKB1 were generated using Flp-In technology. Replicate dishes of cells were incubated for 1 hr with A23187 (10 µM) or phenformin (10 mM). AMPK was immunoprecipitated from cell lysates using anti-AMPK-α1/-α2 antibodies and kinase activity measured using the AMARA peptide substrate (top). Results are mean ± range (n = 2). Cell lysates were also subject to Western blotting with the indicated antibodies.

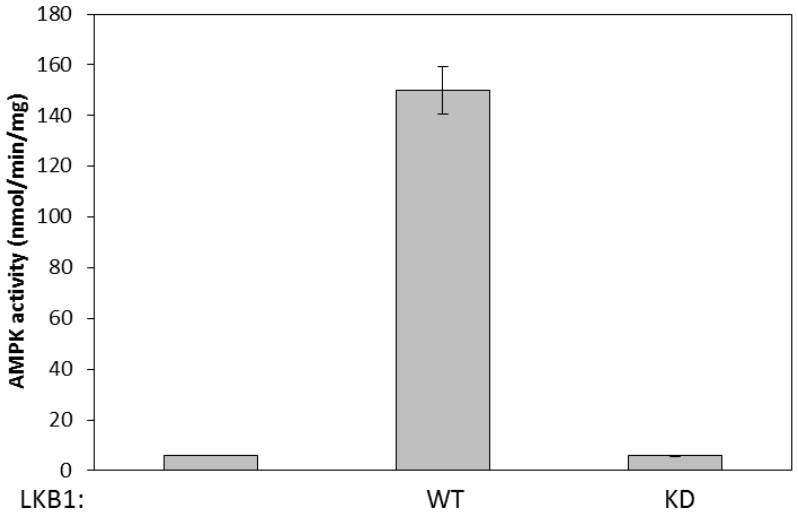

Figure 5.2: LKB1 activity of HeLa cells expressing wild-type or kinase-dead LKB1
LKB1 was immunoprecipitated from either wild-type or kinase-dead LKB1 HeLa cell lysates using anti-LKB1 antibodies. For the control, no lysate was added. LKB1 was incubated with dephosphorylated, bacterially expressed AMPK (α2β2γ1 complex) plus $MgCl_2$ and ATP. The activity of the AMPK complex was then assessed using the AMARA peptide substrate. Results are mean ± SEM (n = 3), except the blank where n = 1.

5.3.2 Effects of AZ4 on LKB1-expressing HeLa cells

The concentration of AZ4 required for inhibition of mTORC1 and mTORC2 in HeLa cells was examined. Phosphorylation of p70 S6 kinase at Thr389 was used as a marker of mTORC1 activity and phosphorylation of PKB at Ser473 used as a marker mTORC2 activity. A concentration of 0.1 µM AZ4 was found to completely inhibit mTORC1, while higher concentrations (> 1 µM) were required for complete inhibition of TORC2 (Fig. 5.3).

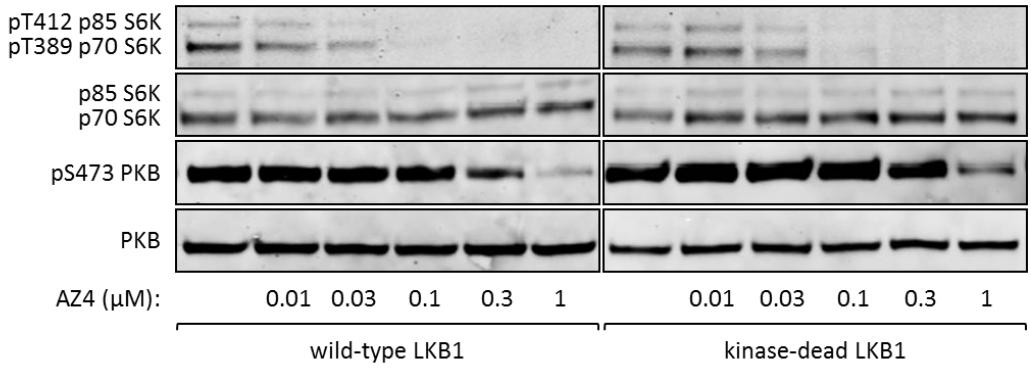

Figure 5.3: Titration of AZ4 in HeLa cells
HeLa cells expressing wild-type or kinase-dead LKB1 were incubated with the indicated concentrations of AZ4 for 1 hr. Cell lysates were subject to Western blotting with the indicated antibodies.

A wide variety of compounds can non-specifically act as mitochondrial poisons, altering cellular metabolism and activating AMPK. To ensure that this did not occur with AZ4, HeLa cells expressing wild-type LKB1 were treated with AZ4 up to 3 µM and the effects on AMPK activity were monitored (Fig. 5.4). No increase in AMPK activity, as measured by kinase assay, Thr172 phosphorylation or ACC phosphorylation was detected. In addition, no effect of AZ4 on the oxygen consumption rate of HeLa cells expressing wild-type or kinase-dead LKB1 was observed (Fig. 5.5). Taken together, these results demonstrate that, in HeLa cells, acute AZ4 treatment has no effect on mitochondrial function or AMPK activity.

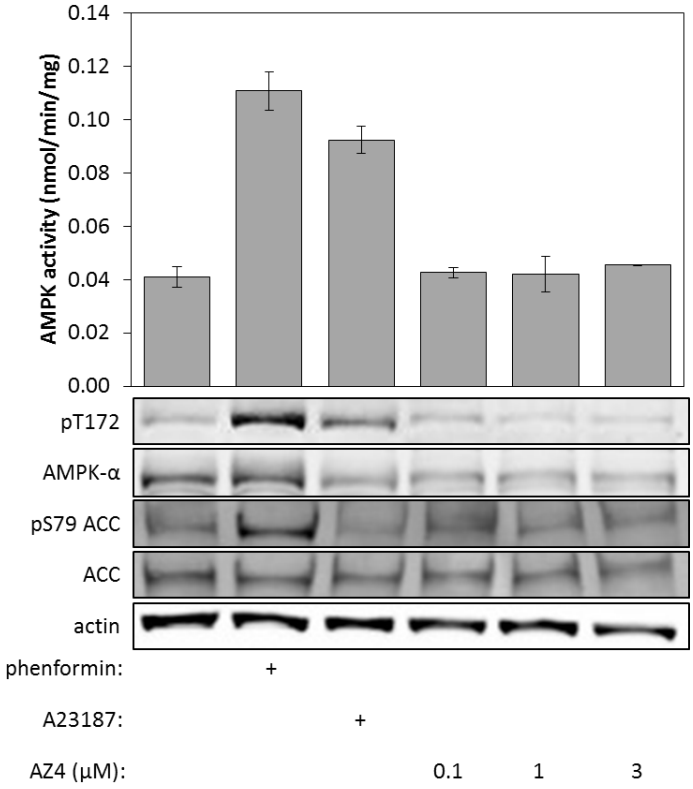

Figure 5.4: Effect of AZ4 on AMPK activity in HeLa cells
HeLa cells expressing wild-type LKB1 were incubated with phenformin (10 mM), A23187 (10 μM) or AZ4 (0.1, 1 or 3 μM) for 1 hr. AMPK was immunoprecipitated from cell lysates using anti-AMPK-α1/α2 antibodies and kinase activity measured using the AMARA peptide substrate (top). Results are mean ± range (n = 2). Cell lysates were also subject to Western blotting with the indicated antibodies (bottom).

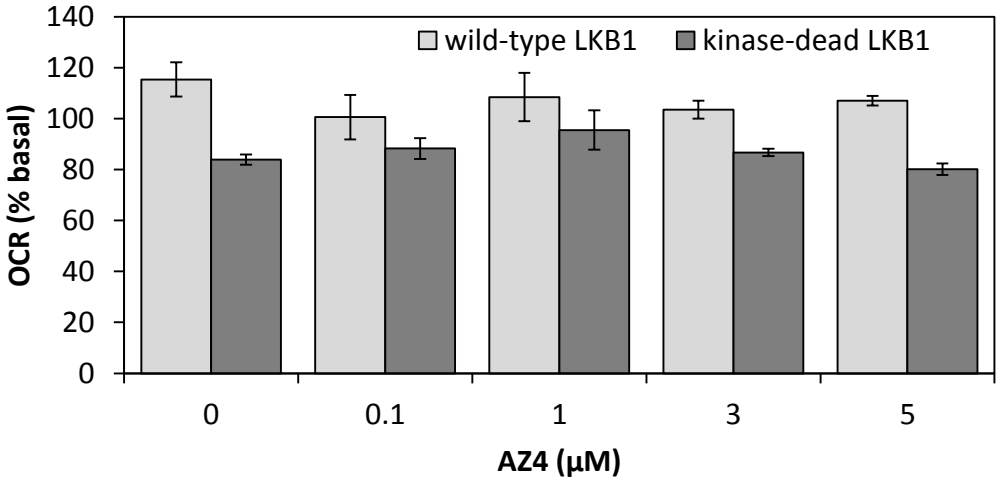

Figure 5.5: Effect of AZ4 on oxygen consumption rate (OCR) in HeLa cells
OCR analysis was performed using a Seahorse Biosciences XF24 extracellular flux analyser. HeLa cells (expressing wild-type or kinase-dead LKB1) were seeded into plates and the basal OCR calculated for every well. AZ4 was injected onto the cells and OCR measured over a 30 min period. Results are expressed as % of basal OCR (mean ± SEM, n = 3).

As mTOR inhibitors are considered promising anti-cancer therapies, the effects of AZ4 on the long-term growth and survival of the wild-type LKB1 and kinase-dead LKB1 HeLa cells were also examined. HeLa cells were treated with AZ4 for a period of 7 days and the number of cells determined. The results in Fig. 5.6 show that AZ4 at 0.1 μM, which was sufficient to inhibit mTORC1, had little effect on the growth of HeLa cells. However, at a concentration of 3 μM, which was sufficient to inhibit mTORC2, AZ4 greatly reduced the number of HeLa cells alive after 7 days, compared to untreated control. Cells expressing wild-type LKB1 appeared to be more resistant to AZ4-induced cell death, as a greater number remained alive after 7 days. To further investigate this, HeLa cells were treated for 48 hours with AZ4 and the effect on apoptosis determined by measuring cleavage of poly (ADP-ribose) polymerase (PARP). PARP is found in the nucleus and is involved in detecting and repairing DNA single strand breaks. PARP binds to single strand breaks and generates a chain of poly (ADP-ribose), which acts as a signal to recruit other DNA-repairing enzymes, such as DNA ligases. During apoptosis, PARP is cleaved by caspase-3 between Asp214 and Gly215, separating the DNA binding domain (24 kDa) from the catalytic domain (89 kDa). PARP helps cells to maintain their viability and its cleavage is used as a common marker for apoptosis. AZ4 did increase PARP cleavage, indicating an increase in apoptosis, and this effect was reduced in the cells expressing wild-type LKB1 compared with the controls expressing kinase-dead LKB1 (Fig. 5.7). These results suggest that a functional LKB1-AMPK pathway can protect cells from AZ4-induced apoptosis.

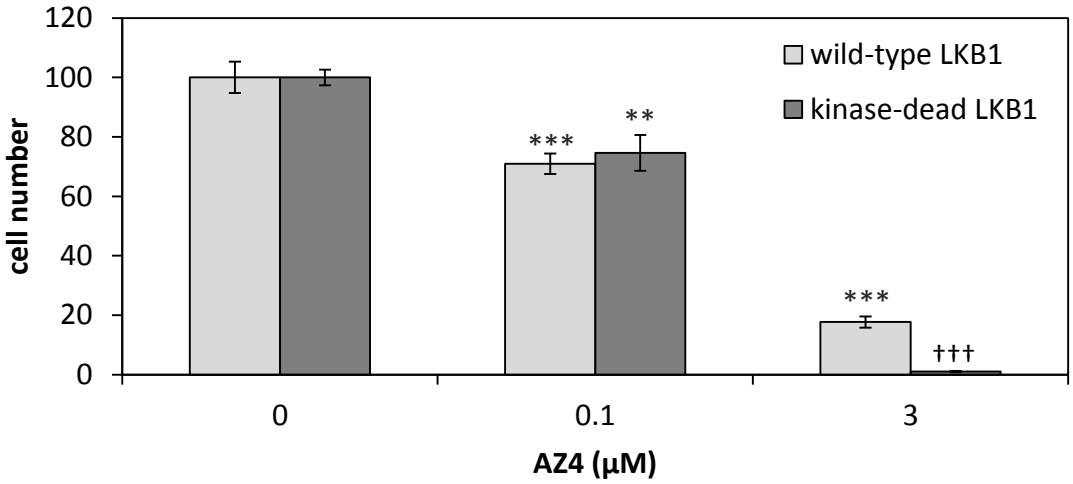

Figure 5.6: Effect of AZ4 on HeLa cell survival
HeLa cells expressing wild-type or kinase-dead LKB1 were incubated with AZ4 at 0.1 or 3 μM for 7 days. At the end of the treatment, cells were stained with trypan blue and the number of viable cells counted using a haemocytometer. Results are expressed as the % of viable cells compared to untreated control plates (mean ± SEM, n = 4). Significantly different from control without AZ4: ** $p < 0.01$, ***$p < 0.001$; significantly different from wild-type LKB1 with 3 μM AZ4: †††$p < 0.001$.

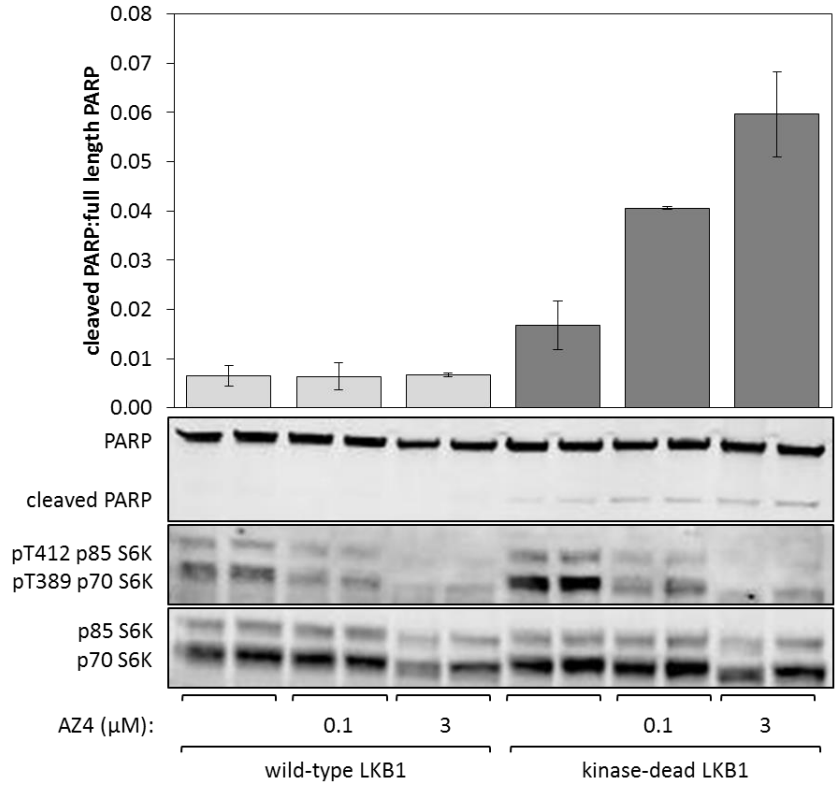

Figure 5.7: Effect of AZ4 on apoptosis in HeLa cells
HeLa cells expressing wild-type or kinase-dead LKB1 were incubated with AZ4 for 48 hr. Cell lysates were subject to Western blotting with the indicated antibodies. The bar chart displays the ratio of cleaved PARP to full-length PARP (mean ± SD, n = 2).

5.3.3 Response of G361 cells to AZ4

Although some effect of LKB1 expression were therefore observed in the HeLa cells they were relatively modest, possibly due to the low levels of LKB1 expression in these cells (the protein was hard to detect by Western blotting) and the resistance of the cells to AZ4-induced apoptosis. The response of other LKB1-null cell lines to AZ4 was therefore examined. G361 cells, as discussed previously, are an LKB1-null cell line isolated from a human melanoma. The effect of AZ4 on G361 cells was examined. The concentration of AZ4 required to inhibit mTORC1 and mTORC2 was similar to that in HeLa cells (Fig. 5.8) and AZ4 had no effect on AMPK activity (Fig. 5.9).

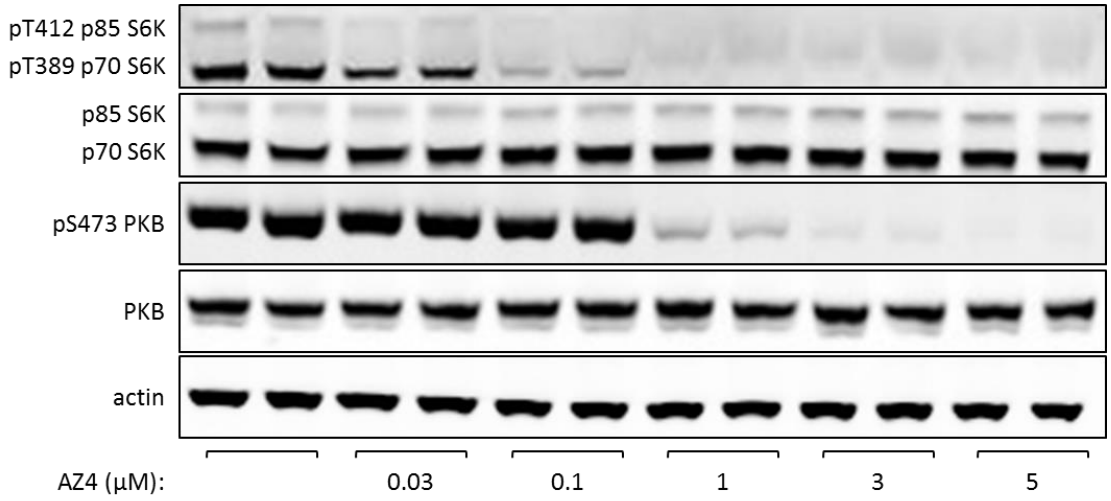

Figure 5.8: Titration of AZ4 in G361 cells
G361 cells were incubated with a range of concentrations of AZ4 for 1 hr. Cell lysates were subject to Western blotting with the indicated antibodies.

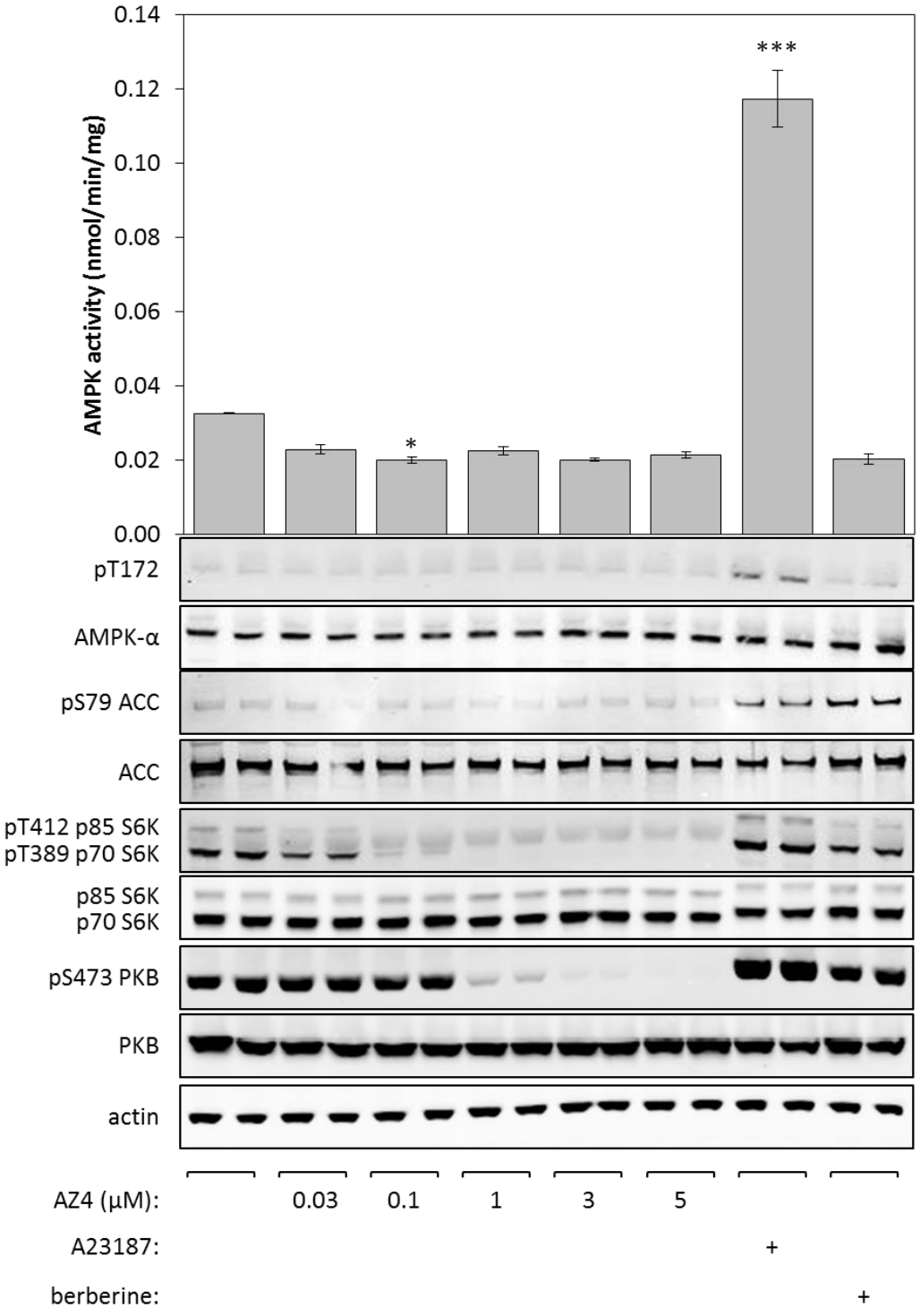

Figure 5.9: Effect of AZ4 on AMPK activity in G361 cells

G361 cells were incubated with AZ4, A23187 (10 μM) or berberine (100 μM) for 1 hr. AMPK was immunoprecipitated from cell lysates using anti-AMPK-α1/α2 antibodies and kinase activity measured using the AMARA peptide substrate (top). Results are mean ± SEM (n = 3). Cell lysates were also subject to Western blotting with the indicated antibodies (bottom). Significantly different from control: *$p < 0.05$, ***$p < 0.001$.

Cancer cells growing in the centre of a solid tumour may be exposed to conditions where growth factors are in limited supply. To simulate this, experiments were carried out in the presence and absence of serum. Cells were treated with AZ4 (3 µM, sufficient to inhibit both TORC1 and TORC2) for a period of 48 hours with and without A769662, a direct activator of AMPK. A769662 was selected as, unlike some other AMPK activators, it does not affect cellular energy status, which might result in cell death. Additionally, some AMPK activators, such as phenformin and quercetin, reduce phosphorylation of PKB at Ser473. This occurs independently of AMPK, as phosphorylation of Ser473 in response to phenformin or quercetin was reduced in both wild-type and AMPK-α1/-α2 double knockout mouse embryo fibroblasts (MEFs). No effect on Ser473 phosphorylation was observed with berberine, A769662 or A23187 (Fig. 5.10).

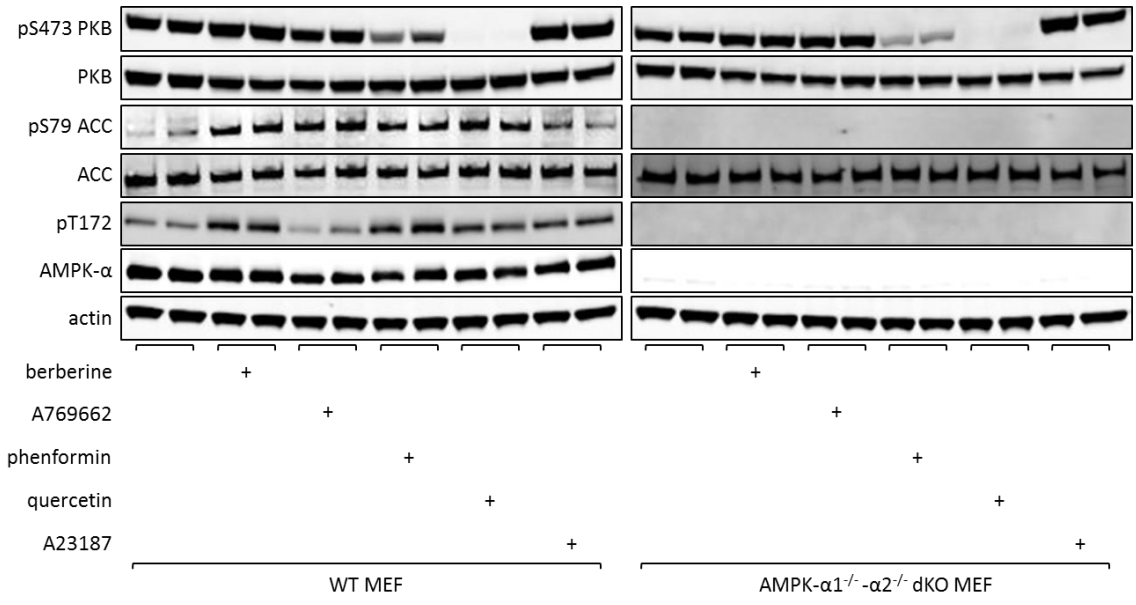

Figure 5.10: Effect of AMPK activators on phosphorylation of PKB at Ser473 in MEFs
Wild-type (WT) or AMPK-$\alpha1^{-/-}$ -$\alpha2^{-/-}$ double knockout (dKO) MEFs were incubated with berberine (300 µM), A769662 (300 µM), phenformin (10 mM), quercetin (300 µM) or A23187 (10 µM) for 1 hr. Cell lysates were also subject to Western blotting with the indicated antibodies.

In the presence of serum, AZ4 had little effect on PARP cleavage in G361 cells (Fig. 5.11). However, under serum-free conditions, a large increase in PARP cleavage was detected. Interestingly, the inclusion of A769662 greatly reduced PARP cleavage, restoring it almost back to basal levels. A769662 alone had no effect on PARP cleavage, and did not interfere with the ability of AZ4 to inhibit mTORC2 as measured by phosphorylation of Ser473 of PKB. The results in Chapter 3 have already demonstrated that A769662 can activate AMPK in LKB1-null cell lines.

The method for harvesting cells used in these experiments involves aspiration of the medium and washing of the cells, followed by rapid lysis with detergent. If A769662 was accelerating cell death it was possible that dead or dying cells had already been removed during the washing step, so that PARP cleavage would not be detected by Western blot. To rule this out, and to investigate the time course for AZ4-induced cell death, G361 cells were treated with AZ4 (0.1 μM or 3 μM) and A769662 in serum-free conditions and samples collected over a period of 48 hours (Fig. 5.12). To confirm that the compounds were active, the phosphorylation of ACC (marker of AMPK activity), PKB (marker of mTORC2 activity), GSK3 (marker of PKB activity) and p70 S6 kinase (marker of mTORC1 activity) were monitored. As expected, A769662 increased ACC phosphorylation. Treatment with 0.1 μM AZ4 decreased p70 S6 kinase phosphorylation, but had no effect on PKB or GSK3 phosphorylation. However, treatment with 3 μM AZ4, by inhibiting both mTORC1 and mTORC2, reduced phosphorylation of PKB, GSK3 and p70 S6 kinase. AZ4 had no effect on AMPK activity assessed by ACC phosphorylation, confirming previous observations. After 2 hours, AZ4 had no effect on PARP cleavage. At 24 hours, 3 μM AZ4 had increased PARP cleavage, but this was prevented by A769662. Similar results were obtained after 32 and 48

hours. Treatment with 0.1 µM AZ4, which does not inhibit mTORC2, had little effect on PARP cleavage until the 48 hour time point where a small increase was observed, although again this was reduced by A769662. Treatment of G361 cells with A769662 protected against AZ4-induced apoptosis.

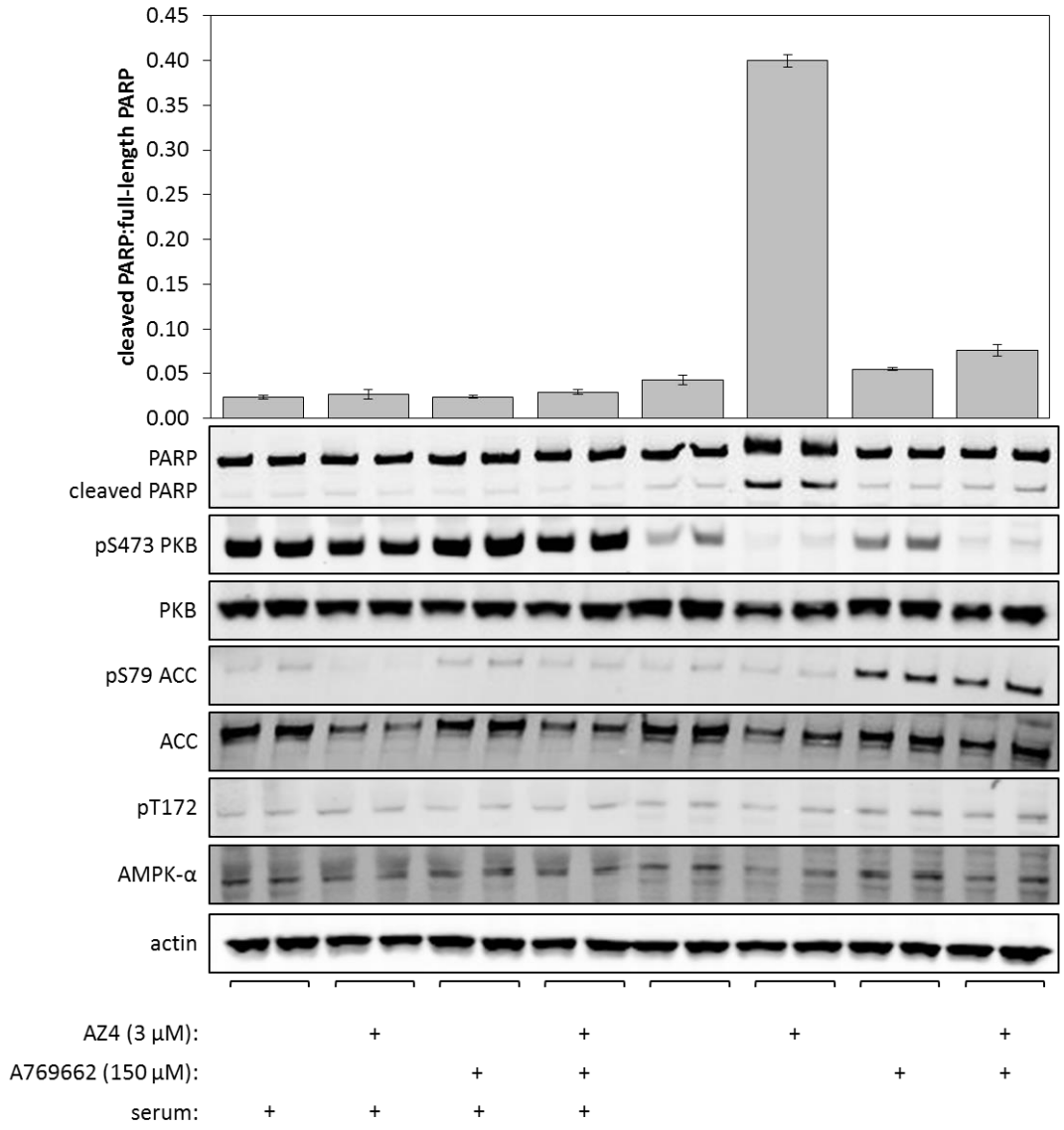

Figure 5.11: Effect of AZ4 on apoptosis in G361 cells
G361 cells were incubated with AZ4 (3 µM), A769662 (150 µM) or both in culture media ± foetal bovine serum for a period of 48 hr. Cell lysates were subject to Western blotting with the indicated antibodies. The bar chart displays the ratio of cleaved PARP to full-length PARP (mean ± SD, n = 2).

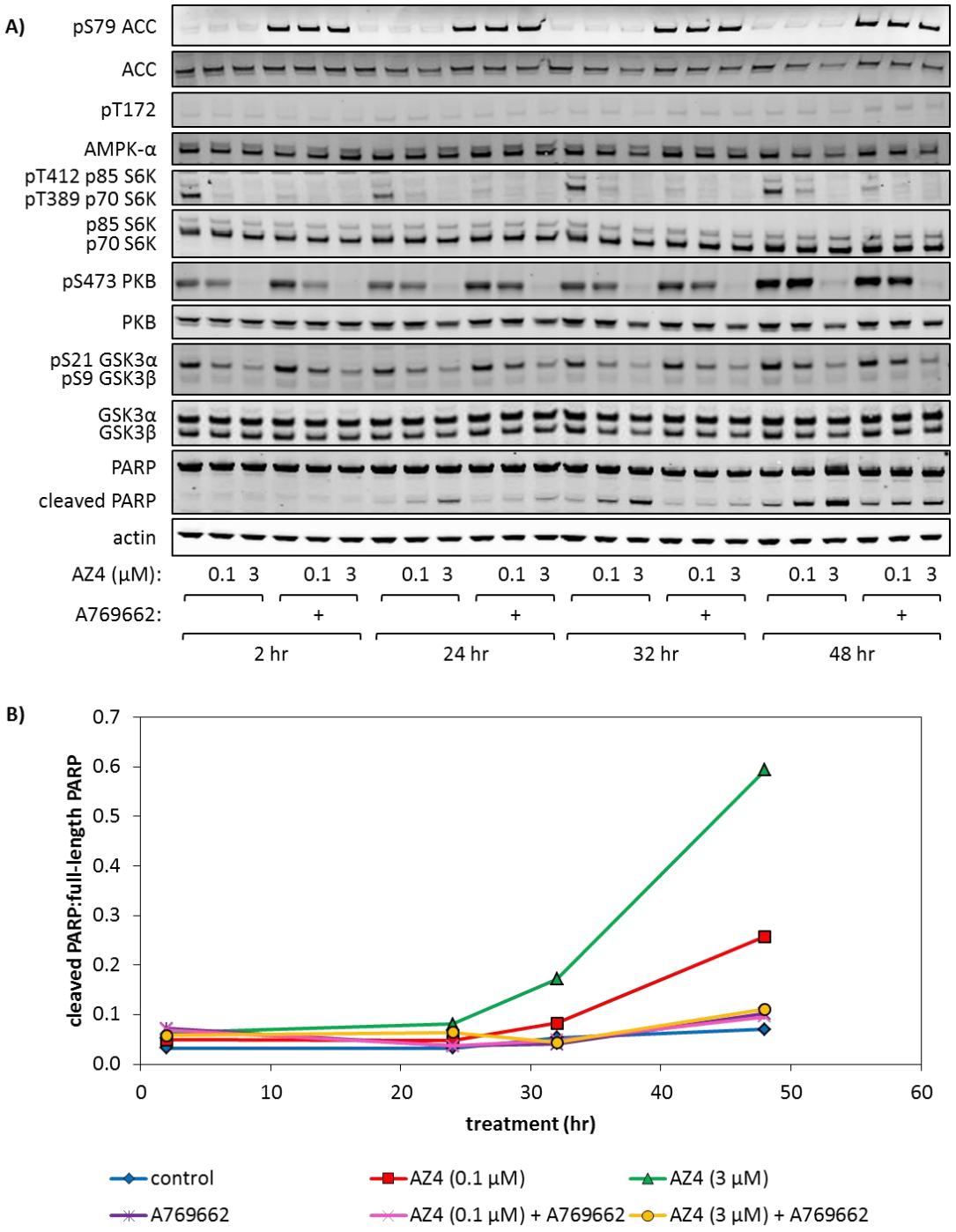

Figure 5.12: Time course of effects of AZ4 on apoptosis in G361 cells
G361 cells were incubated with AZ4 (0.1 or 3 μM), A769662 (150 μM) or both in serum-free culture media for a period of 48 hr. Lysates were prepared at various times throughout the course of the experiment. **(A)** Cell lysates were subject to Western blotting with the indicated antibodies. **(B)** Ratio of cleaved PARP to full-length PARP for each sample.

5.3.4 Effects of AZ4 on wild-type and AMPK-α1$^{-/-}$-α2$^{-/-}$ mouse embryo fibroblasts

The results described previously suggest that, in both HeLa and G361 cells, the presence of an active LKB1-AMPK pathway can protect cells against apoptosis. Although A769662 is a specific activator of AMPK, it is possible that these results are due to off-target effects of the compound. To further investigate the role of AMPK, experiments were performed using wild-type and AMPK-α1$^{-/-}$ -α2$^{-/-}$ knockout mouse embryo fibroblasts. Again, like the other cell lines, a higher concentration of AZ4 was required to inhibit mTORC2 compared with mTORC1 (Fig. 5.13). No effect of AZ4 on AMPK activity was observed (Fig 5.14).

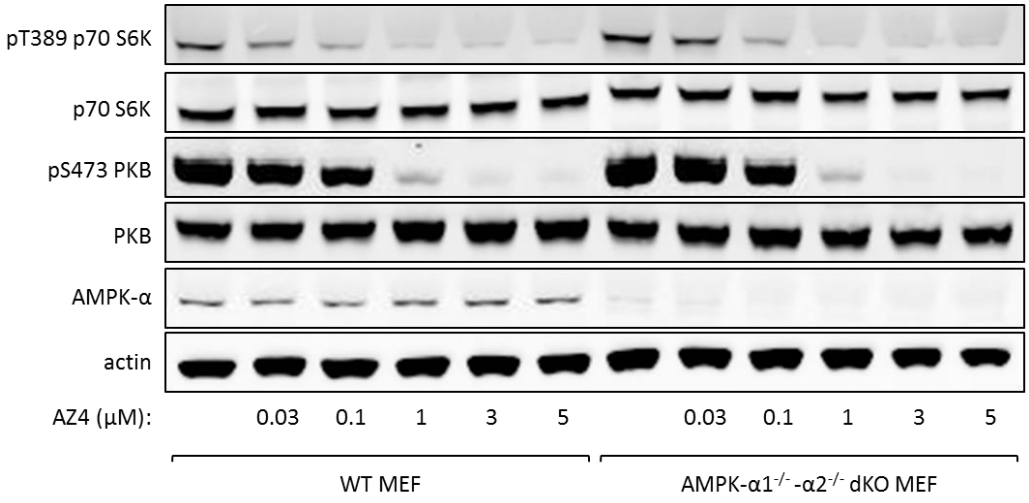

Figure 5.13: Titration of AZ4 in wild-type and AMPK-α1$^{-/-}$-α2$^{-/-}$ MEFs
Wild-type (WT) and AMPK-α1$^{-/-}$-α2$^{-/-}$ dKO mouse embryo fibroblasts were treated with a range of concentrations of AZ4 for 1 hr. Cell lysates were subject to Western blotting with the indicated antibodies.

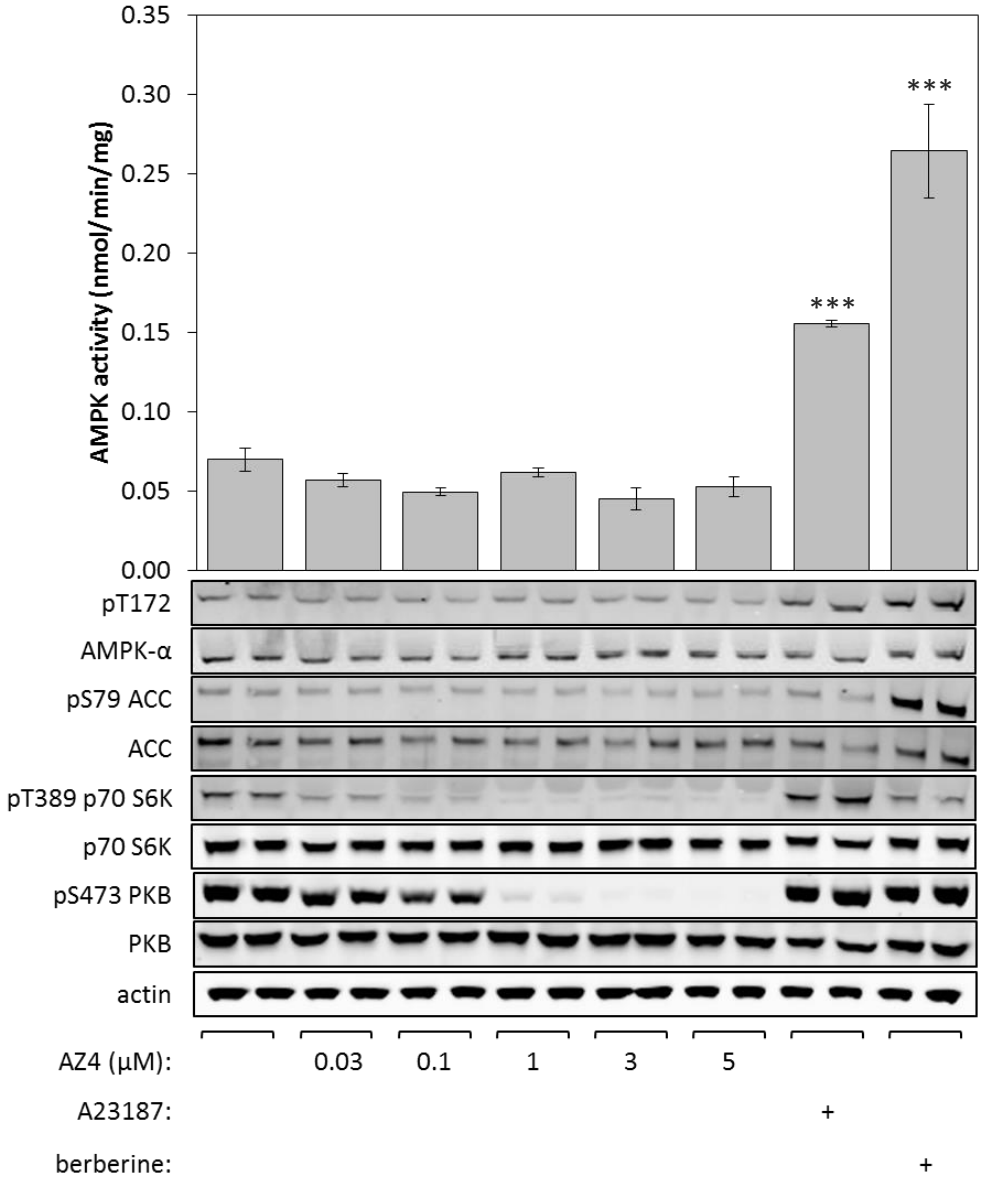

Figure 5.14: Effect of AZ4 on AMPK activity in wild-type MEFs
Wild-type MEFs were incubated with AZ4, A23187 (10 μM) or berberine (300 μM) for 1 hr. AMPK was immunoprecipitated from cell lysates using anti-AMPK-α1/-α2 antibodies and kinase activity measured using the AMARA peptide substrate (top). Results are mean ± SEM (n = 3). Cell lysates were also subject to Western blotting with the indicated antibodies (bottom). Significantly different from control: ***$p < 0.001$.

MEFs were also more sensitive to the serum-free conditions, with periods of greater than 12 hours in serum-free media resulting in the death of all cells (data not shown). Wild-type and AMPK-$\alpha1^{-/-}$-$\alpha2^{-/-}$ knockout MEFs were therefore treated with AZ4 in the presence and absence of serum for 6 hours (Fig. 5.15). Even under serum-free conditions, AZ4 had little effect on PARP cleavage in the wild-type cells. In contrast,

AMPK-$\alpha1^{-/-}$-$\alpha2^{-/-}$ knockout MEFs were sensitive to serum-free conditions, with AZ4 causing an even greater level of PARP cleavage. In contrast to G361 cells, where no signal was observed, it was also possible to monitor the cleavage of caspase-3 in the MEF cells. Caspases (cysteine-aspartic proteases) are a family of proteases that play key roles in the regulation of cell death, via both apoptosis and necrosis. Caspases are regulated at the post-translational level, allowing for rapid activation. Cleavage of caspase-3 mirrored that of PARP, with only small effects observed in the wild-type MEFs compared with AMPK-$\alpha1^{-/-}$-$\alpha2^{-/-}$ knockout MEFs (Fig. 5.15).

The time course of these effects were also investigated (Fig. 5.16). Wild type and AMPK-$\alpha1^{-/-}$-$\alpha2^{-/-}$ knockout MEFs were treated in the presence and absence of serum with AZ4 and samples taken for analysis over a 9 hour period. Results show that, even after 9 hours in serum-free media, AZ4 had no effect on apoptosis of the wild-type MEFs as measured by PARP or caspase-3 cleavage (quantified in Fig. 5.17). The AMPK-$\alpha1^{-/-}$ -$\alpha2^{-/-}$ knockout MEFs, however, were much more sensitive to the absence of serum and AZ4 treatment, and an increase in PARP and caspase-3 cleavage was evident after 6 hours.

In G361 cells, the AMPK activator A769662 protected cells from AZ4-induced apoptosis. To investigate if this was an off-target effect of the compound, the ability of A769662 to protect wild-type and AMPK-$\alpha1^{-/-}$-$\alpha2^{-/-}$ knockout MEFs from apoptosis was examined (Fig. 5.18). As before, AZ4 had little effect on wild-type MEFs but induced apoptosis in the AMPK-$\alpha1^{-/-}$-$\alpha2^{-/-}$ knockout MEFs. However, A769662 did not protect the knockout MEFS from AZ4-induced apoptosis. In fact, A769662 alone increased apoptosis in the knockout MEFs.

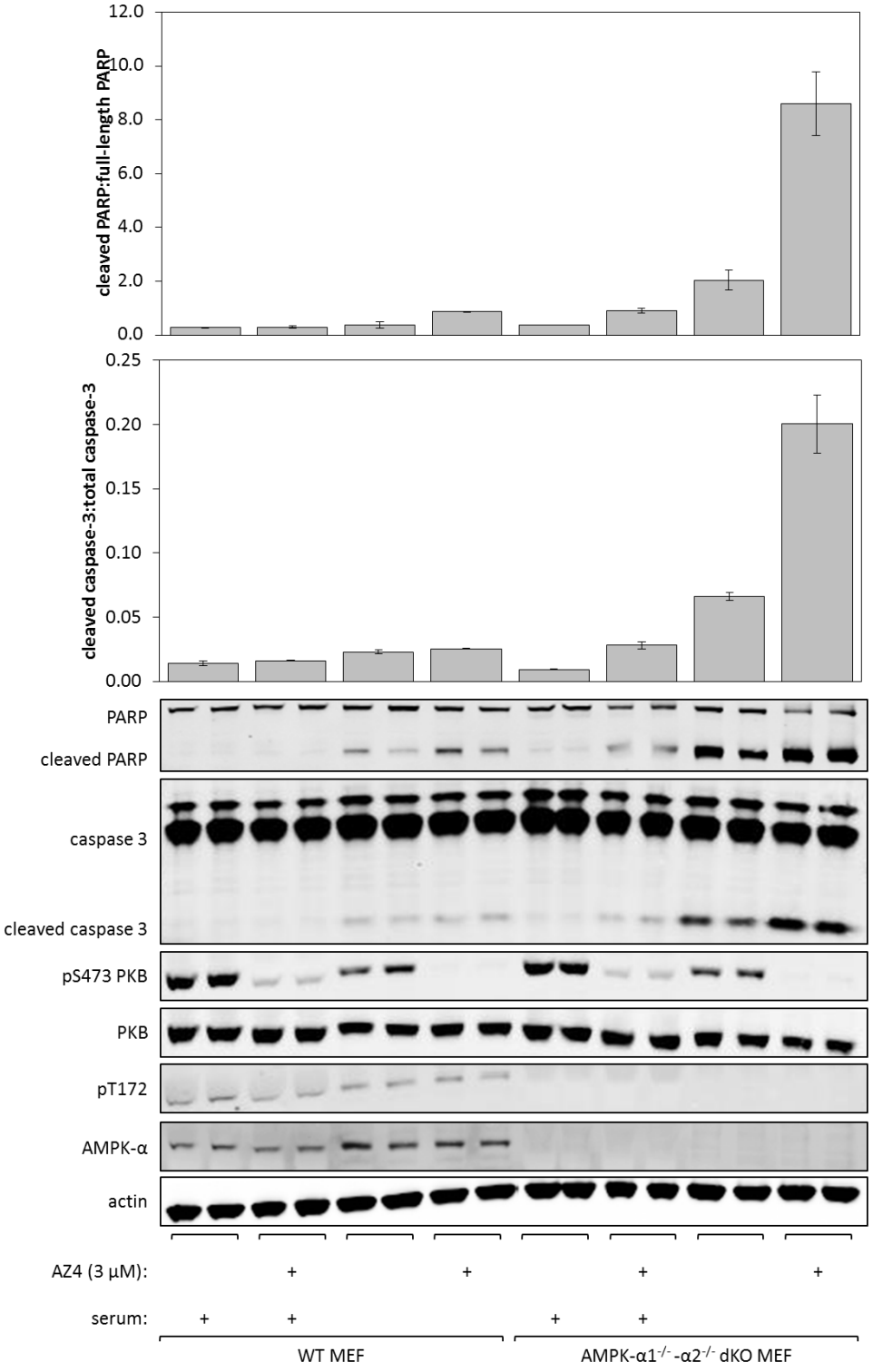

Figure 5.15: Effect of AZ4 on apoptosis of wild-type and AMPK $\alpha1^{-/-}$-$\alpha2^{-/-}$ dKO MEFs
Wild-type (WT) and AMPK-$\alpha1^{-/-}$-$\alpha2^{-/-}$ double knockout (dKO) MEFs were incubated ± AZ4 (3 µM) in the presence or absence of serum for a period of 6 hours. Cell lysates were subject to Western blotting using the indicated antibodies. The bar charts represent quantifications of the PARP and caspase-3 blots and are expressed as mean ± range of cleaved protein: total protein (n = 2).

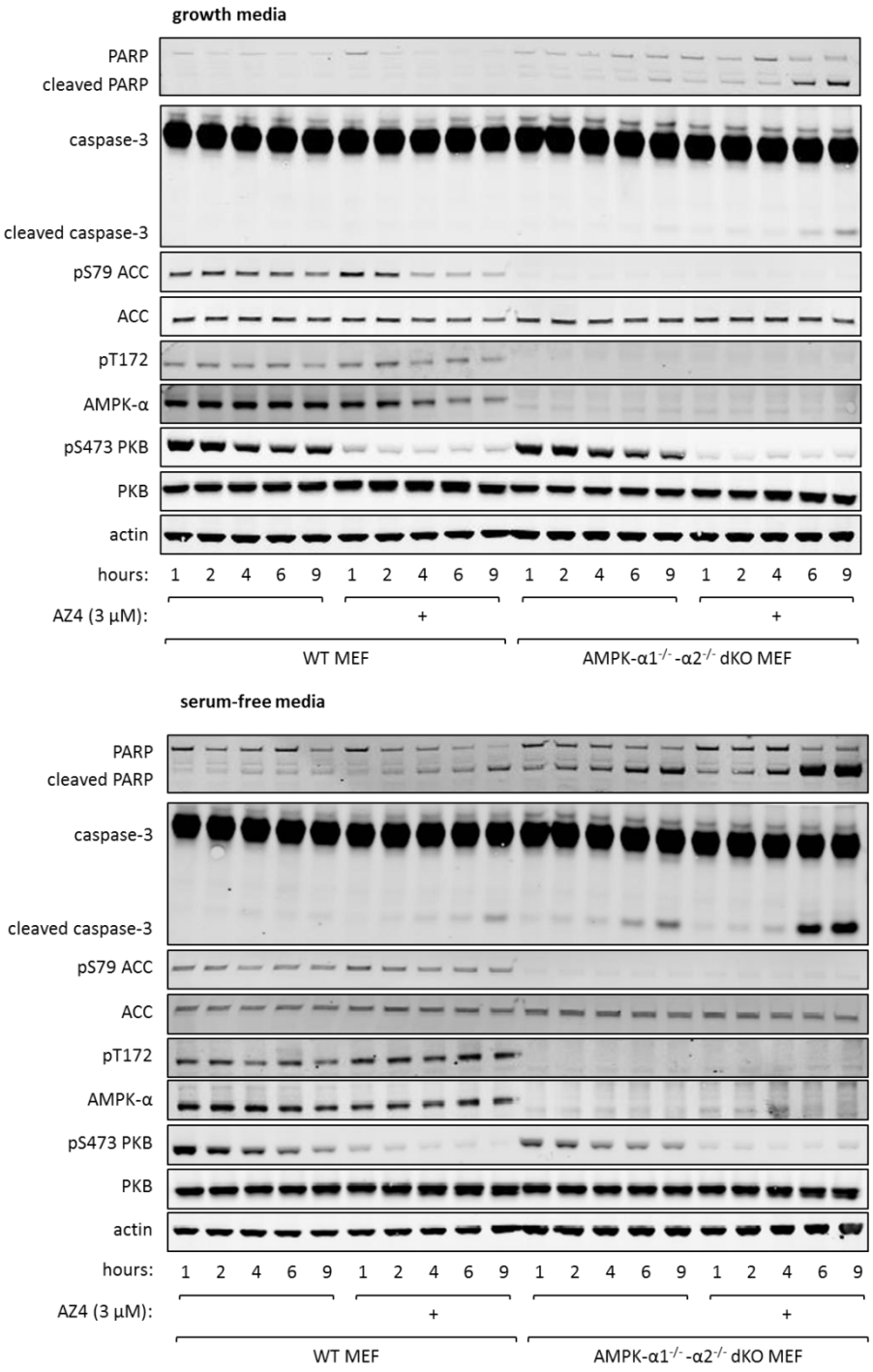

Figure 5.16: Time course of effects of AZ4 on apoptosis of MEF cells
Wild-type and AMPK-$\alpha1^{-/-}$ -$\alpha2^{-/-}$ dKO MEFs were incubated ± AZ4 (3 μM) in the presence of serum (top) or the absence of serum (bottom). Lysates were prepared at the indicated timepoints and subject to Western blotting with the indicated antibodies.

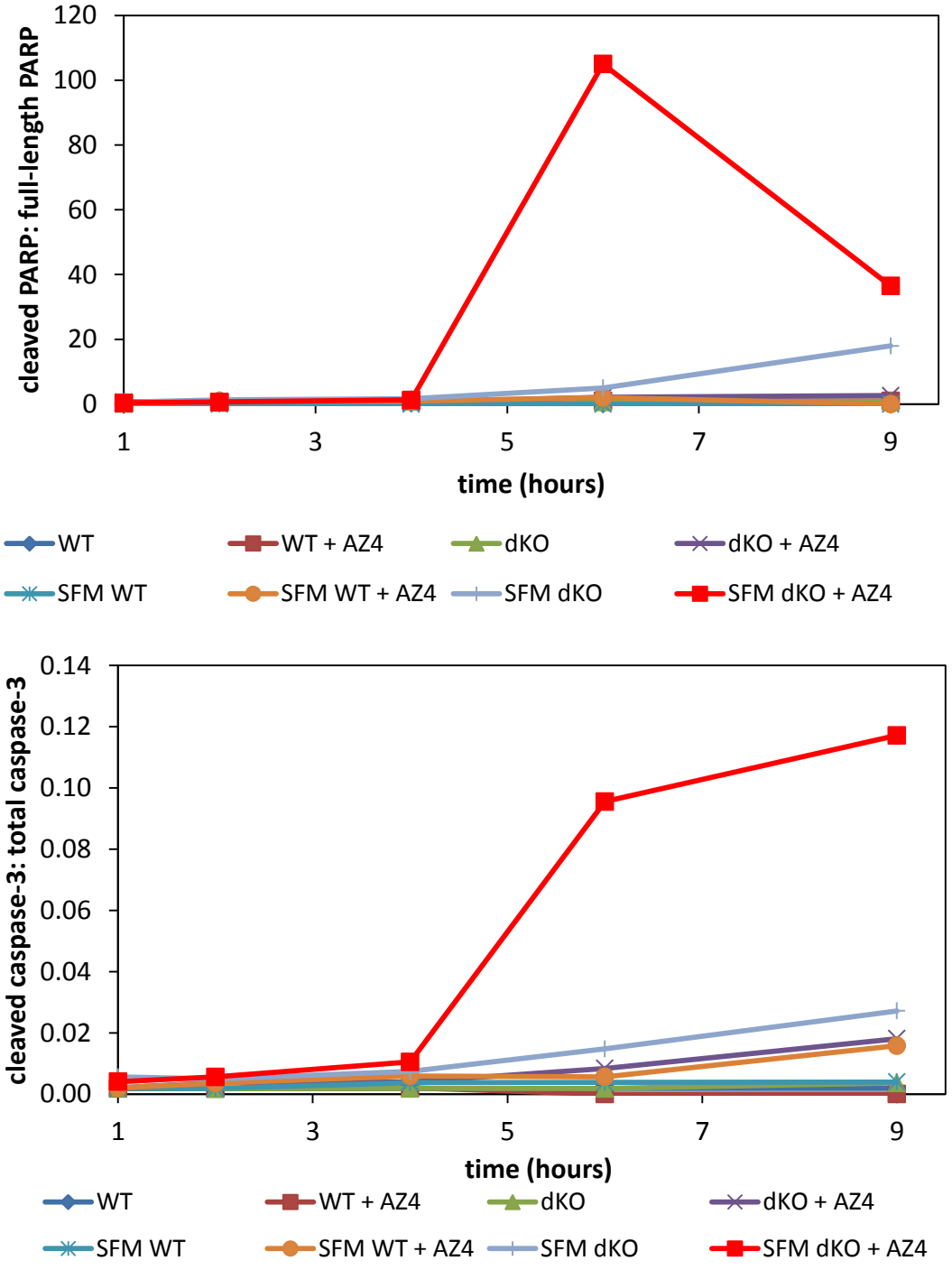

Figure 5.17: Quantification of PARP and caspase-3 blots
The ratio of cleaved PARP:total PARP (top) and cleaved caspase-3:total caspase-3 (bottom) was calculated from the blots in figure 5.16. WT, wild-type MEFs; dKO, AMPK-$\alpha1^{-/-}$-$\alpha2^{-/-}$ dKO MEFs; SFM, serum-free media.

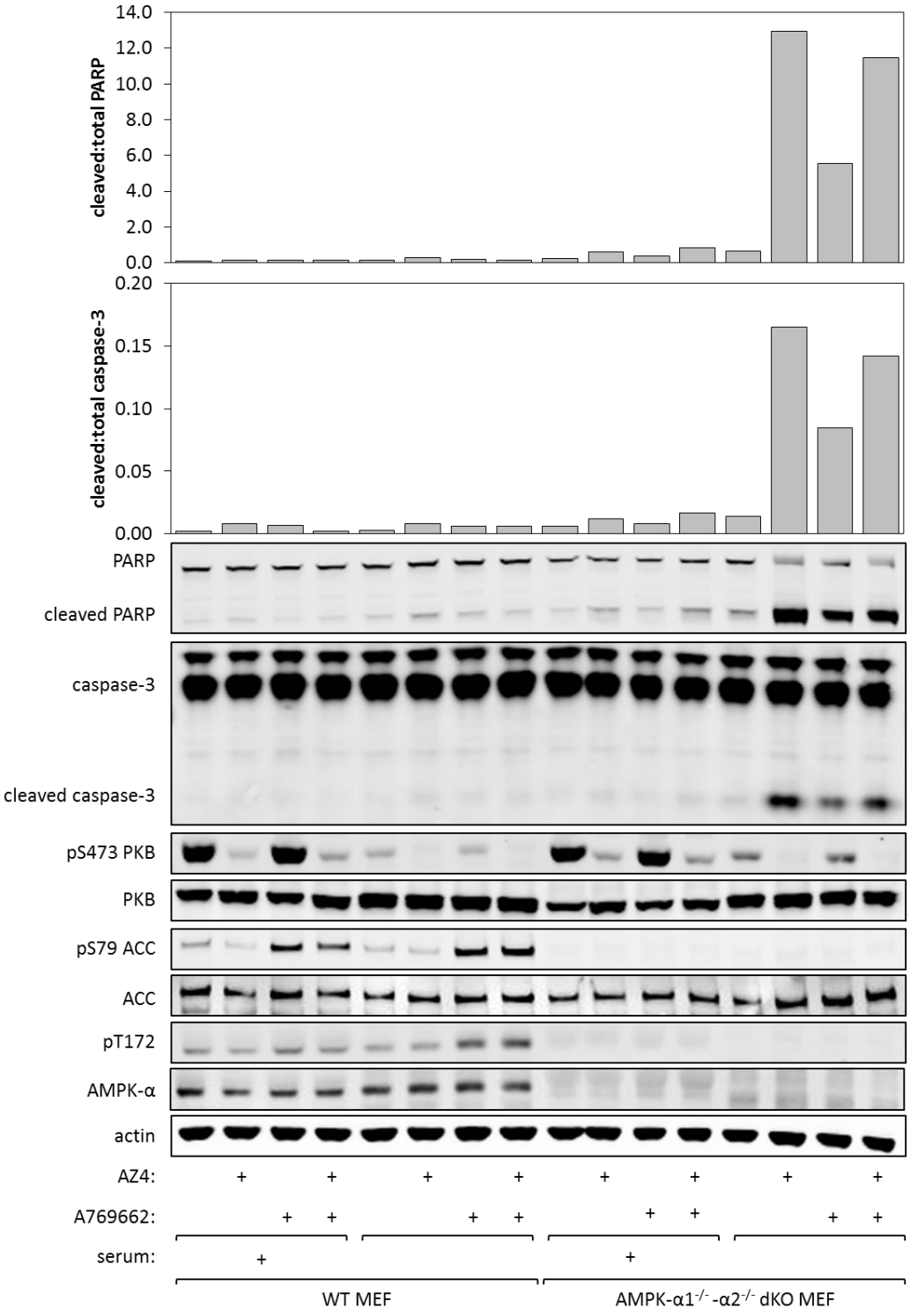

Figure 5.18: Effect of A769662 on AZ4-induced apoptosis in MEFs
Wild-type (WT) and AMPK-$\alpha1^{-/-}$-$\alpha2^{-/-}$ double knockout (dKO) MEFs were incubated ± AZ4 (3 µM) and ± A769662 in the presence or absence of serum for a period of 6 hours. Cell lysates were subject to Western blotting using the indicated antibodies. The bar charts represent quantifications of the PARP and caspase-3 blots and are expressed as mean cleaved protein: total protein (n = 1).

5.4 Discussion

The aim of this chapter was to determine the effect of mTOR inhibition on a range of cell lines, and to determine whether the status of the LKB1-AMPK pathway influenced this response. The evidence presented in this chapter suggests that, in a number of cell lines, inhibition of mTOR by AZ4, particularly under serum-free conditions, can result in apoptosis and cell death. Every cell line tested required higher concentrations of AZ4 to inhibit mTORC2 compared with mTORC1, and the induction of apoptosis appears to require the high concentrations of AZ4 that inhibited mTORC2 as well as mTORC1. Activation of the LKB1-AMPK pathway by A769662, a direct AMPK activator, prevented apoptosis in the LKB1-null G361 cell line. Additionally, genetic deletion of AMPK in mouse embryo fibroblasts sensitized the cells to apoptosis in response to mTOR inhibitors or serum deprivation, as seen when comparing the responses of wild-type and AMPK-$\alpha1^{-/-}$ -$\alpha2^{-/-}$ knockout mouse embryo fibroblasts. This supports the proposed role of the AMPK pathway in protecting cells against AZ4-induced death.

One important consideration in planning the treatment of any given cancer is the nature of the genetic lesion(s) giving rise to the tumour. In some cases, depending on which signalling pathways are hyper- or hypo-activated, the treatment may either have no effect or have detrimental side effects. For example, a recent study has demonstrated that 4E-BPs, which negatively regulate protein synthesis and are lost or strongly inhibited in a number of tumours, are essential for mediating the anti-proliferative effects of dual mTORC1/mTORC2 inhibition (Dowling et al., 2010). Similarly, inhibition of mTORC1 by rapamycin, under conditions where TSC1/TSC2 have been lost, actually promotes cell survival by removing a negative feedback loop to the PI3 kinase pathway (Shah et al., 2004).

The results in this chapter suggest that, whilst treatment of cells with mTOR inhibitors can slow growth and promote apoptosis, cells lacking a functional AMPK pathway are more susceptible to this treatment. The LKB1-AMPK status of a tumour may therefore partly determine the response to mTOR inhibition, and knowledge of this could help in designing effective and specific treatments. It would also be of interest to determine what components of the mTOR pathway require to be inhibited in order to induce apoptosis. From the results in this chapter it seems that it is inhibition of mTORC2 that drives apoptosis, as lower concentrations that only inhibited mTORC1 had much less effect on G361 cells. Using inhibitors of PKB and SGK, or cells lacking these proteins, it might be possible to determine whether either of these proteins are the key mediator of the effects of AZ4. However, it could also be that it is inhibition of 4E-BP1 phosphorylation by mTORC1 that transmits the pro-apoptotic signals, and that loss of 4E-BP1 would reduce the effects of AZ4 on apoptosis, similar to the effects discussed above (Dowling et al., 2010). Work on compounds structurally related to AZ4, such as AZD8055, demonstrates that concentrations of AZD8055 that inhibit phosphorylation of p70 S6 kinase also inhibit phosphorylation of 4E-BP1 (Chresta et al., 2010). This suggests, but does not prove, that apoptosis in response to AZ4 requires inhibition of mTORC2 activity. Equally, although the LKB1-AMPK pathway appears to protect against cell death induced by AZ4, it remains unclear by what mechanism this is occurring.

Given that AMPK regulates cell growth, protein synthesis and energy metabolism via many different pathways, it is not surprising that AMPK activators have been considered as potential anti-cancer therapies. Indeed, treatment of diabetic patients with metformin, an AMPK activator, reduced their risk of cancer by around 30% compared with diabetics on other treatments (Evans, 2005; Bowker et al., 2006).

However, as observed in this chapter, treatment of cells with an AMPK activator may actually protect against apoptosis and thus promote inappropriate survival of the cancer cells. Interestingly, this was observed in LKB1-null cells where the major upstream kinase activity is lost. While it is possible that the effects of A769662 on G361 cells (Fig. 5.12) were due to off-target effects, this seems unlikely because A769662 did not protect AMPK-$\alpha1^{-/-}$ -$\alpha2^{-/-}$ double knockout mouse embryo fibroblasts from apoptosis, suggesting that AMPK is required for this effect (Fig. 5.18).

Supporting the work in this chapter are reports that the LKB1-AMPK pathway determines the response of cells to other types of stress. A549 cells (which were isolated from a lung adenocarcinoma and do not express LKB1) were transfected with wild-type or kinase-dead LKB1 and the effect of phenformin treatment on apoptosis determined. The results show that the presence of wild-type, but not kinase-dead, LKB1 protects cells from the energy stress induced by phenformin (Shackelford et al., 2013).

In conclusion, the results presented in this chapter suggest that the LKB1-AMPK pathway can play an important role in regulating the response to mTOR inhibition.

CHAPTER 6: CONCLUSIONS AND PERSPECTIVES

6.1 Introduction

In this thesis, the regulation of AMPK by adenine nucleotides was investigated. Using studies both in cell-free systems and intact cells, the central role of AMP as an activator of AMPK has been re-established. Phosphorylation of LKB1 by AMPK was also investigated. Whilst this phosphorylation was demonstrated in cell-free assays, its physiological significance remains unclear. Finally, it has been shown that the LKB1-AMPK pathway can play an important role in determining the cellular response to mTOR inhibition. This final chapter discusses the overall implications of the findings in this thesis and suggests directions for future research.

6.2 Regulation of AMPK by AMP

The work in this thesis was initiated by reports in the literature that ADP, and not AMP, may be the main regulator of AMPK. The data presented in Chapter 3 of this thesis demonstrates that while both AMP and ADP can protect AMPK against Thr172 dephosphorylation by protein phosphatases, AMP has the more potent effect. Additionally, AMP was demonstrated to promote the phosphorylation of Thr172 by LKB1, whereas ADP was found to have no effect. Finally, allosteric activation of AMPK by AMP was demonstrated to play a significant role in the overall AMPK activation mechanism.

The results showing that Thr172 phosphorylation by LKB1 is promoted by binding of AMP, and not ADP, are supported by a recent report suggesting that AXIN forms a stable complex with LKB1 and AMPK (Zhang et al., 2013). The formation of this

complex, which was suggested to promote phosphorylation of Thr172 on the AMPK-α, was greatly enhanced by the presence of AMP in cell-free systems, or by glucose deprivation of intact cells. Consistent with the results presented in this thesis, ADP was reported to have no effect on the formation of the LKB1-AMPK-AXIN complex (Zhang et al., 2013). The interaction appeared to be specific for LKB1, as no interaction between AXIN and CaMKKβ was detected, and knockdown of AXIN did not reduce AMPK activation in response to increases in intracellular Ca^{2+} (Zhang et al., 2013). This supports the results presented in Chapter 3, where the phosphorylation of Thr172 of AMPK-α by CaMKKβ was not stimulated by AMP, unlike the LKB1-mediated phosphorylation. These authors also reported that the formation of the complex required myristoylation of the β-subunit of AMPK, supporting the work of Oakhill et al (2010). The AMPK heterotrimer used for the promotion of phosphorylation experiments in Chapter 3 was purified from rat liver, and the LKB1 from insect cells. Using an anti-AXIN antibody, no AXIN was detected in either the LKB1 or AMPK preparations, so preliminary attempts to confirm the observations of Zhang et al (2013) were unsuccessful (data not shown). However, AXIN could be present at levels undetectable by Western blotting. Alternatively, the promotion of phosphorylation of Thr172 may be enhanced if the AMPK purified from rat liver was supplemented with AXIN. Regardless, the work of Zhang et al (2013) does support the observations, reported in Chapter 3, that it is AMP, and not ADP, that is the key regulator of Thr172 phosphorylation and AMPK activity.

One aspect not covered by this thesis is whether the activation of AMPK in LKB1-null cells has a physiological relevance. Treatment of LKB1-null G361 cells with AMPK activators increased phosphorylation of ACC at Ser79 and it would be interesting to

examine whether this resulted in changes in lipid metabolism, although there is no reason to suspect that it would not. AMPK also has significant anti-proliferative properties and activation of AMPK may result in changes in cell growth, survival and cycle progression. The results from Chapter 5, discussed below, suggest that this may be the case.

6.3 Phosphorylation of LKB1 by AMPK

LKB1 has been shown to be phosphorylated in intact cells at Ser31 and this does not occur due to autophosphorylation (Sapkota et al., 2002a). The sequence around Ser31 is well conserved and bears resemblance to the AMPK consensus motif (Dale et al., 1995; Gwinn et al., 2008; Scott et al., 2002). However, although AMPK can phosphorylate Ser31 to a reasonable stoichiometry in cell-free assays, it remains unclear whether this is a physiologically relevant event. To further investigate this, a more specific antibody against phospho-Ser31 would be required. Alternatively, mass spectroscopy of samples from cells treated with a specific AMPK activator may demonstrate whether this phosphorylation can occur in intact cells. The phosphorylation of LKB1 by AMPK was initially an attractive hypothesis, given that it could form part of a feedback loop. However the Ser31 site does not appear to alter LKB1 function, as demonstrated by work in this thesis and from other groups (Sapkota et al., 2002a).

6.4 AMPK protects against apoptosis induced by mTOR inhibition

Another goal of this thesis was to investigate the response of cells to AZ4, a dual mTORC1/mTORC2 inhibitor, and to determine whether the LKB1-AMPK pathway

influenced this response. The results suggest that treatment of intact cells with AZ4 can induce apoptosis and reduce cell number, which was the case in both transformed and non-transformed cell lines. However, more work is required to understand the molecular mechanisms, including the key signalling components underlying these effects. Does apoptosis require inhibition of mTORC2, as suggested by the results in Chapter 5? If so, which of the multiple downstream targets of mTORC2 must be inhibited to induce apoptosis? Alternatively, the effects could be due to increased phosphorylation of the 4E-BPs and a decrease in expression of anti-apoptotic genes. Examining gene expression patterns of cells treated with AZ4 may shed light on this.

Results in Chapter 5 also suggest that the LKB1-AMPK pathway may play a role in determining the response of cells to mTOR inhibition. Treatment with A769662, a direct AMPK activator, decreased AZ4-induced apoptosis of G361 cells; an effect not observed in mouse embryo fibroblasts lacking the AMPK-α1/-α2 subunits. G361 cells do not express LKB1, and the results in Chapter 5 support the observation that A769662 can significantly activate AMPK even in LKB1-null cell lines, and suggests that this activation may be translated into physiologically relevant changes. Additionally, mouse embryo fibroblasts lacking AMPK-α subunits were more susceptible than their wild-type counterparts to AZ4-induced apoptosis. Future work could study whether activation of the LKB1-AMPK pathway in tumours *in vivo*, rather than in cell culture models, regulates the response to mTOR inhibition.

These results suggest that the loss of LKB1-AMPK pathway, a common effect in a number of tumours, may sensitize cancer cells to mTOR inhibition and may have implications for combination therapies, where AMPK activators such as metformin,

which have anti-proliferative properties, are administered together with mTOR inhibitors. The results presented here suggest that this may actually increase the survival of cancer cells and could reduce the efficacy of the treatment. This may also have implications for treatment with inhibitors targeted against other components of the mTOR pathway, such as PI3 kinase. It may even be that inhibition, rather than activation, of the AMPK pathway may be efficacious in treatment of some types of tumour.

Despite this, activating the AMPK pathway may still have benefits in preventing the onset of cancer. AMPK regulates a host of cellular functions that would be expected to reduce tumour formation, including inhibition of protein and lipid synthesis and promotion of autophagy. This idea is supported by emerging evidence that AMPK itself is a tumour suppressor (Evans, 2005; Huang et al., 2008; Faubert et al., 2013), as well as the established tumour suppressor role of LKB1. AMPK may therefore act as a "double-edged sword" in cancer therapy: AMPK activation may prevent the formation of tumours but increase their survival once they are formed. Understanding the status of the LKB1-AMPK pathway in the tumours of individual patients may therefore form an important part of future personalized medicine.

REFERENCES

Abu-Elheiga, L., Brinkley, W.R., Zhong, L., Chirala, S.S., Woldegiorgis, G., Wakil, S.J., 2000. The subcellular localization of acetyl-CoA carboxylase 2. Proc. Natl. Acad. Sci. U. S. A. 97, 1444–1449.

Ahn, J., Lee, H., Kim, S., Park, J., Ha, T., 2008. The anti-obesity effect of quercetin is mediated by the AMPK and MAPK signaling pathways. Biochem. Biophys. Res. Commun. 373, 545–549.

Akman, H.O., Sampayo, J.N., Ross, F.A., Scott, J.W., Wilson, G., Benson, L., Bruno, C., Shanske, S., Hardie, D.G., Dimauro, S., 2007. Fatal infantile cardiac glycogenosis with phosphorylase kinase deficiency and a mutation in the gamma2-subunit of AMP-activated protein kinase. Pediatr. Res. 62, 499–504.

Al-Hakim, A.K., Göransson, O., Deak, M., Toth, R., Campbell, D.G., Morrice, N.A., Prescott, A.R., Alessi, D.R., 2005. 14-3-3 cooperates with LKB1 to regulate the activity and localization of QSK and SIK. J. Cell Sci. 118, 5661–5673.

Alessi, D.R., Andjelkovic, M., Caudwell, B., Cron, P., Morrice, N., Cohen, P., Hemmings, B.A., 1996. Mechanism of activation of protein kinase B by insulin and IGF-1. EMBO J. 15, 6541–6551.

Alessi, D.R., James, S.R., Downes, C.P., Holmes, A.B., Gaffney, P.R., Reese, C.B., Cohen, P., 1997. Characterization of a 3-phosphoinositide-dependent protein kinase which phosphorylates and activates protein kinase Balpha. Curr. Biol. CB 7, 261–269.

Alessi, D.R., Sakamoto, K., Bayascas, J.R., 2006. LKB1-dependent signaling pathways. Annu. Rev. Biochem. 75, 137–163.

Ames, J.B., Ishima, R., Tanaka, T., Gordon, J.I., Stryer, L., Ikura, M., 1997. Molecular mechanics of calcium-myristoyl switches. Nature 389, 198–202.

Anderson, K.A., Ribar, T.J., Lin, F., Noeldner, P.K., Green, M.F., Muehlbauer, M.J., Witters, L.A., Kemp, B.E., Means, A.R., 2008. Hypothalamic CaMKK2 Contributes to the Regulation of Energy Balance. Cell Metab. 7, 377–388.

Andersson, U., Filipsson, K., Abbott, C.R., Woods, A., Smith, K., Bloom, S.R., Carling, D., Small, C.J., 2004. AMP-activated protein kinase plays a role in the control of food intake. J. Biol. Chem. 279, 12005–12008.

Apfeld, J., O'Connor, G., McDonagh, T., DiStefano, P.S., Curtis, R., 2004. The AMP-activated protein kinase AAK-2 links energy levels and insulin-like signals to lifespan in C. elegans. Genes Dev. 18, 3004–3009.

Arad, M., Moskowitz, I.P., Patel, V.V., Ahmad, F., Perez-Atayde, A.R., Sawyer, D.B., Walter, M., Li, G.H., Burgon, P.G., Maguire, C.T., Stapleton, D., Schmitt, J.P., Guo, X.X., Pizard, A., Kupershmidt, S., Roden, D.M., Berul, C.I., Seidman, C.E., Seidman, J.G., 2003. Transgenic mice overexpressing mutant PRKAG2 define the cause of Wolff-Parkinson-White syndrome in glycogen storage cardiomyopathy. Circulation 107, 2850–2856.

Aschenbach, W.G., Sakamoto, K., Goodyear, L.J., 2004. 5' Adenosine Monophosphate-Activated Protein Kinase, Metabolism and Exercise. Sports Med. 34, 91–103.

Bai, Y., Zhou, T., Fu, H., Sun, H., Huang, B., 2012. 14-3-3 Interacts with LKB1 via recognizing phosphorylated threonine 336 residue and suppresses LKB1 kinase function. FEBS Lett. 586, 1111–1119.

Bain, J., Plater, L., Elliott, M., Shpiro, N., Hastie, C.J., McLauchlan, H., Klevernic, I., Arthur, J.S.C., Alessi, D.R., Cohen, P., 2007. The selectivity of protein kinase inhibitors: a further update. Biochem. J. 408, 297–315.

Bar-Peled, L., Chantranupong, L., Cherniack, A.D., Chen, W.W., Ottina, K.A., Grabiner, B.C., Spear, E.D., Carter, S.L., Meyerson, M., Sabatini, D.M., 2013. A Tumor suppressor complex with GAP activity for the Rag GTPases that signal amino acid sufficiency to mTORC1. Science 340, 1100–1106.

Bar-Peled, L., Schweitzer, L.D., Zoncu, R., Sabatini, D.M., 2012. Ragulator Is a GEF for the Rag GTPases that Signal Amino Acid Levels to mTORC1. Cell 150, 1196–1208.

Barnes, K., Ingram, J.C., Porras, O.H., Barros, L.F., Hudson, E.R., Fryer, L.G.D., Foufelle, F., Carling, D., Hardie, D.G., Baldwin, S.A., 2002. Activation of GLUT1 by metabolic and osmotic stress: potential involvement of AMP-activated protein kinase (AMPK). J. Cell Sci. 115, 2433–2442.

Bateman, A., 1997. The structure of a domain common to archaebacteria and the homocystinuria disease protein. Trends Biochem. Sci. 22, 12–13.

Baur, J.A., Pearson, K.J., Price, N.L., Jamieson, H.A., Lerin, C., Kalra, A., Prabhu, V.V., Allard, J.S., Lopez-Lluch, G., Lewis, K., Pistell, P.J., Poosala, S., Becker, K.G., Boss, O., Gwinn, D., Wang, M., Ramaswamy, S., Fishbein, K.W., Spencer, R.G., Lakatta, E.G., Le Couteur, D., Shaw, R.J., Navas, P., Puigserver, P., Ingram, D.K., de Cabo, R., Sinclair, D.A., 2006. Resveratrol improves health and survival of mice on a high-calorie diet. Nature 444, 337–342.

Beall, C., Hamilton, D.L., Gallagher, J., Logie, L., Wright, K., Soutar, M.P., Dadak, S., Ashford, F.B., Haythorne, E., Du, Q., Jovanovic, A., McCrimmon, R.J., Ashford, M.L.J., 2012. Mouse hypothalamic GT1-7 cells demonstrate AMPK-dependent intrinsic glucose-sensing behaviour. Diabetologia 55, 2432–2444.

Beall, C., Piipari, K., Al-Qassab, H., Smith, M.A., Parker, N., Carling, D., Viollet, B., Withers, D.J., Ashford, M.L.J., 2010. Loss of AMP-activated protein kinase alpha2 subunit in mouse beta-cells impairs glucose-stimulated insulin secretion and inhibits their sensitivity to hypoglycaemia. Biochem. J. 429, 323–333.

Beg, Z.H., Allmann, D.W., Gibson, D.M., 1973. Modulation of 3-hydroxy-3-methylglutaryl coenzyme A reductase activity with cAMP and wth protein fractions of rat liver cytosol. Biochem. Biophys. Res. Commun. 54, 1362–1369.

Beg, Z.H., Stonik, J.A., Brewer, H.B., 1978. 3-Hydroxy-3-methylglutaryl coenzyme A reductase: regulation of enzymatic activity by phosphorylation and dephosphorylation. Proc. Natl. Acad. Sci. U. S. A. 75, 3678–3682.

Benkimoun, P., 2009. Police find range of drugs after trawling bins used by Tour de France cyclists. BMJ 339, b4201.

Bergeron, R., Previs, S.F., Cline, G.W., Perret, P., Iii, R.R.R., Young, L.H., Shulman, G.I., 2001. Effect of 5-Aminoimidazole-4-Carboxamide-1-β-d-Ribofuranoside Infusion on In Vivo Glucose and Lipid Metabolism in Lean and Obese Zucker Rats. Diabetes 50, 1076–1082.

Berwick, D.C., Dell, G.C., Welsh, G.I., Heesom, K.J., Hers, I., Fletcher, L.M., Cooke, F.T., Tavaré, J.M., 2004. Protein kinase B phosphorylation of PIKfyve regulates the trafficking of GLUT4 vesicles. J. Cell Sci. 117, 5985–5993.

Bierer, B.E., Mattila, P.S., Standaert, R.F., Herzenberg, L.A., Burakoff, S.J., Crabtree, G., Schreiber, S.L., 1990. Two distinct signal transmission pathways in T lymphocytes are inhibited by complexes formed between an immunophilin and either FK506 or rapamycin. Proc. Natl. Acad. Sci. U. S. A. 87, 9231–9235.

Boudeau, J., Baas, A.F., Deak, M., Morrice, N.A., Kieloch, A., Schutkowski, M., Prescott, A.R., Clevers, H.C., Alessi, D.R., 2003a. MO25alpha/beta interact with STRADalpha/beta enhancing their ability to bind, activate and localize LKB1 in the cytoplasm. EMBO J. 22, 5102–5114.

Boudeau, J., Kieloch, A., Alessi, D.R., Stella, A., Guanti, G., Resta, N., 2003b. Functional analysis of LKB1/STK11 mutants and two aberrant isoforms found in Peutz-Jeghers Syndrome patients. Hum. Mutat. 21, 172.

Boudeau, J., Miranda-Saavedra, D., Barton, G.J., Alessi, D.R., 2006. Emerging roles of pseudokinases. Trends Cell Biol. 16, 443–452.

Bowker, S.L., Majumdar, S.R., Veugelers, P., Johnson, J.A., 2006. Increased cancer-related mortality for patients with type 2 diabetes who use sulfonylureas or insulin. Diabetes Care 29, 254–258.

Brown, E.J., Albers, M.W., Shin, T.B., Ichikawa, K., Keith, C.T., Lane, W.S., Schreiber, S.L., 1994. A mammalian protein targeted by G1-arresting rapamycin-receptor complex. Nature 369, 756–758.

Brown, E.J., Beal, P.A., Keith, C.T., Chen, J., Shin, T.B., Schreiber, S.L., 1995. Control of p70 s6 kinase by kinase activity of FRAP in vivo. Nature 377, 441–446.

Brown, M.S., Brunschede, G.Y., Goldstein, J.L., 1975. Inactivation of 3-hydroxy-3-methylglutaryl coenzyme A reductase in vitro. An adenine nucleotide-dependent reaction catalyzed by a factor in human fibroblasts. J. Biol. Chem. 250, 2502–2509.

Brunet, A., Bonni, A., Zigmond, M.J., Lin, M.Z., Juo, P., Hu, L.S., Anderson, M.J., Arden, K.C., Blenis, J., Greenberg, M.E., 1999. Akt promotes cell survival by phosphorylating and inhibiting a Forkhead transcription factor. Cell 96, 857–868.

Brunet, A., Park, J., Tran, H., Hu, L.S., Hemmings, B.A., Greenberg, M.E., 2001. Protein kinase SGK mediates survival signals by phosphorylating the forkhead transcription factor FKHRL1 (FOXO3a). Mol. Cell. Biol. 21, 952–965.

Brunmair, B., Staniek, K., Gras, F., Scharf, N., Althaym, A., Clara, R., Roden, M., Gnaiger, E., Nohl, H., Waldhäusl, W., Fürnsinn, C., 2004. Thiazolidinediones, Like Metformin, Inhibit Respiratory Complex I A Common Mechanism Contributing to Their Antidiabetic Actions? Diabetes 53, 1052–1059.

Brunn, G.J., Hudson, C.C., Sekulić, A., Williams, J.M., Hosoi, H., Houghton, P.J., Lawrence, J.C., Abraham, R.T., 1997. Phosphorylation of the Translational Repressor PHAS-I by the Mammalian Target of Rapamycin. Science 277, 99–101.

Brunn, G.J., Williams, J., Sabers, C., Wiederrecht, G., Lawrence, J.C., Abraham, R.T., 1996. Direct inhibition of the signaling functions of the mammalian target of rapamycin by the phosphoinositide 3-kinase inhibitors, wortmannin and LY294002. EMBO J. 15, 5256–5267.

Burnett, P.E., Barrow, R.K., Cohen, N.A., Snyder, S.H., Sabatini, D.M., 1998. RAFT1 phosphorylation of the translational regulators p70 S6 kinase and 4E-BP1. Proc. Natl. Acad. Sci. U. S. A. 95, 1432–1437.

Burwinkel, B., Scott, J.W., Bührer, C., van Landeghem, F.K.H., Cox, G.F., Wilson, C.J., Grahame Hardie, D., Kilimann, M.W., 2005. Fatal congenital heart glycogenosis caused by a recurrent activating R531Q mutation in the gamma 2-subunit of AMP-activated protein kinase (PRKAG2), not by phosphorylase kinase deficiency. Am. J. Hum. Genet. 76, 1034–1049.

Carling, D., Aguan, K., Woods, A., Verhoeven, A.J., Beri, R.K., Brennan, C.H., Sidebottom, C., Davison, M.D., Scott, J., 1994. Mammalian AMP-activated protein kinase is homologous to yeast and plant protein kinases involved in the regulation of carbon metabolism. J. Biol. Chem. 269, 11442–11448.

Carling, D., Clarke, P.R., Zammit, V.A., Hardie, D.G., 1989. Purification and characterization of the AMP-activated protein kinase. Copurification of acetyl-CoA carboxylase kinase and 3-hydroxy-3-methylglutaryl-CoA reductase kinase activities. Eur. J. Biochem. FEBS 186, 129–136.

Carling, D., Thornton, C., Woods, A., Sanders, M.J., 2012. AMP-activated protein kinase: new regulation, new roles? Biochem. J. 445, 11–27.

Carling, D., Zammit, V.A., Hardie, D.G., 1987. A common bicyclic protein kinase cascade inactivates the regulatory enzymes of fatty acid and cholesterol biosynthesis. FEBS Lett. 223, 217–222.

Carlson, C.A., Kim, K.H., 1973. Regulation of hepatic acetyl coenzyme A carboxylase by phosphorylation and dephosphorylation. J. Biol. Chem. 248, 378–380.

Carracedo, A., Ma, L., Teruya-Feldstein, J., Rojo, F., Salmena, L., Alimonti, A., Egia, A., Sasaki, A.T., Thomas, G., Kozma, S.C., Papa, A., Nardella, C., Cantley, L.C., Baselga, J., Pandolfi, P.P., 2008. Inhibition of mTORC1 leads to MAPK pathway activation through a PI3K-dependent feedback loop in human cancer. J. Clin. Invest. 118, 3065–3074.

Chen, L., Jiao, Z.-H., Zheng, L.-S., Zhang, Y.-Y., Xie, S.-T., Wang, Z.-X., Wu, J.-W., 2009. Structural insight into the autoinhibition mechanism of AMP-activated protein kinase. Nature 459, 1146–1149.

Chen, L., Wang, J., Zhang, Y.-Y., Yan, S.F., Neumann, D., Schlattner, U., Wang, Z.-X., Wu, J.-W., 2012. AMP-activated protein kinase undergoes nucleotide-dependent conformational changes. Nat. Struct. Mol. Biol. 19, 716–718.

Chen, L., Xin, F.-J., Wang, J., Hu, J., Zhang, Y.-Y., Wan, S., Cao, L.-S., Lu, C., Li, P., Yan, S.F., Neumann, D., Schlattner, U., Xia, B., Wang, Z.-X., Wu, J.-W., 2013. Conserved regulatory elements in AMPK. Nature 498, E8–E10.

Chen, S., Murphy, J., Toth, R., Campbell, D.G., Morrice, N.A., Mackintosh, C., 2008. Complementary regulation of TBC1D1 and AS160 by growth factors, insulin and AMPK activators. Biochem. J. 409, 449–459.

Chen, S., Wasserman, D.H., MacKintosh, C., Sakamoto, K., 2011. Mice with AS160/TBC1D4-Thr649Ala knockin mutation are glucose intolerant with reduced insulin sensitivity and altered GLUT4 trafficking. Cell Metab. 13, 68–79.

Cheung, P.C., Salt, I.P., Davies, S.P., Hardie, D.G., Carling, D., 2000. Characterization of AMP-activated protein kinase gamma-subunit isoforms and their role in AMP binding. Biochem. J. 346, 659–669.

Chresta, C.M., Davies, B.R., Hickson, I., Harding, T., Cosulich, S., Critchlow, S.E., Vincent, J.P., Ellston, R., Jones, D., Sini, P., James, D., Howard, Z., Dudley, P., Hughes, G., Smith, L., Maguire, S., Hummersone, M., Malagu, K., Menear, K., Jenkins, R., Jacobsen, M., Smith, G.C.M., Guichard, S., Pass, M., 2010. AZD8055 is a potent, selective, and orally bioavailable ATP-competitive mammalian target of rapamycin kinase inhibitor with in vitro and in vivo antitumor activity. Cancer Res. 70, 288–298.

Christie, G.R., Hajduch, E., Hundal, H.S., Proud, C.G., Taylor, P.M., 2002. Intracellular sensing of amino acids in Xenopus laevis oocytes stimulates p70 S6 kinase in a target of rapamycin-dependent manner. J. Biol. Chem. 277, 9952–9957.

Chung, J., Kuo, C.J., Crabtree, G.R., Blenis, J., 1992. Rapamycin-FKBP specifically blocks growth-dependent activation of and signaling by the 70 kd S6 protein kinases. Cell 69, 1227–1236.

Clarke, P.R., Hardie, D.G., 1990. Regulation of HMG-CoA reductase: identification of the site phosphorylated by the AMP-activated protein kinase in vitro and in intact rat liver. EMBO J. 9, 2439–2446.

Cohen, P., 1989. The Structure and Regulation of Protein Phosphatases. Annu. Rev. Biochem. 58, 453–508.

Cohen, P., 2002a. The origins of protein phosphorylation. Nat. Cell Biol. 4, E127–E130.

Cohen, P., 2002b. Protein kinases--the major drug targets of the twenty-first century? Nat. Rev. Drug Discov. 1, 309–315.

Cohen, P., Alemany, S., Hemmings, B.A., Resink, T.J., Strålfors, P., Tung, H.Y., 1988. Protein phosphatase-1 and protein phosphatase-2A from rabbit skeletal muscle. Methods Enzymol. 159, 390–408.

Cohen, P., Alessi, D.R., 2013. Kinase drug discovery--what's next in the field? ACS Chem. Biol. 8, 96–104.

Collins, S.P., Reoma, J.L., Gamm, D.M., Uhler, M.D., 2000. LKB1, a novel serine/threonine protein kinase and potential tumour suppressor, is phosphorylated by cAMP-dependent protein kinase (PKA) and prenylated in vivo. Biochem. J. 345 Pt 3, 673–680.

Cool, B., Zinker, B., Chiou, W., Kifle, L., Cao, N., Perham, M., Dickinson, R., Adler, A., Gagne, G., Iyengar, R., Zhao, G., Marsh, K., Kym, P., Jung, P., Camp, H.S., Frevert, E., 2006. Identification and characterization of a small molecule AMPK activator that treats key components of type 2 diabetes and the metabolic syndrome. Cell Metab. 3, 403–416.

Corton, J.M., Gillespie, J.G., Hawley, S.A., Hardie, D.G., 1995. 5-aminoimidazole-4-carboxamide ribonucleoside. A specific method for activating AMP-activated protein kinase in intact cells? Eur. J. Biochem. FEBS 229, 558–565.

Crute, B.E., Seefeld, K., Gamble, J., Kemp, B.E., Witters, L.A., 1998. Functional domains of the alpha1 catalytic subunit of the AMP-activated protein kinase. J. Biol. Chem. 273, 35347–35354.

Da Silva Xavier, G., Leclerc, I., Varadi, A., Tsuboi, T., Moule, S.K., Rutter, G.A., 2003. Role for AMP-activated protein kinase in glucose-stimulated insulin secretion and preproinsulin gene expression. Biochem. J. 371, 761.

Dale, S., Wilson, W.A., Edelman, A.M., Hardie, D.G., 1995. Similar substrate recognition motifs for mammalian AMP-activated protein kinase, higher plant HMG-CoA reductase kinase-A, yeast SNF1, and mammalian calmodulin-dependent protein kinase I. FEBS Lett. 361, 191–195.

Dandapani, M., 2013. The AMPK signalling pathway in cancer and DNA damage. University of Dundee.

Daniel, T., Carling, D., 2002. Functional analysis of mutations in the gamma 2 subunit of AMP-activated protein kinase associated with cardiac hypertrophy and Wolff-Parkinson-White syndrome. J. Biol. Chem. 277, 51017–51024.

Davies, S.P., Carling, D., Hardie, D.G., 1989. Tissue distribution of the AMP-activated protein kinase, and lack of activation by cyclic-AMP-dependent protein kinase, studied using a specific and sensitive peptide assay. Eur. J. Biochem. FEBS 186, 123–128.

Davies, S.P., Carling, D., Munday, M.R., Hardie, D.G., 1992. Diurnal rhythm of phosphorylation of rat liver acetyl – CoA carboxylase by the AMP-activated protein kinase, demonstrated using freeze-clamping. Eur. J. Biochem. 203, 615–623.

Davies, S.P., Hawley, S.A., Woods, A., Carling, D., Haystead, T.A., Hardie, D.G., 1994. Purification of the AMP-activated protein kinase on ATP-gamma-sepharose and analysis of its subunit structure. Eur. J. Biochem. FEBS 223, 351–357.

Davies, S.P., Helps, N.R., Cohen, P.T., Hardie, D.G., 1995. 5'-AMP inhibits dephosphorylation, as well as promoting phosphorylation, of the AMP-activated protein kinase. Studies using bacterially expressed human protein phosphatase-2C alpha and native bovine protein phosphatase-2AC. FEBS Lett. 377, 421–425.

Davies, S.P., Sim, A.T., Hardie, D.G., 1990. Location and function of three sites phosphorylated on rat acetyl-CoA carboxylase by the AMP-activated protein kinase. Eur. J. Biochem. FEBS 187, 183–190.

Dorrello, N.V., Peschiaroli, A., Guardavaccaro, D., Colburn, N.H., Sherman, N.E., Pagano, M., 2006. S6K1- and betaTRCP-mediated degradation of PDCD4 promotes protein translation and cell growth. Science 314, 467–471.

Dowling, R.J.O., Topisirovic, I., Alain, T., Bidinosti, M., Fonseca, B.D., Petroulakis, E., Wang, X., Larsson, O., Selvaraj, A., Liu, Y., Kozma, S.C., Thomas, G., Sonenberg, N., 2010. mTORC1-mediated cell proliferation, but not cell growth, controlled by the 4E-BPs. Science 328, 1172–1176.

Dumont, F.J., Staruch, M.J., Koprak, S.L., Melino, M.R., Sigal, N.H., 1990. Distinct mechanisms of suppression of murine T cell activation by the related macrolides FK-506 and rapamycin. J. Immunol. Baltim. Md 1950 144, 251–258.

Efeyan, A., Sabatini, D.M., 2010. mTOR and cancer: many loops in one pathway. Curr. Opin. Cell Biol. 22, 169–176.

Egan, D.F., Shackelford, D.B., Mihaylova, M.M., Gelino, S., Kohnz, R.A., Mair, W., Vasquez, D.S., Joshi, A., Gwinn, D.M., Taylor, R., Asara, J.M., Fitzpatrick, J., Dillin, A., Viollet, B., Kundu, M., Hansen, M., Shaw, R.J., 2011. Phosphorylation of ULK1 (hATG1) by AMP-activated protein kinase connects energy sensing to mitophagy. Science 331, 456–461.

El-Mir, M.Y., Nogueira, V., Fontaine, E., Avéret, N., Rigoulet, M., Leverve, X., 2000. Dimethylbiguanide inhibits cell respiration via an indirect effect targeted on the respiratory chain complex I. J. Biol. Chem. 275, 223–228.

Evans, A.M., Mustard, K.J.W., Wyatt, C.N., Peers, C., Dipp, M., Kumar, P., Kinnear, N.P., Hardie, D.G., 2005. Does AMP-activated Protein Kinase Couple Inhibition of Mitochondrial

Oxidative Phosphorylation by Hypoxia to Calcium Signaling in O2-sensing Cells? J. Biol. Chem. 280, 41504–41511.

Evans, J.M.M., 2005. Metformin and reduced risk of cancer in diabetic patients. BMJ 330, 1304–1305.

Faubert, B., Boily, G., Izreig, S., Griss, T., Samborska, B., Dong, Z., Dupuy, F., Chambers, C., Fuerth, B.J., Viollet, B., Mamer, O.A., Avizonis, D., DeBerardinis, R.J., Siegel, P.M., Jones, R.G., 2013. AMPK is a negative regulator of the Warburg effect and suppresses tumor growth in vivo. Cell Metab. 17, 113–124.

Feldman, M.E., Apsel, B., Uotila, A., Loewith, R., Knight, Z.A., Ruggero, D., Shokat, K.M., 2009. Active-site inhibitors of mTOR target rapamycin-resistant outputs of mTORC1 and mTORC2. PLoS Biol. 7, e38.

Ferrer, A., Caelles, C., Massot, N., Hegardt, F.G., 1985. Activation of rat liver cytosolic 3-hydroxy-3-methylglutaryl Coenzyme A reductase kinase by adenosine 5'-monophosphate. Biochem. Biophys. Res. Commun. 132, 497–504.

Fischer, E.H., Krebs, E.G., 1955. Conversion of phosphorylase b to phosphorylase a in muscle extracts. J. Biol. Chem. 216, 121–132.

Fischer, G., Schmid, F.X., 1990. The mechanism of protein folding. Implications of in vitro refolding models for de novo protein folding and translocation in the cell. Biochemistry (Mosc.) 29, 2205–2212.

Fogarty, S., Hardie, D.G., 2009. C-terminal phosphorylation of LKB1 is not required for regulation of AMP-activated protein kinase, BRSK1, BRSK2, or cell cycle arrest. J. Biol. Chem. 284, 77–84.

Foretz, M., Hébrard, S., Leclerc, J., Zarrinpashneh, E., Soty, M., Mithieux, G., Sakamoto, K., Andreelli, F., Viollet, B., 2010. Metformin inhibits hepatic gluconeogenesis in mice independently of the LKB1/AMPK pathway via a decrease in hepatic energy state. J. Clin. Invest. 120, 2355–2369.

Frias, M.A., Thoreen, C.C., Jaffe, J.D., Schroder, W., Sculley, T., Carr, S.A., Sabatini, D.M., 2006. mSin1 is necessary for Akt/PKB phosphorylation, and its isoforms define three distinct mTORC2s. Curr. Biol. CB 16, 1865–1870.

Fryer, L.G.D., Parbu-Patel, A., Carling, D., 2002. The anti-diabetic drugs rosiglitazone and metformin stimulate AMP-activated protein kinase through distinct signaling pathways. J. Biol. Chem. 277, 25226–25232.

Fullerton, M.D., Galic, S., Marcinko, K., Sikkema, S., Pulinilkunnil, T., Chen, Z.-P., O'Neill, H.M., Ford, R.J., Palanivel, R., O'Brien, M., Hardie, D.G., Macaulay, S.L., Schertzer, J.D., Dyck, J.R.B., van Denderen, B.J., Kemp, B.E., Steinberg, G.R., 2013. Single phosphorylation sites in Acc1 and Acc2 regulate lipid homeostasis and the insulin-sensitizing effects of metformin. Nat. Med.

García-Martínez, J.M., Alessi, D.R., 2008. mTOR complex 2 (mTORC2) controls hydrophobic motif phosphorylation and activation of serum- and glucocorticoid-induced protein kinase 1 (SGK1). Biochem. J. 416, 375–385.

García-Martínez, J.M., Moran, J., Clarke, R.G., Gray, A., Cosulich, S.C., Chresta, C.M., Alessi, D.R., 2009. Ku-0063794 is a specific inhibitor of the mammalian target of rapamycin (mTOR). Biochem. J. 421, 29–42.

García-Martínez, J.M., Wullschleger, S., Preston, G., Guichard, S., Fleming, S., Alessi, D.R., Duce, S.L., 2011. Effect of PI3K- and mTOR-specific inhibitors on spontaneous B-cell follicular lymphomas in PTEN/LKB1-deficient mice. Br. J. Cancer.

Giardiello, F.M., Brensinger, J.D., Tersmette, A.C., Goodman, S.N., Petersen, G.M., Booker, S.V., Cruz-Correa, M., Offerhaus, J.A., 2000. Very high risk of cancer in familial Peutz-Jeghers syndrome. Gastroenterology 119, 1447–1453.

Goldfine, A.B., Fonseca, V., Jablonski, K.A., Pyle, L., Staten, M.A., Shoelson, S.E., TINSAL-T2D (Targeting Inflammation Using Salsalate in Type 2 Diabetes) Study Team, 2010. The effects of salsalate on glycemic control in patients with type 2 diabetes: a randomized trial. Ann. Intern. Med. 152, 346–357.

Gollob, M.H., 2003. Glycogen storage disease as a unifying mechanism of disease in the PRKAG2 cardiac syndrome. Biochem. Soc. Trans. 31, 228–231.

Gollob, M.H., Seger, J.J., Gollob, T.N., Tapscott, T., Gonzales, O., Bachinski, L., Roberts, R., 2001. Novel PRKAG2 mutation responsible for the genetic syndrome of ventricular preexcitation and conduction system disease with childhood onset and absence of cardiac hypertrophy. Circulation 104, 3030–3033.

Göransson, O., McBride, A., Hawley, S.A., Ross, F.A., Shpiro, N., Foretz, M., Viollet, B., Hardie, D.G., Sakamoto, K., 2007. Mechanism of Action of A-769662, a Valuable Tool for Activation of AMP-activated Protein Kinase. J. Biol. Chem. 282, 32549–32560.

Guertin, D.A., Stevens, D.M., Thoreen, C.C., Burds, A.A., Kalaany, N.Y., Moffat, J., Brown, M., Fitzgerald, K.J., Sabatini, D.M., 2006. Ablation in Mice of the mTORC Components raptor, rictor, or mLST8 Reveals that mTORC2 Is Required for Signaling to Akt-FOXO and PKCα, but Not S6K1. Dev. Cell 11, 859–871.

Gwinn, D.M., Shackelford, D.B., Egan, D.F., Mihaylova, M.M., Mery, A., Vasquez, D.S., Turk, B.E., Shaw, R.J., 2008. AMPK phosphorylation of raptor mediates a metabolic checkpoint. Mol. Cell 30, 214–226.

Hadad, S.M., Baker, L., Quinlan, P.R., Robertson, K.E., Bray, S.E., Thomson, G., Kellock, D., Jordan, L.B., Purdie, C.A., Hardie, D.G., Fleming, S., Thompson, A.M., 2009. Histological evaluation of AMPK signalling in primary breast cancer. BMC Cancer 9, 307.

Hahn-Windgassen, A., Nogueira, V., Chen, C.-C., Skeen, J.E., Sonenberg, N., Hay, N., 2005. Akt activates the mammalian target of rapamycin by regulating cellular ATP level and AMPK activity. J. Biol. Chem. 280, 32081–32089.

Hara, K., Maruki, Y., Long, X., Yoshino, K., Oshiro, N., Hidayat, S., Tokunaga, C., Avruch, J., Yonezawa, K., 2002. Raptor, a binding partner of target of rapamycin (TOR), mediates TOR action. Cell 110, 177–189.

Hara, K., Yonezawa, K., Kozlowski, M.T., Sugimoto, T., Andrabi, K., Weng, Q.P., Kasuga, M., Nishimoto, I., Avruch, J., 1997. Regulation of eIF-4E BP1 phosphorylation by mTOR. J. Biol. Chem. 272, 26457–26463.

Hara, K., Yonezawa, K., Weng, Q.P., Kozlowski, M.T., Belham, C., Avruch, J., 1998. Amino acid sufficiency and mTOR regulate p70 S6 kinase and eIF-4E BP1 through a common effector mechanism. J. Biol. Chem. 273, 14484–14494.

Hardie, D.G., 2007. AMP-activated/SNF1 protein kinases: conserved guardians of cellular energy. Nat Rev Mol Cell Biol 8, 774–785.

Hardie, D.G., Cohen, P., 1979. Dephosphorylation and activation of Acetyl-CoA-carboxylase from lactating rabbit mammary gland. FEBS Lett. 103, 333–338.

Hardie, D.G., Hawley, S.A., 2001. AMP-activated protein kinase: the energy charge hypothesis revisited. BioEssays News Rev. Mol. Cell. Dev. Biol. 23, 1112–1119.

Hardie, D.G., Ross, F.A., Hawley, S.A., 2012a. AMP-activated protein kinase: a target for drugs both ancient and modern. Chem. Biol. 19, 1222–1236.

Hardie, D.G., Ross, F.A., Hawley, S.A., 2012b. AMPK: a nutrient and energy sensor that maintains energy homeostasis. Nat. Rev. Mol. Cell Biol. 13, 251–262.

Hardie, D.G., Salt, I.P., Hawley, S.A., Davies, S.P., 1999. AMP-activated protein kinase: an ultrasensitive system for monitoring cellular energy charge. Biochem. J. 338 (Pt 3), 717–722.

Hawley, S.A., Boudeau, J., Reid, J.L., Mustard, K.J., Udd, L., Mäkelä, T.P., Alessi, D.R., Hardie, D.G., 2003. Complexes between the LKB1 tumor suppressor, STRAD alpha/beta and MO25 alpha/beta are upstream kinases in the AMP-activated protein kinase cascade. J. Biol. 2, 28.

Hawley, S.A., Davison, M., Woods, A., Davies, S.P., Beri, R.K., Carling, D., Hardie, D.G., 1996. Characterization of the AMP-activated protein kinase kinase from rat liver and identification of threonine 172 as the major site at which it phosphorylates AMP-activated protein kinase. J. Biol. Chem. 271, 27879–27887.

Hawley, S.A., Fullerton, M.D., Ross, F.A., Schertzer, J.D., Chevtzoff, C., Walker, K.J., Peggie, M.W., Zibrova, D., Green, K.A., Mustard, K.J., Kemp, B.E., Sakamoto, K., Steinberg, G.R., Hardie, D.G., 2012. The ancient drug salicylate directly activates AMP-activated protein kinase. Science 336, 918–922.

Hawley, S.A., Gadalla, A.E., Olsen, G.S., Hardie, D.G., 2002. The antidiabetic drug metformin activates the AMP-activated protein kinase cascade via an adenine nucleotide-independent mechanism. Diabetes 51, 2420–2425.

Hawley, S.A., Pan, D.A., Mustard, K.J., Ross, L., Bain, J., Edelman, A.M., Frenguelli, B.G., Hardie, D.G., 2005. Calmodulin-dependent protein kinase kinase-β is an alternative upstream kinase for AMP-activated protein kinase. Cell Metab. 2, 9–19.

Hawley, S.A., Ross, F.A., Chevtzoff, C., Green, K.A., Evans, A., Fogarty, S., Towler, M.C., Brown, L.J., Ogunbayo, O.A., Evans, A.M., Hardie, D.G., 2010. Use of cells expressing gamma subunit variants to identify diverse mechanisms of AMPK activation. Cell Metab. 11, 554–565.

Hawley, S.A., Selbert, M.A., Goldstein, E.G., Edelman, A.M., Carling, D., Hardie, D.G., 1995. 5'-AMP activates the AMP-activated protein kinase cascade, and Ca2+/calmodulin activates the calmodulin-dependent protein kinase I cascade, via three independent mechanisms. J. Biol. Chem. 270, 27186–27191.

Hayashi, T., Hirshman, M.F., Kurth, E.J., Winder, W.W., Goodyear, L.J., 1998. Evidence for 5'AMP-Activated Protein Kinase Mediation of the Effect of Muscle Contraction on Glucose Transport. Diabetes 47, 1369–1373.

Heitman, J., Movva, N.R., Hall, M.N., 1991. Targets for cell cycle arrest by the immunosuppressant rapamycin in yeast. Science 253, 905–909.

Helliwell, S.B., Wagner, P., Kunz, J., Deuter-Reinhard, M., Henriquez, R., Hall, M.N., 1994. TOR1 and TOR2 are structurally and functionally similar but not identical phosphatidylinositol kinase homologues in yeast. Mol. Biol. Cell 5, 105–118.

Hemminki, A., Markie, D., Tomlinson, I., Avizienyte, E., Roth, S., Loukola, A., Bignell, G., Warren, W., Aminoff, M., Hoglund, P., Jarvinen, H., Kristo, P., Pelin, K., Ridanpaa, M., Salovaara, R., Toro, T., Bodmer, W., Olschwang, S., Olsen, A.S., Stratton, M.R., de la Chapelle, A., Aaltonen, L.A., 1998. A serine/threonine kinase gene defective in Peutz-Jeghers syndrome. Nature 391, 184–187.

Hong, S.-P., Leiper, F.C., Woods, A., Carling, D., Carlson, M., 2003. Activation of yeast Snf1 and mammalian AMP-activated protein kinase by upstream kinases. Proc. Natl. Acad. Sci. U. S. A. 100, 8839–8843.

Hosokawa, N., Hara, T., Kaizuka, T., Kishi, C., Takamura, A., Miura, Y., Iemura, S., Natsume, T., Takehana, K., Yamada, N., Guan, J.-L., Oshiro, N., Mizushima, N., 2009. Nutrient-dependent mTORC1 association with the ULK1-Atg13-FIP200 complex required for autophagy. Mol. Biol. Cell 20, 1981–1991.

Huang, X., Wullschleger, S., Shpiro, N., McGuire, V.A., Sakamoto, K., Woods, Y.L., McBurnie, W., Fleming, S., Alessi, D.R., 2008. Important role of the LKB1-AMPK pathway in suppressing tumorigenesis in PTEN-deficient mice. Biochem. J. 412, 211–221.

Hudson, E.R., Pan, D.A., James, J., Lucocq, J.M., Hawley, S.A., Green, K.A., Baba, O., Terashima, T., Hardie, D.G., 2003. A novel domain in AMP-activated protein kinase causes glycogen storage bodies similar to those seen in hereditary cardiac arrhythmias. Curr. Biol. CB 13, 861–866.

Hundal, R.S., Krssak, M., Dufour, S., Laurent, D., Lebon, V., Chandramouli, V., Inzucchi, S.E., Schumann, W.C., Petersen, K.F., Landau, B.R., Shulman, G.I., 2000. Mechanism by which metformin reduces glucose production in type 2 diabetes. Diabetes 49, 2063–2069.

Hundal, R.S., Petersen, K.F., Mayerson, A.B., Randhawa, P.S., Inzucchi, S., Shoelson, S.E., Shulman, G.I., 2002. Mechanism by which high-dose aspirin improves glucose metabolism in type 2 diabetes. J. Clin. Invest. 109, 1321–1326.

Hurley, R.L., Anderson, K.A., Franzone, J.M., Kemp, B.E., Means, A.R., Witters, L.A., 2005. The Ca2+/calmodulin-dependent protein kinase kinases are AMP-activated protein kinase kinases. J. Biol. Chem. 280, 29060–29066.

Ikematsu, N., Dallas, M.L., Ross, F.A., Lewis, R.W., Rafferty, J.N., David, J.A., Suman, R., Peers, C., Hardie, D.G., Evans, A.M., 2011. Phosphorylation of the voltage-gated potassium channel Kv2.1 by AMP-activated protein kinase regulates membrane excitability. Proc. Natl. Acad. Sci. U. S. A. 108, 18132–18137.

Imamura, H., Nhat, K.P.H., Togawa, H., Saito, K., Iino, R., Kato-Yamada, Y., Nagai, T., Noji, H., 2009. Visualization of ATP levels inside single living cells with fluorescence resonance energy transfer-based genetically encoded indicators. Proc. Natl. Acad. Sci. 106, 15651–15656.

Ingebritsen, T.S., Cohen, P., 1983. The protein phosphatases involved in cellular regulation. 1. Classification and substrate specificities. Eur. J. Biochem. FEBS 132, 255–261.

Ingebritsen, T.S., Lee, H.-S., Parker, R.A., Gibson, D.M., 1978. Reversible modulation of the activities of both liver microsomal hydroxymethylglutaryl coenzyme a reductase and its inactivating enzyme. Evidence for regulation by phosphorylation-dephosphorylation. Biochem. Biophys. Res. Commun. 81, 1268–1277.

Inoki, K., Li, Y., Xu, T., Guan, K.-L., 2003a. Rheb GTPase is a direct target of TSC2 GAP activity and regulates mTOR signaling. Genes Dev. 17, 1829–1834.

Inoki, K., Zhu, T., Guan, K.-L., 2003b. TSC2 Mediates Cellular Energy Response to Control Cell Growth and Survival. Cell 115, 577–590.

Iseli, T.J., Walter, M., van Denderen, B.J.W., Katsis, F., Witters, L.A., Kemp, B.E., Michell, B.J., Stapleton, D., 2005. AMP-activated protein kinase beta subunit tethers alpha and gamma subunits via its C-terminal sequence (186-270). J. Biol. Chem. 280, 13395–13400.

Iyengar, R.R., Judd, A.S., Zhao, G., Kym, P.R., Sham, H.L., Gu, Y., Liu, G., Liu, M., Zhao, H., Clark, R.F., Frevert, E.U., Cool, B.L., Zhang, T., Keyes, R.F., Hansen, T.M., Xin, Z., 2005. Thienopyridones as AMPK activators for the treatment of diabetes and obesity. 20050038068.

Jacinto, E., Loewith, R., Schmidt, A., Lin, S., Rüegg, M.A., Hall, A., Hall, M.N., 2004. Mammalian TOR complex 2 controls the actin cytoskeleton and is rapamycin insensitive. Nat. Cell Biol. 6, 1122–1128.

Jäger, S., Handschin, C., St-Pierre, J., Spiegelman, B.M., 2007. AMP-activated protein kinase (AMPK) action in skeletal muscle via direct phosphorylation of PGC-1alpha. Proc. Natl. Acad. Sci. U. S. A. 104, 12017–12022.

Jaleel, M., Villa, F., Deak, M., Toth, R., Prescott, A.R., Van Aalten, D.M.F., Alessi, D.R., 2006. The ubiquitin-associated domain of AMPK-related kinases regulates conformation and LKB1-mediated phosphorylation and activation. Biochem. J. 394, 545–555.

Jensen, T.E., Rose, A.J., Hellsten, Y., Wojtaszewski, J.F.P., Richter, E.A., 2007. Caffeine-induced Ca2+ release increases AMPK-dependent glucose uptake in rodent soleus muscle. Am. J. Physiol. - Endocrinol. Metab. 293, E286–E292.

Jiang, R., Carlson, M., 1997. The Snf1 protein kinase and its activating subunit, Snf4, interact with distinct domains of the Sip1/Sip2/Gal83 component in the kinase complex. Mol. Cell. Biol. 17, 2099–2106.

Jin, X., Townley, R., Shapiro, L., 2007. Structural insight into AMPK regulation: ADP comes into play. Struct. Lond. Engl. 1993 15, 1285–1295.

Jørgensen, S.B., Nielsen, J.N., Birk, J.B., Olsen, G.S., Viollet, B., Andreelli, F., Schjerling, P., Vaulont, S., Hardie, D.G., Hansen, B.F., Richter, E.A., Wojtaszewski, J.F.P., 2004a. The alpha2-5'AMP-activated protein kinase is a site 2 glycogen synthase kinase in skeletal muscle and is responsive to glucose loading. Diabetes 53, 3074–3081.

Jørgensen, S.B., Viollet, B., Andreelli, F., Frøsig, C., Birk, J.B., Schjerling, P., Vaulont, S., Richter, E.A., Wojtaszewski, J.F.P., 2004b. Knockout of the alpha2 but not alpha1 5'-AMP-activated protein kinase isoform abolishes 5-aminoimidazole-4-carboxamide-1-beta-4-

ribofuranosidebut not contraction-induced glucose uptake in skeletal muscle. J. Biol. Chem. 279, 1070–1079.

Jung, C.H., Jun, C.B., Ro, S.-H., Kim, Y.-M., Otto, N.M., Cao, J., Kundu, M., Kim, D.-H., 2009. ULK-Atg13-FIP200 Complexes Mediate mTOR Signaling to the Autophagy Machinery. Mol. Biol. Cell 20, 1992–2003.

Kahn, B.B., Alquier, T., Carling, D., Hardie, D.G., 2005. AMP-activated protein kinase: Ancient energy gauge provides clues to modern understanding of metabolism. Cell Metab. 1, 15–25.

Kalender, A., Selvaraj, A., Kim, S.Y., Gulati, P., Brûlé, S., Viollet, B., Kemp, B.E., Bardeesy, N., Dennis, P., Schlager, J.J., Marette, A., Kozma, S.C., Thomas, G., 2010. Metformin, independent of AMPK, inhibits mTORC1 in a rag GTPase-dependent manner. Cell Metab. 11, 390–401.

Kemp, B.E., Oakhill, J.S., Scott, J.W., 2007. AMPK structure and regulation from three angles. Struct. Lond. Engl. 1993 15, 1161–1163.

Kim, D.-H., Sarbassov, D.D., Ali, S.M., King, J.E., Latek, R.R., Erdjument-Bromage, H., Tempst, P., Sabatini, D.M., 2002. mTOR Interacts with Raptor to Form a Nutrient-Sensitive Complex that Signals to the Cell Growth Machinery. Cell 110, 163–175.

Koo, S.-H., Flechner, L., Qi, L., Zhang, X., Screaton, R.A., Jeffries, S., Hedrick, S., Xu, W., Boussouar, F., Brindle, P., Takemori, H., Montminy, M., 2005. The CREB coactivator TORC2 is a key regulator of fasting glucose metabolism. Nature 437, 1109–1111.

Kubota, N., Terauchi, Y., Kubota, T., Kumagai, H., Itoh, S., Satoh, H., Yano, W., Ogata, H., Tokuyama, K., Takamoto, I., Mineyama, T., Ishikawa, M., Moroi, M., Sugi, K., Yamauchi, T., Ueki, K., Tobe, K., Noda, T., Nagai, R., Kadowaki, T., 2006. Pioglitazone Ameliorates Insulin Resistance and Diabetes by Both Adiponectin-dependent and -independent Pathways. J. Biol. Chem. 281, 8748–8755.

Kubota, N., Yano, W., Kubota, T., Yamauchi, T., Itoh, S., Kumagai, H., Kozono, H., Takamoto, I., Okamoto, S., Shiuchi, T., Suzuki, R., Satoh, H., Tsuchida, A., Moroi, M., Sugi, K., Noda, T., Ebinuma, H., Ueta, Y., Kondo, T., Araki, E., Ezaki, O., Nagai, R., Tobe, K., Terauchi, Y., Ueki, K., Minokoshi, Y., Kadowaki, T., 2007. Adiponectin stimulates AMP-activated protein kinase in the hypothalamus and increases food intake. Cell Metab. 6, 55–68.

Kunz, J., Henriquez, R., Schneider, U., Deuter-Reinhard, M., Movva, N.R., Hall, M.N., 1993. Target of rapamycin in yeast, TOR2, is an essential phosphatidylinositol kinase homolog required for G1 progression. Cell 73, 585–596.

Kuo, C.J., Chung, J., Fiorentino, D.F., Flanagan, W.M., Blenis, J., Crabtree, G.R., 1992. Rapamycin selectively inhibits interleukin-2 activation of p70 S6 kinase. Nature 358, 70–73.

Laderoute, K.R., Amin, K., Calaoagan, J.M., Knapp, M., Le, T., Orduna, J., Foretz, M., Viollet, B., 2006. 5’-AMP-Activated Protein Kinase (AMPK) Is Induced by Low-Oxygen and Glucose Deprivation Conditions Found in Solid-Tumor Microenvironments. Mol. Cell. Biol. 26, 5336–5347.

Laplante, M., Sabatini, D.M., 2012. mTOR Signaling in Growth Control and Disease. Cell 149, 274–293.

Lawson, J.W., Veech, R.L., 1979. Effects of pH and free Mg2+ on the Keq of the creatine kinase reaction and other phosphate hydrolyses and phosphate transfer reactions. J. Biol. Chem. 254, 6528–6537.

LeBrasseur, N.K., Kelly, M., Tsao, T.-S., Farmer, S.R., Saha, A.K., Ruderman, N.B., Tomas, E., 2006. Thiazolidinediones can rapidly activate AMP-activated protein kinase in mammalian tissues. Am. J. Physiol. - Endocrinol. Metab. 291, E175–E181.

Lee, K.H., Kim, K.H., 1977. Regulation of rat liver acetyl coenzyme A carboxylase. Evidence for interconversion between active and inactive forms of enzyme by phosphorylation and dephosphorylation. J. Biol. Chem. 252, 1748–1751.

Li, Q., Song, X.-M., Ji, Y.-Y., Jiang, H., Xu, L.-G., 2013. The dual mTORC1 and mTORC2 inhibitor AZD8055 inhibits head and neck squamous cell carcinoma cell growth in vivo and in vitro. Biochem. Biophys. Res. Commun.

Liu, P., Gan, W., Inuzuka, H., Lazorchak, A.S., Gao, D., Arojo, O., Liu, D., Wan, L., Zhai, B., Yu, Y., Yuan, M., Kim, B.M., Shaik, S., Menon, S., Gygi, S.P., Lee, T.H., Asara, J.M., Manning, B.D., Blenis, J., Su, B., Wei, W., 2013. Sin1 phosphorylation impairs mTORC2 complex integrity and inhibits downstream Akt signalling to suppress tumorigenesis. Nat. Cell Biol.

Liu, W., Monahan, K.B., Pfefferle, A.D., Shimamura, T., Sorrentino, J., Chan, K.T., Roadcap, D.W., Ollila, D.W., Thomas, N.E., Castrillon, D.H., Miller, C.R., Perou, C.M., Wong, K.-K., Bear, J.E., Sharpless, N.E., 2012. LKB1/STK11 Inactivation Leads to Expansion of a Prometastatic Tumor Subpopulation in Melanoma. Cancer Cell 21, 751–764.

Liu, Y., Lai, Y., Hill, E.V., Tyteca, D., Carpentier, S., Ingvaldsen, A., Vertommen, D., Lantier, L., Foretz, M., Dequiedt, F., Courtoy, P.J., Erneux, C., Viollet, B., Shepherd, P.R., Tavaré, J.M., Jensen, J., Rider, M.H., 2013. Phosphatidylinositol 3-phosphate 5-kinase (PIKfyve) is an AMPK target participating in contraction-stimulated glucose uptake in skeletal muscle. Biochem. J. 455, 195–206.

Lizcano, J.M., Göransson, O., Toth, R., Deak, M., Morrice, N.A., Boudeau, J., Hawley, S.A., Udd, L., Mäkelä, T.P., Hardie, D.G., Alessi, D.R., 2004. LKB1 is a master kinase that activates 13 kinases of the AMPK subfamily, including MARK/PAR-1. EMBO J. 23, 833–843.

Loewith, R., Jacinto, E., Wullschleger, S., Lorberg, A., Crespo, J.L., Bonenfant, D., Oppliger, W., Jenoe, P., Hall, M.N., 2002. Two TOR complexes, only one of which is rapamycin sensitive, have distinct roles in cell growth control. Mol. Cell 10, 457–468.

Long, X., Lin, Y., Ortiz-Vega, S., Yonezawa, K., Avruch, J., 2005. Rheb binds and regulates the mTOR kinase. Curr. Biol. CB 15, 702–713.

Longnus, S.L., Wambolt, R.B., Parsons, H.L., Brownsey, R.W., Allard, M.F., 2003. 5-Aminoimidazole-4-carboxamide 1-beta -D-ribofuranoside (AICAR) stimulates myocardial glycogenolysis by allosteric mechanisms. Am. J. Physiol. Regul. Integr. Comp. Physiol. 284, R936–944.

Lorenz, M.C., Heitman, J., 1995. TOR mutations confer rapamycin resistance by preventing interaction with FKBP12-rapamycin. J. Biol. Chem. 270, 27531–27537.

Mackintosh, R.W., Davies, S.P., Clarke, P.R., Weekes, J., Gillespie, J.G., Gibb, B.J., Hardie, D.G., 1992. Evidence for a protein kinase cascade in higher plants. 3-Hydroxy-3-methylglutaryl-CoA reductase kinase. Eur. J. Biochem. FEBS 209, 923–931.

Manning, B.D., Cantley, L.C., 2007. AKT/PKB Signaling: Navigating Downstream. Cell 129, 1261–1274.

Manning, G., Whyte, D.B., Martinez, R., Hunter, T., Sudarsanam, S., 2002. The protein kinase complement of the human genome. Science 298, 1912–1934.

Marsin, A.S., Bertrand, L., Rider, M.H., Deprez, J., Beauloye, C., Vincent, M.F., Van den Berghe, G., Carling, D., Hue, L., 2000. Phosphorylation and activation of heart PFK-2 by AMPK has a role in the stimulation of glycolysis during ischaemia. Curr. Biol. CB 10, 1247–1255.

Marsin, A.-S., Bouzin, C., Bertrand, L., Hue, L., 2002. The stimulation of glycolysis by hypoxia in activated monocytes is mediated by AMP-activated protein kinase and inducible 6-phosphofructo-2-kinase. J. Biol. Chem. 277, 30778–30783.

Martineau, Y., Azar, R., Müller, D., Lasfargues, C., El Khawand, S., Anesia, R., Pelletier, J., Bousquet, C., Pyronnet, S., 2013. Pancreatic tumours escape from translational control through 4E-BP1 loss. Oncogene.

Masri, J., Bernath, A., Martin, J., Jo, O.D., Vartanian, R., Funk, A., Gera, J., 2007. mTORC2 activity is elevated in gliomas and promotes growth and cell motility via overexpression of rictor. Cancer Res. 67, 11712–11720.

Mayer, F.V., Heath, R., Underwood, E., Sanders, M.J., Carmena, D., McCartney, R.R., Leiper, F.C., Xiao, B., Jing, C., Walker, P.A., Haire, L.F., Ogrodowicz, R., Martin, S.R., Schmidt,

M.C., Gamblin, S.J., Carling, D., 2011. ADP Regulates SNF1, the Saccharomyces cerevisiae Homolog of AMP-Activated Protein Kinase. Cell Metab.

McBride, A., Ghilagaber, S., Nikolaev, A., Hardie, D.G., 2009. The glycogen-binding domain on the AMPK beta subunit allows the kinase to act as a glycogen sensor. Cell Metab. 9, 23–34.

Menendez, J.A., Vazquez-Martin, A., Ortega, F.J., Fernandez-Real, J.M., 2009. Fatty Acid Synthase: Association with Insulin Resistance, Type 2 Diabetes, and Cancer. Clin. Chem. 55, 425–438.

Merrill, G.F., Kurth, E.J., Hardie, D.G., Winder, W.W., 1997. AICA riboside increases AMP-activated protein kinase, fatty acid oxidation, and glucose uptake in rat muscle. Am. J. Physiol. 273, E1107–1112.

Mihaylova, M.M., Vasquez, D.S., Ravnskjaer, K., Denechaud, P.-D., Yu, R.T., Alvarez, J.G., Downes, M., Evans, R.M., Montminy, M., Shaw, R.J., 2011. Class IIa Histone Deacetylases Are Hormone-Activated Regulators of FOXO and Mammalian Glucose Homeostasis. Cell 145, 607–621.

Milan, D., Jeon, J.-T., Looft, C., Amarger, V., Robic, A., Thelander, M., Rogel-Gaillard, C., Paul, S., Iannuccelli, N., Rask, L., Ronne, H., Lundström, K., Reinsch, N., Gellin, J., Kalm, E., Roy, P.L., Chardon, P., Andersson, L., 2000. A Mutation in PRKAG3 Associated with Excess Glycogen Content in Pig Skeletal Muscle. Science 288, 1248–1251.

Miller, R.A., Chu, Q., Xie, J., Foretz, M., Viollet, B., Birnbaum, M.J., 2013. Biguanides suppress hepatic glucagon signalling by decreasing production of cyclic AMP. Nature 494, 256–260.

Minokoshi, Y., Alquier, T., Furukawa, N., Kim, Y.-B., Lee, A., Xue, B., Mu, J., Foufelle, F., Ferré, P., Birnbaum, M.J., Stuck, B.J., Kahn, B.B., 2004. AMP-kinase regulates food intake by responding to hormonal and nutrient signals in the hypothalamus. Nature 428, 569–574.

Minokoshi, Y., Kim, Y.-B., Peroni, O.D., Fryer, L.G.D., Müller, C., Carling, D., Kahn, B.B., 2002. Leptin stimulates fatty-acid oxidation by activating AMP-activated protein kinase. Nature 415, 339–343.

Mitchelhill, K.I., Michell, B.J., House, C.M., Stapleton, D., Dyck, J., Gamble, J., Ullrich, C., Witters, L.A., Kemp, B.E., 1997. Posttranslational Modifications of the 5'-AMP-activated Protein Kinase β1 Subunit. J. Biol. Chem. 272, 24475–24479.

Mitchelhill, K.I., Stapleton, D., Gao, G., House, C., Michell, B., Katsis, F., Witters, L.A., Kemp, B.E., 1994. Mammalian AMP-activated protein kinase shares structural and functional homology with the catalytic domain of yeast Snf1 protein kinase. J. Biol. Chem. 269, 2361–2364.

Mizushima, N., Levine, B., Cuervo, A.M., Klionsky, D.J., 2008. Autophagy fights disease through cellular self-digestion. Nature 451, 1069–1075.

Mooney, M.H., Fogarty, S., Stevenson, C., Gallagher, A.M., Palit, P., Hawley, S.A., Hardie, D.G., Coxon, G.D., Waigh, R.D., Tate, R.J., Harvey, A.L., Furman, B.L., 2008. Mechanisms underlying the metabolic actions of galegine that contribute to weight loss in mice. Br. J. Pharmacol. 153, 1669–1677.

Moore, F., Weekes, J., Hardie, D.G., 1991. Evidence that AMP triggers phosphorylation as well as direct allosteric activation of rat liver AMP-activated protein kinase. A sensitive mechanism to protect the cell against ATP depletion. Eur. J. Biochem. FEBS 199, 691–697.

Moreno, D., Knecht, E., Viollet, B., Sanz, P., 2008. A769662, a novel activator of AMP-activated protein kinase, inhibits non-proteolytic components of the 26S proteasome by an AMPK-independent mechanism. FEBS Lett. 582, 2650–2654.

Munday, M.R., Campbell, D.G., Carling, D., Hardie, D.G., 1988. Identification by amino acid sequencing of three major regulatory phosphorylation sites on rat acetyl-CoA carboxylase. Eur. J. Biochem. FEBS 175, 331–338.

Narkar, V.A., Downes, M., Yu, R.T., Embler, E., Wang, Y.-X., Banayo, E., Mihaylova, M.M., Nelson, M.C., Zou, Y., Juguilon, H., Kang, H., Shaw, R.J., Evans, R.M., 2008. AMPK and PPARδ Agonists Are Exercise Mimetics. Cell 134, 405–415.

Noda, T., Ohsumi, Y., 1998. Tor, a phosphatidylinositol kinase homologue, controls autophagy in yeast. J. Biol. Chem. 273, 3963–3966.

Nordstrom, J.L., Rodwell, V.W., Mitschelen, J.J., 1977. Interconversion of active and inactive forms of rat liver hydroxymethylglutaryl-CoA reductase. J. Biol. Chem. 252, 8924–8934.

O'Neill, H.M., 2013. AMPK and Exercise: Glucose Uptake and Insulin Sensitivity. Diabetes Metab. J. 37, 1–21.

O'Neill, H.M., Maarbjerg, S.J., Crane, J.D., Jeppesen, J., Jørgensen, S.B., Schertzer, J.D., Shyroka, O., Kiens, B., van Denderen, B.J., Tarnopolsky, M.A., Kemp, B.E., Richter, E.A., Steinberg, G.R., 2011. AMP-activated protein kinase (AMPK) beta1beta2 muscle null mice reveal an essential role for AMPK in maintaining mitochondrial content and glucose uptake during exercise. Proc. Natl. Acad. Sci. U. S. A. 108, 16092–16097.

O'Reilly, K.E., Rojo, F., She, Q.-B., Solit, D., Mills, G.B., Smith, D., Lane, H., Hofmann, F., Hicklin, D.J., Ludwig, D.L., Baselga, J., Rosen, N., 2006. mTOR Inhibition Induces Upstream Receptor Tyrosine Kinase Signaling and Activates Akt. Cancer Res. 66, 1500 –1508.

Oakhill, J.S., Chen, Z.-P., Scott, J.W., Steel, R., Castelli, L.A., Ling, N., Macaulay, S.L., Kemp, B.E., 2010. {beta}-Subunit myristoylation is the gatekeeper for initiating metabolic stress sensing by AMP-activated protein kinase (AMPK). Proc. Natl. Acad. Sci. U. S. A.

Oakhill, J.S., Scott, J.W., Kemp, B.E., 2012. AMPK functions as an adenylate charge-regulated protein kinase. Trends Endocrinol. Metab. 23, 125–132.

Oakhill, J.S., Steel, R., Chen, Z.-P., Scott, J.W., Ling, N., Tam, S., Kemp, B.E., 2011. AMPK is a direct adenylate charge-regulated protein kinase. Science 332, 1433–1435.

Owen, M.R., Doran, E., Halestrap, A.P., 2000. Evidence that metformin exerts its anti-diabetic effects through inhibition of complex 1 of the mitochondrial respiratory chain. Biochem. J. 348 Pt 3, 607–614.

Pan, D.A., Hardie, D.G., 2002. A homologue of AMP-activated protein kinase in Drosophila melanogaster is sensitive to AMP and is activated by ATP depletion. Biochem. J. 367, 179.

Pang, T., Xiong, B., Li, J.-Y., Qiu, B.-Y., Jin, G.-Z., Shen, J.-K., Li, J., 2007. Conserved alpha-helix acts as autoinhibitory sequence in AMP-activated protein kinase alpha subunits. J. Biol. Chem. 282, 495–506.

Pause, A., Belsham, G.J., Gingras, A.C., Donzé, O., Lin, T.A., Lawrence, J.C., Jr, Sonenberg, N., 1994. Insulin-dependent stimulation of protein synthesis by phosphorylation of a regulator of 5'-cap function. Nature 371, 762–767.

Pearce, L.R., Huang, X., Boudeau, J., Pawłowski, R., Wullschleger, S., Deak, M., Ibrahim, A.F.M., Gourlay, R., Magnuson, M.A., Alessi, D.R., 2007. Identification of Protor as a novel Rictor-binding component of mTOR complex-2. Biochem. J. 405, 513–522.

Pearce, L.R., Komander, D., Alessi, D.R., 2010. The nuts and bolts of AGC protein kinases. Nat Rev Mol Cell Biol 11, 9–22.

Pearce, L.R., Sommer, E.M., Sakamoto, K., Wullschleger, S., Alessi, D.R., 2011. Protor-1 is required for efficient mTORC2-mediated activation of SGK1 in the kidney. Biochem. J. 436, 169–179.

Peterson, T.R., Laplante, M., Thoreen, C.C., Sancak, Y., Kang, S.A., Kuehl, W.M., Gray, N.S., Sabatini, D.M., 2009. DEPTOR Is an mTOR Inhibitor Frequently Overexpressed in Multiple Myeloma Cells and Required for Their Survival. Cell 137, 873–886.

Petroulakis, E., Parsyan, A., Dowling, R.J.O., LeBacquer, O., Martineau, Y., Bidinosti, M., Larsson, O., Alain, T., Rong, L., Mamane, Y., Paquet, M., Furic, L., Topisirovic, I., Shahbazian, D., Livingstone, M., Costa-Mattioli, M., Teodoro, J.G., Sonenberg, N., 2009. p53-dependent translational control of senescence and transformation via 4E-BPs. Cancer Cell 16, 439–446.

Polekhina, G., Gupta, A., Michell, B.J., van Denderen, B., Murthy, S., Feil, S.C., Jennings, I.G., Campbell, D.J., Witters, L.A., Parker, M.W., Kemp, B.E., Stapleton, D., 2003. AMPK beta subunit targets metabolic stress sensing to glycogen. Curr. Biol. CB 13, 867–871.

Raught, B., Peiretti, F., Gingras, A.-C., Livingstone, M., Shahbazian, D., Mayeur, G.L., Polakiewicz, R.D., Sonenberg, N., Hershey, J.W.B., 2004. Phosphorylation of eucaryotic translation initiation factor 4B Ser422 is modulated by S6 kinases. EMBO J. 23, 1761–1769.

Rena, G., Pearson, E.R., Sakamoto, K., 2013. Molecular mechanism of action of metformin: old or new insights? Diabetologia.

Rolf, J., Zarrouk, M., Finlay, D.K., Foretz, M., Viollet, B., Cantrell, D.A., 2013. AMPKα1: A glucose sensor that controls CD8 T-cell memory. Eur. J. Immunol. 43, 889–896.

Ross, F.A., Rafferty, J.N., Dallas, M.L., Ogunbayo, O., Ikematsu, N., McClafferty, H., Tian, L., Widmer, H., Rowe, I.C.M., Wyatt, C.N., Shipston, M.J., Peers, C., Hardie, D.G., Evans, A.M., 2011. Selective expression in carotid body type I cells of a single splice variant of the large conductance calcium- and voltage-activated potassium channel confers regulation by AMP-activated protein kinase. J. Biol. Chem. 286, 11929–11936.

Rothwell, P.M., Fowkes, F.G.R., Belch, J.F.F., Ogawa, H., Warlow, C.P., Meade, T.W., 2011. Effect of daily aspirin on long-term risk of death due to cancer: analysis of individual patient data from randomised trials. Lancet 377, 31–41.

Rubenstein, E.M., McCartney, R.R., Zhang, C., Shokat, K.M., Shirra, M.K., Arndt, K.M., Schmidt, M.C., 2008. Access denied: Snf1 activation loop phosphorylation is controlled by availability of the phosphorylated threonine 210 to the PP1 phosphatase. J. Biol. Chem. 283, 222–230.

Ruvinsky, I., Meyuhas, O., 2006. Ribosomal protein S6 phosphorylation: from protein synthesis to cell size. Trends Biochem. Sci. 31, 342–348.

Sabatini, D.M., Erdjument-Bromage, H., Lui, M., Tempst, P., Snyder, S.H., 1994. RAFT1: a mammalian protein that binds to FKBP12 in a rapamycin-dependent fashion and is homologous to yeast TORs. Cell 78, 35–43.

Sabers, C.J., Martin, M.M., Brunn, G.J., Williams, J.M., Dumont, F.J., Wiederrecht, G., Abraham, R.T., 1995. Isolation of a protein target of the FKBP12-rapamycin complex in mammalian cells. J. Biol. Chem. 270, 815–822.

Sabina, R.L., Patterson, D., Holmes, E.W., 1985. 5-Amino-4-imidazolecarboxamide riboside (Z-riboside) metabolism in eukaryotic cells. J. Biol. Chem. 260, 6107–6114.

Saha, A.K., Avilucea, P.R., Ye, J.-M., Assifi, M.M., Kraegen, E.W., Ruderman, N.B., 2004. Pioglitazone treatment activates AMP-activated protein kinase in rat liver and adipose tissue in vivo. Biochem. Biophys. Res. Commun. 314, 580–585.

Sakamoto, K., Göransson, O., Hardie, D.G., Alessi, D.R., 2004. Activity of LKB1 and AMPK-related kinases in skeletal muscle: effects of contraction, phenformin, and AICAR. Am. J. Physiol. Endocrinol. Metab. 287, E310–317.

Sakamoto, K., McCarthy, A., Smith, D., Green, K.A., Grahame Hardie, D., Ashworth, A., Alessi, D.R., 2005. Deficiency of LKB1 in skeletal muscle prevents AMPK activation and glucose uptake during contraction. EMBO J. 24, 1810–1820.

Salt, I.P., Johnson, G., Ashcroft, S.J., Hardie, D.G., 1998. AMP-activated protein kinase is activated by low glucose in cell lines derived from pancreatic beta cells, and may regulate insulin release. Biochem. J. 335 (Pt 3), 533–539.

Sancak, Y., Bar-Peled, L., Zoncu, R., Markhard, A.L., Nada, S., Sabatini, D.M., 2010. Ragulator-Rag complex targets mTORC1 to the lysosomal surface and is necessary for its activation by amino acids. Cell 141, 290–303.

Sancak, Y., Peterson, T.R., Shaul, Y.D., Lindquist, R.A., Thoreen, C.C., Bar-Peled, L., Sabatini, D.M., 2008. The Rag GTPases bind raptor and mediate amino acid signaling to mTORC1. Science 320, 1496–1501.

Sancak, Y., Thoreen, C.C., Peterson, T.R., Lindquist, R.A., Kang, S.A., Spooner, E., Carr, S.A., Sabatini, D.M., 2007. PRAS40 is an insulin-regulated inhibitor of the mTORC1 protein kinase. Mol. Cell 25, 903–915.

Sanchez-Cespedes, M., Parrella, P., Esteller, M., Nomoto, S., Trink, B., Engles, J.M., Westra, W.H., Herman, J.G., Sidransky, D., 2002. Inactivation of LKB1/STK11 Is a Common Event in Adenocarcinomas of the Lung. Cancer Res. 62, 3659 –3662.

Sanders, M.J., Ali, Z.S., Hegarty, B.D., Heath, R., Snowden, M.A., Carling, D., 2007a. Defining the mechanism of activation of AMP-activated protein kinase by the small molecule A-769662, a member of the thienopyridone family. J. Biol. Chem. 282, 32539–32548.

Sanders, M.J., Grondin, P.O., Hegarty, B.D., Snowden, M.A., Carling, D., 2007b. Investigating the mechanism for AMP activation of the AMP-activated protein kinase cascade. Biochem. J. 403, 139–148.

Sapkota, G.P., Boudeau, J., Deak, M., Kieloch, A., Morrice, N., Alessi, D.R., 2002a. Identification and characterization of four novel phosphorylation sites (Ser31, Ser325, Thr336 and Thr366) on LKB1/STK11, the protein kinase mutated in Peutz-Jeghers cancer syndrome. Biochem. J. 362, 481–490.

Sapkota, G.P., Deak, M., Kieloch, A., Morrice, N., Goodarzi, A.A., Smythe, C., Shiloh, Y., Lees-Miller, S.P., Alessi, D.R., 2002b. Ionizing radiation induces ataxia telangiectasia mutated kinase (ATM)-mediated phosphorylation of LKB1/STK11 at Thr-366. Biochem. J. 368, 507–516.

Sapkota, G.P., Kieloch, A., Lizcano, J.M., Lain, S., Arthur, J.S.C., Williams, M.R., Morrice, N., Deak, M., Alessi, D.R., 2001. Phosphorylation of the Protein Kinase Mutated in Peutz-Jeghers Cancer Syndrome, LKB1/STK11, at Ser431 by p90RSK and cAMP-dependent Protein Kinase, but Not Its Farnesylation at Cys433, Is Essential for LKB1 to Suppress Cell Growth. J. Biol. Chem. 276, 19469 –19482.

Sarbassov, D.D., Ali, S.M., Kim, D.-H., Guertin, D.A., Latek, R.R., Erdjument-Bromage, H., Tempst, P., Sabatini, D.M., 2004. Rictor, a novel binding partner of mTOR, defines a rapamycin-insensitive and raptor-independent pathway that regulates the cytoskeleton. Curr. Biol. CB 14, 1296–1302.

Sarbassov, D.D., Ali, S.M., Sengupta, S., Sheen, J.-H., Hsu, P.P., Bagley, A.F., Markhard, A.L., Sabatini, D.M., 2006. Prolonged Rapamycin Treatment Inhibits mTORC2 Assembly and Akt/PKB. Mol. Cell 22, 159–168.

Sarbassov, D.D., Guertin, D.A., Ali, S.M., Sabatini, D.M., 2005. Phosphorylation and regulation of Akt/PKB by the rictor-mTOR complex. Science 307, 1098–1101.

Sato, T., Nakashima, A., Guo, L., Coffman, K., Tamanoi, F., 2010. Single amino-acid changes that confer constitutive activation of mTOR are discovered in human cancer. Oncogene 29, 2746–2752.

Schmelzle, T., Hall, M.N., 2000. TOR, a Central Controller of Cell Growth. Cell 103, 253–262.

Scott, J.W., Hawley, S.A., Green, K.A., Anis, M., Stewart, G., Scullion, G.A., Norman, D.G., Hardie, D.G., 2004. CBS domains form energy-sensing modules whose binding of adenosine ligands is disrupted by disease mutations. J. Clin. Invest. 113, 274–284.

Scott, J.W., Norman, D.G., Hawley, S.A., Kontogiannis, L., Hardie, D.G., 2002. Protein kinase substrate recognition studied using the recombinant catalytic domain of AMP-activated protein kinase and a model substrate. J. Mol. Biol. 317, 309–323.

Scott, J.W., van Denderen, B.J.W., Jorgensen, S.B., Honeyman, J.E., Steinberg, G.R., Oakhill, J.S., Iseli, T.J., Koay, A., Gooley, P.R., Stapleton, D., Kemp, B.E., 2008. Thienopyridone drugs are selective activators of AMP-activated protein kinase beta1-containing complexes. Chem. Biol. 15, 1220–1230.

Shackelford, D.B., Abt, E., Gerken, L., Vasquez, D.S., Seki, A., Leblanc, M., Wei, L., Fishbein, M.C., Czernin, J., Mischel, P.S., Shaw, R.J., 2013. LKB1 inactivation dictates therapeutic response of non-small cell lung cancer to the metabolism drug phenformin. Cancer Cell 23, 143–158.

Shah, O.J., Wang, Z., Hunter, T., 2004. Inappropriate Activation of the TSC/Rheb/mTOR/S6K Cassette Induces IRS1/2 Depletion, Insulin Resistance, and Cell Survival Deficiencies. Curr. Biol. 14, 1650–1656.

Shao, H., Gao, C., Tang, H., Zhang, H., Roberts, L.R., Hylander, B.L., Repasky, E.A., Ma, W.W., Qiu, J., Adjei, A.A., Dy, G.K., Yu, C., 2011. Dual targeting of mTORC1/C2 complexes enhances histone deacetylase inhibitor-mediated anti-tumor efficacy in primary HCC cancer in vitro and in vivo. J. Hepatol.

Shaw, R.J., Kosmatka, M., Bardeesy, N., Hurley, R.L., Witters, L.A., DePinho, R.A., Cantley, L.C., 2004. The tumor suppressor LKB1 kinase directly activates AMP-activated kinase and regulates apoptosis in response to energy stress. Proc. Natl. Acad. Sci. U. S. A. 101, 3329–3335.

Shaw, R.J., Lamia, K.A., Vasquez, D., Koo, S.-H., Bardeesy, N., Depinho, R.A., Montminy, M., Cantley, L.C., 2005. The kinase LKB1 mediates glucose homeostasis in liver and therapeutic effects of metformin. Science 310, 1642–1646.

Smith, D.P., Spicer, J., Smith, A., Swift, S., Ashworth, A., 1999. The Mouse Peutz-Jeghers Syndrome Gene Lkbl Encodes a Nuclear Protein Kinase. Hum. Mol. Genet. 8, 1479–1485.

Song, X.M., Fiedler, M., Galuska, D., Ryder, J.W., Fernström, M., Chibalin, A.V., Wallberg-Henriksson, H., Zierath, J.R., 2002. 5-Aminoimidazole-4-carboxamide ribonucleoside treatment improves glucose homeostasis in insulin-resistant diabetic (ob/ob) mice. Diabetologia 45, 56–65.

Stahmann, N., Woods, A., Carling, D., Heller, R., 2006. Thrombin activates AMP-activated protein kinase in endothelial cells via a pathway involving Ca2+/calmodulin-dependent protein kinase kinase beta. Mol. Cell. Biol. 26, 5933–5945.

Stapleton, D., Mitchelhill, K.I., Gao, G., Widmer, J., Michell, B.J., Teh, T., House, C.M., Fernandez, C.S., Cox, T., Witters, L.A., Kemp, B.E., 1996. Mammalian AMP-activated protein kinase subfamily. J. Biol. Chem. 271, 611–614.

Stein, S.C., Woods, A., Jones, N.A., Davison, M.D., Carling, D., 2000. The regulation of AMP-activated protein kinase by phosphorylation. Biochem. J. 345, 437–443.

Steinberg, G.R., Kemp, B.E., 2009. AMPK in Health and Disease. Physiol. Rev. 89, 1025–1078.

Sun, S.-Y., Rosenberg, L.M., Wang, X., Zhou, Z., Yue, P., Fu, H., Khuri, F.R., 2005. Activation of Akt and eIF4E Survival Pathways by Rapamycin-Mediated Mammalian Target of Rapamycin Inhibition. Cancer Res. 65, 7052 –7058.

Suter, M., Riek, U., Tuerk, R., Schlattner, U., Wallimann, T., Neumann, D., 2006. Dissecting the role of 5'-AMP for allosteric stimulation, activation, and deactivation of AMP-activated protein kinase. J. Biol. Chem. 281, 32207–32216.

Sutherland, C.M., Hawley, S.A., McCartney, R.R., Leech, A., Stark, M.J.R., Schmidt, M.C., Hardie, D.G., 2003. Elm1p is one of three upstream kinases for the Saccharomyces cerevisiae SNF1 complex. Curr. Biol. CB 13, 1299–1305.

Tamás, P., Hawley, S.A., Clarke, R.G., Mustard, K.J., Green, K., Hardie, D.G., Cantrell, D.A., 2006. Regulation of the energy sensor AMP-activated protein kinase by antigen receptor and Ca2+ in T lymphocytes. J. Exp. Med. 203, 1665–1670.

Thomas, A., Beuck, S., Eickhoff, J.C., Guddat, S., Krug, O., Kamber, M., Schänzer, W., Thevis, M., 2010. Quantification of urinary AICAR concentrations as a matter of doping controls. Anal. Bioanal. Chem. 396, 2899–2908.

Thoreen, C.C., Kang, S.A., Chang, J.W., Liu, Q., Zhang, J., Gao, Y., Reichling, L.J., Sim, T., Sabatini, D.M., Gray, N.S., 2009. An ATP-competitive mammalian target of rapamycin inhibitor reveals rapamycin-resistant functions of mTORC1. J. Biol. Chem. 284, 8023–8032.

Thornton, C., Snowden, M.A., Carling, D., 1998. Identification of a novel AMP-activated protein kinase beta subunit isoform that is highly expressed in skeletal muscle. J. Biol. Chem. 273, 12443–12450.

Tiainen, M., Ylikorkala, A., Mäkelä, T.P., 1999. Growth suppression by Lkb1 is mediated by a G(1) cell cycle arrest. Proc. Natl. Acad. Sci. U. S. A. 96, 9248–9251.

Towler, M.C., Fogarty, S., Hawley, S.A., Pan, D.A., Martin, D.M.A., Morrice, N.A., McCarthy, A., Galardo, M.N., Meroni, S.B., Cigorraga, S.B., Ashworth, A., Sakamoto, K., Hardie, D.G., 2008. A novel short splice variant of the tumour suppressor LKB1 is required for spermiogenesis. Biochem. J. 416, 1–14.

Turban, S., Stretton, C., Drouin, O., Green, C.J., Watson, M.L., Gray, A., Ross, F., Lantier, L., Viollet, B., Hardie, D.G., Marette, A., Hundal, H.S., 2012. Defining the Contribution of AMP-activated Protein Kinase (AMPK) and Protein Kinase C (PKC) in Regulation of Glucose Uptake by Metformin in Skeletal Muscle Cells. J. Biol. Chem. 287, 20088–20099.

Turner, N., Li, J.-Y., Gosby, A., To, S.W.C., Cheng, Z., Miyoshi, H., Taketo, M.M., Cooney, G.J., Kraegen, E.W., James, D.E., Hu, L.-H., Li, J., Ye, J.-M., 2008. Berberine and Its More Biologically Available Derivative, Dihydroberberine, Inhibit Mitochondrial Respiratory Complex I A Mechanism for the Action of Berberine to Activate AMP-Activated Protein Kinase and Improve Insulin Action. Diabetes 57, 1414–1418.

Vane, J.R., 1971. Inhibition of Prostaglandin Synthesis as a Mechanism of Action for Aspirin-like Drugs. Nature 231, 232–235.

Vézina, C., Kudelski, A., Sehgal, S.N., 1975. Rapamycin (AY-22,989), a new antifungal antibiotic. I. Taxonomy of the producing streptomycete and isolation of the active principle. J. Antibiot. (Tokyo) 28, 721–726.

Vincent, M.F., Marangos, P.J., Gruber, H.E., Van den Berghe, G., 1991. Inhibition by AICA riboside of gluconeogenesis in isolated rat hepatocytes. Diabetes 40, 1259–1266.

Von Manteuffel, S.R., Gingras, A.C., Ming, X.F., Sonenberg, N., Thomas, G., 1996. 4E-BP1 phosphorylation is mediated by the FRAP-p70s6k pathway and is independent of mitogen-activated protein kinase. Proc. Natl. Acad. Sci. U. S. A. 93, 4076–4080.

Walsh, D.A., Perkins, J.P., Krebs, E.G., 1968. An adenosine 3',5'-monophosphate-dependant protein kinase from rabbit skeletal muscle. J. Biol. Chem. 243, 3763–3765.

Warburg, O., 1956. On the origin of cancer cells. Science 123, 309–314.

Warden, S.M., Richardson, C., O'Donnell, J., Stapleton, D., Kemp, B.E., Witters, L.A., 2001. Post-translational modifications of the beta-1 subunit of AMP-activated protein kinase affect enzyme activity and cellular localization. Biochem. J. 354, 275–283.

Weekes, J., Hawley, S.A., Corton, J., Shugar, D., Hardie, D.G., 1994. Activation of rat liver AMP-activated protein kinase by kinase kinase in a purified, reconstituted system. Effects of AMP and AMP analogues. Eur. J. Biochem. FEBS 219, 751–757.

Willems, L., Chapuis, N., Puissant, A., Maciel, T.T., Green, A.S., Jacque, N., Vignon, C., Park, S., Guichard, S., Herault, O., Fricot, A., Hermine, O., Moura, I.C., Auberger, P., Ifrah, N., Dreyfus, F., Bonnet, D., Lacombe, C., Mayeux, P., Bouscary, D., Tamburini, J., 2011. The dual mTORC1 and mTORC2 inhibitor AZD8055 has anti-tumor activity in acute myeloid leukemia. Leuk. Off. J. Leuk. Soc. Am. Leuk. Res. Fund UK.

Wilson, W.A., Hawley, S.A., Hardie, D.G., 1996. Glucose repression/derepression in budding yeast: SNF1 protein kinase is activated by phosphorylation under derepressing conditions, and this correlates with a high AMP:ATP ratio. Curr. Biol. CB 6, 1426–1434.

Winder, W.W., Hardie, D.G., 1996. Inactivation of acetyl-CoA carboxylase and activation of AMP-activated protein kinase in muscle during exercise. Am. J. Physiol. 270, E299–304.

Winder, W.W., Holmes, B.F., Rubink, D.S., Jensen, E.B., Chen, M., Holloszy, J.O., 2000. Activation of AMP-activated protein kinase increases mitochondrial enzymes in skeletal muscle. J. Appl. Physiol. Bethesda Md 1985 88, 2219–2226.

Winder, W.W., Wilson, H.A., Hardie, D.G., Rasmussen, B.B., Hutber, C.A., Call, G.B., Clayton, R.D., Conley, L.M., Yoon, S., Zhou, B., 1997. Phosphorylation of rat muscle acetyl-CoA carboxylase by AMP-activated protein kinase and protein kinase A. J. Appl. Physiol. Bethesda Md 1985 82, 219–225.

Wingo, S.N., Gallardo, T.D., Akbay, E.A., Liang, M.-C., Contreras, C.M., Boren, T., Shimamura, T., Miller, D.S., Sharpless, N.E., Bardeesy, N., Kwiatkowski, D.J., Schorge, J.O., Wong, K.-K.,

Castrillon, D.H., 2009. Somatic LKB1 mutations promote cervical cancer progression. PloS One 4, e5137.

Wojtaszewski, J.F.P., Jørgensen, S.B., Hellsten, Y., Hardie, D.G., Richter, E.A., 2002. Glycogen-dependent effects of 5-aminoimidazole-4-carboxamide (AICA)-riboside on AMP-activated protein kinase and glycogen synthase activities in rat skeletal muscle. Diabetes 51, 284–292.

Wojtaszewski, J.F.P., Nielsen, P., Hansen, B.F., Richter, E.A., Kiens, B., 2000. Isoform-specific and exercise intensity-dependent activation of 5'-AMP-activated protein kinase in human skeletal muscle. J. Physiol. 528, 221–226.

Woods, A., Cheung, P.C., Smith, F.C., Davison, M.D., Scott, J., Beri, R.K., Carling, D., 1996a. Characterization of AMP-activated protein kinase beta and gamma subunits. Assembly of the heterotrimeric complex in vitro. J. Biol. Chem. 271, 10282–10290.

Woods, A., Dickerson, K., Heath, R., Hong, S.-P., Momcilovic, M., Johnstone, S.R., Carlson, M., Carling, D., 2005. Ca2+/calmodulin-dependent protein kinase kinase-beta acts upstream of AMP-activated protein kinase in mammalian cells. Cell Metab. 2, 21–33.

Woods, A., Johnstone, S.R., Dickerson, K., Leiper, F.C., Fryer, L.G.D., Neumann, D., Schlattner, U., Wallimann, T., Carlson, M., Carling, D., 2003. LKB1 is the upstream kinase in the AMP-activated protein kinase cascade. Curr. Biol. CB 13, 2004–2008.

Woods, A., Munday, M.R., Scott, J., Yang, X., Carlson, M., Carling, D., 1994. Yeast SNF1 is functionally related to mammalian AMP-activated protein kinase and regulates acetyl-CoA carboxylase in vivo. J. Biol. Chem. 269, 19509–19515.

Woods, A., Salt, I., Scott, J., Hardie, D.G., Carling, D., 1996b. The alpha1 and alpha2 isoforms of the AMP-activated protein kinase have similar activities in rat liver but exhibit differences in substrate specificity in vitro. FEBS Lett. 397, 347–351.

Wyatt, C.N., Mustard, K.J., Pearson, S.A., Dallas, M.L., Atkinson, L., Kumar, P., Peers, C., Hardie, D.G., Evans, A.M., 2007. AMP-activated protein kinase mediates carotid body excitation by hypoxia. J. Biol. Chem. 282, 8092–8098.

Xiao, B., Heath, R., Saiu, P., Leiper, F.C., Leone, P., Jing, C., Walker, P.A., Haire, L., Eccleston, J.F., Davis, C.T., Martin, S.R., Carling, D., Gamblin, S.J., 2007. Structural basis for AMP binding to mammalian AMP-activated protein kinase. Nature 449, 496–500.

Xiao, B., Sanders, M.J., Underwood, E., Heath, R., Mayer, F.V., Carmena, D., Jing, C., Walker, P.A., Eccleston, J.F., Haire, L.F., Saiu, P., Howell, S.A., Aasland, R., Martin, S.R., Carling, D., Gamblin, S.J., 2011. Structure of mammalian AMPK and its regulation by ADP. Nature.

Yamauchi, T., Kamon, J., Minokoshi, Y., Ito, Y., Waki, H., Uchida, S., Yamashita, S., Noda, M., Kita, S., Ueki, K., Eto, K., Akanuma, Y., Froguel, P., Foufelle, F., Ferre, P., Carling, D., Kimura, S., Nagai, R., Kahn, B.B., Kadowaki, T., 2002. Adiponectin stimulates glucose utilization and fatty-acid oxidation by activating AMP-activated protein kinase. Nat. Med. 8, 1288–1295.

Yang, Q., Inoki, K., Ikenoue, T., Guan, K.-L., 2006. Identification of Sin1 as an essential TORC2 component required for complex formation and kinase activity. Genes Dev. 20, 2820–2832.

Yang, Y., Atasoy, D., Su, H.H., Sternson, S.M., 2011. Hunger States Switch a Flip-Flop Memory Circuit via a Synaptic AMPK-Dependent Positive Feedback Loop. Cell 146, 992–1003.

Yeh, L.A., Lee, K.H., Kim, K.H., 1980. Regulation of rat liver acetyl-CoA carboxylase. Regulation of phosphorylation and inactivation of acetyl-CoA carboxylase by the adenylate energy charge. J. Biol. Chem. 255, 2308–2314.

Yin, M.J., Yamamoto, Y., Gaynor, R.B., 1998. The anti-inflammatory agents aspirin and salicylate inhibit the activity of I(kappa)B kinase-beta. Nature 396, 77–80.

Yip, C.K., Murata, K., Walz, T., Sabatini, D.M., Kang, S.A., 2010. Structure of the human mTOR complex I and its implications for rapamycin inhibition. Mol. Cell 38, 768–774.

Yuan, T.L., Cantley, L.C., 2008. PI3K pathway alterations in cancer: variations on a theme. Oncogene 27, 5497–5510.

Yue, Z., Jin, S., Yang, C., Levine, A.J., Heintz, N., 2003. Beclin 1, an autophagy gene essential for early embryonic development, is a haploinsufficient tumor suppressor. Proc. Natl. Acad. Sci. U. S. A. 100, 15077–15082.

Zeqiraj, E., Filippi, B.M., Deak, M., Alessi, D.R., van Aalten, D.M.F., 2009a. Structure of the LKB1-STRAD-MO25 complex reveals an allosteric mechanism of kinase activation. Science 326, 1707–1711.

Zeqiraj, E., Filippi, B.M., Goldie, S., Navratilova, I., Boudeau, J., Deak, M., Alessi, D.R., van Aalten, D.M.F., 2009b. ATP and MO25alpha regulate the conformational state of the STRADalpha pseudokinase and activation of the LKB1 tumour suppressor. PLoS Biol. 7, e1000126.

Zhang, H., Bajraszewski, N., Wu, E., Wang, H., Moseman, A.P., Dabora, S.L., Griffin, J.D., Kwiatkowski, D.J., 2007. PDGFRs are critical for PI3K/Akt activation and negatively regulated by mTOR. J. Clin. Invest. 117, 730–738.

Zhang, Y.-L., Guo, H., Zhang, C.-S., Lin, S.-Y., Yin, Z., Peng, Y., Luo, H., Shi, Y., Lian, G., Zhang, C., Li, M., Ye, Z., Ye, J., Han, J., Li, P., Wu, J.-W., Lin, S.-C., 2013. AMP as a Low-Energy Charge Signal Autonomously Initiates Assembly of AXIN-AMPK-LKB1 Complex for AMPK Activation. Cell Metab. 18, 546–555.

Zheng, B., Jeong, J.H., Asara, J.M., Yuan, Y.-Y., Granter, S.R., Chin, L., Cantley, L.C., 2009. Oncogenic B-RAF negatively regulates the tumor suppressor LKB1 to promote melanoma cell proliferation. Mol. Cell 33, 237–247.

Zheng, X.F., Florentino, D., Chen, J., Crabtree, G.R., Schreiber, S.L., 1995. TOR kinase domains are required for two distinct functions, only one of which is inhibited by rapamycin. Cell 82, 121–130.

Zhou, G., Myers, R., Li, Y., Chen, Y., Shen, X., Fenyk-Melody, J., Wu, M., Ventre, J., Doebber, T., Fujii, N., Musi, N., Hirshman, M.F., Goodyear, L.J., Moller, D.E., 2001. Role of AMP-activated protein kinase in mechanism of metformin action. J. Clin. Invest. 108, 1167–1174.

Zinzalla, V., Stracka, D., Oppliger, W., Hall, M.N., 2011. Activation of mTORC2 by association with the ribosome. Cell 144, 757–768.

Zoncu, R., Bar-Peled, L., Efeyan, A., Wang, S., Sancak, Y., Sabatini, D.M., 2011a. mTORC1 senses lysosomal amino acids through an inside-out mechanism that requires the vacuolar H^+-ATPase. Science 334, 678–683.

Zoncu, R., Efeyan, A., Sabatini, D.M., 2011b. mTOR: from growth signal integration to cancer, diabetes and ageing. Nat. Rev. Mol. Cell Biol. 12, 21–35.

Zong, H., Ren, J.M., Young, L.H., Pypaert, M., Mu, J., Birnbaum, M.J., Shulman, G.I., 2002. AMP kinase is required for mitochondrial biogenesis in skeletal muscle in response to chronic energy deprivation. Proc. Natl. Acad. Sci. U. S. A. 99, 15983–15987.